



Ingrid Milena Reyes Martinez Belchior

Behavior of a Lime-Treated Expansive Soil

TESE DE DOUTORADO

Thesis presented to the Programa de Pós-Graduação em Engenharia Civil of the Departamento de Engenharia Civil, PUC-Rio as partial fulfillment of the requirements for the degree of Doutor em Engenharia Civil

Advisor: Michéle Dal Toé Casagrande
Co-advisor: Jorge Gabriel Zornberg

Rio de Janeiro
August 2016



Ingrid Milena Reyes Martinez Belchior

Behavior of a Lime-Treated Expansive Soil

Thesis presented to the Programa de Pós-Graduação em Engenharia Civil of the Departamento de Engenharia Civil do Centro Técnico Científico da PUC-Rio, as partial fulfillment of the requirements for the degree of Doutor.

Profa. Michéle Dal Toé Casagrande

Advisor

Departamento de Engenharia Civil – PUC-Rio

Prof. Jorge Gabriel Zornberg

Co-advisor

Civil, Architectural and Environmental Engineering Department –
University of Texas at Austin

Prof. Euripedes do Amaral Vargas Jr

Departamento de Engenharia Civil – PUC-Rio

Prof. Nilo Cesar Consoli

Departamento de Engenharia Civil – UFRGS

Prof. Roberto Francisco de Azevedo

Departamento de Engenharia Civil – UFV

Prof. Ben-Hur de Albuquerque e Silva

Seção de Engenharia de Fortificação e Construção – IME

Prof. Márcio da Silveira Carvalho

Coordinator of the Centro Técnico Científico da PUC-Rio

Rio de Janeiro, August 1st 2016

All rights reserved.

Ingrid Milena Reyes Martinez Belchior

Graduated in Civil Engineering from University of Nariño (UDENAR), Pasto – Colombia in 2008. She received her master's degree in Civil Engineering at Pontifical Catholic University of Rio de Janeiro (PUC-Rio) in 2012. She was Visiting Graduate Student at the University of Texas at Austin (U.S.) in the Department of Civil, Architectural and Environmental Engineering to conduct part of her Doctoral researches in the Geotechnical Engineering area (March 2015 - February 2016).

Bibliographic Data

Belchior, Ingrid Milena Reyes Martinez

Behavior of a lime-treated expansive soil / Ingrid Milena Reyes Martinez Belchior ; advisor: Michéle Dal Toé Casagrande ; co-advisor: Jorge Gabriel Zornberg – 2016.
191f. : il. ; 30 cm

Tese (Doutorado) – Pontifícia Universidade Católica do Rio de Janeiro, Departamento de Engenharia Civil, 2016.

Inclui bibliografia

1. Engenharia Civil – Teses. 2. Solo expansivo. 3. Potencial de expansão. 4. Tratamento com cal. 5. Ensaio de centrífuga. I. Casagrande, Michéle Dal Toé. II. Zornberg, Jorge Gabriel. III. Pontifícia Universidade Católica do Rio de Janeiro. Departamento de Engenharia Civil. IV. Título.

CDD: 624

To my beloved husband Mairon whose
love and support contributed to this achievement.

Acknowledgement

Certainly, this accomplishment is not only mine. Immeasurable appreciation and deepest gratitude for help and support are extended to the following persons who in one way or another have contributed in making this study possible.

First of all, my deepest acknowledgment goes to my advisor, Professor Michéle Dal Toé Casagrande, for her friendship and enormous support for this study. I am very thankful because she allowed me to be part of the “Casagrande’s academic family”. She constantly motivated me to do an excellent work, afforded me of great opportunities and trusted me since the beginning.

I would like to express my sincere gratitude to my co-advisor Dr. Jorge Zornberg, for giving me the opportunity to work in his lab during my exchange program at the University of Texas at Austin. Certainly, his insightful discussions and constant support during the development of this research were crucial for reaching this important step.

I want to thank my committee members, Prof. Euripedes do Amaral Vargas Jr, Prof. Nilo Cesar Consoli, Prof. Roberto Francisco de Azevedo and Prof. Ben-Hur de Albuquerque e Silva, for their valuable reviews and comments that helped to improve the quality of the final version of this thesis.

I would like to thank all of my friends at PUC-Rio that struggled side by side with me over the past 4 years. A special thanks goes out to Nathalia Passos, Nathalia Louzada, Carla Carrapatoso, Carlos Emmanuel Lautenschläger, Guilherme Righetto, Perlita Esaine, Julia Camargo, Adriano Malko, Giobana Garcia, Eliana Marin, Maria Isabel Ramos, Alexander Mera, Lorena Chamorro, and other friends for the many precious memories along this way.

I would like to thank the staff at the PUC-Rio, including Rita Leite, Amauri Fraga, Edson Silva e Josue Martins, and the IC students Lucas Repsold and Bianca Fernades. To Adriano Malko e Nathalia Louza for helping me with the Micro-CT and to professor Franklin Antunes for his valuable comments.

I would like to thank my lab-mates at the University of Texas for their friendship, help and teachings: Chris Armstrong, Dr. Chunlei Zhang, Gaston Quaglia, Xin Peng, Amr Morsy, Federico Castro Jr., Alejandro Ortiz, Hossein Roodi, Larson Snyder, André Cavalcante, Calvin Blake, Aaron Potkay, Ivan Garcia, Ryan Phillips, José Martinez and Kristen Van Hoosier.

I would like to thank the special friends from Austin-TX, specially to my “Italian sister” Luigia Muto, because her great friendship made me feel like at home, talking for long hours, sharing delicious food and exploring new places. In a

similar manner, I also would like to thank Marieke Baas-deRuijter and Bert-Jan Baas, and the IGSM group, especially to Mary Kim and Maria Villarreal.

A very special thanks from the bottom of my heart to my beloved husband Mairon Belchior. His unconditional love has been my rock of support through my good and difficult moments. He comprehensively understood that I had to stay away during our first year of marriage in order to achieve this goal. This accomplishment would not have been possible without the continuous encouragement, help, care and support that he provides me. I am truly thankful for having you in my live.

I also want to express my very profound gratitude to my parents, Floriberto Reyes and Gloria Martinez, and to my siblings, Monica Reyes and Alexander Reyes, because, even the long distances separating us, their love is always present in my life. A special thanks to my sister Monica for allowing me to share happy moments with my niece Luciana Rodriguez and my nephew Juan Ignacio Rodriguez every weekend by the web cam.

I would like to thank the financial support of National Council for Scientific and Technological Development (CNPq) and Coordination for the Improvement of Higher Level or Education Personnel (CAPES), for providing me scholarships to develop this study in Brazil and abroad.

And above all, thanks God for giving me grace to accept with serenity the things that cannot be changed, courage to change the things which can be changed, and wisdom to distinguish the one from the other.

Abstract

Belchior, Ingrid Milena Reyes Martinez; Casagrande, Michéle Dal Toé (Advisor); Zornberg, Jorge Gabriel (Co-advisor). **Behavior of a Lime-Treated Expansive Soil**. Rio de Janeiro, 2016. 191p. DSc Thesis, – Departamento de Engenharia Civil, Pontifícia Universidade Católica do Rio de Janeiro.

The main objectives of this research are to investigate the effect of hydrated lime (HL) treatment on the swelling behavior of a natural expansive soil, Eagle Ford clay from Texas (USA), and to measure the efficiency of lime treatment on swelling reduction due to variations in the condition of specimen preparation. This study involved conventional free swell tests and centrifuge tests, which are a new technique developed by the University of Texas at Austin (USA). So far, no studies have been performed using this centrifuge to analyze the swelling reduction in expansive soils by stabilization treatments. Also, no studies have measured the improving of lime treatment efficiency due to variables controlled during preparation of lime-soil mixtures (i.e. compaction moisture content, compaction dry density, mellowing and curing time), as well as the applied effective stress. This work also involved investigations about modifications of geotechnical properties, mineralogical composition and microstructural constitution due to the addition of lime. From the analysis of the swelling vs. time curves, three values were defined to examine the swelling behavior: the swelling potential (Sp), the primary swelling slope (PSS) and the secondary swelling slope (SSS). Assessment of the lime treatment efficiency, as quantified by the Swelling Potential Reduction Ratio (SPR) indicates: (i) the elimination of 97% of Sp with 4% HL; (ii) SPR enhancement with increasing curing time; (iii) adverse effect of mellowing periods on the SPR; (iv) the possibility to decrease the necessary lime dosage by increasing the compaction moisture and/or reducing the compaction dry density; and (v) dependency of the hydrated lime dosage to prevent swelling on the applied g-level (i.e. applied stress).

Keywords

Expansive soil; swelling potential; lime treatment; centrifuge test.

Resumo

Belchior, Ingrid Milena Reyes Martinez; Casagrande, Michéle Dal Toé (Advisor); Zornberg, Jorge Gabriel (Co-advisor). **Comportamento de um Solo Expansivo Melhorado com Cal**. Rio de Janeiro, 2016. 191p. Tese de Doutorado – Departamento de Engenharia Civil, Pontifícia Universidade Católica do Rio de Janeiro.

Os principais objetivos desta pesquisa são investigar o efeito da cal hidratada (HL) no comportamento de um solo expansivo, Eagle Ford do Texas (USA), e medir a eficiência do tratamento com cal sobre a redução da expansão através de variações das condições de preparação das amostras. Este estudo envolveu ensaios edométricos e ensaios de centrífuga, que é uma nova técnica desenvolvida pela Universidade do Texas em Austin (EUA). Até o presente trabalho, nenhum estudo tem sido desenvolvido usando esta centrífuga para analisar a redução da expansão em solos expansivos estabilizados. Além disso, nenhum estudo tem medido o melhoramento da eficiência do tratamento com cal devido às variáveis controladas durante a preparação das misturas solo-cal (ou seja, umidade, densidade, período entre a mistura e a compactação e tempo de cura), como também da tensão aplicada. Este trabalho também incluiu investigações sobre modificações das propriedades geotécnicas, composição mineralógica e constituição microestrutural, devido à adição de cal. A partir da análise das curvas de expansão vs. tempo, três valores foram definidos para examinar o comportamento expansivo: o potencial expansivo (S_p) e as inclinações de expansão primária (PSS) e secundária (SSS). A avaliação da eficiência do tratamento com cal, quantificada através do parâmetro “Razão da Redução do Potencial Expansivo” (SPR), indica: (i) eliminação de 97% de S_p com 4% de HL; (ii) melhoramento do SPR pelo aumento do tempo de cura; (iii) efeito adverso na SPR de períodos longos entre mistura e a compactação; (iv) possibilidade de diminuir a dosagem de cal necessária para reduzir a expansão através do aumento da umidade de compactação e/ou redução da densidade seca de compactação; e (v) dependência da dosagem da cal para prevenir a expansão no nível-g.

Palavras-chave

Solo expansivo; potencial de expansão; tratamento com cal; ensaio de centrífuga.

Contents

1 Introduction	24
1.1. Objectives of the Research	28
1.2. Research Organization	29
2 Literature Review	31
2.1. Origin and Distribution of Expansive Soils	31
2.2. Factors of Swelling Behavior	32
2.2.1. Clay Mineralogy	33
2.2.2. Soil Water Chemistry	36
2.2.3. Soil Suction	37
2.2.4. Plasticity	37
2.2.5. Soil Structure and Fabric	39
2.2.6. Moisture Variations and Initial Moisture Conditions	41
2.2.7. Dry Density	42
2.2.8. Stress Conditions	43
2.3. Water Adsorption Mechanism and Swelling	43
2.3.1. Diffuse Double Layer	44
2.3.2. Cation Exchange Capacity (CEC)	45
2.3.3. Inner-Crystalline and Osmotic Swelling	45
2.4. Methods for Classification and Evaluation of Swelling Potential of Expansive Clays	48
2.4.1. Potential Vertical Rise Method	51
2.4.2. Conventional Free Swell Test and Swell Pressure	54
2.4.3. Centrifuge Testing For Evaluation of Swelling Behavior	55
2.5. Treatments to control swelling of expansive clays	60
2.6. Lime Treatment in Expansive Soils	62
2.6.1. Lime Soil Reactions	63
2.6.1.1. Deleterious Chemical Reactions	65
2.6.2. Effect of Mellowing Period on the Lime Treatment	66
2.6.3. Modification of Soil Properties by Lime Addition	68

3 Materials, Methods and Equipment	72
3.1. Materials	73
3.1.1. Expansive Soil	73
3.1.2. Hydrated Lime	74
3.1.3. Soil Preparation	74
3.2. Basic Tests	75
3.2.1. Atterberg Limits	75
3.2.2. Chemical Tests	77
3.2.2.1. pH Test	77
3.2.2.2. Blue Methylene Test	78
3.2.3. Specific Gravity	80
3.2.4. Hydrometer Test	80
3.2.5. Standard Proctor Compaction Tests	81
3.2.6. Unconfined Compressive Strength (UCS) Test	82
3.3. Swelling Potential Tests	83
3.3.1. Conventional Free Swell Test	84
3.3.2. Centrifuge Test	86
3.3.2.1. Centrifuge Set-Up	87
3.3.2.2. Specimen Preparation	88
3.3.2.3. Testing Procedure	90
3.3.2.4. Typical Results	92
3.3.2.5. Measured Variables and Calculated Properties	94
3.4. Mineralogical Test and Microscopic Observations	99
3.4.1. Mineralogical Test Using X-Ray Diffraction (XRD)	99
3.4.2. Microscopic Observations through Environmental Scanning Electron Microscopy (ESEM)	101
3.4.3. X-Ray Computer Micro-Tomography (Micro-CT)	104
4 Experimental Results and Analysis	106
4.1. Basic Tests	107
4.1.1. Atterberg Limits	107
4.1.2. Chemical Evaluation	110
4.1.2.1. pH	110

4.1.2.2. Cation Exchange Capacity (CEC) Evaluation by Blue Methylene Test	112
4.1.3. Specific Gravity	113
4.1.4. Grain Size Distribution Analysis by Hydrometer Test	113
4.1.5. Compaction Analysis	114
4.1.6. Unconfined Compressive Strength (UCS) Analysis	115
4.2. Swelling Potential Reduction Analysis	120
4.2.1. Conventional Free Test Results and Analysis	122
4.2.1.1. Evaluation of Lime Percentage Effect on Swelling Behavior	122
4.2.1.2. Evaluation of Curing Time Effect on Swelling Behavior	129
4.2.1.3. Evaluation of Mellowing Period Effect on Swelling Behavior	134
4.2.2. Centrifuge Test Results and Analysis	138
4.2.2.1. Evaluation of Compaction Moisture Condition Effect on Swelling Behavior	139
4.2.2.2. Evaluation of Compaction Dry Density Effect on Swelling Behavior	148
4.2.2.3. Evaluation of G-Level Effect on Swelling Behavior	153
4.3. Mineralogical and Micro-structural Observations	160
4.3.1. X-Ray Diffraction (XRD) Analysis	160
4.3.2. Environmental Scanning Electron Microscopy (ESEM) Analysis	162
4.3.2.1. Curing and Mellowing Period Effect on Micro-Structural Features	167
4.3.3. Micro-CT Analysis	169
5 Conclusions and Recommendations	174
5.1. Conclusions	174
5.2. Future Works	180
6 References	181

List of Figures

Figure 2.1. Basic structural unit in the silica sheet (Forouzan, 2016)	33
Figure 2.2. Basic structural units in the octahedral sheet (Forouzan, 2016)	34
Figure 2.3. Structure of kaolinite (Forouzan, 2016)	35
Figure 2.4. Structure of smectite / montmorillonite (Forouzan, 2016)	35
Figure 2.5. Structure of illite (Forouzan, 2016)	36
Figure 2.6. Liquid limit of bentonite (W_{LB}) and soil-bentonite mixture (W_{LM}) as function of free swell of bentonite (Mishra <i>et al.</i> , 2011)	38
Figure 2.7. Vertical swell strain with PI for different initial moisture conditions (Puppala <i>et al.</i> , 2014)	38
Figure 2.8. Effect of compaction on soil structure (Lambe, 1958)	39
Figure 2.9. Swelling potential vs. compaction method (Attom <i>et al.</i> , 2001)	40
Figure 2.10. Effect of cycling wetting and drying on the swelling behavior of natural expansive soils (Basma <i>et al.</i> , 1996)	41
Figure 2.11. Relationship between maximum swelling pressure and initial dry density (Komine, 2004)	42
Figure 2.12. Diffuse Double Layer (DDL) of clay minerals (Baser, 2009)	44
Figure 2.13. Inner-crystalline swelling of sodium montmorillonite: layer distances and maximum number of water molecules per sodium ion are showed (Madsen & Müller-Vonmoos, 1989)	47
Figure 2.14. Osmotic swelling representation: C_1 is the ion concentration between clay layers and C_2 is the ion concentration in the pore water.	48
Figure 2.15. Commonly used criteria for swelling potential classification (Yilmaz, 2006)	51
Figure 2.16. Percent volumetric change vs. plasticity index (Armstrong, 2014)	53
Figure 2.17. Load vs. potential vertical rise (PVR) relationship (Armstrong, 2014)	53
Figure 2.18. Schematic of centrifuge swelling test (Plaisted, 2009)	56
Figure 2.19. Comparison between single infiltration centrifuge test and conventional free swell test results (Plaisted, 2009)	57

Figure 2.20. Schematic view of permeameter cup of large centrifuge (Kuhn, 2010)	57
Figure 2.21. Swell vs. Total stress for 10 mm thick specimens with water pressure of 400 psf (19 kPa) (Kuhn, 2010)	58
Figure 2.22. Swell vs. compaction dry unit weight for Eagle Ford clay specimens (Walker, 2012)	59
Figure 2.23. Comparison between double infiltration centrifuge and ASTM D4546-08 (2008) (free swell) curves (Armstrong, 2014)	60
Figure 2.24. Sequence illustrating influence of early lime-clay reactions upon clay particle arrangements and soil structure (Beetham <i>et al.</i> 2014)	64
Figure 2.25. Effect of mellowing duration on strength at different lime additions (Holt & Freer-Hewish, 1998)	67
Figure 2.26. Effect of mellowing duration and temperature on the volume change of lime-treated British soils (Holt <i>et al.</i> , 2000)	68
Figure 2.27. Variation in liquid limit and plastic limit with lime content for an expansive soil (Dash & Hussain, 2011)	69
Figure 2.28. Effect of lime treatment on pore size distribution. Results of mercury intrusion porosimetry (MIP) (Tran <i>et al.</i> , 2014)	69
Figure 2.29. Variation of swell potential with percent lime and curing time. (Nalbantoglu & Tuncer, 2001)	70
Figure 2.30. Effect of lime and curing time on the compression and rebound indices C_c and C_r .(Nalbantoglu & Tuncer, 2001)	71
Figure 3.1. Localization of Eagle Ford Clay excavation	73
Figure 3.2. Determination of pH	77
Figure 3.3. Example of a methylene blue test	79
Figure 3.4. Hydrometer test	81
Figure 3.5. Divided molds and hammer for UCS specimen preparation	82
Figure 3.6. Automated loading system by GeoJac	83
Figure 3.7. Standard consolidation frame used for conventional free swell testing	85
Figure 3.8. Consolidation cell diagram (Zornberg <i>et al.</i> , 2009)	85
Figure 3.9. Compaction specimen procedure	85
Figure 3.10. Consolidation cell assembly	86

Figure 3.11. Damon IEC CRU-5000 centrifuge: external view (left) and internal view (right)	87
Figure 3.12. Data Acquisition System (DAS) components	88
Figure 3.13. Tools set for specimen preparation	89
Figure 3.14. Compaction specimen procedure	90
Figure 3.15. Centrifuge cup preparation and testing assembly.	91
Figure 3.16. Screenshot of <i>LabView</i> program monitoring a centrifuge test (Walker, 2012)	92
Figure 3.17. Typical result from centrifuge test	93
Figure 3.18. Schematic view of soil specimen into the centrifuge	96
Figure 3.19. Schematic representation of the components of an X-ray diffractometer (Ulery, 2008)	100
Figure 3.20. Bruker D8 Advance X-Ray diffractometer	100
Figure 3.21. XRD sample preparation.	101
Figure 3.22. Schematic cross section of an ESEM (Romero and Simms, 2008)	102
Figure 3.23. Environmental Scanning Electron Microscope Philips/FEI XL30 (ESEM). Department of Geological Sciences of the University of Texas at Austin	103
Figure 3.24. ESEM specimen holders (left) and specimen placement into the ESEM (right)	104
Figure 3.25. Zeiss XRadia Versa 510 micro-tomograph (http://lpdipuc.jimdo.com/english/microtomography/zeiss-xradia-versa-510/)	105
Figure 4.1. Atterberg limits variation of Eagle Ford clay with different percentages of hydrated lime	107
Figure 4.2. Liquid limit variation of Eagle Ford clay with different percentages of hydrated lime at different curing time	109
Figure 4.3. Plastic limit variation of Eagle Ford clay with different percentages of hydrated lime at different curing time	109
Figure 4.4. Plastic index of Eagle Ford clay with different percentages of hydrated lime at different curing time	109
Figure 4.5. Casagrande's plasticity chart for natural and	

lime-treated Eagle Ford clay.	110
Figure 4.6. Results of pH tests for lime-treated Eagle Ford clay with different curing times	111
Figure 4.7. Specific gravity variation of Eagle Ford clay with different percentages of hydrated lime	113
Figure 4.8. Grain size distribution measured by hydrometer tests using untreated Eagle Ford clay and lime-treated Eagle Ford clay with 2% and 4% of hydrated lime	114
Figure 4.9. Standard Proctor compaction curves for untreated Eagle Ford clay (0% HL) and expansive soil treated with 4% hydrated lime (4% HL).	115
Figure 4.10. Unconfined Compressive Strength (UCS) of untreated and lime-treated expansive soils at different curing time.	116
Figure 4.11. Unconfined Compressive Strength (UCS) of lime-treated Eagle Ford clay allowed to mellow for 3 and 7 days (M3 and M7, respectively) and without mellowing period (NM)	118
Figure 4.12. Different failure mode in specimens with no mellowing (NM) and with 7 days of mellowing (M7)	119
Figure 4.13. Typical swelling percent vs. log time curve	121
Figure 4.14. Semi-log plot of conventional free swell tests results for lime-treated Eagle Ford clay with lime variation between 0% and 2%.	123
Figure 4.15. Semi-log plot of conventional free swell tests results for lime-treated Eagle Ford clay with lime variation between 2.5% and 4.0%.	123
Figure 4.16. Swelling potential (Sp) and swelling potential reduction ratio (SPR) vs. hydrated lime percentage	125
Figure 4.17. Primary swelling slope (PSS) variation with hydrated lime percentage	126
Figure 4.18. Secondary swelling slope (SSS) variation with hydrated lime percentage	126
Figure 4.19. Relationship between primary and secondary swelling slope at different lime contents	127

Figure 4.20. Semi-log plot of percentage of total swelling potential vs. time for untreated and lime-treated Eagle Ford clay with lime additions between 0% and 2%.	128
Figure 4.21. Semi-log plot of percentage of total swelling potential vs. time for lime-treated soils with lime additions between 2.5% and 4.0%.	128
Figure 4.22. Semi-log plot of conventional free swell test results for lime-treated soil with 1% of hydrated lime at different curing times	130
Figure 4.23. Semi-log plot of conventional free swell test results for lime-treated soil with 2% of hydrated lime at different curing times	131
Figure 4.24. Curing time (days) effect on swelling potential	131
Figure 4.25. Swelling potential reduction ratio (SPR) for different curing times	132
Figure 4.26. Curing time effect on primary swelling slope	133
Figure 4.27. Curing time effect on secondary swelling slope	134
Figure 4.28. Semi-log plot of conventional free swell test results evaluating the effect of mellowing periods	136
Figure 4.29. Semi-log plot of centrifuge test results from specimens with 0% and 0.5% of hydrated lime compacted at different moisture conditions	141
Figure 4.30. Semi-log plot of centrifuge test results from specimens with 1% and 2% of hydrated lime compacted at different moisture conditions	141
Figure 4.31. Semi-log plot of centrifuge test results from specimens with 3% and 4% of hydrated lime compacted at different moisture conditions	142
Figure 4.32. Compaction moisture condition effect on swelling potential for different hydrated lime percentages	143
Figure 4.33. Swelling potential reduction ratio (SPR) at different compaction moisture conditions	144
Figure 4.34. Compaction moisture condition effect on primary swelling slope	146
Figure 4.35. Compaction moisture condition effect on	

secondary swelling slope	147
Figure 4.36. Semi-log plot of centrifuge test results of specimens with 0% and 0.5% of hydrated lime and compacted at 94% and 100% relative compaction (RC)	149
Figure 4.37. Semi-log plot of centrifuge test results of specimens with 1%, 2%, 3% and 4% of hydrated lime and compacted at 94% and 100% relative compaction (RC)	149
Figure 4.38. Relative compaction effect on swelling potential for different hydrated lime percentages	150
Figure 4.39. Relative compaction effect on swelling potential reduction ratio (SPR) for different hydrated lime percentages	151
Figure 4.40. Relative compaction effect on primary swelling slope	152
Figure 4.41. Relative compaction effect on secondary swelling slope	153
Figure 4.42. Semi-log plot of centrifuge test results of untreated Eagle Ford clay specimens subjected to different g-levels.	155
Figure 4.43. Semi-log plot of centrifuge test results at different g-levels for lime-treated soils with 1% and 2% of hydrated lime.	155
Figure 4.44. Relationship between g-level and swelling potential in centrifuge tests of specimens with different percentage of hydrated lime	156
Figure 4.45. g-level effect on swelling potential reduction ratio (SPR) for different hydrated lime percentages	157
Figure 4.46. g-level effect on primary swelling slope	159
Figure 4.47. g-level effect on secondary swelling slope	159
Figure 4.48. X-ray diffractogram of untreated and treated Eagle Ford clay with 3% of hydrated lime	161
Figure 4.49. X-ray diffractogram of lime-treated Eagle Ford clay with 3% of hydrated lime at 0 and 7 days of curing	161
Figure 4.50 X-ray diffractogram of lime-treated Eagle Ford clay with 3% of hydrated lime with no mellowing and 7 days of mellowing period	162
Figure 4.51. ESEM micrograph amplification of 200x of untreated Eagle Ford Clay	163
Figure 4.52. ESEM micrograph amplification of 1000x	

of untreated Eagle Ford Clay	164
Figure 4.53. EDX spectra of untreated Eagle Ford clay	165
Figure 4.54. ESEM micrograph amplification of 200x of Eagle Ford clay treated with 3% of hydrated lime	165
Figure 4.55. ESEM micrograph amplification of 1000x of Eagle Ford clay treated with 3% of hydrated lime	166
Figure 4.56. EDX spectra of Eagle Ford Clay treated with 3% hydrated lime	167
Figure 4.57. ESEM micrograph amplification of 1000x of untreated and lime-treated Eagle Ford clay with 3% of hydrated lime and with 1 and 7 days of curing	168
Figure 4.58. ESEM micrograph amplification of 1000x of lime-treated Eagle Ford clay with 3% of hydrated lime (HL) with no mellowing (NM) and 7 days of mellowing period (7M)	169
Figure 4.59. Micro-CT images taken from untreated Eagle Ford clay specimen	170
Figure 4.60. Micro-CT images taken from lime-treated specimen with 4% HL	170
Figure 4.61. Micro-CT images before and after pre-processing	171
Figure 4.62. Micro-CT images after segmentation depicting pore distribution	172
Figure 4.63. Pore area distribution for untreated and lime-treated Eagle Ford clay	173

List of Tables

Table 2.1. Typical values of CEC for clay minerals (Mitchell & Soga, 1976)	45
Table 2.2. Methods for evaluating swelling potential of expansive clays	49
Table 2.3. Empirical correlations for determining swelling potential	49
Table 2.4. Swelling potential criteria classification	50
Table 3.1. Chemical analysis of hydrated lime (Austin White Lime Company)	74
Table 3.2. Experimental plan of basic tests	75
Table 3.3. Experimental plan of conventional free swell tests	84
Table 3.4. Experimental plan of centrifuge tests	84
Table 3.5. Equations for properties calculation in centrifuge test (Armstrong, 2014)	94
Table 3.6. Experimental plan of mineralogical test and microscopic observations	99
Table 4.1. Atterberg limits results of Eagle Ford clay with different percentages of hydrated lime at different curing times	108
Table 4.2. Blue methylene test results of Eagle Ford clay with different percentages of hydrated lime	112
Table 4.3. Unconfined Compressive Strength (UCS) and Young's modulus of untreated and lime-treated expansive soils at different curing time.	116
Table 4.4. Unconfined Compressive Strength (UCS) data for evaluation of mellowing period effect	118
Table 4.5. Variations of moisture content, void ratio and saturation during conventional free swell tests for evaluating the hydrated lime effect	122
Table 4.6. Swelling potential, SPR, and slopes of primary and secondary swelling of unthread and lime-treated Eagle Ford clay with different hydrated lime percentage.	124

Table 4.7. Variation of Moisture content, Void ratio and saturation during conventional free swell tests for evaluating the curing time effect	129
Table 4.8. Variations of moisture content, void ratio and saturation during conventional free swell tests for evaluating the mellowing period effect	136
Table 4.9. Swelling potential and slopes of primary and secondary swelling of specimens with and without mellowing	137
Table 4.10. Swelling potential reduction ratio (SPR) for different mellowing periods	138
Table 4.11. Variation of moisture content, void ratio and saturation during centrifuge tests for evaluating the compaction moisture effect	140
Table 4.12. Variation of moisture content, void ratio and saturation during centrifuge tests for evaluating the compaction dry density effect	148
Table 4.13. Variation of moisture content, void ratio and saturation during centrifuge tests for evaluating the g-level effect	154
Table 4.14. Swelling potential, SPR values and primary and secondary swelling slopes for untreated and lime-treated Eagle Ford clay subjected at different g-levels in centrifuge test	156

List of Abbreviation

AFNOR	<i>Association Française de Normalisation</i>
ASTM	American Society for Testing and Materials
CAH	Calcium-Aluminate-Hydrates
CSH	Calcium-silicate-hydrates
CEC	Cation Exchange Capacity
DAS	Data Acquisition System
DDL	Diffuse Double Layer
ESEM	Environmental Scanning Electron Microscopy
FS	Free Swell
GSED	Gaseous Secondary Electron Detector
HL	Hydrated Lime
LL	Liquid Limit
LPS	Linear Position Sensor
LVDT	Linear Variable Differential
Micro-CT	Computer Micro-Tomography
MDD	Maximum Dry Density
PFS	Percent of Free Swell
PI	Plastic Index
PL	Plastic Limit
PSS	Primary Swelling Slope
PVC	Percent Volumetric Change
PVR	Potential Vertical Rise
UCS	Unconfined Compressive Strength
SEM	Scanning Electron Microscope
SL	Shrinkage Limit
Sp	Swelling Potential
SPR	Swelling Potential Reduction Ratio
SSS	Secondary Swelling Slope
TGA	Thermo-gravimetric Analysis
TxDOT	Texas Department of Transportation
XRD	X-Ray Diffraction

List of Symbols

Al^{+3}	Aluminum
$Al_2(OH)_6$	Aluminum hydroxide
C	Clay content
C_c	Compression index
C_r	Rebounded index
Ca^{+2}	Calcium
$Ca(OH)_2$	Hydrated high-calcium lime
$CaCl_2$	Calcium chloride
$Ca_3[Si(OH)_6](CO_3)(SO_4) \cdot 12H_2O$	Thaumasite
$Ca_6[Al(OH)_6]_2 \cdot (SO_4)_3$	Ettringite
CaO	Quicklime
DOP	Dry of optimum moisture content
K	Potassium
KCl	Potassium chloride
Li	Lithium
Mg^{+2}	Magnesium
Na	Sodium
NaCl	Sodium chloride
NH_4^+	Ammonium
NaOH	Sodium hydroxide
NASH	Sodium aluminum silicate hydroxide hydrates
NM	Specimen without mellowing period
M3	Specimen mellow for 3 days
M7	Specimen mellow for 7 days
OPT	Optimum moisture content
SiO_4	Silicate
$Si_8Al_4O_{20}(OH)_4nH_2O$	Montmorillonite
$2SiO_2Al_2O_3 \cdot 2H_2O$	Kaolinite
ε_{af}	Failure strain

$\varepsilon_{s,ver}$	Vertical Swell Strain
γ_d	Dry unit weight
ω	Moisture content for PVR method
ω_d	Dry moisture condition for PVR method
ω_a	Moisture average for PVR method
W_n	Natural water content
W_{LB}	Liquid Limit of Bentonite
W_{LM}	Liquid Limit of Soil-Bentonite Mixture
WOP	Wet of optimum moisture content

1 Introduction

Expansive soils typically involve high plastic clays found around the world, which undergo considerable volumetric changes, in terms of swelling or shrinkage, due to changes in moisture content. The swelling of these soils is led by changes in environmental conditions either due to natural causes, such as drought and heavy rains, or from construction issues, such as inadequate drainage of surface water from the structure, leaks in water pipes or sanitary sewer lines.

The volumetric changes undergone by expansive soils have been responsible for significant damages on transportation infrastructure, shallow foundations and lightweight constructions, such as pavements, canals and reservoir linings, retaining walls and single-story buildings. According to Wise & Hudson (1971), the principal forms of swelling soil damages in pavements are unevenness along a stretch of pavement, longitudinal cracks which run parallel to the center line of the pavement, transverse cracking and localized failure of the pavement caused by decrease in strength and bearing capacity.

The annual damage caused by expansive soils costs about \$1 billion in the USA, £150 million in the United Kingdom and billions of dollars all over the world (Das & Sobhan, 2013). In Brazil, there is no clear estimate of the damage caused by expansive soils, but it is known that they are present in many regions, including the South region (states of *Paraná*, *São Paulo* and *Santa Catarina*) and the North East region (states of *Bahia*, *Pernambuco* and *Ceará*) (Ferreira, 2008; Simões *et al.*, 2006). Thus, the development of these regions might be compromised by the potential damages caused by expansive soils.

Extensive studies have attempted to determine the factors that influence the swelling behavior of expansive soils, such as, type and amount of clay minerals, properties of pore fluid, soil density, moisture content, surcharge pressure and temperature (Holtz & Gibbs, 1956; Satyanarayana & Ranganatham, 1969; Gens *et al.*, 1992; Basma *et al.*, 1996; Delage *et al.*, 1998; Du *et al.*, 1999; Shi *et al.*, 2002;

Sivapullaiah, 2005; Arasan *et al.*, 2007; Lin, 2012; Azam *et al.*, 2013; Armstrong, 2014).

Moreover, other studies have focused on the prediction of the swelling behavior in expansive soils (Frydman & Weisberg, 1991; Gadre & Chandrasekaran, 1994; Chiappone, 2004; Zornberg *et al.*, 2009; Kuhn, 2010; Forouzan, 2016). The swelling behavior prediction has been conducted using both direct and indirect methods. The indirect methods include the use of approximate correlations of swelling with index properties. The direct methods are the conventional free swell test and the centrifuge test. The free swell test is a widely applied technique for measuring the swelling potential and it is based on the use of one dimensional consolidometer. Since the free swell test is typically time consuming, the centrifuge technology was developed with the aim to overcome this problem. The centrifuge test for evaluating swelling behavior of expansive soils is a new technique developed at the University of Texas at Austin. This technique allows the testing of multiple specimens simultaneously and the testing time is usually significant less than that required from conventional free swell test. The rotation within the centrifuge imposes a gravitational field across the specimen, accelerating the water flow through the specimen and facilitating full water permeation and, consequently, entering into the microporous structure of the soil. Because of this, the centrifuge also allows measurement in an expedited way by an in-flight data acquisition system (Zornberg *et al.*, 2009). So far, a number of studies have confirmed the capability of this centrifuge test to measure accurately and quickly the expansion of natural soils (Plaisted, 2009; Kuhn, 2010; Walker, 2012; Armstrong, 2014; Das, 2014; Snyder, 2015). However, no studies have been performed using this centrifuge technology to analyze the swelling reduction in expansive soils by stabilization treatments.

Several studies have been conducted to explore techniques and methods to overcome or prevent the damages generated by expansive soils in earthworks (Basma & Tuncer, 1991; Puppala & Musenda, 2000; Petry & Little, 2002; Baser, 2009; Al-Rawas *et al.*, 2012). These methods comprise soil stabilization, soil replacement, compaction control, pre-wetting, moisture control, surcharge loading, mixing with non-swelling soil, and the use of geosynthetics.

Soil stabilization is the most used technique to overcome issues related with problematic soils, such as expansive clays, around the world. In locations without

availability of good aggregates or appropriate soils, the stabilization of available soils, in order to improve the geotechnical properties, is an effective solution. In roads, for instance, the stabilization technique avoids the necessity to borrow granular bases from faraway places from the construction site. Also, in another cases, stabilization can avoid the requirement of deep foundations in soils with poor bearing capacity that usually results in unaffordable cost for low-budget building project.

Among the techniques used to stabilize expansive soils in order to mitigate its swelling behavior, lime addition has been the most common technique due to the low cost of lime and its availability. In fact, some researchers have shown that lime treatment may reduce the swelling potential of expansive soils (Holt *et al.*, 2000; Al-Rawas *et al.*, 2005; Panjaitan, 2014, Schanz & Elsayy, 2015, Nalbantoglu & Tuncer, 2001). For instance, Schanz & Elsayy (2015) concluded that the swelling potential, i.e. ratio between height increase due to wetting to initial height, of an expansive soil reduced from 34.5% to about 26.5% in specimens mixed with 10% of limestone, and from 34.5% to about 1% in specimens with 10% of hydrated lime. Also, Nalbantoglu & Tuncer (2001) found that the swelling potential was drastically reduced from 20% for the untreated specimen to 1.5% when treated with 2% of lime with no curing time.

Even though the lime addition effect on the swelling potential of expansive soils has been well characterized, no studies have been identified that thoroughly address the effect of lime on the mechanism of swelling. Only few studies have been found about the mechanism of swelling in natural expansive soils, such as the research carried out by Sivapullaiah *et al.* (1996), which concluded that the size, shape, type, and amount of the non-clay fraction play significant role in governing the swelling behavior. Das (2014), by using the centrifuge testing on natural expansive soils, found that the secondary swelling increased with the increase in compaction moisture content and compaction dry density, and reduced with increasing gravitational gradient. Also, this study concluded that clays with flocculated structure (compacted dry of optimum) develop rapid primary swelling but less secondary swelling, as compared to clays with a disperse structure (compacted wet of optimum).

Several studies have only reported the swelling potential reduction obtained with certain amount of lime, leaving aside the analysis of the effect of lime

treatment on the expansion process. Furthermore, no studies have measured the improving of lime treatment efficiency due to variables controlled during preparation of lime-soil mixtures (i.e. moisture condition, density condition, mellowing, curing time, etc.).

Thus, the main purposes of this research are to investigate the modification of swelling behavior due to lime treatment, and to measure the efficiency of lime treatment on swelling reduction due to variations of specimen preparation conditions. The modification of swelling behavior due to variations in lime-soil mixtures preparation is studied by analyzing the swelling vs. time curves obtained from both conventional free swell tests and centrifuge tests carried out in the expansive soil Eagle Ford clay. The analysis of these curves was made considering three important values: the primary swelling slope (PSS), the secondary swelling slope (SSS) and the swelling potential (S_p). The PSS provides an idea of the water flow rate into the specimen that generates the most representative percentage of the total swelling. The primary swelling occurs at a faster rate and it develops when the voids are not able to accommodate further swelling clay particle. In this study, the development of primary swelling was attributed to capillarity process. The S_p is the inflection point of the curve and usually represents around 80% to 90% of total swelling potential. The secondary swelling occurs slowly at lower rate, after the swelling potential is reached. The SSS allows predicting long-term swelling and is attributed to a final hydration process at particle scale.

Based on the swelling potential (S_p) values obtained for untreated and lime-treated Eagle Ford clay specimens prepared at different conditions, the parameter designated as Swelling Potential Reduction Ratio (SPR) was introduced to estimate the efficiency of lime treatment on swelling mitigation. The SPR compares the swelling potential of untreated Eagle Ford clay and the swelling potential of lime-treated Eagle Ford clay subjected at different parametric variations.

This study also includes investigations about modifications of geotechnical properties undergone by the expansive soil Eagle Ford clay due to lime addition, based on basic test such as, Atterberg limits, pH and Cation Exchange Capacity (CEC) test, specific gravity, particle size by hydrometer test, standard Proctor compaction and Unconfined Compressive Strength (UCS). Finally, mineralogical test (X-Ray Diffraction - XRD) and micro-structural observations (via Environmental Scanning Electron Microscopy – ESEM and X-Ray Computer

Micro-Tomography – Micro-CT) were carried out in order to support and complete this study.

1.1. Objectives of the Research

The main objectives of this research are (i) to investigate the combined effect of hydrated lime addition with different specimen preparation conditions, such as curing time, mellowing periods, compaction moisture content, compaction dry density and effective stress on the swelling behavior in the natural expansive soil Eagle Ford clay and (ii) to estimate the swelling potential reduction due to these conditions in order to formulate recommendations to achieve greater lime treatment efficiency in reduction of swelling behavior.

From these overall objectives, the following specific objectives were established:

1. To evaluate the common geotechnical and physicochemical characteristics of the untreated and lime-treated Eagle Ford clay, including soil classification, basic tests, such as, Atterberg limits, specific gravity, particle size distribution, Unconfined Compressive Strength (UCS), moisture-density relationship by standard Proctor effort, pH and Cation Exchange Capacity (CEC);
2. To investigate the effect of lime percentage, mellowing period and curing time on the swelling behavior through conventional free swell tests;
3. To investigate the effect of compaction moisture, compaction dry density and effective stress on the swelling behavior through centrifuge tests;
4. To analyze the time vs. swelling curves obtained from both conventional free swell test and centrifuge test in order to identify the effect of lime addition on swelling potential and slopes of primary and secondary swelling;
5. To estimate the efficiency of lime treatment on swelling mitigation by comparing the swelling potential of the untreated Eagle Ford clay with

the swelling potential obtained from lime-treated Eagle Ford clay specimens prepared at different conditions.

6. To conduct X-Ray Diffraction (XRD), Environmental Scanning Electron Microscopy (ESEM) and X-Ray Computer Micro-Tomography (Micro-CT) tests to observe the mineralogical and micro-structural changes of the expansive soil subjected to lime addition.

1.2. Research Organization

A comprehensive literature review was carried out and summarized in Chapter 2, which aims to obtain a state of art about the geotechnical problems generated by expansive soils, the origin and composition of this type of soils and the current methods for evaluating and predicting the swelling potential. After the description of expansive soils, the literature review comprises the description of lime treatment, the main reactions that take place between soil minerals and lime, and principal modifications of soil properties due to lime addition.

Chapter 3 describes the materials, methods and equipments used in this study. The materials include Eagle Ford clay and hydrated lime. This chapter also contains the description of basic tests (Atterberg limits, specific gravity, particle size distribution, Unconfined Compressive Strength, moisture-density relationship by standard Proctor effort, pH and Cation Exchange Capacity), swelling potential tests (conventional free swell and centrifuge test), mineralogical test using X-Ray Diffraction, and micro-structural observations employing ESEM and Micro-CT carried out on untreated and lime-treated soils.

Chapter 4 includes the results obtained from the performed experimental tests and the interpretation and analysis of these data. The main properties modifications undergone by Eagle Ford clay due to lime addition are explained. The changes in swelling behavior are analyzed detailing the swelling vs. log-time curves considering the effect of lime on swelling potential and on the slopes of primary and secondary swelling. Also, a parameter called Swelling Potential Reduction Ratio (SPR) was introduced to estimate the efficiency of lime treatment on swelling mitigation. This chapter finalizes with the study of lime treatment influence on soil

mineralogy and micro-structural composition in order to support and complete this analysis.

Chapter 5 provides the main conclusions and contributions derived from this study, the recommendations to improve the lime addition efficiency on mitigation of expansive behavior and the future research works needed to complement this study.

2 Literature Review

Accomplishing the objectives of this research requires a good understanding of the general characteristics of expansive soils and important aspects about lime treatment for swelling reduction. This chapter begins with a brief description about the origin of expansive soils and factors that influence the expansive behavior of this type of soils. Afterwards, the mechanisms of swelling and methods for classification and evaluation of swelling potential of expansive clays are reported. This literature review finalizes with a brief state of art about lime treatment for expansive soils, including description of the lime effect on the principal properties of this type of soils.

2.1. Origin and Distribution of Expansive Soils

Expansive soils are originated from a complex combination of geological processes and diagenetic conditions that conduct the formation of clay minerals susceptible to volumetric changes with moisture variations. According to Chen (1975), these processes and conditions depend on the composition of the parent material and the degree of chemical and physical weathering that the parent material has been exposed into its environment. Donaldson (1969) cited by Chen (1975) classified the parent materials associated with expansive soils in two groups: the first group includes basic igneous rocks with comparatively low silica portions (45% to 52%), such as pyroxenes, amphiboles, olivine and biotite. The second group is composed of sedimentary rocks that contain montmorillonites as a constituent of shale and claystone, along with magnesium rich limestone and marl.

The diagenesis of expansive soils is strongly influenced by the weathering process of the parent material. The physical weathering processes include the degradation of the parent material, expansion due to unloading, crystal growth, thermal expansion and contraction, organic activity, and colloidal plucking. The chemical weathering processes include hydration, hydrolysis, oxidation and

carbonation. Favorable environments for expansive soil formation should be alkaline, with absence of leaching, and with presence of ferromagnesium minerals in the parent material.

The expansive soils are particularly located in arid and semi-arid regions with tropical and temperate climate zones. In these regions, evapotranspiration exceeds the precipitation. Potentially expansive soils can be found anywhere in the world. Chen (1975) summarized the countries in which expansive soils have been reported as follows: Argentina, Australia, Brazil, Canada, Cuba, Ethiopia, Ghana, India, Israel, Iran, Mexico, Morocco, South Africa, Spain, Turkey, U.S.A and Venezuela. In Brazil, expansive soils have been reported in South, Center South, and North East regions; especially in the states of *Pernambuco, Bahia, Ceará, São Paulo, Santa Catarina e Paraná* (Simões *et al.*, 2006; Ferreira, 2008).

2.2. Factors of Swelling Behavior

Changes in the soil water system disturb the internal stress equilibrium and cause expansion. According to Nelson & Miller (1992), clay particles generally are platelets with negative electrical charges on their surface and positively charged edges. The negative charges are balanced by cations in the soil water that become attached to the surfaces of the platelets by electrical forces. The electrical inter-particle force field is a function of both the negative surface charges and the electrochemistry of the soil water. The internal electrochemical force system must be in equilibrium with the externally applied stresses and capillary tension in the soil water. If the resulting change in internal forces is not balanced by a corresponding change in the externally applied state of stress, then expansion takes place and the particle spacing will change so as to adjust the inter-particle forces until equilibrium is reached.

Multiple factors influence the mechanism of swelling of expansive clays. These factors can be intrinsic such as, clay mineralogy, soil water chemistry, soil suction, plasticity, soil structure and fabric and dry density; and extrinsic factors such as, moisture variations and stress conditions. Each of these factors is briefly described below.

2.2.1. Clay Mineralogy

Different kinds of clay minerals exhibit different variations in the electrical field and thus, different swelling potentials. The swelling potential of an entire soil mass depends on the portion and type of clay minerals existent in the soil. In order to facilitate the structural analysis and only for engineering purposes, the clay minerals have been classified in three important structural groups: kaolinite, smectite and illite. Kaolinite is generally non-expansive, whereas illite (vermiculites) and smectite (includes montmorillonite) are expansive (Mitchell & Soga, 2005).

The main structural units of clay minerals are two fundamental crystal sheets, the silica and alumina sheets. Variety of combinations and arrangements of these blocks constitute various clay minerals. The silica sheet is a combination of tetrahedral units that consists of a single silicon atom and four oxygen atoms enclosing it (Figure 2.1). On the other hand, the alumina sheet results from combination of octahedral units that possess six oxygen or hydroxyls surrounding aluminum, magnesium, iron, or other atom (Figure 2.2).

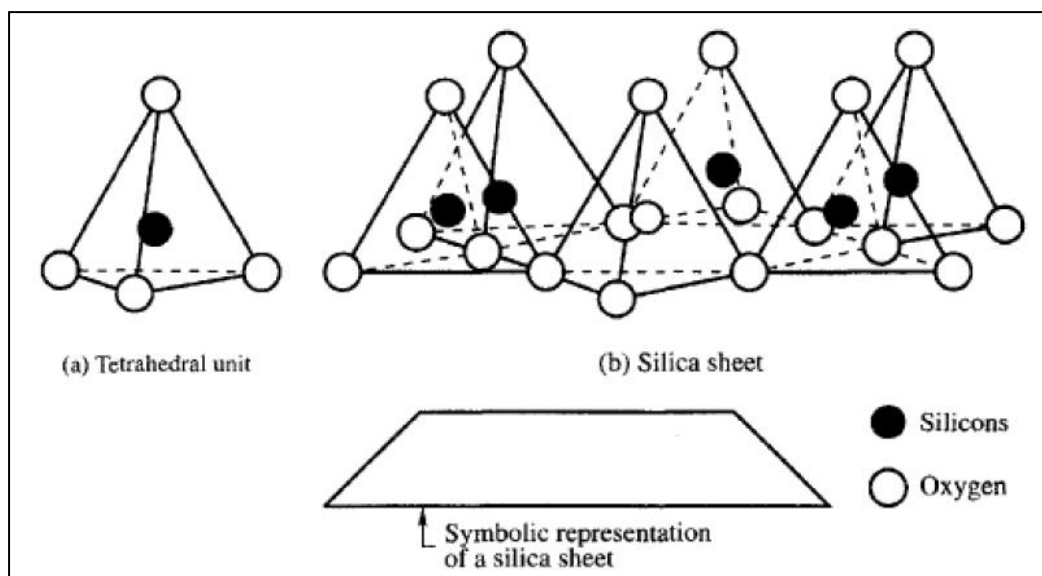


Figure 2.1. Basic structural unit in the silica sheet (Forouzan, 2016)

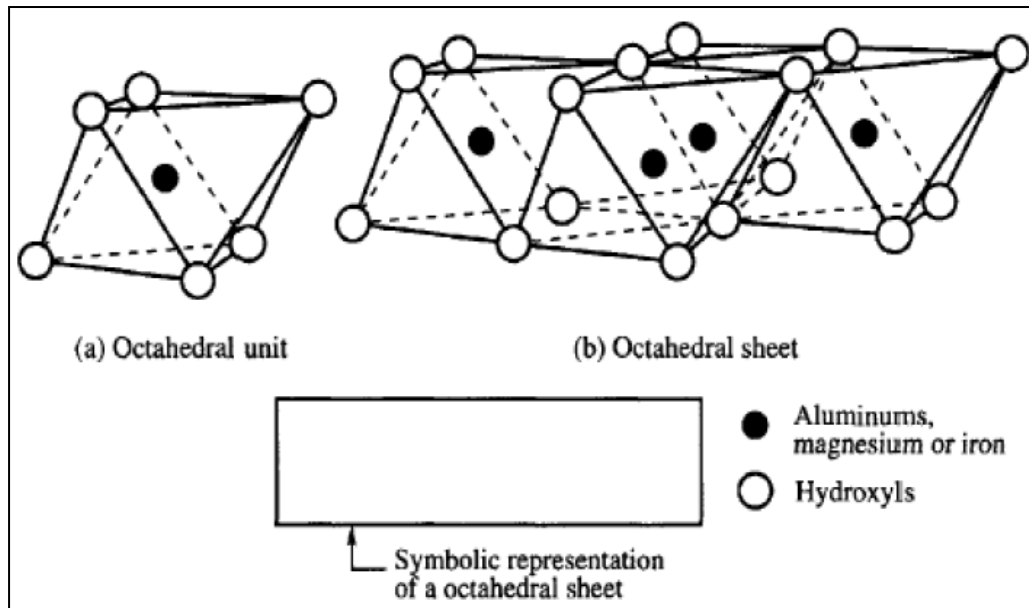


Figure 2.2. Basic structural units in the octahedral sheet (Forouzan, 2016)

According to Mitchell & Soga (2005), atoms are assembled into tetrahedral and octahedral units, followed by the formation of sheets and their stacking to form layers that combine to produce the different clay mineral groups. These minerals are identified using the nomenclature 1:1 and 2:1, that represents the number of tetrahedral layers of SiO_4 and octahedral layers of $\text{Al}_2(\text{OH})_6$, respectively.

Kaolinite is a soft, earthy and usually white mineral, with the chemical composition $2\text{SiO}_2\text{Al}_2\text{O}_3\cdot 2\text{H}_2\text{O}$ is generated from the chemical weathering of aluminum silicate minerals like feldspar. As described by Holtz & Kovacs (1981) and shown in Figure 2.3, kaolinite consists basically of repeating layers of one tetrahedral (silica) sheet and one octahedral (alumina or gibbsite) sheet. Because of the staking of one layer of each basic sheet, kaolinite is called a 1:1 clay mineral. According to Mitchell & Soga (2005), in kaolinite there is no swelling in the presence of water because of sufficient bonding between layers that avoids interlayer swelling.

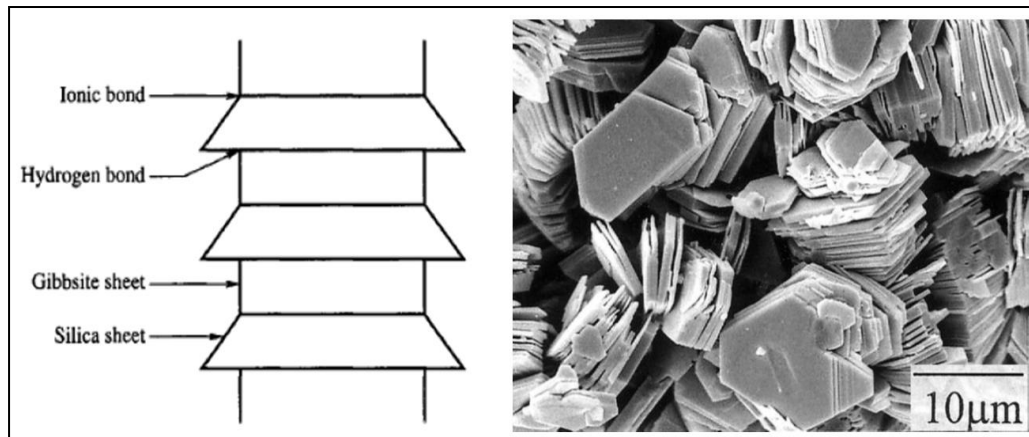


Figure 2.3. Structure of kaolinite (Forouzan, 2016)

The smectite group is composed of two silica sheets and one alumina (gibbsite) sheet, thus, smectite is called 2:1 mineral (Figure 2.4). The main mineral of this group is montmorillonite, which the chemical composition is $\text{Si}_8\text{Al}_4\text{O}_{20}(\text{OH})_4\text{nH}_2\text{O}$. The smectites can expand when they come into contact with water because of the weak bonds, which are prone to break when any polar cationic fluid, such as water, penetrates between structural sheets.

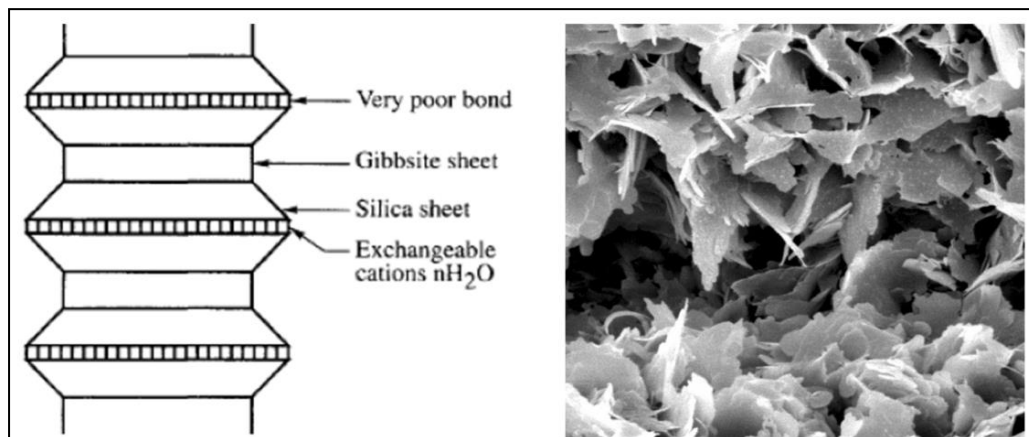


Figure 2.4. Structure of smectite / montmorillonite (Forouzan, 2016)

The illite group also has a 2:1 structure similar to montmorillonite, but the inter-layers are bonded together with non-exchangeable potassium cations (Figure 2.5). In comparison with hydrogen bonds, these bonds are weaker. It results in less swelling potential than smectite minerals.

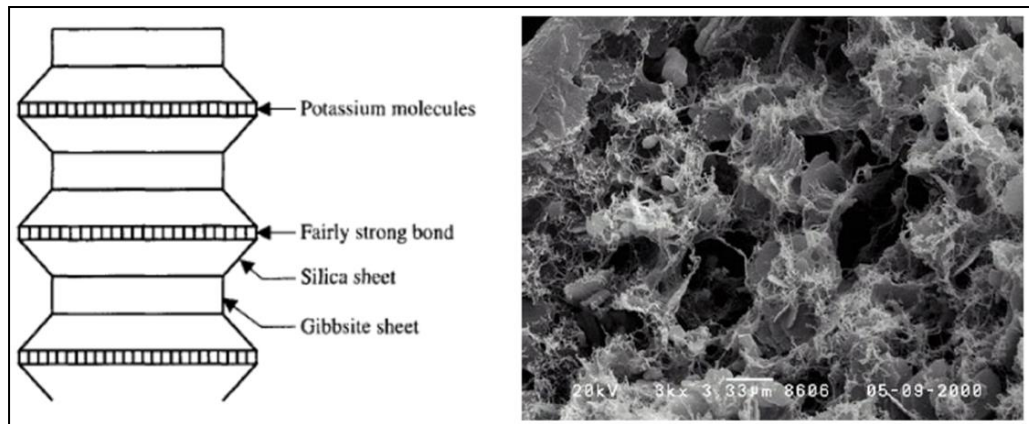


Figure 2.5. Structure of illite (Forouzan, 2016)

The 2:1 clay minerals bond their structure by Van der Waals' forces, which are weak fluctuating dipole bonds. Due to the weak Van der Waals' bonding the layers of silica and alumina are very susceptible to water infiltration (Soga & Mitchell, 2005). The 1:1 clay minerals bond their structure by a hydrogen bond. This hydrogen bond is much stronger than the Van der Waals' forces thus, kaolinite is less susceptible to water infiltration.

2.2.2. Soil Water Chemistry

Salt cations, such as sodium, calcium, magnesium and potassium, are dissolved in the soil water and are adsorbed on the clay surfaces as exchangeable cations to balance the negative electrical surface charges. Hydrations of these cations and adsorptive forces exerted by the clay crystal themselves can cause the accumulation of a large amount of water between the clay particles (Nelson & Miller, 1992).

Montes-H (2005), through the study of swelling behavior of a bentonite (MX80) saturated with Na-solution and Ca-solution, reported that the swelling potential is governed by the nature of the interlayers cations. The results showed an excellent capacity of swelling in the bentonite saturated with Na-solution, while the Ca-saturated bentonite swelled significantly less. Di Maio (1996) investigated volume changes of bentonite exposed to NaCl, KCl or CaCl₂ solutions, and observed decreasing of large swelling potential. Similarly, Arasan *et al.* (2007) reported that the swelling pressure decreased when the concentration of salt

solutions increased for high plasticity clays. Moreover, Sivapullaiah (2005) indicated that NaOH solution caused to formation of new swelling type of compounds (i.e., sodium aluminum silicate hydroxide hydrates – NASH) and these new compounds increased the swelling of clay.

2.2.3. Soil Suction

Soil suction is an influent parameter which is an independent effective stress variable. In unsaturated soils, soil suction is represented by the negative pore pressure. Soil suction is related to gravity, surface tension, pore size and shape, saturation, electrical and chemical characteristics of the soil particles and moisture.

The water retention properties of compacted unsaturated clay (FoCa7 clay) were determined by Delage *et al.* (1998). Results plotted in a void ratio vs. logarithm suction diagram showed fairly linear and reversible behavior at all suctions smaller than the initial one (113 kPa). A constant volume of air equal to the initial value was observed, showing that total volume changes were equal to the volume of exchanged water

It has been observed that soil-water retention curves present hysteretic behavior, which means that different moisture changes under varying suctions must be expected when samples are subjected to drying or wetting paths. Gens & Alonso (1992) showed that expansive soils submitted to suction changes had an approximately elasto-plastic response: whereas the first application of a low suction never previously supported by the sample induced large irrecoverable swelling strains, subsequent suction cycles in the same range induced approximately reversible cyclic strains.

2.2.4. Plasticity

There is a general agreement about that greater swelling potential is related with high plastic index and higher liquid limit. It has been reported a linear relationship between the liquid limit and free swell (Al-Zoubi, 2008; Mishra *et al.*, 2011) (Figure 2.6). Since both liquid limit and swelling depend on the net particle repulsive force between clay particles, thereby this linear relationship was expected.

Puppala *et al.* (2014) studied the volume change behaviors of five different types of expansive soils from Texas (U.S) and found clear relationship between vertical swell strain (i.e. swelling potential) and plastic index (Figure 2.7).

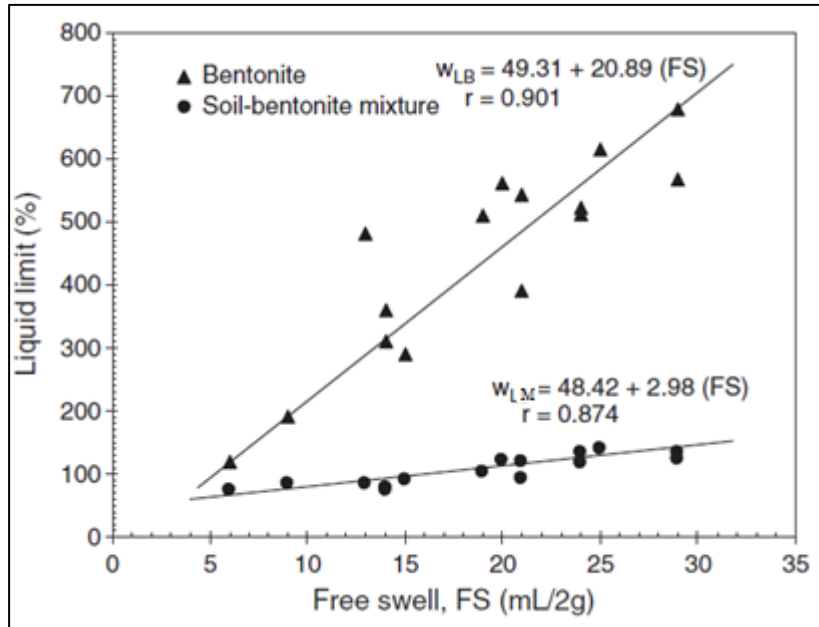


Figure 2.6. Liquid limit of bentonite (W_{LB}) and soil-bentonite mixture (W_{LM}) as function of free swell of bentonite (Mishra *et al.*, 2011)

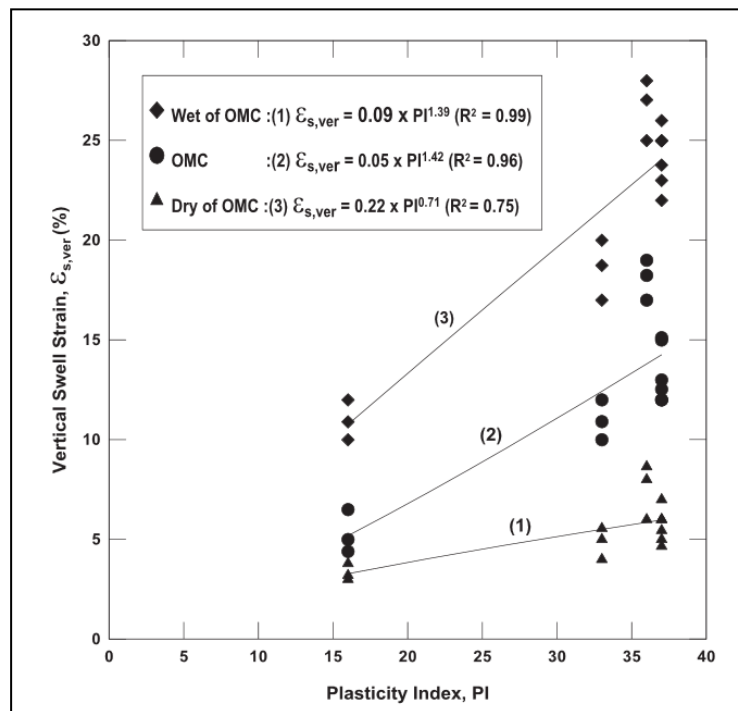


Figure 2.7. Vertical swell strain with PI for different initial moisture conditions (Puppala *et al.*, 2014)

There are many correlations between plasticity properties and swelling potential described in the literature and based on experimental observations. Some of these correlations will be summarized later in section 2.4. Furthermore, methods to estimate the swelling potential of expansive soils based on plasticity properties have been proposed, such as the Potential Vertical Rise (PVR) method. This method was developed by the Texas Department of Transportation (TxDOT) and will be detailed in section 2.4.1.

2.2.5. Soil Structure and Fabric

Fabric and structure of clay change because of compaction at high water content or remolding. Lambe (1958) considered the microstructure of soil specimens compacted on the dry side of the compaction curve as flocculated: soil particles are typically configured in face to face and edge to face contacts which allow the development of soil swelling. The rearrangement of particles on the wet side of the compaction curve, instead, comes out in a more regular configuration, with only face to face contacts, but in a disperse manner, as reported in Figure 2.8. Furthermore, kneading compaction can cause dispersed structures with lower swelling potential than soils which are compacted statically with lower water contents.

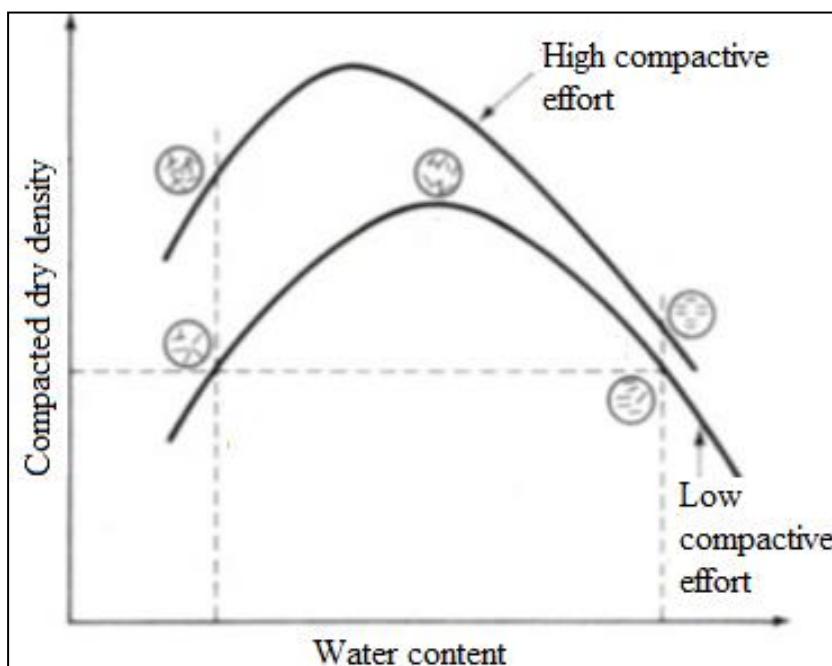


Figure 2.8. Effect of compaction on soil structure (Lambe, 1958)

Armstrong (2014) carried out centrifuge tests in order to study the effect of fabric on the swelling of highly plastic clay, and concluded that samples with a flocculated structure swell more rapidly and have less secondary swelling than those samples with a disperse structure for tests at the same initial moisture content.

Attom *et al.* (2001) observed the effect of soil sample preparation on swelling behavior. It was compared the swelling potential obtained in undisturbed samples against the swelling potential of samples compacted by applying a vertical static load, compacted by kneading with a pneumatic compactor, and compacted dynamically via the standard Proctor test. The results identified that undisturbed sample showed the highest amount of swelling for all three soils as the same prepared moisture content and density for the compacted tests based upon the undisturbed samples (Figure 2.9). Moreover, the type of compaction had a significant influence on the swelling; since the densities were the same, the difference in the swell can be explained by the difference in the fabric of the clays based on their microstructures. As the undisturbed sample had a significant amount of time to sediment and form, thixotropy could have caused the micro-pores to begin at a much smaller value, leading to an increased amount of swell. Thus, re-compacted specimens may not accurately depict the conditions in the field to determine the vertical strain of a soil.

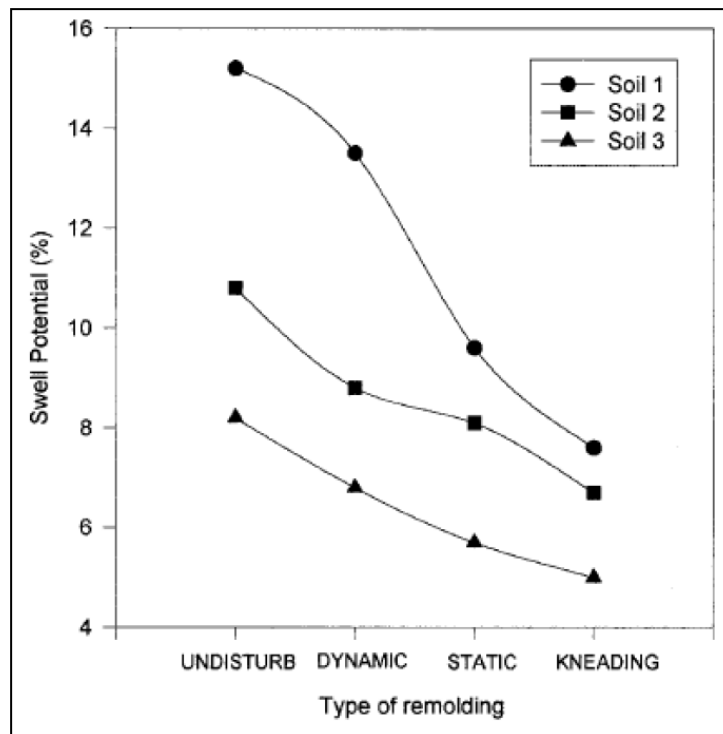


Figure 2.9. Swelling potential vs. compaction method (Attom *et al.*, 2001)

2.2.6. Moisture Variations and Initial Moisture Conditions

The moisture variations are due to climatic cycles and alterations of drainage conditions. The initial moisture content of expansive soils controls the amount of swelling of both undisturbed and remolded samples. According to Chen (1975), very dry clays with natural moisture content below 15 percent usually indicate danger. Such clays can easily absorb moisture to as high as 35 percent with resultant damaging expansion to structures. Conversely, clays with moisture contents above 30 percent indicate that most of the expansion has already taken place and further expansion will be small.

A desiccated expansive soil has higher affinity for water, or higher suction, than the same soil at higher water content, lower suction. Conversely, a wet soil profile will lose water more readily on exposure to drying influences, and shrink more than a relatively dry initial profile (Nelson & Miller, 1992).

Furthermore, several researchers have also studied the influence of cycling wetting and drying on the swelling behavior of natural expansive soils (Osipov & Rumjantseva, 1987; Alonso *et al.*, 2005). Some studies have reported that swelling potential decreases when expansive soil is repeatedly subject to swell then allowed to dry their initial water content (i.e. partial shrinkage) (Al-Homoud *et al.*, 1995; Basma *et al.*, 1996) whereas, other studies have found out that swelling potential increase after first cycle when the expansive soil is allowed to fully desiccate to the shrinkage limit (i.e. full shrinkage) (Osipov & Rumjantseva, 1987) (Figure 2.10).

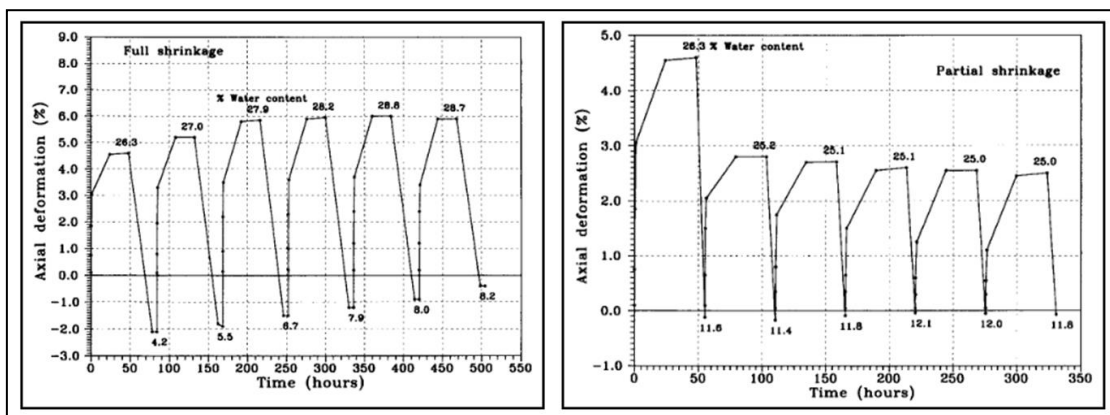


Figure 2.10. Effect of cycling wetting and drying on the swelling behavior of natural expansive soils (Basma *et al.*, 1996)

2.2.7. Dry Density

The initial void ratio of expansive soils influences the volume changes associated with the adsorption and desorption of water. It has been reported that specimens compacted at a lower density undergo less total axial strain when following a wetting path. This behavior was attributed to inefficient translation of interlayer swelling to bulk swelling for loosely compacted specimens. The interlayer volume changes that take place on the particle scale are internally adsorbed by the larger scale pores. Conversely, denser specimens have more efficient translation from particle-scale swelling to bulk-scale swelling because the interlayer volume changes cannot accommodate into the internal pores.

Villar & Lloret (2008) carried out swelling test with compacted bentonite and the results suggested an exponential relationship between swelling pressure and final dry density. In this case, final dry density was reported slightly different from the dry density to which samples were initially compacted, due to the small deformations allowed by the used equipment. The same trend was reported by Komine (2004) in the study about swelling characteristics of four kinds of bentonites, as shown in Figure 2.11.

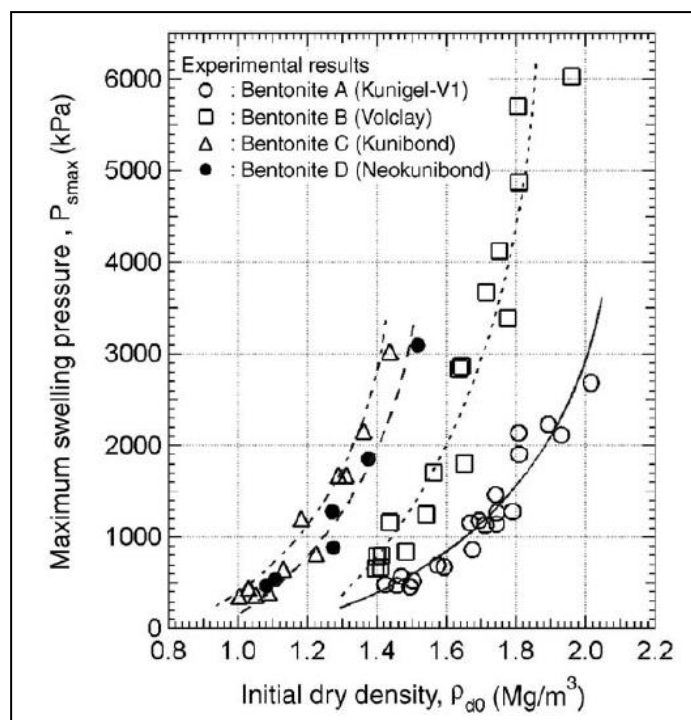


Figure 2.11. Relationship between maximum swelling pressure and initial dry density (Komine, 2004)

2.2.8. Stress Conditions

Volume change is directly related to change in the state of stress in the soil. A reduction in total stress due to excavation of overlying material will result in rebounding and heaving of the surface. Heaving in unsaturated soils is accompanied by imbibitions of water and is time dependent (Nelson & Miller, 1992).

The magnitude of surcharge load specifies the quantity of volume change that will occur for special moisture content and density. Exerted external load acts to reduce expansion and balance inter-particle repulsive forces.

An over-consolidated soil might expand more than the same soil which is consolidated normally at the same void ratio. The pressure caused through soil swelling increases in aging of compacted clays, but swelling degree is not affected under light loading by aging.

2.3. Water Adsorption Mechanism and Swelling

Three micro-scale mechanisms for water adsorption are important in expansive soil behavior: hydration, capillarity, and osmosis. Of these, hydration and osmosis play an important role in the two main clay swelling processes: inner-crystalline and osmotic swelling (Wayllace, 2008).

Hydration of clay mineral surface results of attractive forces developed on the negatively charged clay particle and interlayer surfaces due to hydrogen bonding, charged surface-dipole attraction, or a combination of both (Mitchell, 1976). Water molecules may form hydrogen bonds with exposed oxygens or hydroxyls on tetrahedral layer surfaces. Cation hydration, results in an increase of the ionic radii of the cation, an increase of the interlayer pore space, and an overall volume change of the soil mass. The hydration mechanisms in soils is associated with the particle surfaces rather than the particle fabric, thus water adsorption is relative unaffected by disturbance as compaction.

Capillarity results from the curvature of air-water interfaces within the porous soil fabric. Water adsorption driven by capillarity depends largely on the geometric features of the larger scale inter-particle pore space and thus is sensitive to disturbance associated with compaction. Capillarity may be defined in terms of

matric suction, and depends on the surface tension of the pore fluid, the degree of saturation, and capillary radius. As saturation increases, the pore-water menisci are enlarged and matric suction decreases (Wayllace, 2008).

Osmotic water adsorption is due to concentration differences of dissolved ions between the interlayer pore water and the free water. Depending on the ionic concentration, the type of exchangeable ion (e.g., Ca vs. Na), pH of the pore water, and clay mineralogy, the osmotic water adsorption will take place. Corresponding osmotic swelling results from the balance of attractive and repulsive forces that develop between overlapping electrical double layers.

2.3.1. Diffuse Double Layer

The diffuse double layer (DDL) is formed by the negatively charged clay particle surface and the concentration of positive ions in solution adjacent to the clay particle. Overlapping DDLs between clay particles generates inter-particle repulsive forces or micro-scale “swelling pressures”. Therefore, interaction of the DDL and, hence swelling potential, is related to the increasing in thick of DDL (Baser, 2009).

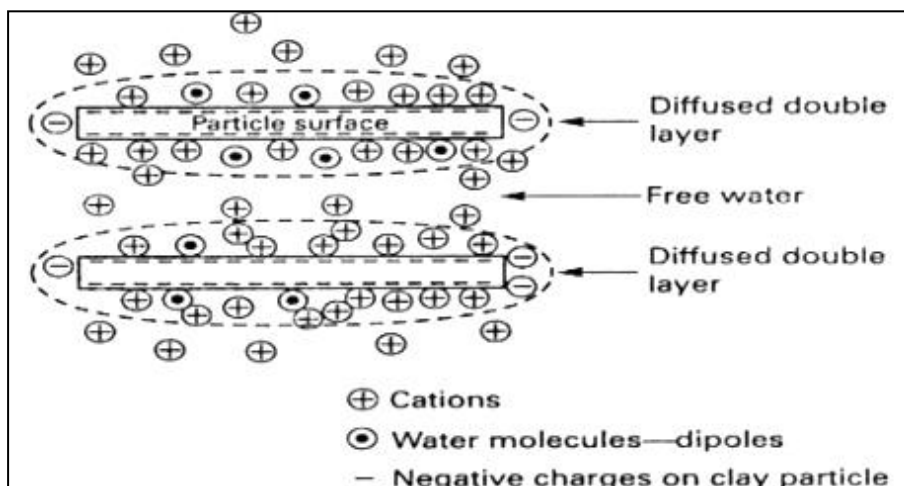


Figure 2.12. Diffuse Double Layer (DDL) of clay minerals (Baser, 2009)

The lower valences of cations results in increase in DDL thickness. Thus, for the same soil mineralogy, more swelling would occur in a sample having

exchangeable sodium cations (Na^+) than in a sample with calcium (Ca^{+2}) or magnesium (Mg^{+2}) cations (Nelson & Miller, 1992).

The high concentration of cations near the surface of clay particle creates a repulsive force between the diffuse double layer system (Chen, 1975). In general, a thicker DDL and greater swelling are associated with lower cation concentrations (Mitchell & Soga, 2005).

2.3.2. Cation Exchange Capacity (CEC)

Cations that neutralize the negative charge net around the surface of soil particles in water are readily exchangeable with other cations. The exchange reaction depends mainly on the relative concentrations of cations in the water and also on the electrovalence of cations. The Cation Exchange Capacity (CEC) is the quantity of exchangeable cations required to balance the negative charge on the surface of the clay particles. CEC is expressed in milliequivalents per 100 grams of dry clay (Nelson & Miller, 1992). Typical values of the CEC for different clay minerals are given in Table 2.1.

Table 2.1. Typical values of CEC for clay minerals (Mitchell & Soga, 1976)

Mineral	Cation Exchange Capacity (CEC) (meq/100g)
Kaolinite	3-15
Illite	10-40
Montmorillonite	80-150

2.3.3. Inner-Crystalline and Osmotic Swelling

The swelling of clays is result of the layer structure of the clay minerals and of the cations adsorbed for the charge equilibrium. Thus, two categories of swelling were described by Madsen & Müller-Vonmoos (1989): inner-crystalline swelling and osmotic swelling. The inner-crystalline swelling is caused by the hydration of the exchangeable cations of the dry clay, whereas the osmotic swelling results from the large difference in the ion concentrations close to the clay surfaces and in the pore water.

In the fully dry montmorillonite, the exchangeable interlayer cations are located on the surface of the layers or in the hexagonal holes of the tetrahedral

sheets. Thus, the montmorillonite layers lie so close together that they are almost in contact. The negatively charged layers are held together very strongly by the interlayer cations and the Van der Waals attraction at this small distance. The cations hydrate upon contact with water and order themselves on a plane halfway between the clay layers. This leads to widening of the spacing between the layers. The volume of montmorillonite can double in the process of inner-crystalline swelling (Figure 2.13). Inner-crystalline swelling can be reduced through the intercalation of organic compounds. The organic cation replaces another ion in the interlayer space and the carbohydrate chain makes the surface hydrophobic (Madsen & Müller-Vonmoos, 1989).

Unlike inner-crystalline swelling, which acts over small distances (up to 1nm), osmotic swelling, which is based on the repulsion between electric double layers, can act over much larger distances. The driving force for the osmotic swelling is the large difference in concentration between the ions electrostatically held close to the clay surface and the ions in the pore water of the soil (Figure 2.14 (a)).

Irregularities in the crystal lattice are manifested by an excess negative charge, which must be compensated by positive ions close to the surface of the clay. The concentration of positive ions close to the surface is thus extremely high, while that of negative ions is very small. The positive ion concentration decreases with increasing distance from the surface, whereas the concentration of negative ions increases. The negatively charged clay surface and the cloud of ions form the diffuse electric double layer.

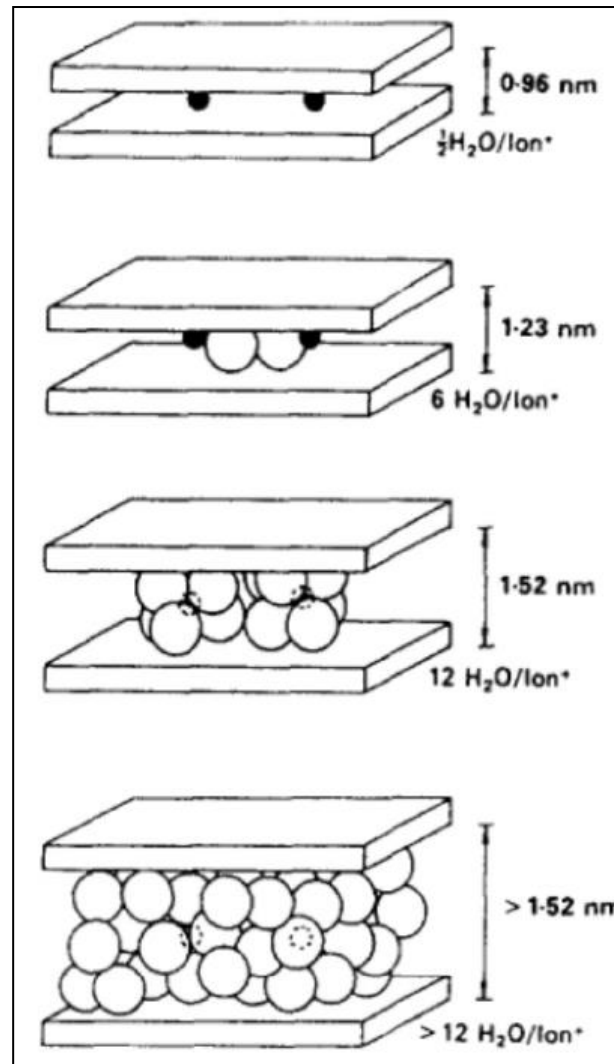


Figure 2.13. Inner-crystalline swelling of sodium montmorillonite: layer distances and maximum number of water molecules per sodium ion are showed (Madsen & Müller-Vonmoos, 1989)

High negative potential exists directly at the surface of the clay layer. The value of this potential is reduced with increasing distance from the surface and reaches zero in the pore water. When two such negative potential fields overlap, they repel each other, and cause the swelling in clay. The profile of the potential curves, and therefore the repulsion at a given distance, vary with the valence and the radius of the ions contained in the double layer and with the concentration of electrolytes in the pore water.

The osmotic swelling can be prevented, in laboratory as well as in field scale, by the application of a counter-pressure. Usually, the maximum pressure necessary to prevent any volume increase is referred to as swelling pressure (Figure 2.14 (b) and (c)).

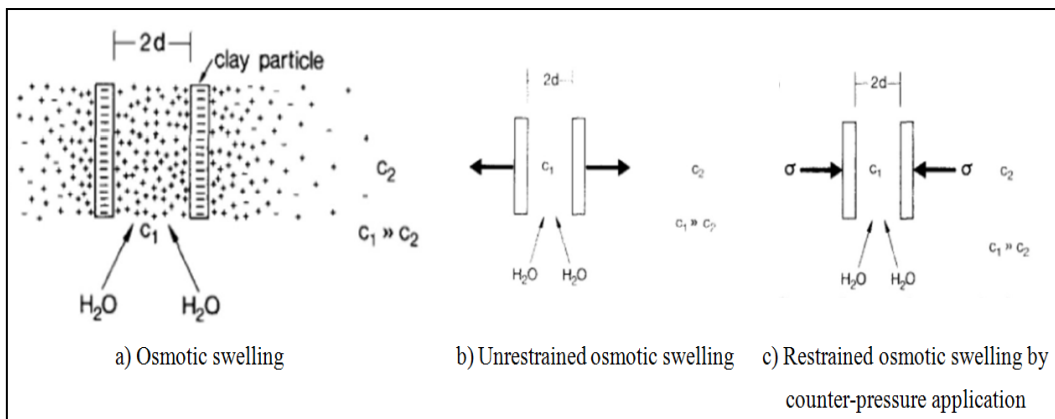


Figure 2.14. Osmotic swelling representation: C_1 is the ion concentration between clay layers and C_2 is the ion concentration in the pore water.

2.4. Methods for Classification and Evaluation of Swelling Potential of Expansive Clays

Early recognition of soil of expansive soils, during exploration and preliminary stages of a project, is essential for designing appropriate foundation. This section discusses test and classification procedures that have been used to identify expansion or swelling potential.

The identification and evaluation of expansive clays can be made by indirect and direct methods. Indirect methods include the mineralogical identification, index properties, consistence limits or parameters related with texture and soil composition. On the other hand, direct methods are based on measurements of induced expansion and pressure needed to avoid expansion. Table 2.2 summarizes some of these methods.

Numerous empirical correlations for indirect swelling potential estimation have been reported in the literature. These correlations are based on index properties (liquid limit, plastic index, shrinkage index, clay content, etc.) and placement conditions (initial dry unit weight, initial water content and sub-charge pressure). Some empirical correlations for determining swelling potential are summarized in Table 2.3.

Table 2.2. Methods for evaluating swelling potential of expansive clays

Method	Sub-classification	Standard	References
Indirect	Identification	X-Ray Diffraction (XRD), Scanning electron microscope (SEM), Thermo-gravimetric Analysis (TGA)	Al-Rawas et al. (2005), Katti & Shanmugasundaram (2001), Liu et al., (2005), Du et al., (1999). Azam et al., (2013).
	Qualitative	Particle size distribution, consistency limits, geotechnical classification.	McDowell (1959), Seed et al. (1962), Satyanarayana & Ranganatham (1969), Nayak & Christensen (1971), Vijayvergiya & Ghazzaly (1973), Chen (1975)
	Descriptive	Geology, pedology, geomorphology and visual identification.	Snethen et al. (1975), Shi et al. (2002); Simões et al. (2006)
Direct	Quantitative	Conventional free swell test, potential volume change meter, centrifuge test	Nelson & Miller (1992), Holtz & Gibbs (1956), Zornberg et al. (2009).

Table 2.3. Empirical correlations for determining swelling potential

Reference	Empirical correlations
Vijayvergiya & Ghazzaly (1973)	$\log Sp = \frac{1}{12}(0.4LL - w_n + 5.5)$ $\log Sp = \frac{1}{19.5}(6.242\gamma_d + 0.65LL - 130.5)$
Nayak & Christensen (1971)	$Sp = (2.29 \times 10^{-2})(PI)^{1.45} \frac{C}{w_i} + 6.38$
O'Neil and Ghazzaly (1977) in Yilmaz (2006)	$Sp = 2.77 + 0.131LL - 0.27w_n$
Johnson and Snethen (1978) in Yilmaz (2006)	$\log Sp = 0.036LL - 0.0833w_n + 0.458$

Sp: swelling potential (%); LL: liquid limit (expressed in decimal); w_n : natural water content (expressed in decimal); γ_d : dry unit weight in kN/m^3 ; PI: plastic index; w_i : initial moisture content of the sample; C: clay content, by weight, of soil as a percentage.

Although there is no a general agreement about the swelling potential classification, the literature contains a considerable number of classification schemas. Some swelling potential classification criteria are shown in Table 2.4 and

Figure 2.15. The classification of the swelling potential showed in Figure 2.15 (a) is based on the test using compacted specimen, percentage of clay and activity. Liquid limit and plasticity index are used for classification in Figure 2.15 (b), which is based on the plasticity chart. Classification depicted in Figure 2.15 (c) takes into consideration the plasticity index and percent of clay in whole sample. The classification in Figure 2.15 (d) is based on measurements of soil water content, suction and volume change in drying.

Table 2.4. Swelling potential criteria classification

Reference	Criteria	Remarks
Holtz & Gibbs (1956)	$C > 28, PI > 35, SL < 11$ (Very high)	Based on C, P, SL
	$20 \leq C \leq 31, 25 \leq PI \leq 41, 7 \leq SL \leq 12$ (High)	
	$13 \leq C \leq 23, 15 \leq PI \leq 28, 10 \leq SL \leq 16$ (Medium)	
Raman (1967) in Yilmaz (2006)	$PI > 32$ and $SI > 40$ (Very high)	Based on PI and SI
	$23 \leq PI \leq 32, 30 \leq SI \leq 40$ (High)	
	$12 \leq PI \leq 23, 15 \leq SI \leq 30$ (Medium)	
	$PI < 12$ and $SI < 15$ (low)	
Chen. (1975)	$PI \geq 35$ (Very high)	Based on PI
	$20 \leq PI \leq 55$ (High)	
	$10 \leq PI \leq 35$ (Medium)	
	$PI \leq 15$ (low)	
C: clay content, % (< 0.002mm); PI: plastic index, %; SL: shrinkage limit, % (lower limit of volume change)		

In the next sections only three methods for evaluation of swelling will be described: the indirect method proposed by McDowell (1959), herein called potential vertical rise (PVR) method; and two direct methods, the conventional free swell test and the centrifuge test. These methods were chosen because, the indirect method PVR has been a widely used in transportation projects developed by the Texas Department of Transportation (TxDOT), and the direct methods, conventional free swell test and centrifuge test were used in the present research.

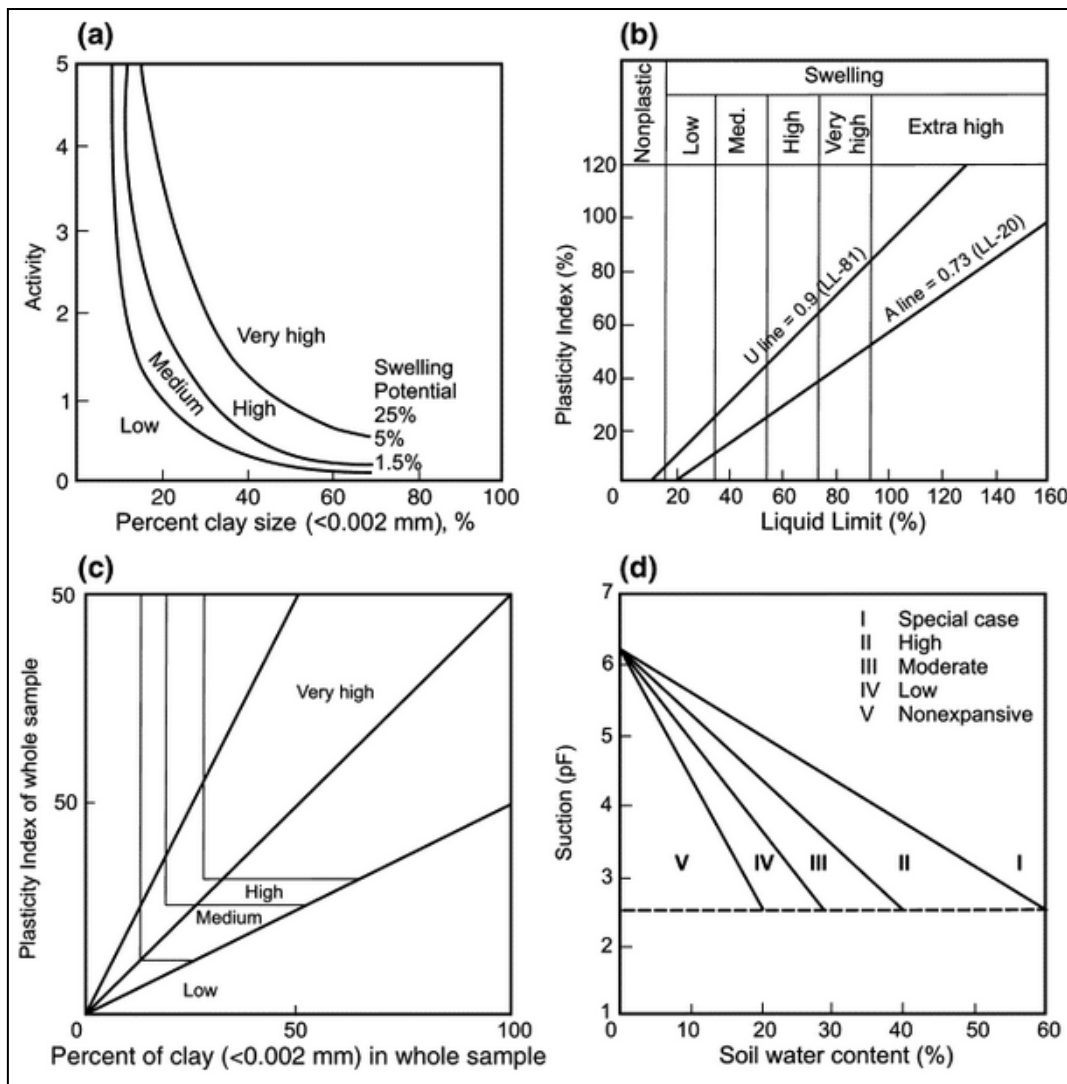


Figure 2.15. Commonly used criteria for swelling potential classification (Yilmaz, 2006)

2.4.1. Potential Vertical Rise Method

The potential vertical rise method (PVR) was developed the Texas Highway Department in 1956 in order to understand the vertical movement of the surface caused by the shrinking and swelling of soils. In this method, the plasticity index of the soil and the field loading are used to predict the vertical rise.

The uncertainty of the PVR method has led many districts of Texas Department of Transportation (TxDOT) avoid the use this method. The lack of a reliable method to assess the potential impact of swelling clays has resulted in considerable improper pavement designs, numerous cases of roads underlain by expansive soils that without stabilization might result in significant amount of resources spent on maintenance cracking repairs in these areas (Snyder, 2015).

The PVR estimation has been used as an index property for projects in areas with known expansive soils, because this method only requires the plasticity index (PI) to predict the volumetric change. As summarized by Armstrong (2014), the method divides the sub-grade into two feet strata (0.6 m), taking into account the depth of sub-grade, with a known or assumed moisture content (ω), unit weight (γ) in pcf, liquid limit (LL), plasticity index (PI), and percent soil binder (i.e. the percent of the stratum that passes through the No. 40 sieve). The moisture condition of each layer is divided into three conditions, dry (ω_d), wet (ω_w), and average (ω_a), as determined by which condition the moisture content of the soil strata is closest to. The dry condition is representative of a condition in which little shrinkage but maximum swell occurs, and the wet condition is considered to be where the maximum capillary absorption occurs. Equations (2.1) to (2.3) show how each moisture condition is calculated:

$$\omega_d = 0.2 * LL + 9\% \quad (2.1)$$

$$\omega_w = 0.47 * LL + 2\% \quad (2.2)$$

$$\omega_a = \frac{\omega_d + \omega_w}{2} \quad (2.3)$$

Once the moisture condition is known or assumed, the percent volumetric change (PVC) of a soil under a one psi (6.9 kPa) surcharge is determined from Figure 2.16 via the PI and moisture condition of the strata.

The percent volumetric change (PVC) must be converted to the percent of free swell (PFS) as indicated in equation (2.4). After PFS is obtained, the load at the top and bottom of each stratum should be assessed from the projects plans and/or boring logs. Then, the PVR of the top and bottom of the strata is calculated by using Figure 2.17, considering the load at each location and the PFS of the strata. The difference between the PVR at the top and bottom of the strata is considered the PVR of the entire strata. However, some corrections are needed for the PVR as the method assumes that the unit weight of the soil is 125 pcf (19.7kN/m³) and that the entire soil strata passes the No. 40 sieve. These corrections are taken as the ratio of the actual unit weight and the percentage of the soil that passes the No. 40 sieve. After these corrections are added, the final PVR is then obtained.

$$PFS = (PVC) * 1.07 + 2.6\% \quad (2.4)$$

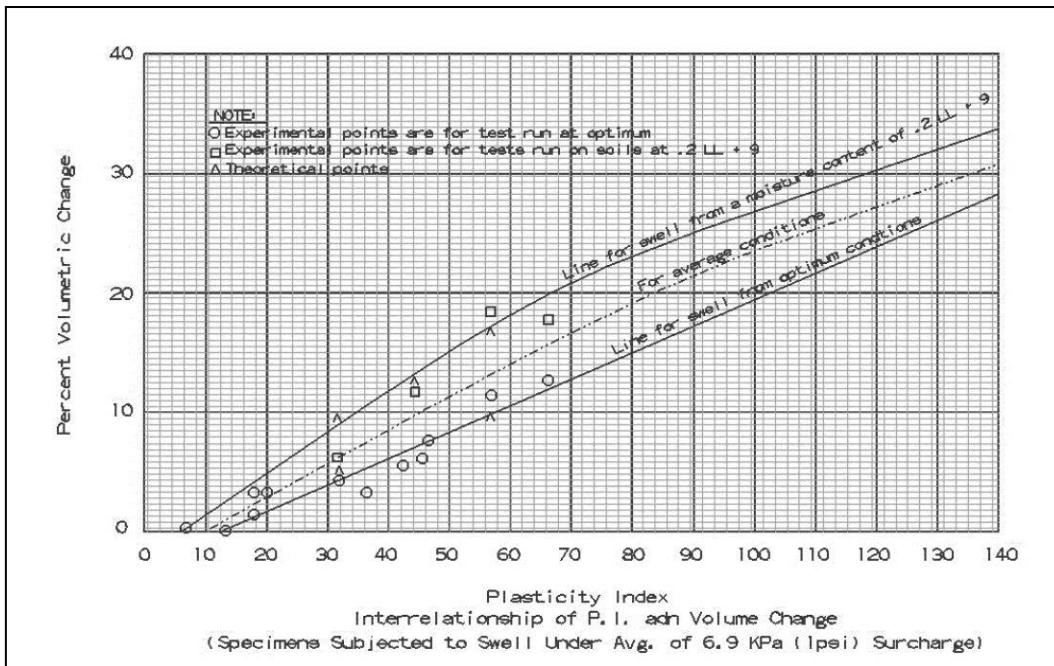


Figure 2.16. Percent volumetric change vs. plasticity index (Armstrong, 2014)

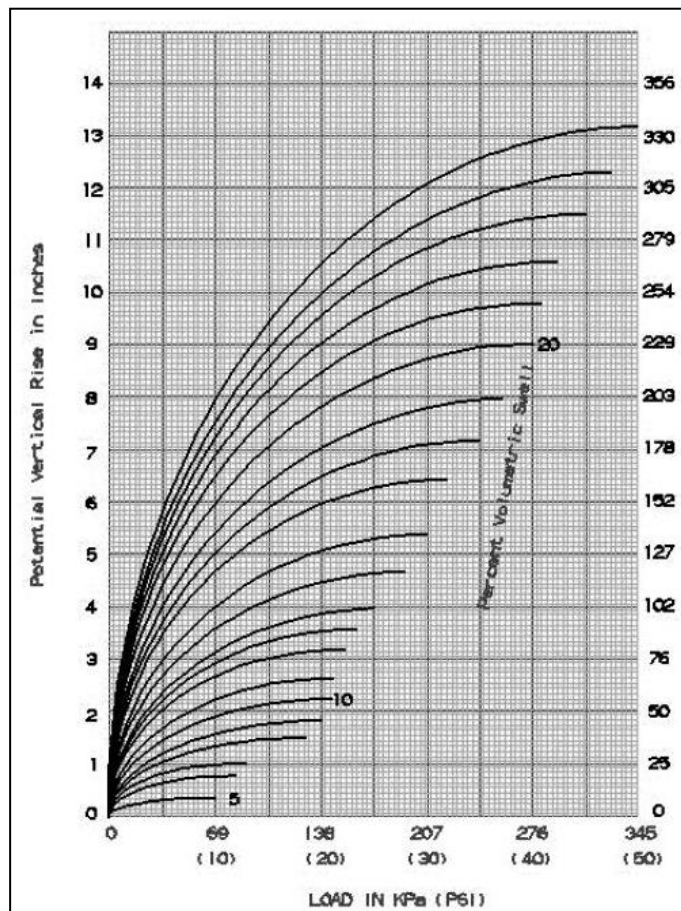


Figure 2.17. Load vs. potential vertical rise (PVR) relationship (Armstrong, 2014)

The first limitation of this method is based on the fact that, even though the plasticity index is a good indicator of swelling potential, does not consider how a soil may behave in-situ due to its mineralogy. Furthermore, this limitation is magnified by the fact that McDowell used only a limited amount of soil samples from Guadalupe County, Texas to create the poorly fit relationship for the moisture condition curves, as seen in Figure 2.16. In addition, the moisture condition curves were extrapolated to a plasticity index (PI) of 140 without further testing near those plasticity index values.

Another limitation exists due to the fact that these soils were not tested at a moisture condition any lower than that calculated from equation (2.1), or at any point in between the dry, wet, and average curves for that matter. From previous research, it is known that the initial moisture condition change of +/- 3% can play a major role in the swelling behavior of a soil (Walker, 2012).

2.4.2. Conventional Free Swell Test and Swell Pressure

The conventional free swell test is described in ASTM D 4546-08 testing procedure. The swelling potential is measured using a consolidation frame (oedometer). The specimen is compacted or trimmed into a consolidation ring, placed between two filter papers and porous stones. The standard method ASTM D4546-08 (2008) includes three types of tests identified as A, B and C. Method A is known as the “wetting-after-loading tests on multiple specimens”, where soil specimens having the same compaction conditions are subjected to a vertical stress and then, water is added to the consolidation ring. Method “A” requires at least four soil specimens to be tested under different overburden pressures, in order to establish a relationship between swell and vertical effective stress. Method “B” is referred to the “single point wetting-after-loading test on a single specimen”, in which the single specimen is tested under representative in-situ conditions of interest. Method “C” allows the soil to swell first before application of desired overburden pressure.

The conventional free swell test results are affected by number of factors which include the effect of oversized particles, sampling disturbance, and the differences in the percentage of wetting between the lab tests and the field. The

main limitation of this test is that the measuring is only one dimensional because lateral strain is restricted. In addition, the conventional free swell test fully inundates the specimen resulting in the most extreme case of a 100% saturated sample. In comparison, values of saturation rarely exceed 95% in the field, which leads to possibility of smaller strains occurring in the field than the values measured in the lab. Also, the reconstituted samples used in these tests may not have the same structure as the in-situ soil in the field, since they should be prepared with soil sieved through the No.10 sieve. These alterations could create differences between the lab tested specimens and the soil in the field.

The swell pressure is the vertical pressure applied to the soil specimen in order to inhibit the swelling of the soil. The swell pressure can be determined from the swell vs. vertical stress curve obtained from test Method “A” of ASTM D4546-08 (2008). The swell pressure can also be obtained by continuously varying the overburden pressure of a specimen until the initial sample height remains unchanged.

2.4.3. Centrifuge Testing For Evaluation of Swelling Behavior

The centrifuge testing for characterization of volumetric changes in expansive clays has been early documented in the literature (Frydman & Weisberg, 1991; Gadre & Chandrasekaran, 1994)), but in the last years it has become an important testing method for measurement of swelling characteristics of expansive soils (Snyder, 2015; Armstrong, 2014; Das, 2014; Walker, 2012; Kuhn, 2010).

The specimen is subjected to an increased gravitational field induced by the rotation within the centrifuge. This imposes a gravitational gradient across the sample, accelerating the flow of the water through the sample. Depending on the test setup, water infiltrates the soil either from the top (Frydman & Weisberg, 1991; Plaisted, 2009; Kuhn, 2010) or the bottom (Gadre & Chandrasekaran, 1994) of the specimen.

The development of centrifuge technology at the University of Texas at Austin began with the research conducted by Plaisted (2009). Plaisted’s research involved testing reconstituted specimens of the Eagle Ford clay using a set of plastic permeameter cups referred to as the single infiltration set-up. The single infiltration

setup was composed of two parts, the top cup and the base cup. The top cup was designed to hold the soil specimen and contain the ponded water. The bottom cup was designed to collect the outflow of water that has passed through the soil specimen, and was used to back calculate the total height of water ponded on top of the sample at the end of testing. Two identical porous disks were designed out of the same material as the permeameter cup to allow the flow of water through the soil specimen. One of the disks was used to support the specimen in the bottom of the top cup, while the other was placed on top of the specimen to provide a boundary between the overburden pressure and water ponded on top. A diagram of the single infiltration set-up can be seen in Figure 2.18.

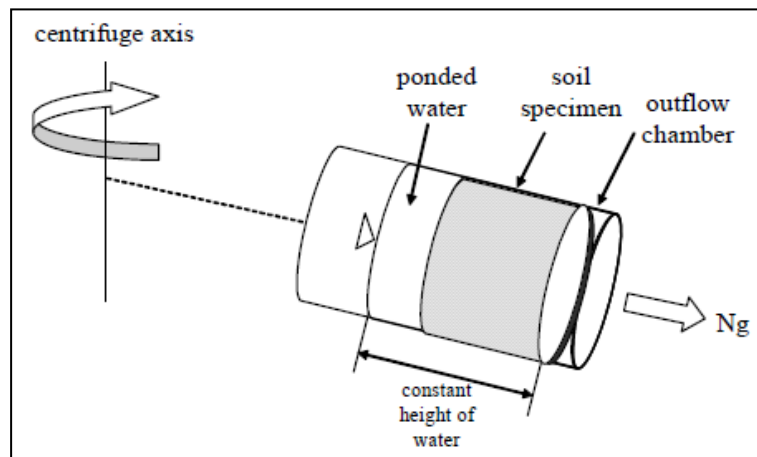


Figure 2.18. Schematic of centrifuge swelling test (Plaisted, 2009)

The results reported that the strain induced during the centrifuge test had more scatter behavior and it was higher than that from the conventional free swell test (Figure 2.19). This discrepancy was attributed to the fact of the specimens had to be removed from the increased gravitational field, and reintroduced to the 1-g environment (specimen was removed from the centrifuge) in order to take height measurements periodically.

Kuhn (2010) developed parallel research about the swelling behavior of the Eagle Ford clay in a larger scale centrifuge. This centrifuge has the capability to measure the swelling during the testing process without having to remove the sample from its loading condition. This was possible due to the installation of a data acquisition system combined with a linear positioning system inside the centrifuge. These advancements avoided the need for stopping the centrifuge to measure the

changes in height due to swelling, and make possible a fair comparison between centrifuge and conventional free swell test results. A schematic view of the permeameter cup inside the large centrifuge is depicted in Figure 2.20.

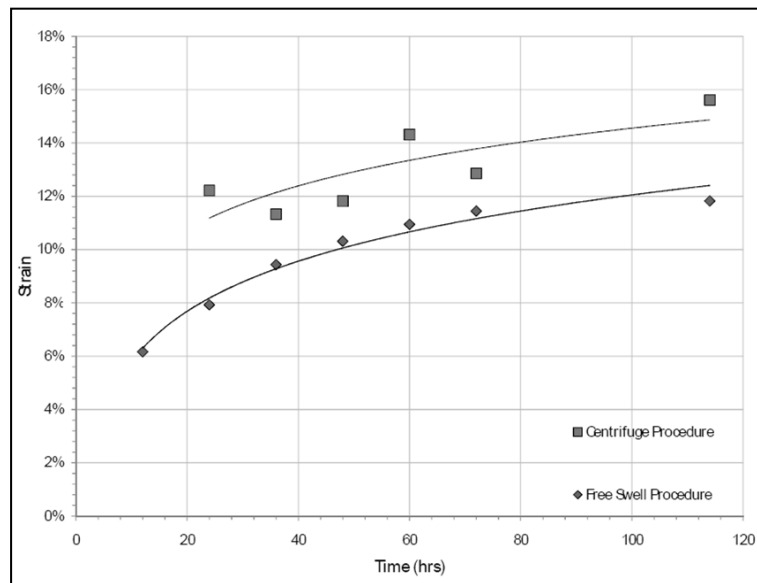


Figure 2.19. Comparison between single infiltration centrifuge test and conventional free swell test results (Plaisted, 2009)

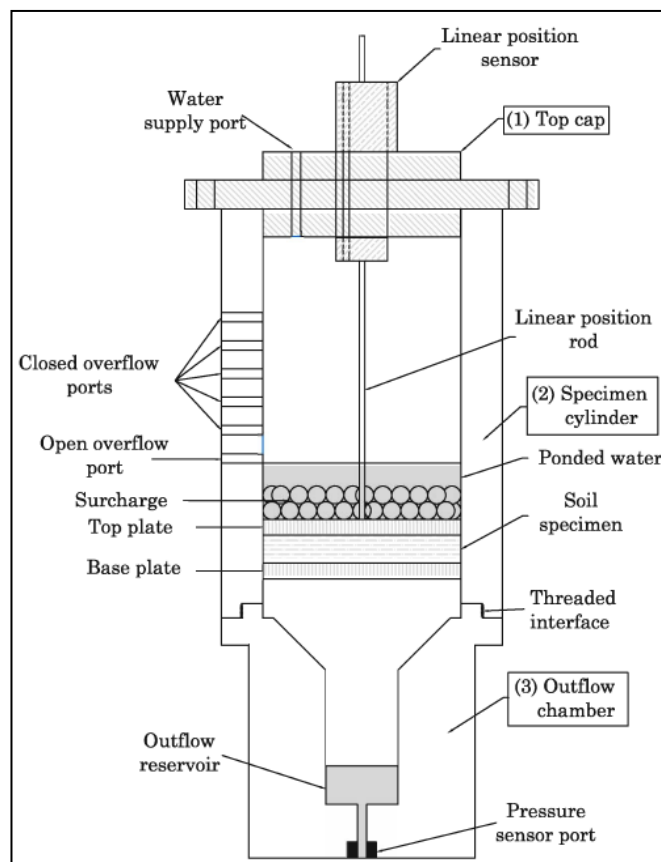


Figure 2.20. Schematic view of permeameter cup of large centrifuge (Kuhn, 2010)

Kuhn (2010) carried out two testing series. The first series (i) involved testing specimens with a constant height of water and surcharge mass, which results in the only factor changing is the total stress applied at different g-levels. The second series (ii) involved testing under a constant water pressure and total stress during the test. In the second scenario, various water and surcharge pressures were applied at the same g-level. The results indicating the relationship between the total stress applied and the swelling measured in the centrifuge are shown in Figure 2.21 for both series. This research pointed out that the total swelling of the specimens decreased with increased g-level for the first series, and the total swelling of the specimens decreased with increased height of water, or water pressure, as well as, increases in the surcharge pressure.

Despite the large centrifuge test produced is comparable to results with conventional free swell test, this equipment is somewhat impractical for conducting a large scale testing program on soils. Consequently, it was necessary to design a similar data acquisition system for the smaller centrifuge which can run multiple samples at the same time.

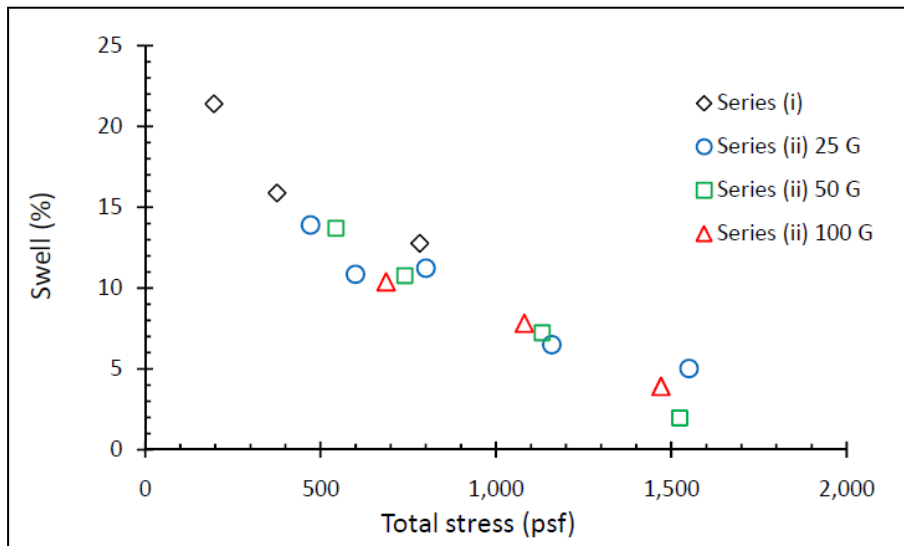


Figure 2.21. Swell vs. Total stress for 10 mm thick specimens with water pressure of 400 psf (19 kPa) (Kuhn, 2010)

Afterwards, Walker (2012) conducted research which focused on the implementation of a data acquisition system with linear position sensors in the smaller centrifuge. The data acquisition system consisted of a custom built Arduino board designed with an analog to digital converter, an accelerometer to measure g-

levels and a power supply of 4 AA batteries. Along with the internal Arduino board, an Arduino receiver plugged into a computer via USB outside the centrifuge was used to wirelessly collect the data. The centrifuge contained six cups for testing; two of the cups were used to store the Arduino board and power supply, leaving space for 4 specimens to be analyzed for each test. A modified top cap was designed to install the linear position sensor.

After installing the new setup, Walker (2012) carried out tests to estimate the swelling potential of Eagle Ford clay, Houston Black clay, and Tan Taylor clay. The testing program included examination of the effect of initial compaction conditions (i.e. the initial moisture content and dry density) of these soils on their swelling behavior. This research demonstrated that increasing dry unit weight resulted in increasing swelling potential, as well as the increase in water content decreased the swelling potential (Figure 2.22). Furthermore, it was verified that the linear position sensors could be used to measure the swelling behavior of expansive soils in the small centrifuge.

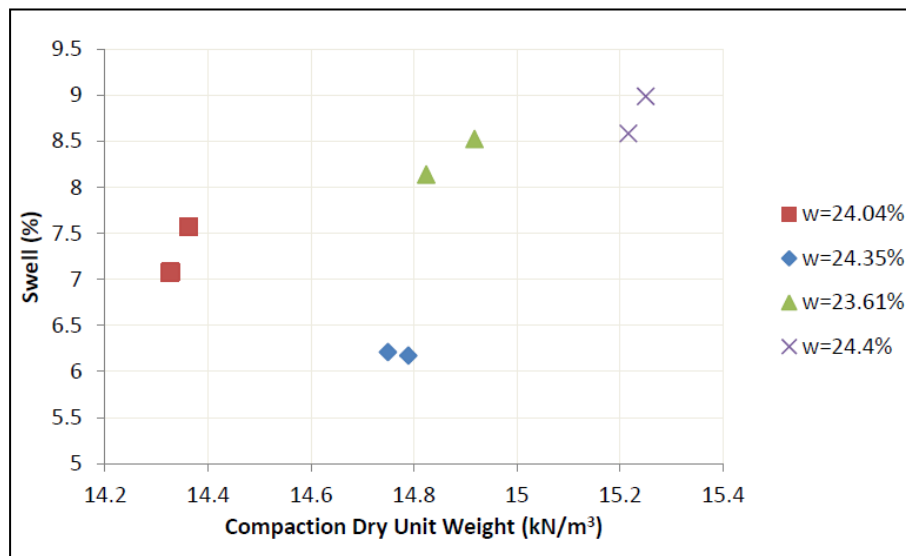


Figure 2.22. Swell vs. compaction dry unit weight for Eagle Ford clay specimens (Walker, 2012)

The final improvement made in the centrifuge of the University of Texas at Austin was developed by Armstrong (2014), who designed a new permeameter cup that matched the boundary conditions from the ASTM D4546-08 (2008) tests and allows infiltration at both the top and base of a specimen. This new permeameter cup, identified as the double infiltration set-up, also represented a progress as the

cutting ring could not only be used to compact reconstituted specimens in but also use trimmed specimens of “undisturbed” samples. The final version of the centrifuge set-up is widely described in section 3.3.2, since it was used in the present research.

During his research, Armstrong (2014) identified the effects of the clay fabric on the swelling behavior of highly expansive soil called Cook Mountain clay. The specimens were test in the single and double infiltration set-up, as well as, conventional free swell tests to confirm the results. Observations from the testing suggested that the fabric of the soil had an impact on the swelling behavior. Specimens with a flocculated structured reached the end of primary swelling faster, and had less secondary swelling than specimens with a dispersed structure. In addition, it was proven that the double infiltration set-up matched results from the conventional free swell test, as seen in Figure 2.23. Therefore, the double infiltration set-up provided more precise results than the single infiltration set-up due to less variability in the confining stress as well as less dependence on the height of water to apply an effective stress during test and produces results more rapidly than conventional free swell test.

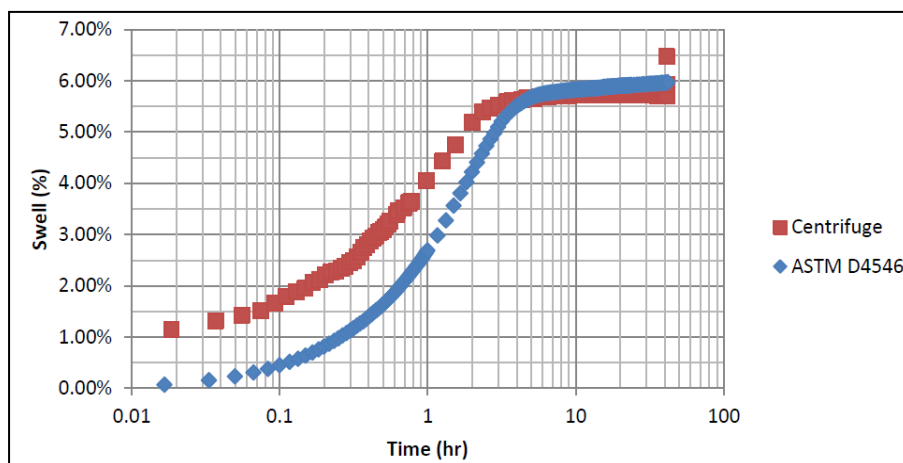


Figure 2.23. Comparison between double infiltration centrifuge and ASTM D4546-08 (2008) (free swell) curves (Armstrong, 2014)

2.5. Treatments to control swelling of expansive clays

According to Nelson & Miller (1992), the available treatment procedures to control swelling of expansive soils before and after construction of structures and

highways include: prewetting, removal and replacement, remolding and compacting, surcharge loading, moisture barriers and chemical modification. These alternatives may be employed either singly or in combination, to control swelling. However, depending on the specific conditions, such as economic factors, site characteristics and time available for the treatment, one or more methods can be ineffective.

Prewetting or ponding procedure is addressed to increase the moisture content in the expansive soil in order to cause heave prior to construction and thereby eliminate problems afterwards. This procedure may present problems that limit its application. For instance, expansive soils typically exhibit low hydraulic conductivity and the time required for adequate wetting can be several years (Nelson & Miller, 1992). Furthermore, the long periods of contact between water and the expansive soil can produce loss of soil strength, reducing the bearing capacity and slope stability.

The procedure of removal of expansive soils and replacement with non-expansive soils might be unfeasible in cases when the expansive layer extends to a very high depth making uneconomically its complete removal. However, non-expansive soils compacted at high density usually exhibit higher bearing capacity than expansive clays. This method might be preferred when construction delays are not allowed.

The procedure of remolding and compacting an expansive soil is indicated when the soil has low swelling potential. The bearing capacity of the remolded soil is usually lower since the soil is generally compacted at wet of optimum moisture content and moderate density (Nelson & Miller, 1992).

Surcharge loading is the procedure where the expansive soil is loaded with a surcharge large enough to counteract the probable swell pressures. This alternative becomes less efficient in soils with high swell pressures, because of the nonlinear nature of the pressure-swell relationship (Nelson & Miller, 1992). Thus, this procedure is generally applicable only for soils with low to moderate swelling pressures.

Since soil expansion problems are resulted from fluctuations in water content, uneven heave can be resulted from uneven water content changes. So that, the problems generated by expansive soils also can be mitigated by using horizontal and vertical moisture barriers that promote the uniform water content distribution

into the soil. According to Nelson & Miller (1992), the basic principle on which moisture barriers act is to move edge effects away from the foundation or pavement and minimize seasonal fluctuations of water content directly below the structure. Also, the time during which moisture changes occur is long because the barrier increases the path length for water migration under the structure. This allows for water content to be more uniformly distributed due to capillary action in the subsoil. Thus, the heave will occur more slowly and in a more uniform manner.

Among the chemical modifications to control swelling of expansive soils are the use of Portland cement, lime-fly ash combinations and hydrated lime. Nelson & Miller (1992) stated that even the Portland cement produces similar lime-effects in clay soils, it is not as effective as lime stabilization of highly plastic clays. Some clay soils have such a high affinity for water that the cement may not hydrate sufficiently to produce the complete pozzolanic reaction. So that, Portland cement is usually advantageous when soils are not lime reactive.

There is a wide variety of fly ash that can be mixed with lime in order to produce different mechanical and chemical properties into the soil, so that, for specific application of this type of modification, it is necessary a comprehensive testing program to determine the design criteria for its use. In this study, the use of hydrated lime for modifying expansive soil is studied, so that, more detailed description about it is presented in the following sections.

2.6. Lime Treatment in Expansive Soils

Among the techniques for improvement the behavior of expansive soils, lime treatment may be the most practical and worthwhile in preventing the potential damages associated with large volume changes.

When lime is added to a clay-water-system, the divalent calcium cations virtually always replace the cations normally adsorbed at the clay surface. This cation exchange occurs because divalent calcium cations can normally replace cations of single valence, and ions in a high concentration will replace those in a lower concentration (Little, 1994).

The fact that calcium will replace most cations available in the water system is documented by the Lyotropic series which generally states that higher valence

cations replace those of a lower valence, and larger cations replace smaller cations of the same valence. The Lyotropic series is written as: $\text{Li}^+ < \text{Na}^+ < \text{K}^+ < \text{NH}_4^+ \ll \text{Mg}^{+2} < \text{Ca}^{+2} \ll \text{Al}^{+3}$, where the cation to the right replaces the one to the left. Therefore, in equal concentration, Ca^{+2} can easily replace the cation commonly present in most clays.

2.6.1. Lime Soil Reactions

The chemical reactions that take place when lime is mixed with soil in presence of water can be classified as immediate and long-term reactions. Immediate reactions are commonly referred as “lime treatment” and long-term reactions as “lime-stabilization”.

When lime is added to a clay soil, it has an immediate effect on the properties of the soil as cation exchange begins to take place between the metallic ions associate with the surface of the clay particles and the calcium ions of the lime (Bell, 1996). The free calcium of the lime exchanges with the adsorbed cations of the clay mineral, resulting in reduction in size of the diffused water layer surrounding the clay particles (Figure 2.24 (a) and (b)). This reduction in the diffused water layer allows the clay particles to come into closer contact with one another, causing flocculation/agglomeration of the clay particles, which transforms the clay into a more silt-like or sand-like material. Dash & Hussain (2011) suggested that the decreasing of the thickness of the diffuse double layer may increase the charge concentration and thereby the viscosity of the pore fluid, leading to an increase in the plastic limit of lime-treated samples.

As described by Beetham *et al.* (2014), opposing negative charges of parallel aligned (face to face) clay particles are repelled and reconfigure to promote a flocculated, positive/negative charge (e.g. edge to face) arrangement (Figure 2.24 (c)). This causes silt-sized aggregations of clay particles to group together and two influences on the clay soil structure are suggested: an increase in microporosity or intra-aggregate porosity of flocculated particles (Figure 2.24 (c)); and a change to the meso-porosity or inter-aggregate porosity (Figure 2.24 (d)). This reduces the effective surface area of clay minerals in contact with the inter-aggregate pore water accounting for much of the immediate change in physical properties of the clay soil

associated with lime improvement (reduced plasticity, promotion of brittle/friable behavior, increased permeability).

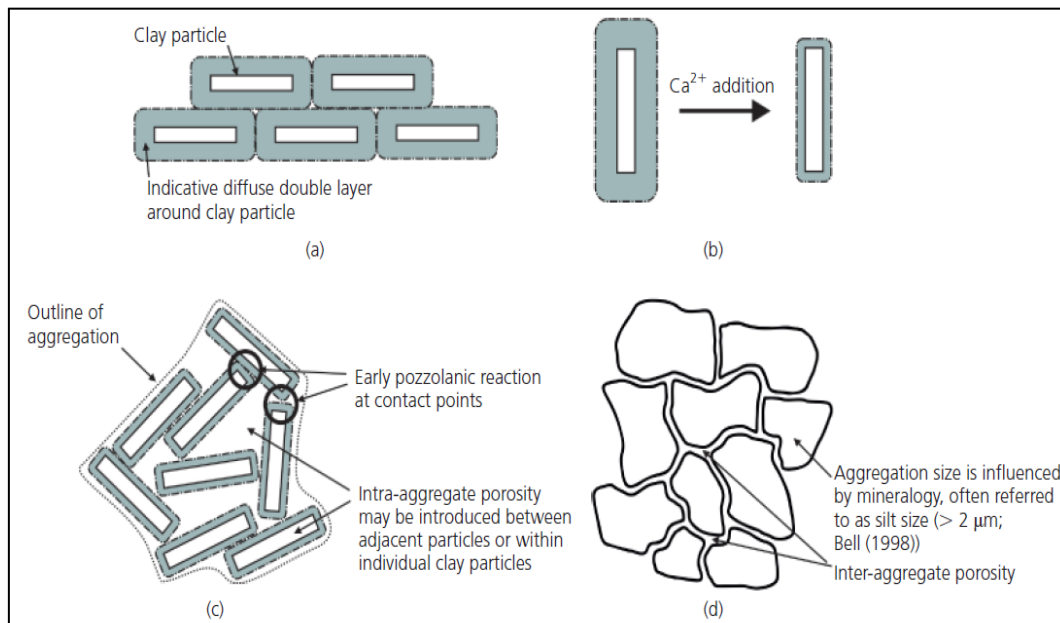
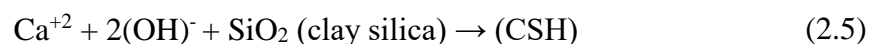
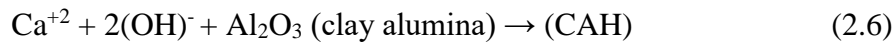


Figure 2.24. Sequence illustrating influence of early lime-clay reactions upon clay particle arrangements and soil structure (Beetham *et al.* 2014)

Long-term reactions are more complex and are strongly influenced by soil conditions and mineralogical properties. However, many clay soils are pozzolanically reactive when stabilized with lime and respond with an appreciable strength gain due to the development of a cemented matrix among the soil particles.

Little (1994) defined a pozzolan as a finely divided siliceous or aluminous material which in the presence of water and calcium hydroxide will form a cemented product. The cemented products are calcium-silicate-hydrates (CSH) and calcium-aluminate-hydrates (CAH). Clay is a pozzolan because it is a source of silica and alumina for the pozzolanic reaction. Clay-silica and clay-alumina become soluble or available in a high pH environment. The pH of water saturated with lime is 12.4 at 25°C. Thus a lime-soil-water system has a pH high enough to solubilize silica and alumina for pozzolanic reaction. As long as enough residual calcium remains in the system to combine with the clay-silica and clay-alumina and as long as the pH remains high enough to maintain solubility, the pozzolanic reaction will continue. The reaction is illustrated as follows:

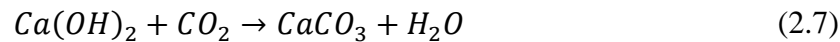




With base on this fact, Eades & Grim (1966) adopted the pH variation due to lime addition in order to design a procedure for determining the amount of lime required for satisfying all immediately occurring reactions, and yet provide enough residual lime to maintain a pH of 12.4 for sustaining the strength-producing reaction.

2.6.1.1. Deleterious Chemical Reactions

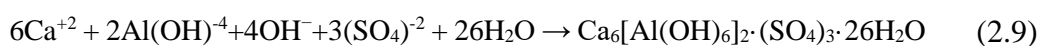
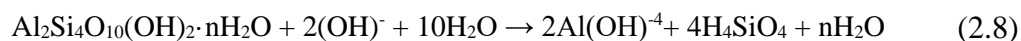
Lime-treated soils can undergo two undesirable chemical reactions. The first is lime carbonation and the second is the reaction with the sulfate existing in the soil. Carbonation is the reaction that occurs between free lime and atmospheric carbon dioxide and results in formation of calcium carbonate, as shown in the equation below:



The carbonation reaction is recommended to be controlled because it causes weak bounding and consumes calcium ions affecting negatively pozzolanic reactions.

On the other hand, several studies have found that calcium-based stabilizers treatments of natural expansive soil rich with sulfates may lead to a new heave distress problem instead of mitigating it. Heave and loss strength of lime stabilized soils have been associated with high sulfur contents in the treated soil, leading to the formation of the expansive and strength reducer minerals ettringite ($\text{Ca}_6[\text{Al}(\text{OH})_6]_2 \cdot (\text{SO}_4)_3$) and thaumasite ($\text{Ca}_3[\text{Si}(\text{OH})_6](\text{CO}_3)(\text{SO}_4) \cdot 12\text{H}_2\text{O}$).

Puppala *et al.* (2005) stated that sulfate content as a percent of dry weight of soil needed to induce heaving varied from 320 mg/kg (or ppm) to as high as 43.500 mg/kg. The time of sulfate heave appearance after chemical stabilization ranged from a few days to 18 months. Hunter (1988) reported a chemical relationship model of time-treated montmorillonite sulfate-rich clays to explain the formation of ettringite. The chemical reactions are the dissolution of clay minerals at $\text{pH} > 5$ and the formation of ettringite, as shown in equations (2.8) and (2.9), respectively.



The chemical reaction model points out that dissolution of any clay minerals (alumina and amorphous silica) will occur due to the high pH conditions caused by the addition of lime stabilizer. Ettringite formation affects clay properties such as consistency, compaction characteristics and the cation exchange process (Rajasekaran & Rao, 2005). Ettringite can be extremely detrimental because it has the potential to swell up to 250 percent of its original volume (Puppala & Cerato, 2009).

Little & Nair (2009) suggested two possible theories to explain the expansion of ettringite. First, the expansion in the matrix might result from crystallization pressure, crystal interlocking, and oriented crystal growth. Second, water absorption by ettringite molecules are the reason of expansion. It is probable that the expansion is a combination of the two theories, but either way, water is crucial to ettringite expansion. If the initial water used in mixing and compaction of stabilized soils is too low to dissolve all sulfates available into solution for ettringite formation, water from an external source, such as heavy rainfall, will be able to dissolve more of the soluble sulfate than the mix water, making the ions more available for ettringite formation and expansion later on.

2.6.2. Effect of Mellowing Period on the Lime Treatment

The effectiveness of lime treatment in expansive soils depend on the appropriate preliminary laboratory testing that considerers the influence of diverse environmental factors during construction. One of them is a possible compaction delay after lime adding and mixing due to hitches or technical breaks for logistic reasons.

The time elapse between lime-soil mixing and compaction is known as “mellowing”. There are conflicting recommendations in the literature about the influence of mellowing periods during lime treatments: researches developed by the Louisiana Department of Transport in the early sixties indicated that a delay longer than 48 hours involves a lower strength of the lime-soil mixtures (Taylor & Arman, 1960); Mitchell & Hooper (1961) found that a 24 hour delayed compaction reduced the dry unit weight and the long-term strength, whereas the swelling was found to increase. Holt & Freer-Hewish (1998) examined the long-term effect of mellowing

by using UCS (Unconfined Compressive Strength) testing on specimens that had been cured for various periods up to a maximum of 195 days. The results obtained are shown in Figure 2.25. The specimens treated with 2% lime decreased in strength with prolonged curing while those treated with 4% lime maintained a similar strength or demonstrated increases in strength. They suggested that 2% of lime was not enough to achieve full stabilization. In addition, at the end of 195 days of curing, the specimens mellowed for 24 hours in both cases were always significantly weaker than specimens mellowed for 1 hour before compaction. The strength of the specimen with 4% lime and mellowed for 1 hour before curing was approximately double that of the specimen mellowed for 24 hours. Similar trends in strength loss were observed in studies conducted by Talluri *et al.* (2013).

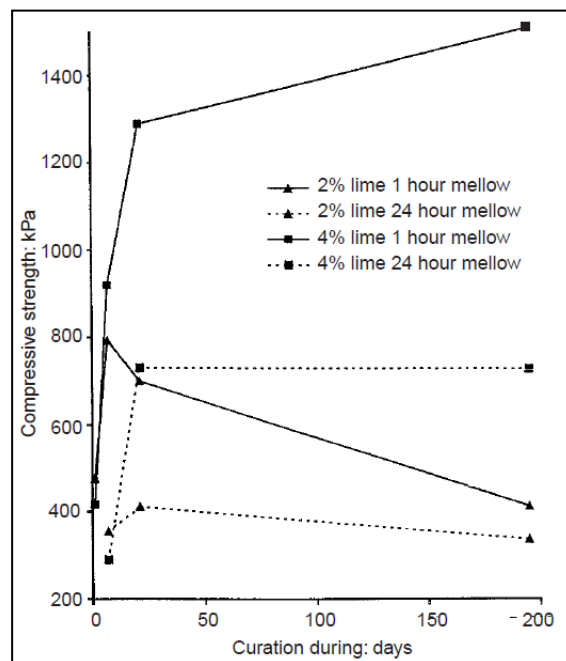


Figure 2.25. Effect of mellowing duration on strength at different lime additions (Holt & Freer-Hewish, 1998)

Some authors recommend compaction to be executed immediately after lime addition (Osinubi & Nwaiwu, 2006) while others advise a wait of few days (typically 3 to 7 days) in order to obtain a higher quality material or to mitigate swelling in sulfate-bearing soil (Harris *et al.*, 2004; Talluri, 2013). Harris *et al.* (2004) reported that using 3 days mellowing period resulted in acceptable swell in soils with sulfate contents around 7,000ppm, whereas mellowing of 3 days and 6% lime did not result in acceptable swell with 10,000-ppm sulfates.

Holt *et al.* (2000) studied the effect of mellowing periods on the modification process of four British soils treated with quicklime and found that a half day mellowing period decreased the volume change (volume calculated by measuring of height and diameter of specimens subjected to soaking), but mellowing periods above half a day produced progressive increase in volume change, so that generally after a one day mellowing period the volume change was greater than that without mellowing (Figure 2.26).

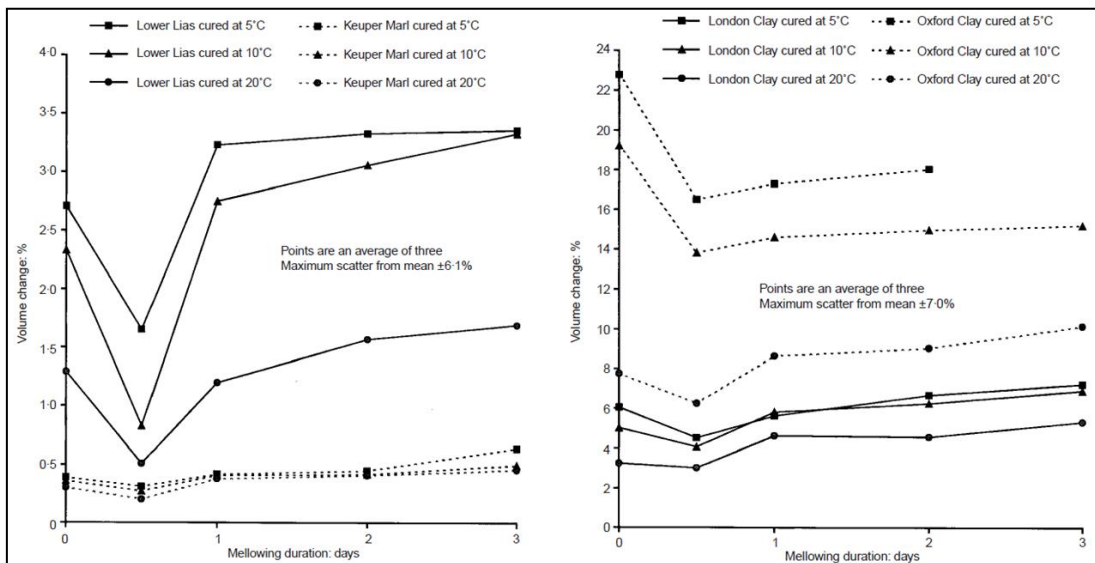


Figure 2.26. Effect of mellowing duration and temperature on the volume change of lime-treated British soils (Holt *et al.*, 2000)

2.6.3. Modification of Soil Properties by Lime Addition

Many of engineering properties of clay soils improve with lime addition. The effect of lime on the plasticity has been reported as instantaneous and resulting from the flocculation process. Very small quantities of lime are required to bring about different plastic behavior, around 1 to 3% of lime, depending on the type of clay minerals present in soil. Whereas the liquid limit of clays soils is found to decrease with increased lime content (Wang *et al.*, 1963; Bell, 1996), the plastic limit generally shows an increasing trend (Dash & Hussain, 2011) (Figure 2.27). Correspondingly, the plastic index, the arithmetic difference between the liquid limit and the plastic limit, is generally found to decrease with lime content, making the soil more friable and therefore more workable.

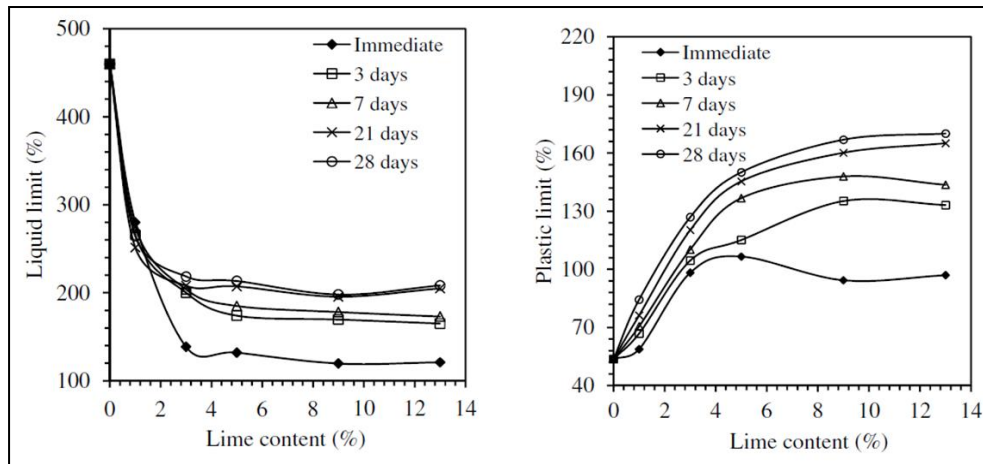


Figure 2.27. Variation in liquid limit and plastic limit with lime content for an expansive soil (Dash & Hussain, 2011)

Bell (1996) observed that the addition of lime to clay materials increases their optimum moisture content and reduces their maximum dry density for the same compactive effort. The reduction in dry density was attributed to an immediate formation of cemented products which reduce compactibility and hence the density of the treated soil. The flocculation and agglomeration processes enlarge particle size causing increasing in void ratio, and consequently the hydraulic conductivity increases as well (Cuisinier *et al.*, 2011; Tran *et al.*, 2014).

Tran *et al.* (2014) demonstrated that the lime treatment only increased the modal size of inter-aggregates (from 1.5 μm to 3 μm) and there was no effect on the intra-aggregate pore sizes (around 0.015 μm) and thus, the increasing in hydraulic conductivity was attributed only to the change in the inter-aggregate pore size (Figure 2.28).

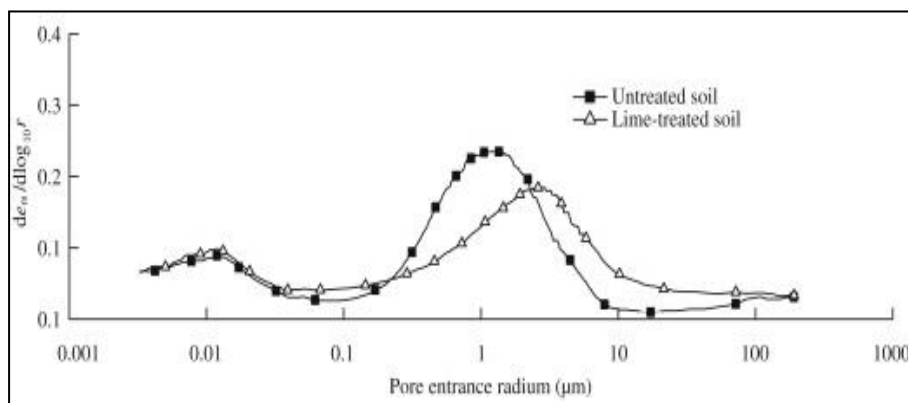


Figure 2.28. Effect of lime treatment on pore size distribution. Results of mercury intrusion porosimetry (MIP) (Tran *et al.*, 2014)

Swelling potential is normally significantly reduced by lime treatment, as demonstrated from results obtained by Nalbantoglu & Tuncer (2001), using an expansive soil from Cyprus treated with hydrated lime and subjected to conventional free swell test (Figure 2.29). In fact, the reduction in PI associated with virtually all fine-grained soils upon the addition of lime is a significant indication of the reduction of swelling potential (Little, 1994). At the same time that lime reduces the swelling potential, lime has been reported to increase the compression resistance. The compression and rebounded indices (C_c and C_r , respectively) obtained from one-dimensional consolidation test, developed by Nalbantoglu & Tuncer 2001), indicated a dramatic decrease with an increase in the percent lime (Figure 2.30).

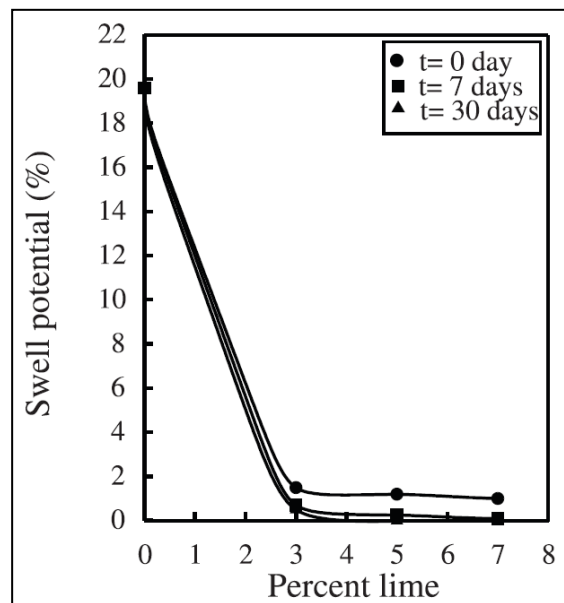


Figure 2.29. Variation of swell potential with percent lime and curing time. (Nalbantoglu & Tuncer, 2001)

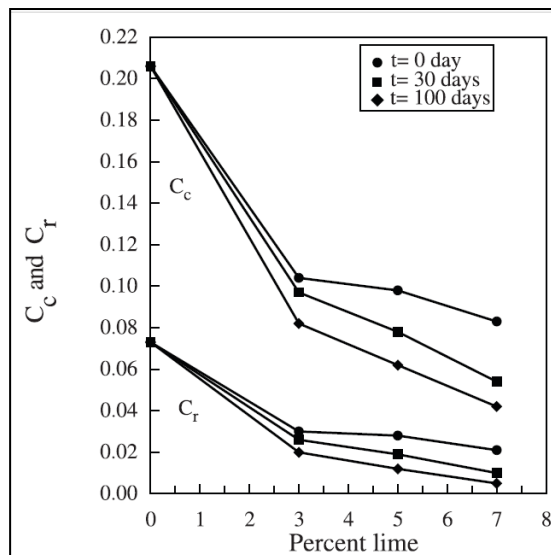


Figure 2.30. Effect of lime and curing time on the compression and rebound indices C_c and C_r . (Nalbantoglu & Tuncer, 2001)

Furthermore, studies have also examined the effect of cyclic wetting and drying on the swelling potential in expansive soil treated with lime (Stoltz *et al.*, 2012; Guney *et al.*, 2007). These studies have reported negative effect of wetting and drying cycle on lime treatment through observations of increasing of swelling potential after various cycles (4 to 6). The beneficial effect of lime treatment in controlling swelling potential is partially lost when lime-treated soil is subject to cycles of wetting and drying (Guney *et al.*, 2007).

On the other hand, lime can stabilize the soils through cementation, producing increases in strength and stiffness (Bell, 1996; Consoli *et al.*, 2011)). Consoli *et al.* (2009), reported that Unconfined Compressive Strength increased linearly with the increase in the lime content, however, Bell (1996) stated that an excessive addition of lime might reduce the strength because lime has no good frictional properties. Furthermore, Consoli *et al.* (2009) found that the unconfined compression strength increased approximately linearly with a reduction in the porosity of the compacted mixture and that there is no relationship between the unconfined compression strength and the water/lime ratio.

Among the different variable affecting the strength of lime stabilized clay soil, curing is of major importance. Its effect on strength is a function of time, temperature and relative humidity (Mitchel & Soga, 2005). The strength increases rapidly at first, generally during the first 7 days of curing, then increases more slowly at a more or less constant rate.

3 Materials, Methods and Equipment

The present chapter contains four main sections that describe the materials, experimental methods and equipment employed in this research. The first section (section 3.1) describes the principal characteristics of the expansive soil and lime used in this study, and the sample preparation methods. Section 3.2 briefly describes the basic tests for soil characterization carried out to examine the effect of lime treatment on different geotechnical properties. The basic tests include: Atterberg limits, pH and Cation Exchange Capacity (CEC) determination, specific gravity, particle size by hydrometer test, standard Proctor compaction and Unconfined Compressive Strength (UCS).

The methods executed for measuring the swelling potential are described in section 3.3. Two methods were applied at this point: the conventional free swell test and the centrifuge test. The conventional free swell test is the most traditional heave prediction test that involves the use of the one-dimensional consolidation apparatus, whereas the centrifuge test is a new technology developed by the University of Texas at Austin. Since there is no standard specification about the centrifuge test procedure, special attention is given to the description of this new technology.

Finally, section 3.4 describes the techniques used to obtain mineralogical analysis and micro-structural observations in order to understand the changes due to lime treatment of the expansive soil Eagle Ford clay. The mineralogical test was executed by X-Ray Diffraction (XRD) technique and the micro-structural observations were performed by using Environmental Scanning Electron Microscopy (ESEM) and X-Ray Computer Micro-Tomography (Micro-CT).

3.1. Materials

3.1.1. Expansive Soil

The natural expansive soil selected for this study was a highly clayey soil named Eagle Ford predominant in Texas, United States. Since this soil has been widely studied in previous researches, the Eagle Ford clay used in this study was obtained from the available stockpiles of the geotechnical laboratories of the University of Texas at Austin.

According to previous researches (Walker, 2012 and Das, 2014), the stored Eagle Ford clay was excavated from the Eagle Ford formation located at the intersection of Hester's Crossing and Interstate 35 on the outskirts of South Round Rock, at Austin city area, approximately 25 km north from the University of Texas campus (Figure 3.1). The soil was excavated using a backhoe from a depth of 3 meters, and transported using 50 gallon plastic drums. According to Lin (2012), the untreated Eagle Ford clay has as principal compounds: montmorillonite (28%); illite (27%) and kaolinite (11%).

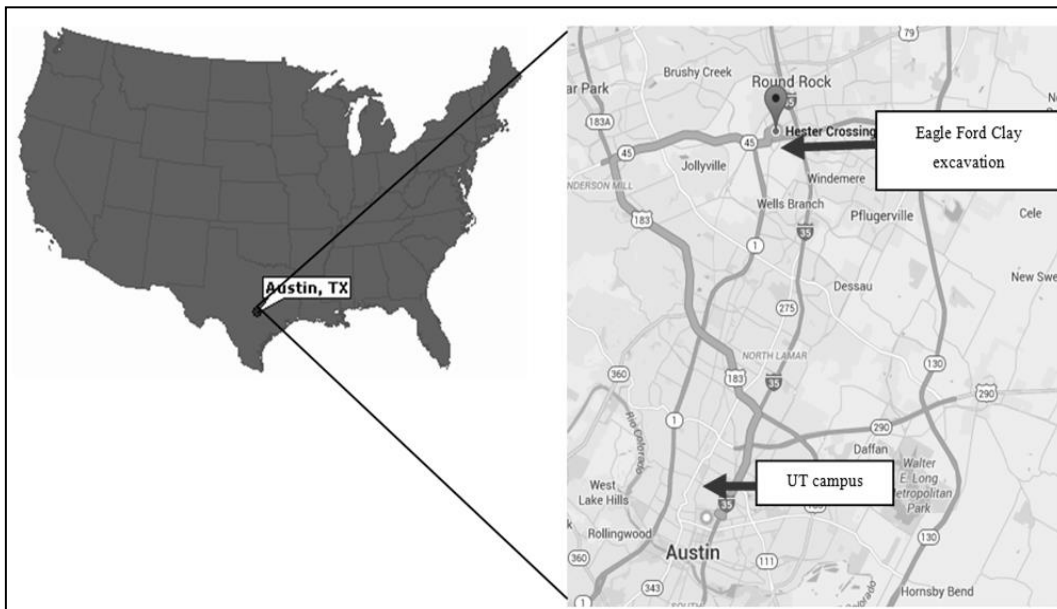


Figure 3.1. Localization of Eagle Ford Clay excavation

3.1.2. Hydrated Lime

Lime can be produced in various forms, however for stabilization applications the most typically used are: hydrated high-calcium lime ($\text{Ca}(\text{OH})_2$), and quicklime (CaO). In this study, hydrated high-calcium lime, henceforward called “hydrated lime” was used in this research because this type of lime enables to control the moisture content of the lime-soil mixtures easier than quicklime. Quicklime needs to consume a considerable amount of water when it hydrates in an exothermic reaction before reacting with the soil particles, but hydrated lime does not need additional water during the mixing with soil.

The chemical composition of the hydrated lime was provided by Austin White Lime Company¹ and is listed in Table 3.1. This material is odorless white of grayish-white granular powder, with molecular weight of 74.08 and specific gravity of 2.24.

Table 3.1. Chemical analysis of hydrated lime (Austin White Lime Company)

Chemical analysis	(%)
$\text{Ca}(\text{OH})_2$	94
Free CaO	0.1
Free H_2O	0.4
Inerts	3.5
LOI (loss of ignition)	24.16
CaCO_3	2.0

3.1.3. Soil Preparation

Testing for this study was only performed on remolded samples proceed as follows. Prior to testing, the soil was air-dried in room temperature until the soil was dried enough to be crushed. Then, the air-dried soil was processed using a mechanical soil crusher to break the large clods of the collected soil. During crushing operation, fossil or rock fragments that could potentially alter the soil characteristics were removed. After crushing, the soil was passed through the No. 10 sieve and stored in sealed 5 gallon buckets until further use.

Lime-soil mixtures were prepared with dosage rates based on the dry weight of soil to be treated. Lime was added to the air-dried soil and mixed for approximately 5 minutes, before water addition, enabling the lime to be evenly

¹ <http://www.austinwhitelime.com/>

distributed throughout the mix. Distilled water was added to the lime-soil mixture to achieve the desired moisture content. Taking into account the evaporation water due to the slaking reaction, additional 1% of moisture content was added. Thus, lime-soil mixtures and water were hand mixed with the spatula for approximately 5 minutes more and finally stored in Ziploc bags.

The mellowing period was established between the end time of lime-soil-water mixing and the specimen compaction time. After the mixing process, the lime-soil mixtures were transferred to Ziploc bags that were stored at room temperature ($23^{\circ}\text{C} \pm 2^{\circ}\text{C}$) and relative humidity about 95%. At the end of the mellowing period, the material was remixed and compacted for different tests.

3.2. Basic Tests

A complete series of basic tests was performed on untreated and lime-treated soils. In particular, the tests consisted in determining Atterberg limits, chemical tests (pH and Cation Exchange Capacity – CEC), specific gravity, particle size distribution (by hydrometer test), compaction properties and Unconfined Compressive Strength (UCS). Table 3.2 summarizes the experimental plan of basic tests.

Table 3.2. Experimental plan of basic tests

Test	Lime percentages (%)	Curing days	Mellowing days	Total test
Atterberg limits	0, 1, 2, 3, 4	0, 7, 28	-	12
pH	0, 1, 2, 3, 4	0, 7, 28	-	12
CEC	0, 1, 2, 3, 4	-	-	12
Specific gravity	0, 1, 2, 3, 4	-	-	12
Hydrometer	0, 2, 4	-	-	3
Compaction	0, 4	1	1	2
UCS	0, 1, 2, 3	0, 7	3, 7	13

3.2.1. Atterberg Limits

The Atterberg limits identify moisture content boundaries between states of consistency of fine-grained soils. The moisture contents at the boundaries between the different states are defined as the shrinkage, plastic and liquid limits.

The liquid limit (LL), plastic limit (PL), and plasticity index (PI) of soils are also used extensively, either individually or together, with other soil properties to correlate with engineering behavior such as compressibility, hydraulic conductivity (permeability), compactibility, shrink-swell, and shear strength (ASTM D4318-10, 2010).

Atterberg limits tests were conducted in accordance to the testing procedure detailed by standard ASTM D4318-10 (2010). These tests were conducted in order to determine the plasticity properties of the untreated Eagle Ford clay and lime-treated of clay with different percentages of lime.

The plastic limit (PL) was determined by rolling out a thread of the fine portion of a soil (passing through a No. 40 sieve) on a flat, non-porous surface. If the soil was at moisture content where its behavior was plastic, this thread retained its shape down to a very narrow diameter. The thread soil was remolded making the moisture content fell down due to evaporation. The test was repeated until the thread begins to break apart at larger diameters. The plastic limit was defined as the moisture content where the thread broke apart at a diameter of 3.2 mm approximately.

The liquid limit (LL) was defined as the moisture content at which the behavior of a clayey soil changes from plastic to liquid. The LL was determined using the Casagrande's apparatus and material passing through a 475 μ m (No. 40) sieve. Untreated and lime-treated soils were mixed at various water contents, placed and spread in a uniform manner in the brass cup, and then a groove of determined size was carved down the sample vertically. Once the sample was prepared in the cup, the apparatus arm was cranked at a rate of 2 cycles per second to induce drop blows to the sample. The number of blows was counted until the groove was closed. The number of blows for each water content value was collected and plotted on a log plane. The moisture content pertaining to 25 blows on the plot was considered the liquid limit of the material.

The plastic index (PI) was defined as the moisture content where the soil exhibits plastic properties. Its value was computed as the difference between the liquid limit and the plastic limit ($PI = LL - PL$).

3.2.2. Chemical Tests

In order to understand the chemical and mineralogical changes associated with lime treatment in expansive soils, simple tests to analyze the Cation Exchange Capacity (CEC) by blue methylene test and pH were performed, as described in the following sections.

3.2.2.1. pH Test

The pH test was conducted in accordance with the TxDOT Designation: Tex-121-E (TxDOT, 2002). This test allows determining the minimum of lime percentage needed for a lime-soil mixture to attain a pH of 12.4. This percentage of lime represents a rough approximation of the optimum lime content need to pozzolanic reactions with clay soil.

The pH of untreated and lime-treated soils was tested using a Thermo Scientific Orion ROSS ultra pH electrode with a pH range of 0-14, temperature range of 0° to 100°C, and precision of 0.01. The pH meter was calibrated with manufactured buffer solutions of known pH (4.01, 7.00 and 10.01). The pH meter probe, stir plate and solutions can be seen in Figure 3.2.

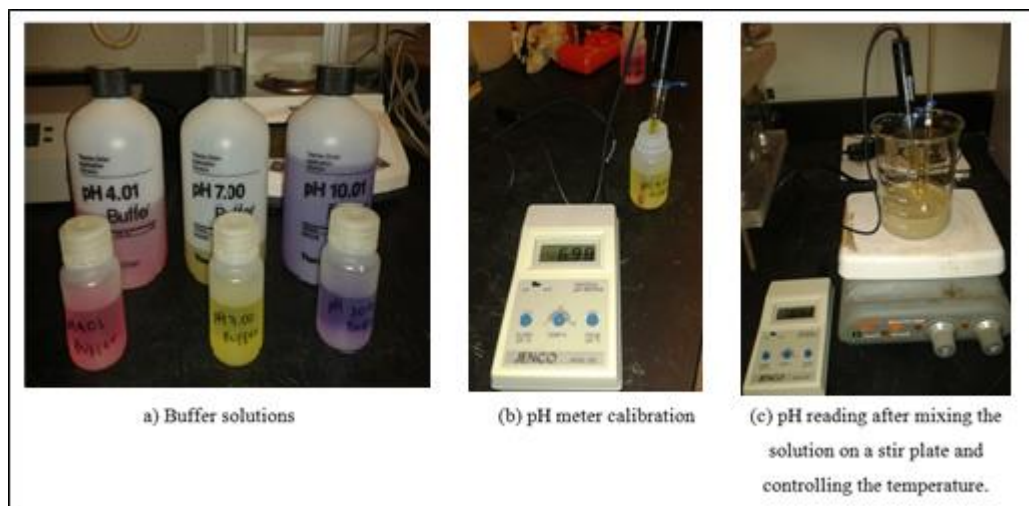


Figure 3.2. Determination of pH

The solutions for testing pH were prepared placing 30g samples of soil and the quantity of lime equivalent to 0, 1, 2, 3 and 4% of the total dry soil sample, and adding 150 ml of distilled water to each combination. The distilled water was

previously heated to 45-60°C. Each solution was stirred using a stir plate for 1 hour to disperse the soil and make sure all soluble material was in solution. At the end of an hour, the temperature of the mixture was recorded and the pH meter was adjusted at that temperature. The electrode was cleaned with distilled water before each pH reading.

3.2.2.2.

Blue Methylene Test

The Cation Exchange Capacity (CEC) is defined as the sum of the exchangeable cations and expressed as milliequivalents per 100g of soil. The excess in negative electric charges, attached to the clay particle, attracts cations (positive ions) towards the surface of the clay producing ionic exchange phenomena. This can take place between the easily exchangeable cations of the clay and the cations released by methylene blue upon being dissolved in water.

Cation exchange is also an important reaction in lime treatments. Low valence cations are replaced by high valence and small cations are replaced by big cations having the same valence. When sufficient lime is added to the soil, the calcium cations from lime replace weak cations from the soil. This cation exchange reduces the thickness of diffuse water layer surrounding the clay particle, thus clay particles come closer to each other and flocculation-agglomeration occurs.

The methylene blue stain test allows quantifying the ionic absorption capacity of a soil by measuring the quantity of methylene blue required to cover the total (external and internal) surface of the clay particles contained in the soil.

In this study, the methylene blue stain test described by French Standard AFNOR NF P 94-068 (1998) was selected to measure the CEC, because this standard has been successfully applied in different studies about lime-treated soils (Chiappone, 2004; Cambi, 2012).

AFNOR standard test is based on the same test procedure established in the standard test method for methylene blue index of clay described in ASTM C837-09 (2014). The ASTM and AFNOR testing procedures differ in terms of the quantity of material to be analyzed and the concentration of the methylene blue solution. The ASTM testing procedure is recommended for high clay content samples and homogeneous materials where small samples are representatives.

Furthermore, the ASTM procedure has to be performed in controlled pH conditions (acid environment). These last two conditions about material homogeneity and acid environment make difficult the use of ASTM standard to measure the CEC of lime-treated soils.

Following the AFNOR standard, the blue methylene was conducted taking 10g of soil dissolved in 500ml of distilled water. The methylene blue solution was prepared with 10g/L concentration and added to the soil sample solution 5 by 5ml. After 1 minute of blue methylene addition, one drop of the mixture solution was placed onto the filter paper. The test was ended when the dye forms a second light blue halo around the aggregate-dye spot and stayed stable for 2 minutes. This reflects the presence of an excess quantity of methylene blue that is no longer absorbed by the clay minerals and remains in suspension. Figure 3.3 shows an example of a methylene blue test and how to recognize the end of the test.

The Cation Exchange Capacity (CEC) is calculated as the methylene blue index as follows:

$$CEC \left(\frac{meq}{100 g} \right) = \frac{EV}{W} \times 100 \quad (3.1)$$

where:

CEC: Cation Exchange Capacity in meq/100g clay

E: milliequivalents of methylene blue per milliliter (0.0268 meq/ml)

V: milliliters of methylene blue solution required for the titration, and

W: grams of dry material (10 g)

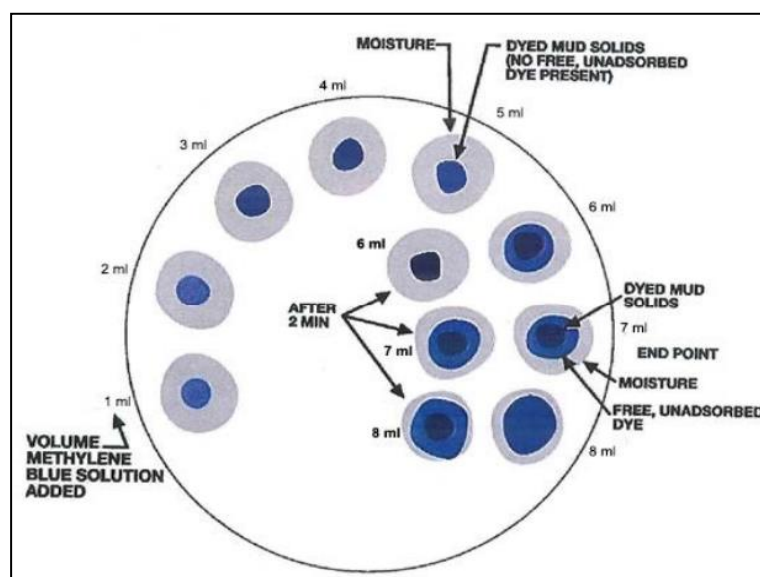


Figure 3.3. Example of a methylene blue test

3.2.3. Specific Gravity

The specific gravity testing was conducted in accordance with standard Specific Gravity of soil Solids by Water Pycnometer described in ASTM D854-14 (2014). This procedure determines the specific gravity of a soil that is the ratio of the weight in air of an aggregate unit volume to the weight in air of an equal volume of distilled water, both at a determined temperature.

Air-dried expansive soil was weighed to a specific amount per the standards and placed in the pycnometer (50 grams). The pycnometer was then filled with distilled water until the specific mark. The sample in the pycnometer was placed under a vacuum for 15 minutes in order to remove the entrapped air bubbles. After that, the pycnometer was placed into water bath for at least 12 hours (overnight). Finally, the mass of the pycnometer plus soil and water was recorded in order to determine the specific gravity (G_s) as shown in the following equation.

$$G_s = (W_2 - W_1) / [(W_2 - W_1) - (W_3 - W_4)] \quad (3.2)$$

where:

W_1 = Empty weight of pycnometer

W_2 = Weight of pycnometer + oven dry soil

W_3 = Weight of pycnometer + oven dry soil + filled water

W_4 = Weight of pycnometer + filled with water only

3.2.4. Hydrometer Test

Hydrometer test was carried out in accordance to the standard method for particle size analysis of soils described by ASTM D422-63 (2007). This test was conducted in order to determine the effect of lime treatment on particle size distribution.

The method requires taking 50g of air dried soil passed through a No. 200 sieve and mixing it with a solution containing 4% of dispersing agent (sodium hexametaphosphate solution) and soaking it for about 24 hours. At the end of the soaking period, the prepared soil was thoroughly mixed in a stirring apparatus (Figure 3.4 (b)), and all the soil solids inside the mixing cup were transferred to a graduate cylinder and filled with distilled water until the total volume was 100ml

(Figure 3.4 (a)). The slurry was agitated during one minute and after that the hydrometer readings were recorded at cumulative times of 2, 5, 15, 30, 60, 250 and 1440 minutes.



Figure 3.4. Hydrometer test

3.2.5. Standard Proctor Compaction Tests

The compaction test was conducted in accordance with ASTM D698-12 (2012). This test method is used to determine the relationship between moisture content and dry density of soils. The two important values calculated by this test are: the Maximum Dry Density (MDD) and the Optimum Moisture Content (OPT). The MDD is the maximum value obtained by the compaction curve using the specified compactive effort and the OPT is the moisture content at which the soil can be compacted to the MDD.

The standard Proctor test was conducted using a mechanical compactor model G-132-M100, manufactured by Ploog Engineering. This compactor automatically compacts and rotates the mold that contains the soil after each blow. It is able to track the number of hammer blows and to stop when the required number of blows is reached. The compactor was used to perform standard compaction tests using a 5.5lb (2.5kg) hammer with 12 inches (305mm) height of drop.

The lime-soil mixtures were prepared 24 hours before compaction test in order to allow the complete lime reactions and the moisture equilibration. The soil,

previously prepared at five different moisture contents, was compacted in three layers using a mold with volume of 944cm^3 , internal diameter of 10cm, and height of 11.68 cm. Once compaction was completed, the collar was removed and the soil excess was trimmed until the top of the sample is uniform and flat. The weight of the mold and sample was then recorded and the sample was extruded from the mold using a hydraulic jack. Once the sample was extruded, its actual moisture content was measured.

3.2.6. Unconfined Compressive Strength (UCS) Test

The Unconfined Compressive Strength (UCS) is the most widely used property in order to evaluate soil strength. The UCS test was conducted according the procedure described by ASTM D2166 (2013). This test allows to obtain quick measure of compressive strength for those soils that possess sufficient cohesion to permit tests in an unconfined state.

The UCS tests were conducted on compacted soil specimens of 1.5 inches (3.8 cm) in diameter and 3 inches (7.6 cm) in height. The samples used in UCS tests were compacted using a divided mold and a special hammer that provides the same effort as the traditional standard Proctor hammer (Figure 3.5). This compaction was performed placing the soil into the mold in three layer of approximately equal thickness, and each layer received 25 blows of a 1.5kg hammer. At the end of compaction, the specimen was wrapped in a plastic inside of an aluminum foil and stored for curing in an environmental chamber at 23°C and 70% of relative humidity.



Figure 3.5. Divided molds and hammer for UCS specimen preparation

The UCS measurement was performed using an automated loading system by GeoJac, as shown in Figure 3.6. The strain rate for the tests was 1% per minute for all samples. Once broken, the samples were kept for X-Ray Diffraction (XRD) and Environmental Scanning Electron Microscopy (ESEM) tests described later in sections 3.4.1 and 3.4.2, respectively.



Figure 3.6. Automated loading system by GeoJac

3.3. Swelling Potential Tests

The swelling potential tests were carried out using two different methodologies: the conventional free swell test and the centrifuge test. The effects of curing time and mellowing period were evaluated using the conventional free swell test, because de samples needed to be compacted directly into the ring and kept for long periods. It was not convenient to use the rings from centrifuge equipment for this purpose, because the centrifuge would be stopped for long time waiting the curing to be done.

The centrifuge test was used to evaluate the effect of compaction moisture condition, compaction dry density (relative compaction – RC %) and effective stress (by g-level) on swelling behavior of the expansive soil treated with different percentages of lime. Table 3.3 and Table 3.4 report the total of tests done with each of these methodologies.

Table 3.3. Experimental plan of conventional free swell tests

Set No.	Curing time (days)	Mellowing period (days)	Percentages of lime (%)	Tests done
1	0	0	0, 0.5, 1.0, 1.5, 2.0, 2.5, 3.0, 3.5, 4.0	9
2	1, 7, 28	0	1.0, 2.0, 3.0, 4.0	12
3	7	3, 7	1.0, 3.0	4
Total Conventional free swell tests				25

Table 3.4. Experimental plan of centrifuge tests

Set No.	g-level	Compaction moisture condition	Compaction dry density (RC %)	Percentage of lime (%)	Test done
1	5	DOP; OPT; WOP	100%	0, 0.5, 1, 2, 3, 4	18
2	5	OPT	100%; 94%	0, 0.5, 1, 2, 3, 4	6
3	5; 50; 200	OPT	100%	0, 1, 2	6
Total Centrifuge Tests					30

3.3.1. Conventional Free Swell Test

The conventional free swell test was conducted according to ASTM D4546-08 (2008) using a standard consolidation frame from Wykeham Farrance Engineering, shown in Figure 3.7. A typical assembly of a consolidation cell used in conventional free swell test is depicted in Figure 3.8. The conventional free swell test is described as follows. The soil specimen was compacted in a metal ring, which was prepared with vacuum grease to eliminate the friction between soil and the ring wall (Figure 3.9). Filter paper was placed in the top and bottom of compacted soil specimen in order to avoid clogging. The metal ring was placed between two porous stones and held into a water reservoir by a clamping flange secured with a series of knurled clamping nuts (Figure 3.10). The specimen compaction procedure is described in Figure 3.9 and the consolidation cell assembly is displayed in Figure 3.10.



Figure 3.7. Standard consolidation frame used for conventional free swell testing

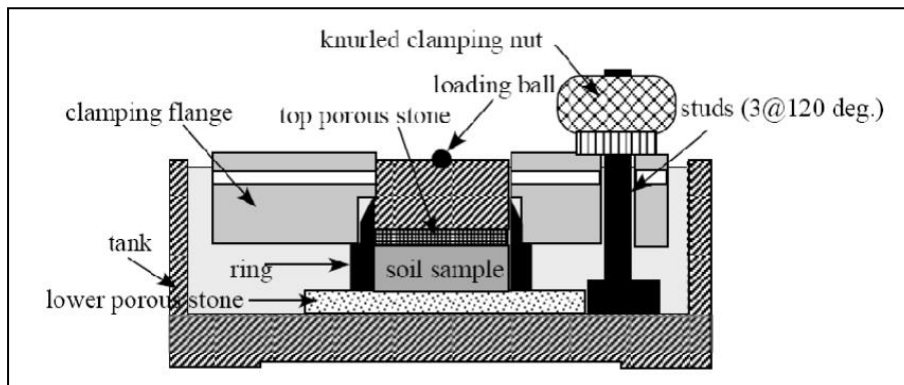


Figure 3.8. Consolidation cell diagram (Zornberg *et al.*, 2009)

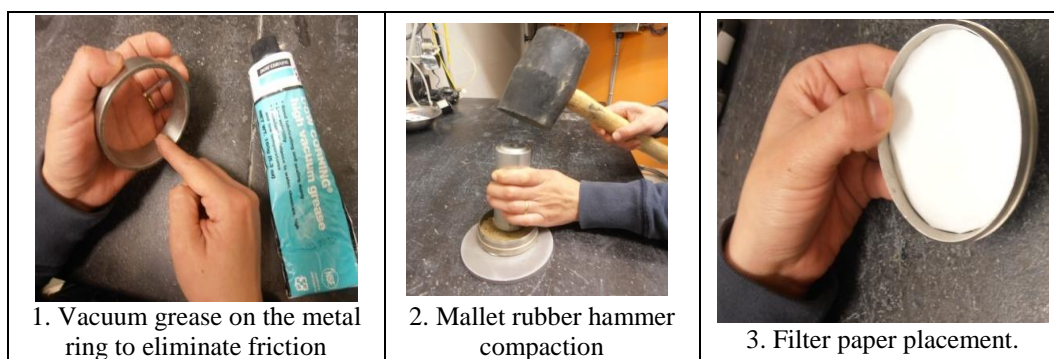


Figure 3.9. Compaction specimen procedure

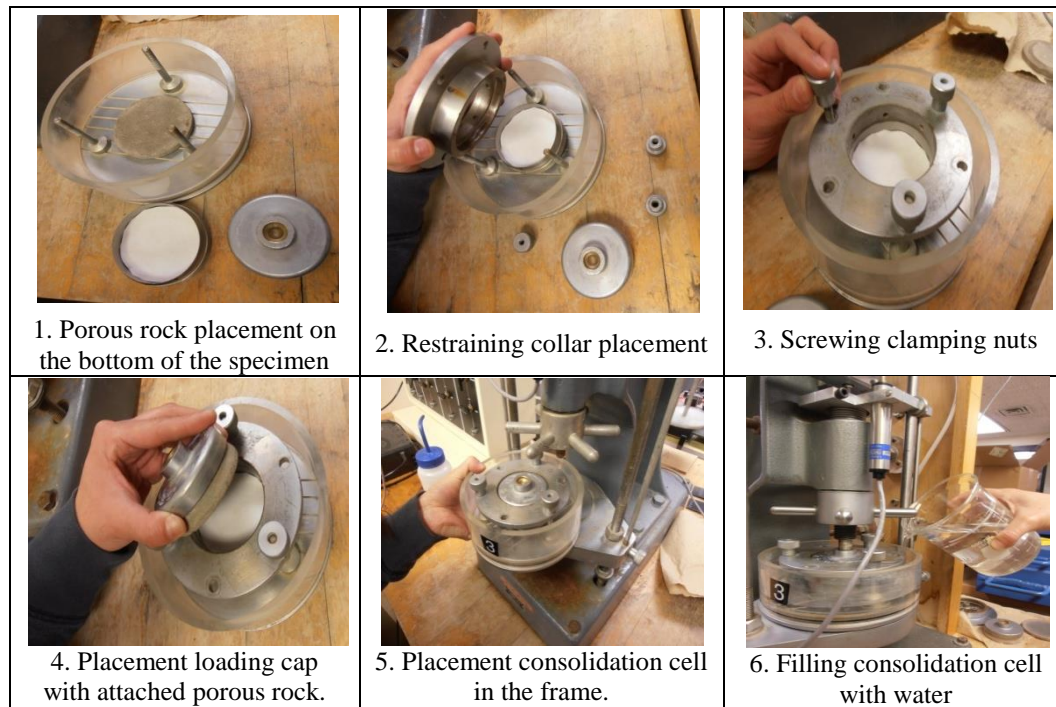


Figure 3.10. Consolidation cell assembly

After the consolidation cell and the specimen were placed into the frame, the setting load was applied and the specimen height was monitored. Once the specimen height was equilibrated, the data logging was started and tap water was added to the reservoir in which the soil specimen was sitting. The height variation of the specimen was taken via dial gauge and a linear variable differential transformer (LVDT) in order to generate swelling vs. time curves.

3.3.2. Centrifuge Test

The centrifuge test for evaluating swelling behavior of expansive soils is a new technique developed at the University of Texas at Austin. Recent researches have demonstrated that the use of centrifuge can be useful in the characterization of expansive soils (Walker, 2012; Armstrong, 2014; Das, 2014; Snyder, 2015). The centrifuge allows testing up to six soil specimens simultaneously, which facilitates the repeatability of results among identical specimens in order to obtain more reliable results. The rotation of the specimen within the centrifuge imposes a gravitational gradient across it by accelerating the water flow. Thus, the centrifuge testing can take short time to permeate the water into the specimen and to enter into the microporous structure of the soil.

3.3.2.1. Centrifuge Set-Up

The centrifuge set-up is composed by a Damon IEC CRU-5000 centrifuge with a Model 259 rotor, a Data Acquisition System (DAS), six centrifuge cups and a control board. Figure 3.11 shows an external and internal view of the centrifuge. The control board has knobs for controlling the speed and temperature, and buttons to start and stop the rotation. The centrifuge's rotor allows hanging the metal centrifuge cups that contain the specimens and let them spin perpendicular to axis of rotation of the centrifuge. The specimens are subjected to an increased gravitational field induced by the rotation within the centrifuge that is able to reach g-levels up to 200g's.

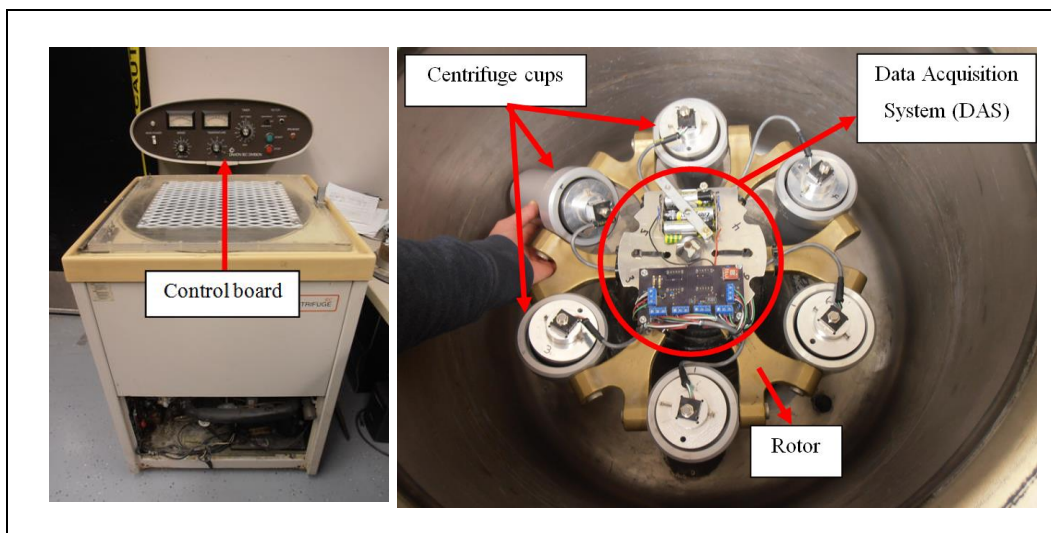


Figure 3.11. Damon IEC CRU-5000 centrifuge: external view (left) and internal view (right)

Figure 3.12 shows the Data Acquisition System (DAS) components. The DAS includes a battery supply, an accelerometer, an analog to digital converter and a Linear Position Sensors (LPS). The LPS is attached at the lid of the centrifuge cup and is used for monitoring the vertical deformations of the soil specimens. The DAS is able to transmit wirelessly the sensors data to a computer, which records voltage values over time from LPS and accelerometer.

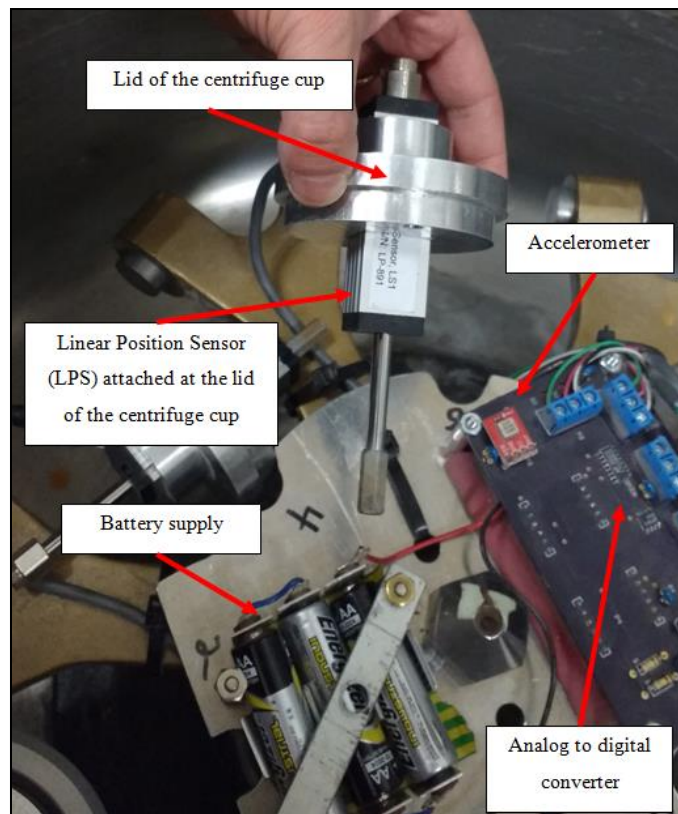


Figure 3.12. Data Acquisition System (DAS) components

3.3.2.2. Specimen Preparation

In order to conduct the centrifuge test, the specimen preparation was carried out using the tools set showed in Figure 3.13. The compaction specimen procedure shown in Figure 3.14 is described as follows. The metal ring was prepared applying vacuum grease to reduce the friction between the specimen and ring walls during testing. Afterwards, the ring was assembled with a brass porous disk and a filter paper, and the soil was poured into the ring using a funnel. The soil mass required to achieve the desired dry density was controlled with a scale.

The specimen was compacted to 1cm height and 5cm diameter into the metal ring using a rubber mallet and a cylindrical compactor. The specimen height was constantly monitored across the specimen surface using a caliper. The specimen height established was 1cm based on previous works (Plaisted, 2009; Kuhn, 2010), because that height has shown to reduce the testing durations and keeps the accurate and consistent swelling test results.

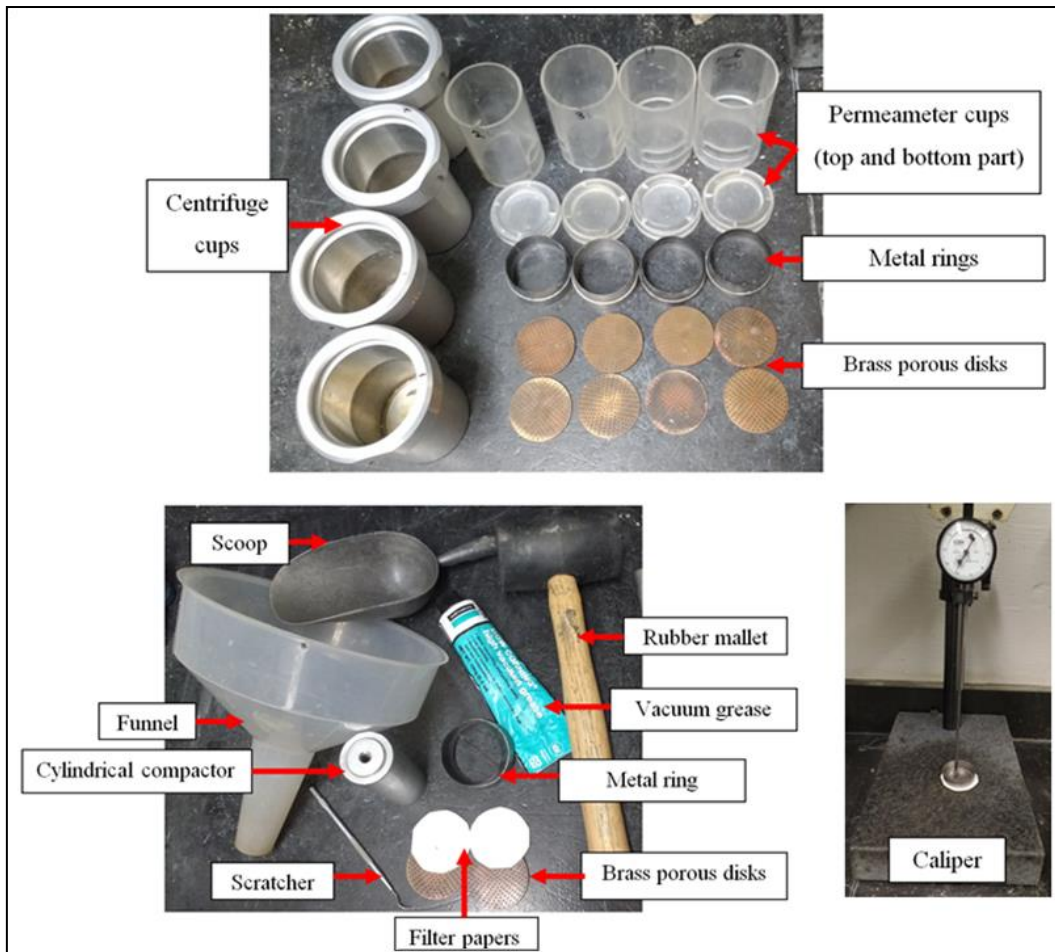


Figure 3.13. Tools set for specimen preparation

Once the specimen height was reached, the remained soil on the ring wall was removed using a scratcher. Finally, the specimen preparation was completed placing a second filter paper and brass porous disk on the top of the specimen. These brass porous disks were used to increase the applied effective stress and the filter papers to avoid the soil migration.

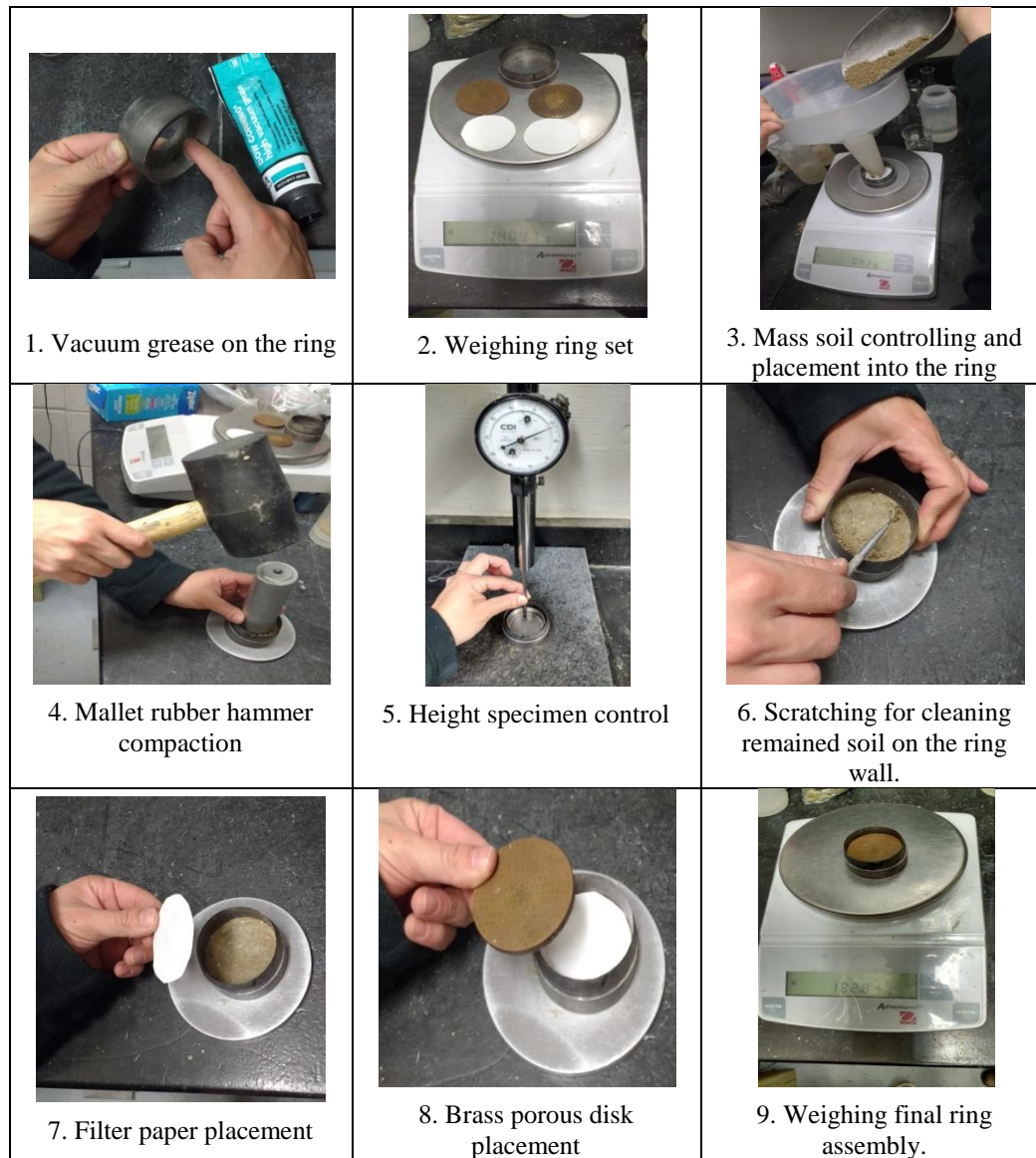


Figure 3.14. Compaction specimen procedure

3.3.2.3. Testing Procedure

After specimen compaction, each ring was placed into a permeameter cup, which allows water infiltration from both sides, i.e., the top and base side of the specimen. Thus, the permeameter cup was inserted into the centrifuge cup in order to be hung on the centrifuge arms rotor. The lid of the centrifuge cup was placed to close the permeameter cup in order to finalize the testing assembly (Figure 3.15). Afterwards, the centrifuge was turned on and a *LabView*² program was started to

² <http://www.ni.com/labview/>

acquire the LPS and accelerometer data. A screenshot of the *LabView* program is shown in Figure 3.16 and details about it can be found in Walker (2012).

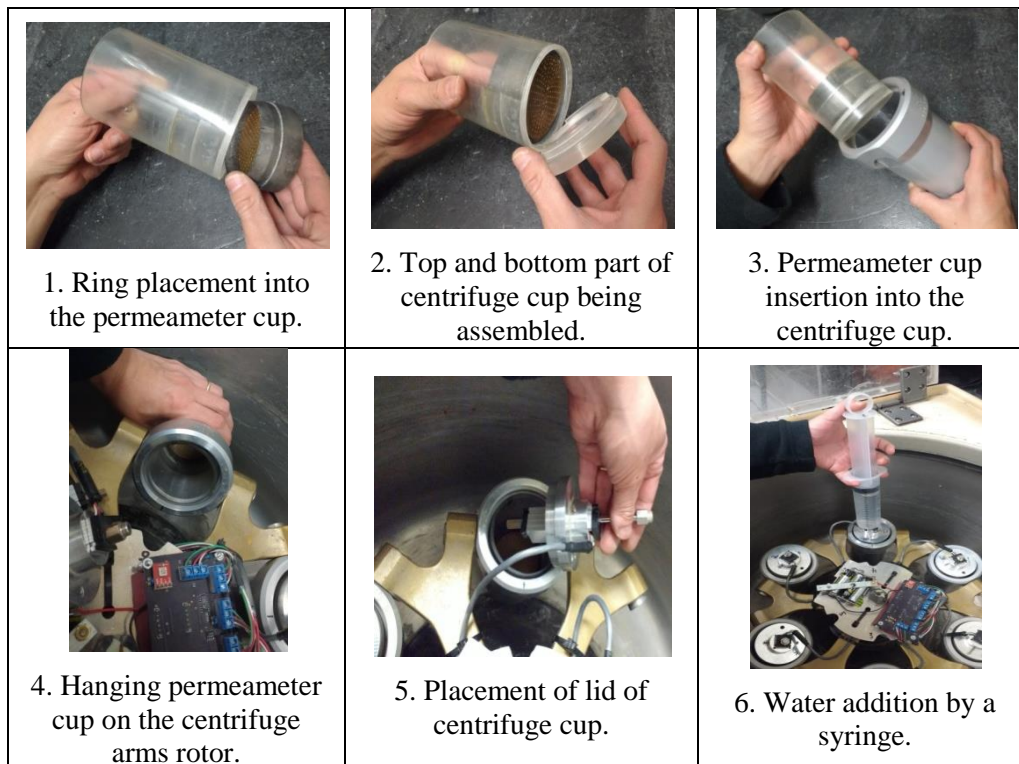


Figure 3.15. Centrifuge cup preparation and testing assembly.

The specimens were spun into the centrifuge applying g-level between 2 and 3g's in order to apply a seating load during 5 minutes. This time have been demonstrated to be enough to guarantee the full contact between all the assemblage components, porous disks, filter papers and soil specimen (Walker, 2012; Armstrong, 2014). After the seating load cycle was completed, the g-level was adjusted for the desired testing g-level. At the desired g-level, the specimen underwent a compression for approximately an hour, or until the compression reached the original height specimen. After the compression cycle was completed, the centrifuge was stopped and around 80 grams of distilled water were added to the specimen, using a syringe, through a little hole on the lid of the cups (Figure 3.15). After that, the centrifuge was restarted and allowed to spin for approximately 24 hours. During this time, the water was infiltrated into the specimen generating the soil expansion.

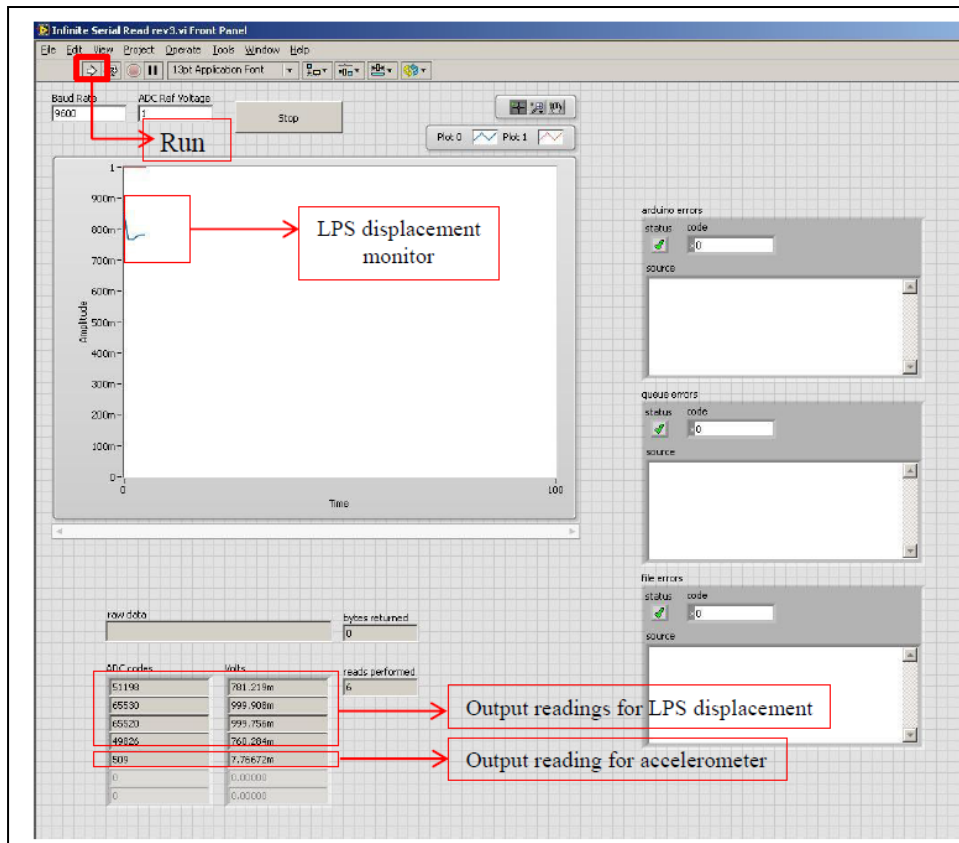


Figure 3.16. Screenshot of *LabView* program monitoring a centrifuge test (Walker, 2012)

When the centrifuge test was finalized, the centrifuge cups were removed to record the final weights of the total assembly and permeameter cups. The water in the cup was poured out and the metal ring with the specimen was taken out. The porous disks were removed and the solids dry mass was determined placing the metal ring, wet specimen and filter papers into the oven at 110°C.

3.3.2.4. Typical Results

The Data Acquisition System (DAS) records voltage data from the LPS and the accelerometer through the *LabView* program. These data were converted in specimen height and g-level using a Python script, developed by Plaisted (2009) and modified by Armstrong (2014). Thus, the converted data were exported in a text file that can be analyzed using an Excel spreadsheet. The g-level average can be determined by the recorded data, and the swelling percent can be calculated

based on the deflections registered by the LPS. A typical result from centrifuge test is shown in Figure 3.17.

As described by Armstrong (2014), there are four general regions in the centrifuge test as labeled in Figure 3.17. The first region is the application of the seating load at which there is very little change in strain observed due to the small amount of stresses applied (g-level between 2 and 3g's). The second region corresponds to the compression load application in order to attain the initial specimen height. There is a gap between the second and third region that represents the time when the centrifuge is stopped in order to add water into the specimen. The third region represents the primary swelling undergone by the specimen and the fourth region corresponds to the secondary swelling.

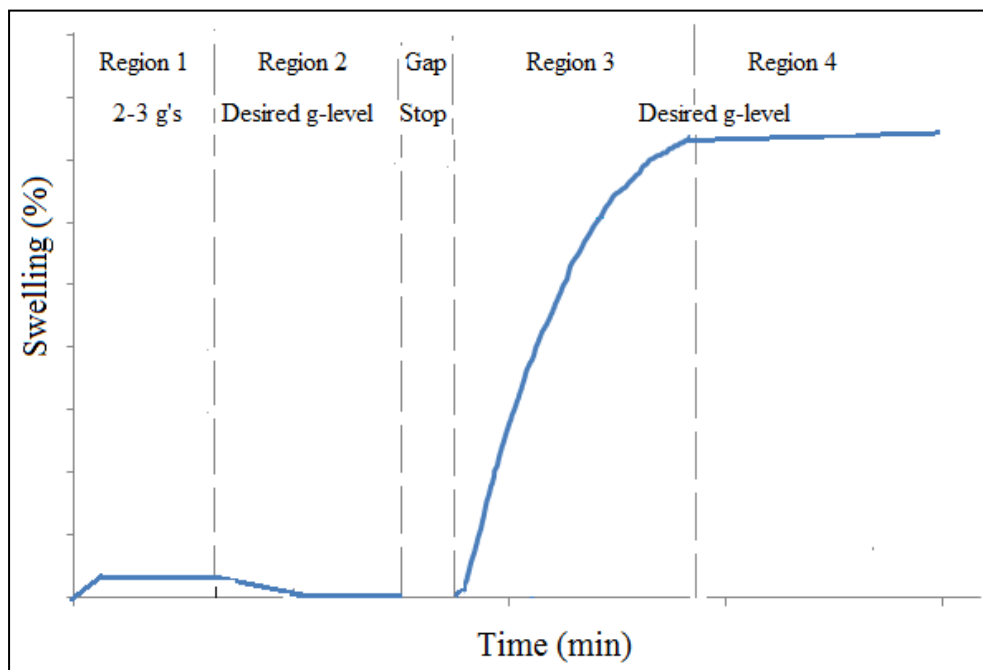


Figure 3.17. Typical result from centrifuge test

Even though the typical results were obtained in this way, only the third and fourth regions were considered interesting to analyze the behavior of expansion during the centrifuge test. Furthermore, in the next chapter, the analysis of expansive behavior over time is facilitated by plotting the swelling vs. time data with logarithmic scale to represent the time.

3.3.2.5. Measured Variables and Calculated Properties

The input variables during the centrifuge test were centrifuge cup mass, the soil mass before and after testing, the specimen height after compaction, the change in specimen height during testing, and the g-level from the accelerometer in the centrifuge. From these input variables, the calculated properties were the swelling during the testing, the initial and final moisture content, the initial and final void ratio, the initial and final saturation, the initial dry density, the initial and final volume, primary and secondary swelling slopes, and the equivalent stress felt in the specimen. Table 3.5 contains the equations used for processing the testing data.

Table 3.5. Equations for properties calculation in centrifuge test (Armstrong, 2014)

Property	Equation	Variables
Initial Height, h_i	$h_i = h_c + (\Delta h_{cs} - \Delta h_s)$	h_c Height of sample at compaction Δh_{cs} Change in height of sample at the end of compression Δh_s Change in height of sample at end of seating load
Strain or Swelling, S	$S = \frac{\Delta h_t}{h_i} * 100\%$	Δh_t Change in height of sample at time, t
Volume, V	$V = (h_c + \Delta h_t) * A$	A Area of sample
Dry Density of Soil, ρ_d	$\rho_d = \frac{m_s}{V_f} \frac{1}{1 + \omega_i}$	m_s Mass of soil at beginning of the test ω_i Initial moisture content of soil V_f Final Volume
Void Ratio, e	$e = \frac{SG * \rho_w}{\rho_d} - 1$	SG Specific Gravity of the Soil ρ_w Density of Water
Saturation, S	$S = \frac{SG * \omega}{e}$	
Slope of Swelling Curve, s	$s = \frac{\Delta h_{t2} - \Delta h_{t1}}{\ln(t_2) - \ln(t_1)} * \ln(10)$	Δh_{ti} Change in height at time i t_i Time i

The equivalent effective stress (σ'_{eq}) represents an average of the effective stress undergone through the specimen from the top to the bottom. As reported by Plaisted (2009), the equivalent effective stress can be calculated by equation (3.3), which assumes a log-linear variation between the effective stress on the top (σ'_t) to the effective stress on the bottom (σ'_b) of the specimen:

$$\sigma'_{eq} = (\sigma'_b - \sigma'_t) * \left[\frac{\frac{1}{e} SR^{\left(\frac{1}{SR-1} + 1\right)} - 1}{SR - 1} \right] + \sigma'_t \quad (3.3)$$

where SR is the stress ratio ($SR = \sigma'_b / \sigma'_t$).

In order to calculate the equivalent effective stresses, by application of the principle of effective stress introduced by Terzaghi, the total stresses (σ_t and σ_b) and pore pressures ($u_{(t)}$ and $u_{(b)}$) at top and bottom of the specimen need to be calculated as function of the centripetal acceleration (ω) undergone by the specimen into the centrifuge.

The total stresses (σ_t and σ_b) were calculated as follows. First, it should be considered that the centripetal acceleration experimented in the specimen is calculated as shown in equation (3.4):

$$a_c = \omega^2 * r = N * g \quad (3.4)$$

where a_c is the centripetal acceleration, ω is the angular velocity, r is the radial distance from the central axis in the centrifuge, N is the artificial g-level that represents the scalar factor between the centripetal acceleration and the standard acceleration of gravity, and g symbolizes the standard gravitational acceleration. Since the gravitational acceleration (a_c) varies with the radius (r), the unit weight (γ) varies along the specimen's height as follows:

$$\gamma = \rho_s * a_c = \rho_s (\omega^2 * r) \quad (3.5)$$

The density (ρ_s) was assumed to be constant throughout the specimen and is calculated by equation (3.6):

$$\rho_s = \frac{[(V_f - V_d) * \rho_w] + (SG * \rho_w * V_d)}{V_f} \quad (3.6)$$

with V_f being the final volume of the soil specimen, V_d being the dry volume of the soil specimen, SG being the soil specific gravity, and ρ_w being the density of water (1 g/cm³). Considering this assumption, the total stress ($\sigma_{(r)}$) caused by the soil at

any point through the soil mass can be calculated by integrating the unit weight (equation (3.5)) and adding the pressure exerted at the top of the soil (σ'_{ob}) as shown in equation (3.7).

$$\sigma(r) = \sigma'_{ob} + \int_{r_t}^r (\rho_s * \omega^2 * r) dr = \sigma'_{ob} + \frac{1}{2}(\rho_s * \omega^2)(r^2 - r_t^2) \quad (3.7)$$

Consequently, the total stress at the top σ_t and bottom σ_b of the specimens are defined by equations (3.8) and (3.9), respectively, with r_b being distance from the central axis in the centrifuge to the bottom of the specimen and r_t to the top of the specimen (Figure 3.18).

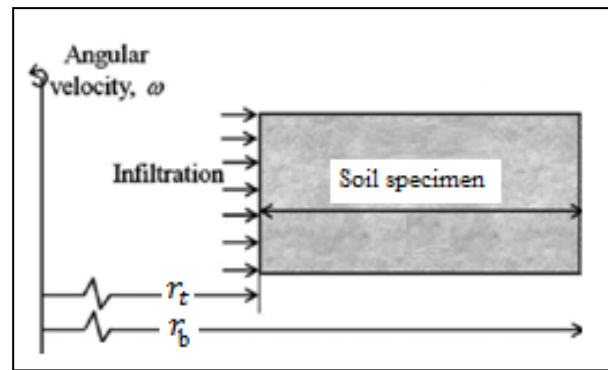


Figure 3.18. Schematic view of soil specimen into the centrifuge

$$\sigma_t = \sigma'_{ob} + \frac{1}{2}(\rho_s * \omega^2)(r_t^2 - r_t^2) = \sigma'_{ob} \quad (3.8)$$

$$\sigma_b = \sigma'_{ob} + \frac{1}{2}(\rho_s * \omega^2)(r_b^2 - r_t^2) \quad (3.9)$$

The σ'_{ob} value represents the effective overburden stress and takes into account the overburden from the linear position sensor (LPS), porous disk and the water column above of the specimen. The calculation of this value is made as described below.

Since the cutting ring is submerged, it must be taking into account the buoyant, and not the total weight of the overburden. For the LPS rod, the overburden mass ($m_{rod,b}$) is taken as follows:

$$m_{rod,b} = \frac{\pi d_{rod}^2}{4} \quad (3.10)$$

$$* [(h_{rod} - h_w) * SG_{Al} * \rho_w - (SG_{Al} - 1) * h_{rod} * \rho_w]$$

where d_{rod} is the rod diameter (0.495cm), h_{rod} is the rod height (13.1 cm), h_w is the water height above of the specimen, and SG_{Al} is the specific gravity of the aluminum (2.70), which is the rod material.

The overburden mass of the brass porous disk is calculated based on the porous disk volume (V_{brass}). The V_{brass} is calculated by taking the mass of the dry porous disk and dividing it by the specific gravity of the brass (8.42). So, the submerged mass of the porous disk ($m_{pd,b}$) is determined as follows:

$$m_{pd,b} = (SG_{brass} - 1) * V_{brass} \quad (3.11)$$

Thus, the effective overburden stress (σ'_{ob}) at the top of the specimen can be calculated as indicated in (3.12):

$$\sigma'_{ob} = \frac{m_{ob} * a_c}{A_s} = \frac{(m_{rod,b} + m_{pd,b})\omega^2 r_t}{A_s} \quad (3.12)$$

where, A_s is the soil specimen area.

The pore pressures at top and bottom of the specimen ($u_{(t)}$ and $u_{(b)}$, respectively) are calculated as described below. According to Dell'Avanzi *et al.* (2004), the discharge velocity (v_c) of water through the soil specimen can be calculated as follows:

$$v_c = -\frac{k_s}{g} * \frac{\delta\Phi_c}{\delta r} \quad (3.13)$$

where k_s is the saturated hydraulic conductivity, g is the gravitational constant and $\frac{\delta\Phi_c}{\delta r}$ is the gradient in fluid potential at radius (r). Taking the specimen base (r_b) as the elevation datum, the fluid potential (Φ_c) can be calculated as shown in equation (3.14):

$$\Phi_c = \frac{1}{2} * \omega^2 * (r_b^2 - r^2) + \frac{u_{(r)}}{\rho_w} \quad (3.14)$$

with $u_{(r)}$ being the pore water pressure in the specimen at a radius (r). Thus, the gradient of the soil can be calculated by derivation of the equation (3.14) with respect to the radius r , as shown in equation (3.15). Substituting this result in equation (3.13), the discharge velocity equation (v_c) is calculated in (3.16):

$$\frac{\delta\Phi_c}{\delta r} = -\rho_w * \omega^2 * r + \frac{\delta u_{(r)}}{\delta r} \quad (3.15)$$

$$v_c = -\frac{k_s}{g} * \left(-\rho_w * \omega^2 * r + \frac{\delta u_{(r)}}{\delta r} \right) \quad (3.16)$$

Assuming that the discharge velocity remains constant over the radius as the volumetric moisture content stays the same with time, due to saturation, the derivative of equation (3.16) with respect to the radius becomes as follows:

$$\frac{\delta v_c}{\delta r} = 0 = \frac{k_s * \rho_w * \omega^2}{g} - \frac{k_s}{g} * \frac{\delta^2 u(r)}{\delta r^2} \quad (3.17)$$

The saturated hydraulic conductivity (k_s) and the gravity acceleration (g) both were cancelled out, so equation (3.17) is left with:

$$\rho_w * \omega^2 = \frac{\delta^2 u(r)}{\delta r^2} \quad (3.18)$$

which, when integrated, becomes:

$$u(r) = \frac{1}{2} \rho_w \omega^2 r^2 + C_1 r + C_2 \quad (3.19)$$

Since the top and bottom of the specimen are connected in the permeameter cup and the pore water pressure is known, the boundary conditions can be imposed for C_1 and C_2 using the equations (3.20) and (3.21) in order to calculate the water pressure at any given point:

$$P_1 = \frac{1}{2} \rho_w \omega^2 (r_t^2 - r^2) = u(t) \quad (3.20)$$

$$P_2 = \frac{1}{2} \rho_w \omega^2 (r_b^2 - r^2) = u(b) \quad (3.21)$$

It should be considered that r_0 is taken as the radius from the central axis to the top of the water above of the specimen. Thus, the resulting constants C_1 and C_2 can be determined as follows:

$$C_1 = \frac{P_2 - P_1 + \frac{1}{2} \rho_w \omega^2 (r_t^2 - r_b^2)}{r_b - r_t} \quad (3.22)$$

$$C_2 = P_1 - \frac{1}{2} \rho_w \omega^2 r_t^2 - C_1 r_t \quad (3.23)$$

Finally, the equation (3.24) allows to calculate the pore water pressure through the specimen:

$$u(r) = \frac{1}{2} \rho_w \omega^2 (r^2 - r_t^2) + \frac{P_2 - P_1 + \frac{1}{2} \rho_w \omega^2 (r_t^2 - r_b^2)}{r_b - r_t} (r - r_t) + P_1 \quad (3.24)$$

The pore pressures at top $u(t)$ and bottom $u(b)$ of the specimen were obtained by replacing, r with r_t or r with r_b , respectively, in equation (3.24), as follows:

$$u(t) = P_1 = \frac{1}{2} \rho_w \omega^2 (r_t^2 - r_t^2) = 0 \quad (3.25)$$

$$u(b) = \frac{1}{2} \rho_w \omega^2 (r_b^2 - r_t^2) + \frac{1}{2} \rho_w \omega^2 (r_t^2 - r_b^2) \quad (3.26)$$

The total pressures (equations (3.8) and (3.9)) and the pore pressures (equations (3.25) and (3.26)) at the top and bottom of the specimen are already known. Consequently, the effective stresses at the top (σ'_t) and bottom (σ'_b) of the specimen can be calculated as indicated in equations (3.27) and (3.28), respectively. So that, the equivalent effective stress defined in equation (3.3) can be calculated.

$$\sigma'_t = \sigma'_{ob} \quad (3.27)$$

$$\sigma'_b = \sigma'_{ob} + \frac{1}{2}\rho_s\omega^2(r_b^2 - r_t^2) - \frac{1}{2}\rho_w\omega^2(r_b^2 - r_t^2) \quad (3.28)$$

3.4. Mineralogical Test and Microscopic Observations

The mineralogical test was executed by X-Ray Diffraction (XRD) technique, whereas the micro-structural observations were performed by using Environmental Scanning Electron Microscopy (ESEM) and X-Ray Computer Micro-Tomography (Micro-CT). Table 3.6 summarizes the variable examined in the experimental plan of mineralogical test and microscopic observations.

Table 3.6. Experimental plan of mineralogical test and microscopic observations

Test	Curing time (days)	Mellowing period (days)	Percentages of lime (%)	Tests done
XRD	1, 7	0, 7	0, 3	4
ESEM	1, 7	0, 7	0, 3	4
Micro- CT	-	0	0, 4	2
Total mineralogical test and microscopic observations				10

3.4.1. Mineralogical Test Using X-Ray Diffraction (XRD)

In order to understand the mineralogical composition of the untreated Eagle Ford expansive soil and the changes associated with the lime treatment, X-Ray Diffraction (XRD) tests were performed. X-Ray Diffraction is a technique used to determine the crystallographic structure and chemical composition of diverse materials. In this test, X-Rays are emitted from an X-Ray source to the analyzed specimen. Due to the interaction with the specimen, the X-Rays undergo elastic scattering with a certain incident angle, which is unique for a particular crystallographic structure. Figure 3.19 shows the schematic representation of the components of an X-Ray Diffractometer. In XRD tests, a spectrum of the scattering

intensity, as a function of the incident angle, is obtained. The diffracted X-Rays are then detected, processed and counted.

In this study, the XRD tests were conducted using the Bruker D8 Advance X-Ray Diffractometer shown in Figure 3.20. Resulting data were analyzed with EVA program that contains a large database of XRD spectra for various materials. The EVA program allows matching the peaks of the unknown spectrum with the spectrums from its database. Operating and safety procedures were provided by the staffs from the Electron Microbeam Laboratory at the University of Texas at Austin.

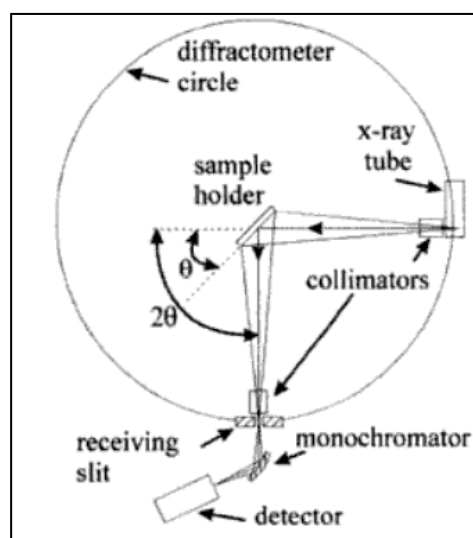


Figure 3.19. Schematic representation of the components of an X-ray diffractometer (Ulery, 2008)

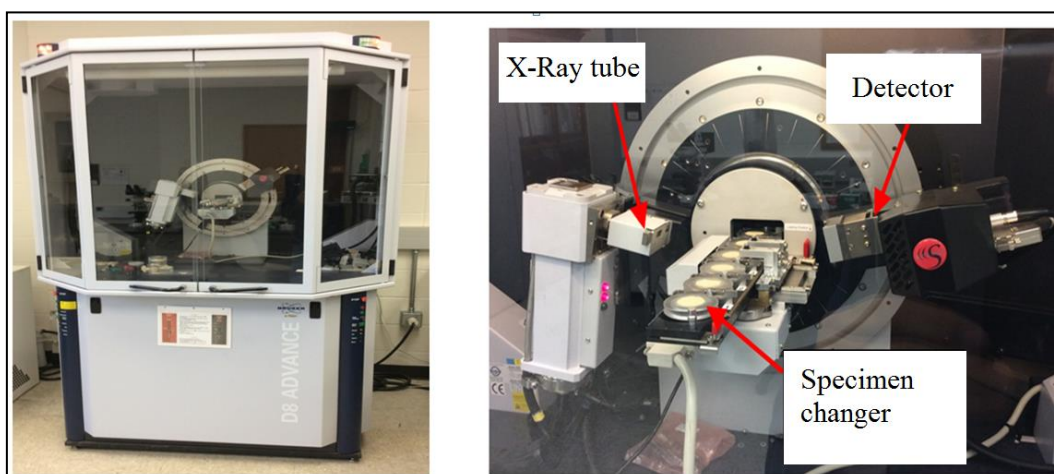


Figure 3.20. Bruker D8 Advance X-Ray diffractometer

The XRD tests were performed in specimens previously used in Unconfined Compressive Strength tests (UCS). After UCS estimation, the specimens were reduced to powder using a mortar and pestle, and the obtained powder was placed into the XRD holders (Figure 3.21). XRD tests were conducted at voltage of 40kV and amperage of 40mA, and the X-Ray source was a 2.2kW Cu X-Ray tube. The scan of 2θ angle was carried out through 5° to 70° at the speed of 19.2 second/deg and increments of 0.01836° .



Figure 3.21.XRD sample preparation.

3.4.2. Microscopic Observations through Environmental Scanning Electron Microscopy (ESEM)

The Environmental Scanning Electron Microscopy (ESEM) has become one of the newer and most promising qualitative method for studying the arrangements of aggregations, particles and voids of soils. According Romero and Simms (2008), ESEM is a special type of scanning electron microscope that works under controlled environmental conditions and requires no conductive coating on the specimen, thus, the micrographs are more representative of how the structure exists in nature. This makes the examination of wet specimens possible, without specimens disturbance concerns, which is an obvious advantage of ESEM compared to conventional SEM (Scanning Electron Microscopy). According to Lin & Cerato (2014), among the specimen disturbances produced by SEM specimen preparation are: (1) air drying induces volumetric shrinkage in wet clayey soils; (2) freeze drying introduces overall swelling owing to inevitable partial re-crystallization of water to ice; (3) critical drying can cause particle breakup.

A schematic cross section of ESEM equipment is shown in Figure 3.22. The sample chamber works at higher pressure (absolute pressure up to 3kPa) and separated from the increasing vacuum regions by the pressure-limiting apertures. In order to maintain high vacuum (10^{-5} Pa) in the electron gun, and poor vacuum in the specimen chamber, the vacuum should not diffuse from one level to another through the small holes bored in the aperture discs.

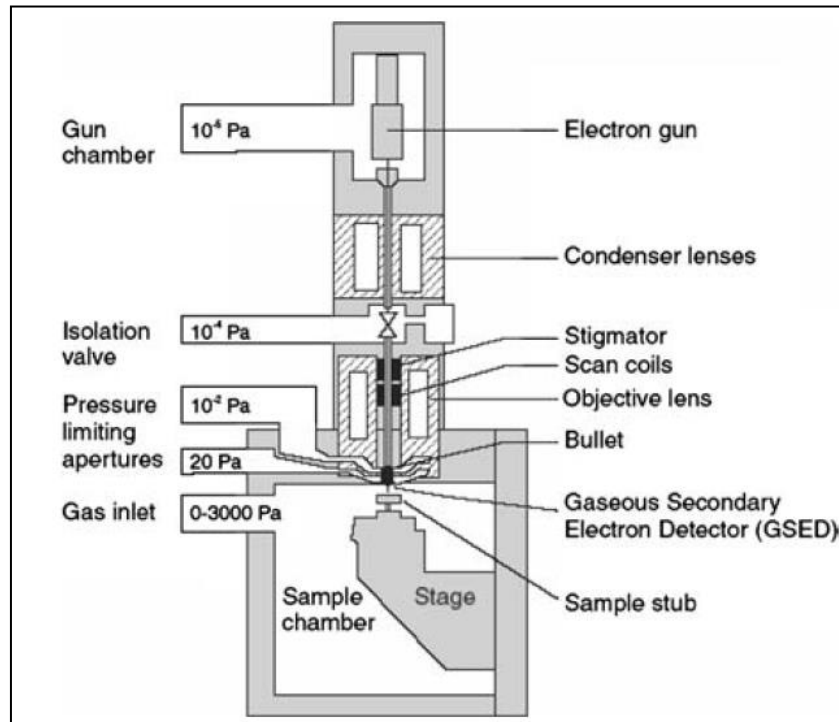


Figure 3.22. Schematic cross section of an ESEM (Romero and Simms, 2008)

Romero and Simms (2008) summarized the operation of ESEM as follows: ESEM is equipped with a gaseous secondary electron detector (GSED), as shown in Figure 3.22, to produce surface images, which is based on the principle of gas ionisation and allows imaging of non-conductive samples. The energetic primary electron beam, emitted from the electron gun, penetrates the gas chamber with little apparent scatter and hits the specimen, scanning across the surface of the specimen. This causes the specimen to emit secondary electrons, which are accelerated towards the positively charged GSED. As they travel through the gaseous environment, collisions occur between the secondary electrons and the gas particles. This results in emission of additional secondary electrons that provide more signal and ionization of the gas molecules (positive gaseous ions). The

positively charged gas ions are attracted to the negatively charged specimen and it has a negative charge from the primary electrons that have been bombarding it, suppressing the charging effects. This charge suppression allows imaging non-conductive specimens without the need of conductive coating. The difference in signal intensity of secondary electrons emitted from different locations on the specimen and collected at the positively charged GSED allows an image to be formed during a scan.

The ESEM equipment used in this study was a Philips /FEI XL30, owned by Department of Geological Sciences of the University of Texas at Austin (Figure 3.23). The maximum permissible vapor pressure of this equipment is 1.333kPa (10torr). For the ESEM tests concerned here, the temperature was set constant at 15⁰C and the vapor pressure was 0.2Torr.



Figure 3.23. Environmental Scanning Electron Microscope Philips/FEI XL30 (ESEM). Department of Geological Sciences of the University of Texas at Austin

The microscopic observations were done using specimens of natural soil (Eagle Ford clay) and mixtures of natural soil with 1% and 3% of hydrated lime. These percentages of hydrated lime were chosen because the most substantial

reduction of swelling and plastic index was observed with 1% of hydrated lime and the high reduction of swelling was obtained with 3% of hydrated lime.

The observations were done in specimens previously used in UCS tests. After the UCS measurement, a little chunk of soil was trimmed from each compacted specimen using a scalpel, trying to generate a flat bottom on the specimen for making easy to fix it on the ESEM specimen holder. Carefully, each chunk of soil was stuck on the ESEM specimen holder with a special adhesive carbon tape and was placed into the chamber using a tweezers (Figure 3.24). Detached particles on the ESEM specimen holder were cleaned off using an air blaster that provided gentle puffs of air.



Figure 3.24. ESEM specimen holders (left) and specimen placement into the ESEM (right)

3.4.3. X-Ray Computer Micro-Tomography (Micro-CT)

The X-Ray Computer Micro-Tomography (Micro-CT) is a non-destructive and non-invasive technique used to investigate the attributes of the ‘inside’ of objects of interest, and is based on the principle of the attenuation of an electromagnetic wave beam that is focused on the object (Pires *et al.*, 2010). Its implementation is based on the computer processing of numerous snapshots of the sample taken at different angles by an X-Ray source. The development of Micro-CT has allowed to carry out studies in three dimensions (3D) in micrometric scale in order to investigate several phenomena in soil physics (Baveye *et al.*, 2002; Monga *et al.*, 2007; Tippkötter *et al.*, 2009).

The Micro-CT is a method used for image reconstruction that makes a ‘crossing’ of different radiation beams that interact with the specimen. The

attenuated intensity of the radiation passing through a specimen can be compared to the original intensity of the radiation with its origins on the radiation source, which makes it possible to measure the attenuation of the radiation passing through the specimen. The computer-processed combinations of X-Ray images taken from different angles allow to produce cross-sectional (tomographic) images (virtual slices) of specific areas of a scanned specimen.

Quantitative characterization of aggregate pore structure can be provided by Micro-CT. The lime addition is responsible for modifications in the aggregate pore structure, so that the Micro-CT technique might be used to examine the pore structure modifications undergone by the expansive soil Eagle Ford after lime addition. The Zeiss XRadia Versa 510 micro-tomograph, shown in Figure 3.25, was used in this study. This micro-tomograph is owned by the Department of Chemistry and Materials Engineering of the Pontifical Catholic University of Rio de Janeiro (PUC-Rio). The Micro-CT tests were done using natural Eagle Ford clay specimen and lime-treated specimen with 4% of hydrated lime. These specimens were previously used in swelling tests and dried using an oven.

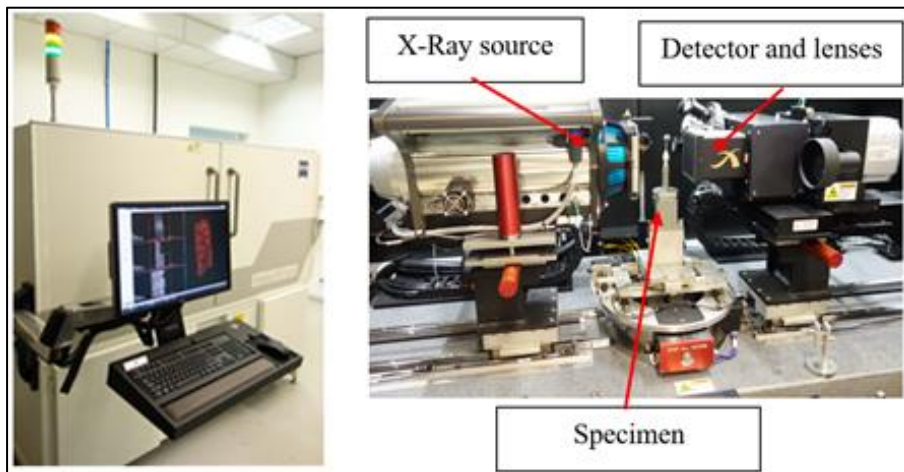


Figure 3.25. Zeiss XRadia Versa 510 micro-tomograph
(<http://lpdipuc.jimdo.com/english/microtomography/zeiss-xradia-versa-510/>)

4 Experimental Results and Analysis

The literature review presented in Chapter 2, revealed a number of distinctive features in expansive soil behavior, such as, dependent swelling behavior of clay mineralogy, plasticity, and soil structure and soil fabric. Also, it was established that the lime treatment in expansive soils is beneficial for swelling reduction and strength improvement. However there are no studies about combined effect of different percentages of lime and variations of soil preparation parameters, such as, compaction moisture condition, compaction dry density, mellowing period, curing time, effective stress. Thus, these results and analysis aim to identify the most efficient variations of these parameters for swelling reduction of expansive soils by lime treatment.

Results from the experimental plans proposed in Table 3.2, Table 3.3, Table 3.4 and Table 3.6 are presented and analyzed in this chapter. The basic tests were carried out as a general vision of the modifications undergone by the expansive soil Eagle Ford clay due to lime addition. The basic tests include: Atterberg limits, pH and Cation Exchange Capacity (CEC) determination, specific gravity, particle size by hydrometer test, standard Proctor compaction and Unconfined Compressive Strength (UCS).

Afterwards, the modification of swelling behavior due to lime treatment is examined in detail. The swelling vs. time curves were detailed analyzed considering the effect of lime on swelling potential and on the slopes of primary and secondary swelling. Also, a parameter called Swelling Potential Reduction Ratio (SPR) is introduced to estimate the efficiency of lime treatment on swelling mitigation. The SPR compares the swelling potential of untreated Eagle Ford clay and the swelling potential of lime-treated Eagle Ford clay subjected at different parametric variations. This chapter finalizes with the study of lime treatment influence on soil mineralogy and micro-structural composition in order to support and complete this analysis.

4.1. Basic Tests

4.1.1. Atterberg Limits

The addition of hydrated lime brought about a notable reduction in Eagle Ford clay plasticity. Figure 4.1 shows the Atterberg limits variation with hydrated lime percentage. It can be seen that liquid limit (LL) decreases with the increase in hydrated lime percentage, while plastic limit (PL) increases slightly (initially) and remains relatively constant while the hydrated lime percentage increases. Consequently, the reduction in plasticity index (PI) was generated from the addition of hydrated lime. Also, it can be observed that the largest change in PI took place with only 1% of hydrated lime (HL) that reduced the PI from 59.3% (for untreated Eagle Ford clay) to 17.9% (for Eagle Ford clay treated with 1% HL), as shown in Table 4.1, in column “0 curing days”.

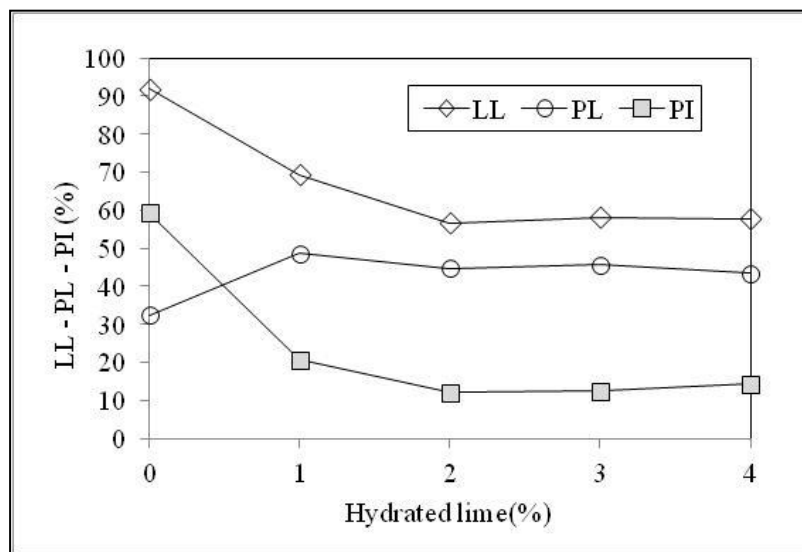


Figure 4.1. Atterberg limits variation of Eagle Ford clay with different percentages of hydrated lime

From the natural soil Eagle Ford clay PI obtained, and according to the classification of expansive soils based on Plastic Index (PI) proposed by Chen (1975), this clay with PI = 59.3% can be classified as soil with very high swelling potential (PI > 35%), whereas the lime-treated Eagle Ford clay reported PI can be

classified as soils with low or medium swelling potential ($PI < 35\%$), as shown in Table 4.1, in column “0 curing days”.

Three series of tests with different curing times were conducted (0, 7 and 28 days). The results are summarized in Table 4.1 and plotted in Figure 4.2 to Figure 4.4. The first line of Table 4.1 contains untreated Eagle Ford clay data (0% HL) and the remainder lines contain lime-treated Eagle Ford clay. Even though it can be observed small variations in LL and PL by using curing time, it should be noted that the PI values in specimens with 28 days of curing were slightly higher than those obtained from shorter curing time, except when HL was 1%.

Similarly to the results shown in Figure 4.2, Dash & Hussain (2011) detected that the increased curing time leads to increasing the liquid limit. They stated that the prolonged curing time stimulates the pozzolanic reactions, thus, the products derived from these reactions are able to hold more water, resulting in a further increase in the liquid limit. Furthermore, this increase in liquid limit was attributed to a possible change in soil fabric. The flocculated structure produced by lime treatment is more remarkable with the time. Therefore, the soil structure becomes relatively more open and allows holding more water. It also can be observed that PI appears to remain relatively constant, regardless the curing time, when the lime percentage is greater or equal than 2%.

Table 4.1. Atterberg limits results of Eagle Ford clay with different percentages of hydrated lime at different curing times

Hydrated lime (%)	0 curing days			7 curing days			28 curing days		
	LL (%)	PL (%)	PI (%)	LL (%)	PL (%)	PI (%)	LL (%)	PL (%)	PI (%)
0	91.8	32.5	59.3	91.8	32.5	59.3	91.8	32.5	59.3
1	66.5	48.6	17.9	76.4	37.0	39.4	70.4	39.4	31.0
2	56.7	44.6	12.1	65.4	49.2	16.2	65.4	48.2	17.1
3	58.1	45.6	12.5	63.6	47.3	16.3	69.6	48.2	21.4
4	57.8	43.5	14.3	63.4	46.4	17.0	71.0	53.0	18.0

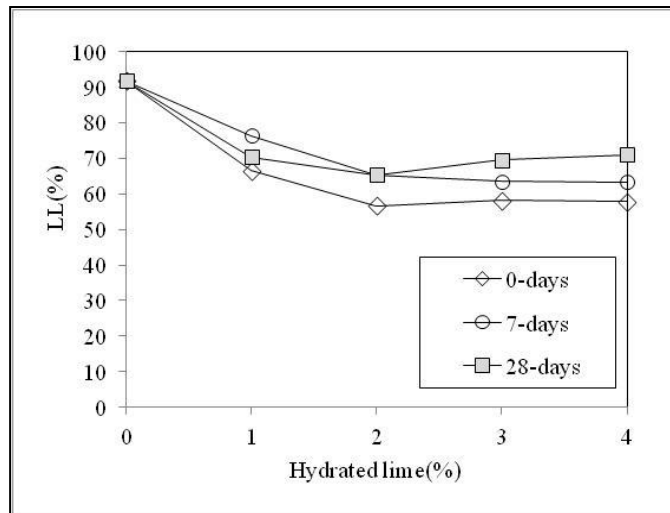


Figure 4.2. Liquid limit variation of Eagle Ford clay with different percentages of hydrated lime at different curing time

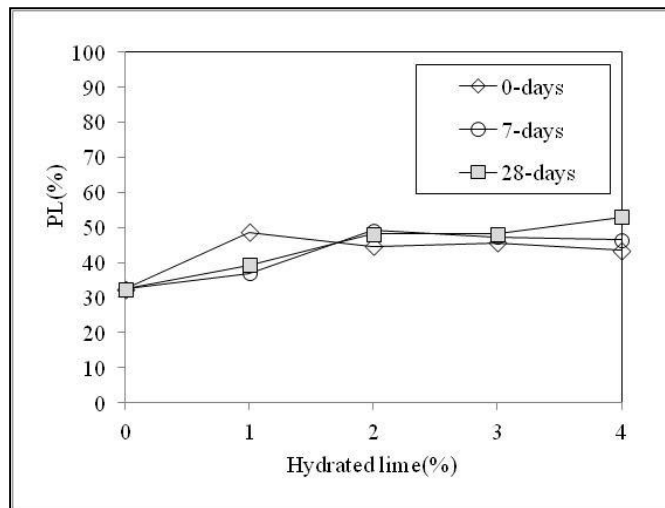


Figure 4.3. Plastic limit variation of Eagle Ford clay with different percentages of hydrated lime at different curing time

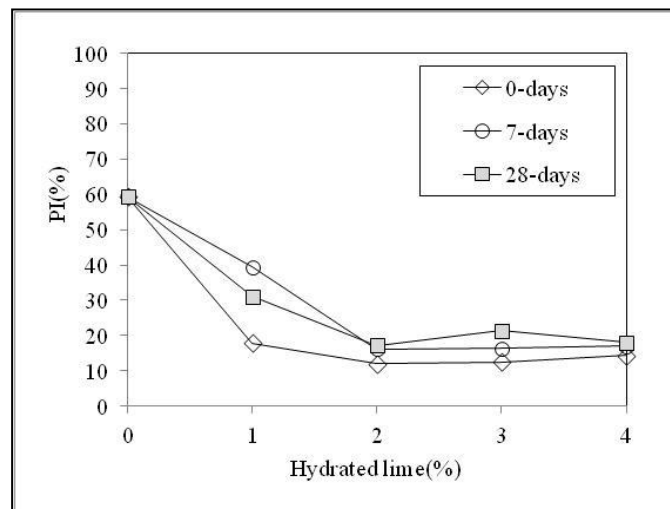


Figure 4.4. Plastic index of Eagle Ford clay with different percentages of hydrated lime at different curing time

The plasticity index reduction of the expansive soil Eagle Ford clay due to the lime addition may suggested changes in the soil texture. The data presented in Table 4.1 were plotted on a Casagrande's plasticity chart, as depicted in Figure 4.5. The natural soil Eagle Ford clay is classified as clay with high plasticity (CH) because its PI is placed above the A-line in Casagrande's plasticity chart. After lime addition, regardless the curing time, all lime-treated Eagle Ford data are plotted below the A-line, showing the substantial reduction in plasticity and a new silty texture.

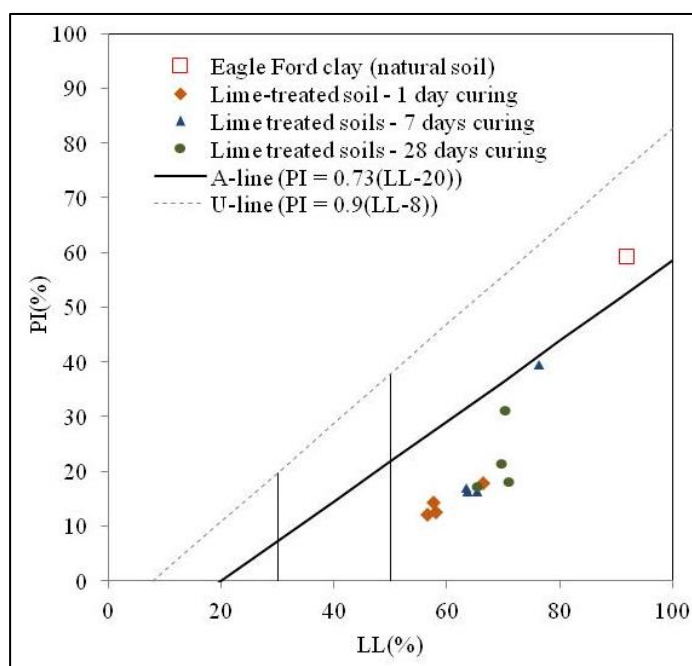


Figure 4.5. Casagrande's plasticity chart for natural and lime-treated Eagle Ford clay.

4.1.2. Chemical Evaluation

4.1.2.1. pH

Figure 4.6 shows the results of pH tests for lime-treated Eagle Ford clay with different curing times. As expected, the pH of all lime-treated Eagle Ford clay specimens increased because of the hydrated lime. The hydrated lime, or calcium hydroxide, is relatively stable in water, although it can partially dissociate to provide calcium ions and hydroxyl groups, which may react with the clay minerals.

The hydroxyl groups are able to elevate the pore water pH to the maximum value of approximately 12.4 (Beetham *et al.*, 2014).

The natural pH of the untreated Eagle Ford clay (0% HL) was found 8.4. The measurements done at the same day that the lime-soil mixtures were prepared (0 days of curing) showed a stable value of 12.4 with hydrate lime additions between 3% and 4%. It also can be noticed that there is a decrease of pH values between the different curing times for hydrated lime percentages of 1, 2 and 3%. However, for hydrated lime percentage of 4%, there was not a reduction of pH between the different curing times, i.e. its pH value was kept around 12.4.

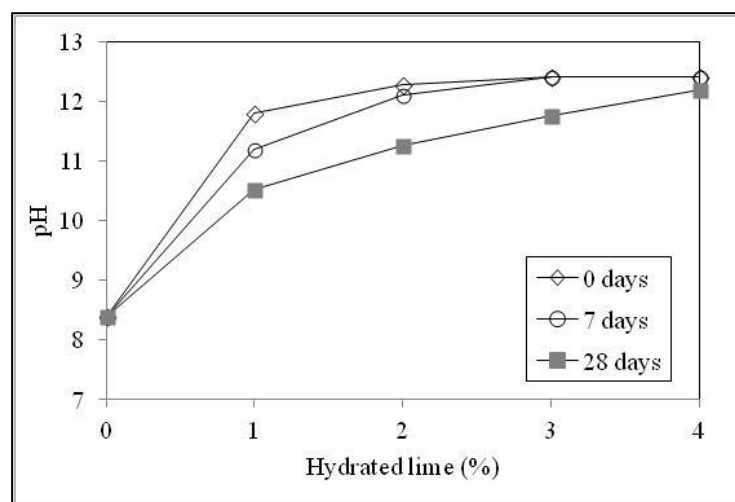


Figure 4.6. Results of pH tests for lime-treated Eagle Ford clay with different curing times

The above reductions in pH between the different curing times infer that the lime was consumed during the curing time as result of modification process. The reductions in pH were insignificant between 0 days and 7 days of curing time, but the reduction between 0 days and 28 days of curing time showed that 3% of hydrated lime was not enough to reach pH of 12.4, which is the appropriated pH for pozzolanic reactions, according Eades & Grim (1966).

Therefore, 4% of hydrated lime might be the percentage of lime needed to induce the highly alkaline environment to promote the dissolution of aluminosilicate constituents of Eagle Ford clay. These constituents are able to react with cations (Ca^{+2}) of lime to induce the cemented products formation.

4.1.2.2.

Cation Exchange Capacity (CEC) Evaluation by Blue Methylene Test

The Cation Exchange Capacity (CEC) was determined by blue methylene tests, since the methylene blue dye is capable of replacing the exchangeable cations available in the clay particles. The lime treatment in expansive soils mainly involves a rapid cation exchange process on the clay particle surface. Thus the alteration of CEC due to lime treatment might be detected by blue methylene test.

The Cation Exchange Capacity values are usually related with the specific surface area of clay particles. Clays with large specific surface area usually have high CEC, high surface activity and, consequently, high water absorption potential. Clay particles typically exhibit surface charge imbalance and the negative charges can be balanced by hydrated cations. Accordingly, individual clay particles are surrounded by absorbed water in the diffuse double layer arrangement. The thickness of the diffuse double layer is controlled by several factors, although the charge valence has primary influence (Reeves *et al.*, 2006). The charge balances in the clay surface can be altered by few cations coming from the lime and the diffuse double layer shrinks as consequence of the charge balances (Beetham *et al.*, 2014).

The results obtained from blue methylene tests are shown in Table 4.2. It can be observed that the CEC decreased while the hydrated lime percentage was increased. This is in accordance with other studies, which reported the CEC reduction is due to lime addition (Cambi *et al.*, 2011).

Table 4.2. Blue methylene test results of Eagle Ford clay with different percentages of hydrated lime

Hydrated lime (%)	Blue methylene (ml)	CEC (meq/100g)
0	130	34.8
1	75	20.1
2	60	16.1
3	55	14.7
4	50	13.4

The decrease in CEC values verifies the formation of new pozzolanic reaction minerals, which results in big size particle, and consequently small specific surface responsible for less water absorption potential and high hydraulic conductivity. Also, since some clay cations were already exchanged due to lime addition, it was

expected that less cations around the clay particles were available in lime-treated clay specimens, and consequently less CEC might be identified after lime addition. According to the values of CEC reported by Mitchell & Soga (1976) and presented in Table 2.1, the natural soil Eagle Ford clay exhibited a typical CEC value of the expansive mineral illite (10 - 40 meq/100g). After lime addition, the CEC decreased and reached CEC values similar to non expansive minerals, such as, kaolinite (3 – 15 meq/100g).

4.1.3. Specific Gravity

The specific gravity value of hydrated lime was reported by the Austin Lime Company and is 2.24. Figure 4.7 shows the specific gravity obtained from mixtures of Eagle Ford clay and hydrated lime ranging from 0% to 4% and the specific gravity of pure hydrated lime (100% HL). The specific gravity decreases as the hydrated lime percentage increases in the mixture due to the low specific gravity of the hydrated lime.

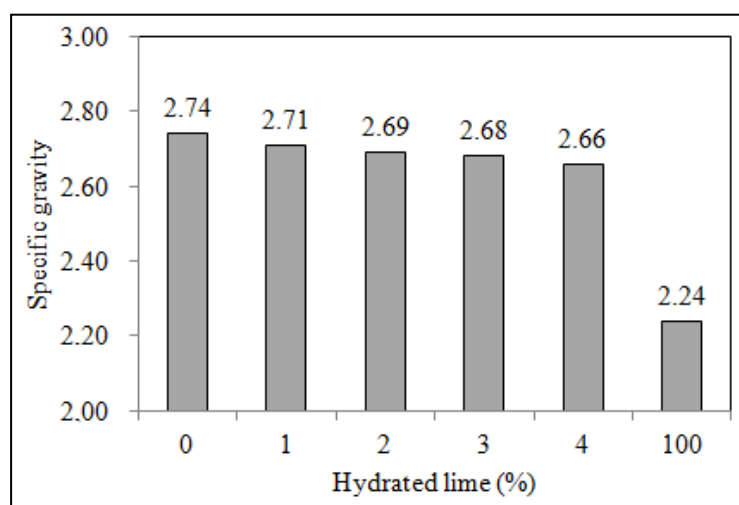


Figure 4.7. Specific gravity variation of Eagle Ford clay with different percentages of hydrated lime

4.1.4. Grain Size Distribution Analysis by Hydrometer Test

The grain size distribution was evaluated by hydrometer test and was conducted using a sample of untreated Eagle Ford clay (0% HL) and two lime-treated samples (2% HL and 4% HL) in order to determine the effect of lime treatment on the grain size distribution. Figure 4.8 shows the grain size distribution

measured by hydrometer tests. It can be observed that when the hydrated lime is added, the percent of smaller particles reduces. For instance, the percentage of particles finer than 0.001 mm is around 60% for untreated Eagle Ford clay, whereas for lime-treated Eagle Ford clay with 4% of hydrated lime, this percentage drops to 30%. The flocculation process occurs immediately after lime addition and particle aggregates are formed. The grain size distribution curve of fine-grains moved toward down because the grain size was increased.

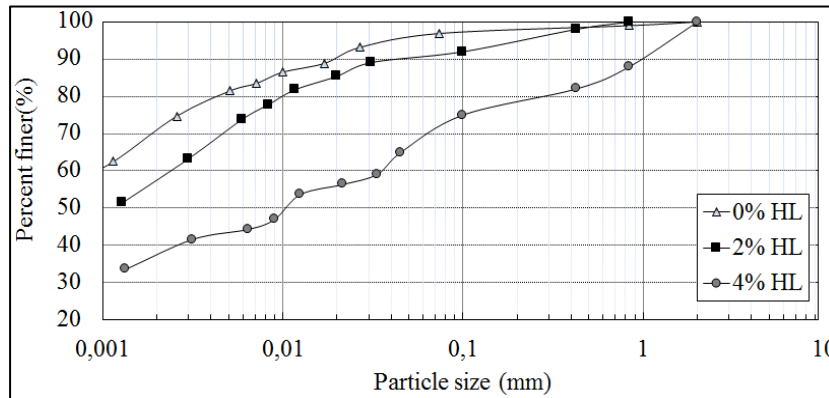


Figure 4.8. Grain size distribution measured by hydrometer tests using untreated Eagle Ford clay and lime-treated Eagle Ford clay with 2% and 4% of hydrated lime

4.1.5. Compaction Analysis

Standard Proctor compaction tests were conducted to determine the compaction moisture content and dry density relationship for Eagle Ford clay (untreated soil or 0% HL) and lime-treated Eagle Ford clay with 4% hydrated lime (4% HL). The results are showed in Figure 4.9. The standard Proctor curves present an optimum moisture content of 22% with a corresponding maximum dry density of 14.8 kN/m^3 (1.51 g/cm^3) for untreated Eagle Ford clay (0% HL). The lime-treated Eagle Force clay with 4% hydrated lime had optimum moisture around 26% with a corresponding maximum dry density of 14 kN/m^3 (1.43 g/cm^3).

These results show how the immediate reactions took place after lime addition, producing changes in the physical properties of the soil. The flocculation process increases the air void content, and reduces the compactibility and the dry density of the lime-treated soil. Some studies have suggested that the decrease in dry density due to lime addition is associated with a strong modification of the soil microstructure with the formation of a small class of pores between 0.01 and 0.2 μm (Le Runigo, 2009). According to Beetham *et al.* (2014), the pore space size

resultant from the flocculation process is smaller than $0.3 \mu\text{m}$, thus the alteration of intra-aggregate porosity due to lime addition is improbable. Therefore, the dry density reduction might be due only to the increase of void space between clay clods or inter-aggregate porosity (pore size bigger than $100 \mu\text{m}$).

Likewise, the optimum moisture content was varied due to lime addition. The resultant curve of lime-treated Eagle Ford clay with 4% of hydrated lime was shifted toward the wet side compared with the untreated Eagle Ford clay curve. Enough water is required for the lime-soil reactions, thus the optimum moisture content is increased. This type of results has been reported by many researchers, such as Little *et al.* (1995), Bell (1996), Holt & Freer-Hewish (1998) and Beetham *et al.* (2014).

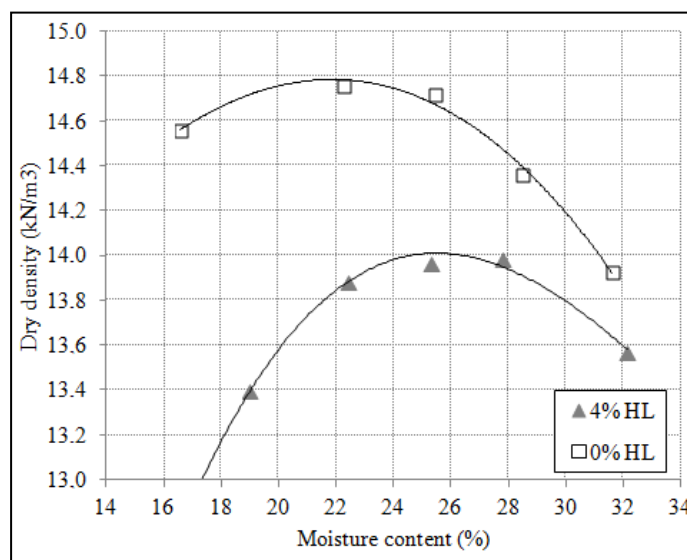


Figure 4.9. Standard Proctor compaction curves for untreated Eagle Ford clay (0% HL) and expansive soil treated with 4% hydrated lime (4% HL).

4.1.6. Unconfined Compressive Strength (UCS) Analysis

The Unconfined Compressive Strength (UCS) was measured in untreated and lime-treated Eagle Ford clay with the purpose of determining the effect of the amount of lime, curing time and mellowing period on the compressive strength. The specimens for curing time analysis were compacted at the same day that the lime-soil mixtures were prepared. After compaction, the specimens were enveloped in plastic wrap and aluminum foil, and placed in the environmental chamber for the specific curing time. The stress-strain curves obtained from UCS tests for different

curing times and hydrated lime percentage are given in Figure 4.10. The peak stress (UCS), axial strain at the failure and Young's modulus deduced from these curves are summarized in Table 4.3.

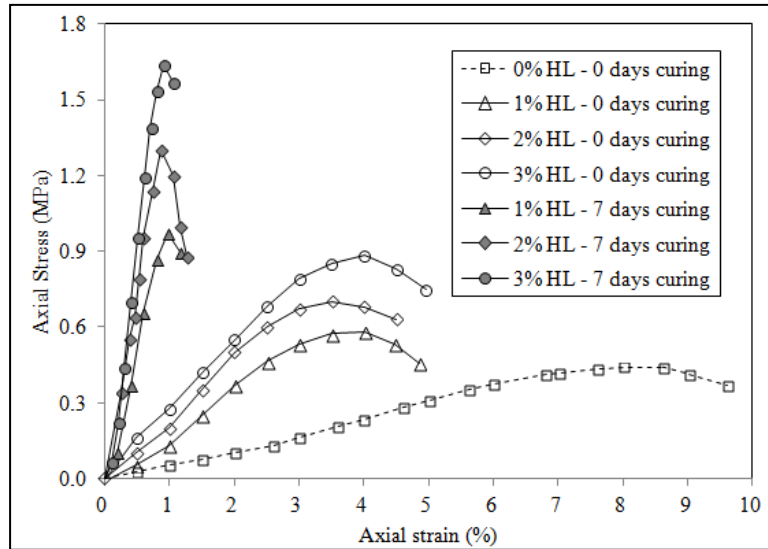


Figure 4.10. Unconfined Compressive Strength (UCS) of untreated and lime-treated expansive soils at different curing time.

It can be noticed an enhancement of the peak strength while the hydrated lime content and curing time were increased. In comparison to untreated Eagle Ford clay (0% HL), the improvement of peak strength was 32% for the specimen with 1% of hydrated lime (1% HL) and 100% for the specimen with 3% of hydrated lime (3% HL) at 0 days of curing. In addition, the specimen with 1% HL and 7 days of curing obtained an improvement of 120% of strength, whereas the specimen with 3% HL and 7 days of curing almost trebled the strength of the untreated Eagle Ford clay.

Table 4.3. Unconfined Compressive Strength (UCS) and Young's modulus of untreated and lime-treated expansive soils at different curing time.

Hydrated lime (%)	Curing time (days)	UCS (MPa)	Failure strain ϵ_{af} (%)	Young's modulus (MPa)
0	0	0.44	7.6	0.08
1	0	0.58	4.0	0.24
2	0	0.70	3.5	0.25
3	0	0.88	4.0	0.30
1	7	0.97	1.0	1.05
2	7	1.30	0.9	2.55
3	7	1.64	0.9	2.58

The stiffness and brittleness of the lime-soil mixtures also increased with the increase of curing time. The Young's modulus, reported in Table 4.3, demonstrated that the stiffness of lime-treated Eagle Ford clay is between 3 and 21 times greater than the stiffness of the natural Eagle Ford clay. This agrees with the earlier findings of Bell (1996). However, it is important to clarify that the Young's moduli reported here were calculated with base on the strength-stress curves and not based on direct measurements on the specimens.

Another feature that is depicted in Figure 4.10 is the decreasing of failure strain with the lime addition. In this study, the failure strain seems to depend only on the curing time and not the percentages of lime, at least not with the percentages of lime used here.

The mellowing period effect was also examined by using Unconfined Compressive Strength test. Before compaction, the lime-soil mixtures were kept in Ziploc bags into the environmental chamber. The specimens with no mellowing (NM) were the same used above for evaluating the 7 days curing effect, since those specimens were compacted immediately after the lime-soil mixtures were prepared, and stored in compacted state into the environmental chamber. The specimens that were allowed to mellow were only compacted after 3 and 7 days of mixtures preparation, and were designated as specimens M3 and M7, respectively. All specimens (NM, M3 and M7) were subjected to UCS test at the same day, corresponding to 7 days after mixing.

Figure 4.11 presents the results obtained for this evaluation. Table 4.4 contains the strength properties of all these specimens. The specimens that were allowed to mellow (M3 and M7) were slightly weaker than specimens with no mellowing (NM), i.e. the UCS reduced with long mellowing periods, such as 3 and 7 days. This reduction in UCS might be due to different factors, such as, loss of water, lime consumption and high air void generation during mellowing period. Also, the late compaction after lime-soil mixture preparation might be responsible for breaking the bonds produced during flocculation process, resulting in weaker behavior.

Table 4.4. Unconfined Compressive Strength (UCS) data for evaluation of mellowing period effect

Hydrated lime (%)	Mellowing period (days)	Specimen label	UCS (MPa)	Failure strain ϵ_{af} (%)	Young's modulus (MPa)
1	0	NM	0.97	1.0	1.45
	3	M3	0.95	1.5	1.03
	7	M7	0.95	2.8	0.45
3	0	NM	1.64	1.0	1.72
	3	M3	1.45	1.2	0.86
	7	M7	1.45	5.6	0.39

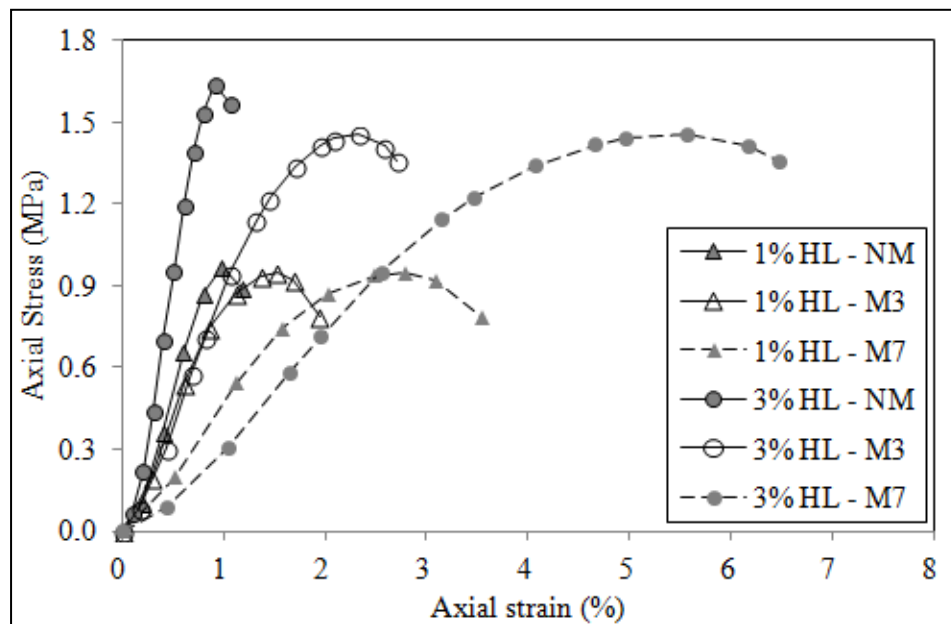


Figure 4.11. Unconfined Compressive Strength (UCS) of lime-treated Eagle Ford clay allowed to mellow for 3 and 7 days (M3 and M7, respectively) and without mellowing period (NM)

Bell (1996) indicated that the amount of water, available for hydration and reaction to form cemented bonds, influences the strength that can be attained. Thus, if some moisture content is supposed to be lost during mellowing period, then less strength would be obtained in the samples allowed to mellow. Additionally, the consumption of lime seems to be increased in the lime-soil mixtures when they are not compacted due to higher contact between air and lime-treated soil particles. It can be seen, from Figure 4.11, that mellowing period inclusion on lime treatment can change the brittle behavior to a more ductile one.

Also this change was observed in different failure mode by the specimens, as shown in Figure 4.12. Specimens compacted immediately after lime-soil mixing

(no mellowing) presented a 45° failure plan, whereas specimens compacted seven days after lime-soil mixing (mellowing of seven days) exposed vertical failure plans. The prolonged mellowing period seems to produce micro-cracks inside of the specimens, and when the specimens is subjected to compression, these micro-cracks extend to the principal compression direction, like it happens in rocks.

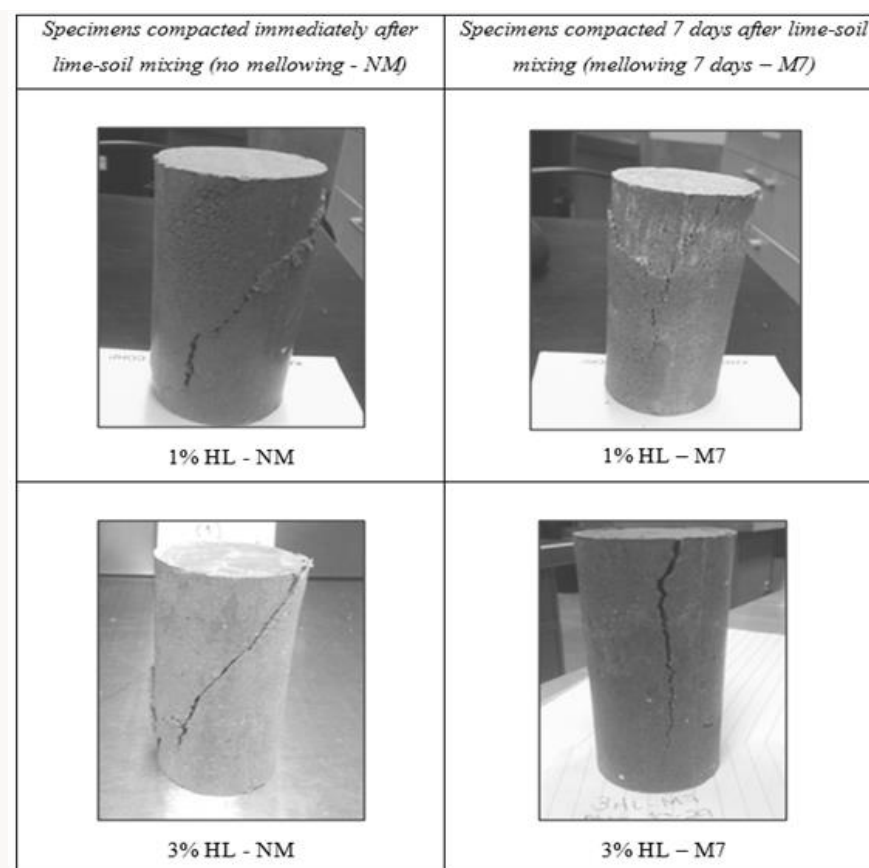


Figure 4.12. Different failure mode in specimens with no mellowing (NM) and with 7 days of mellowing (M7)

Holt & Freer-Hewish (1998) also examined the long-term effect of mellowing by using UCS (Unconfined Compressive Strength) testing on specimens that had been cured for various periods up to 195 days. They observed that, at the end of 195 days of curing, the specimens mellowed for 24 hours were always significantly weaker than specimens mellowed for 1 hour before compaction. The strength of the specimen with 4% of lime and mellowed for 1 hour before compaction was approximately the double of the strength of specimen mellowed for 24 hours. West (1959) also studied two granular soils and a cohesive soil in order to analyze the effect of elapsed time between the mixing and the compaction on the strength of

soil-cement mixtures. His results showed that a lapse of time between mixing and compaction (i.e. mellowing) resulted in a significant reduction of the state of compaction and the strength of the stabilized clay and sandy gravel. Thus, the results obtained in the present study with lime-treated Eagle Ford clay agreed with this early finding. West (1959) also recommended using a construction procedure, which involves a short time between mixing and compaction or an increase of compactive effort to minimize the effect of the mellowing period on the strength.

4.2. Swelling Potential Reduction Analysis

The swelling potential test was estimated by two direct methods: the conventional free swell test and the centrifuge test. Regardless the testing method, the swelling was defined as the ratio of the increase in height to the original specimen height, expressed as a percentage, and as shown in equation (4.1).

$$\text{Swelling (\%)} = \frac{h_t - h_0}{h_0} * 100 \quad (4.1)$$

where h_t is the specimen height at time t and h_0 is the specimen height at the beginning of the swelling potential test.

Figure 4.13 shows a typical swelling percent vs. log time curve. It can be seen that the increase of swelling percent is fast at the initial phase and then it gets slow in order to reach gradually an asymptotic level. If tangent lines are constructed about the point of inflection, it is possible to extract three important values from this curve: the primary swelling slope (PSS), the secondary swelling slope (SSS) and the swelling potential (S_p). The swelling potential is considered to be the point of the curve in which the slope inflects (Figure 4.13).

These three values are important to describe the swelling behavior of natural or lime-treated soils. The primary swelling slope provides an idea of the rate of flow into the specimen that generates the most representative percentage of the total swelling. The primary swelling occurs at a faster rate and it develops when the voids are not able to accommodate further swelling clay particle. The swelling potential represents around 80% to 90% of total swelling potential. The secondary swelling occurs slowly at lower rate, after the swelling potential is reached. The secondary swelling slope allows predicting long-term swelling, that usually is ignored, but it can result in significant structural damages.

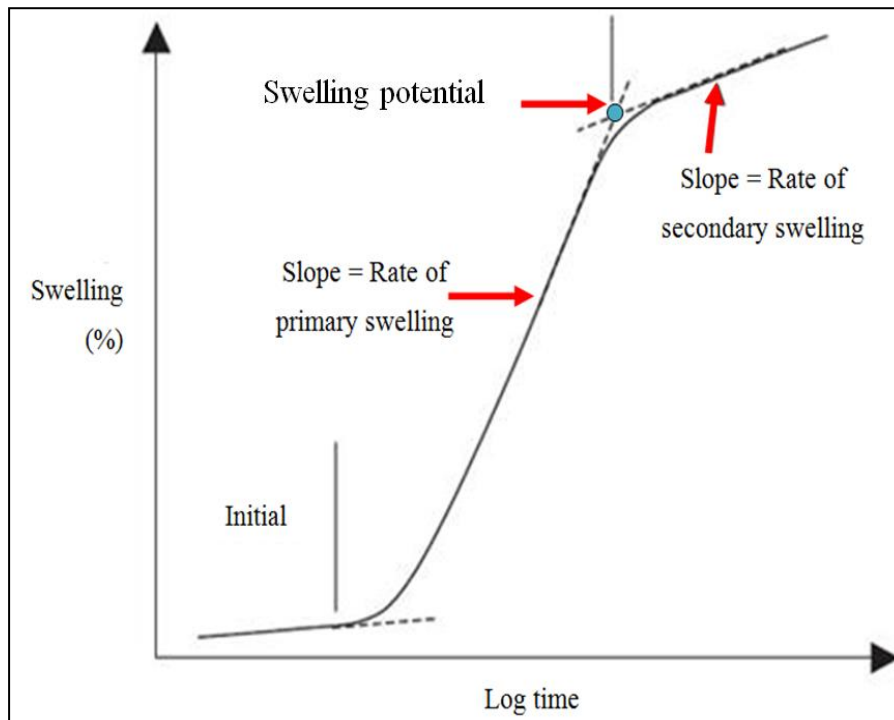


Figure 4.13. Typical swelling percent vs. log time curve

In order to analyze the efficiency of lime percentage on the reduction of swelling potential, a new parameter, called Swelling Potential Reduction Ratio (SPR), was introduced. SPR measures the reduction on swelling potential produced by hydrated lime additions, at different specimen preparation conditions, regarding to swelling potential in natural soil. SPR is defined by equation (4.2).

$$SPR = 1 - \frac{Sp_{(n\%HL)}}{Sp_{(0\%HL)}} \quad (4.2)$$

where $Sp_{(0\%HL)}$ is the swelling potential in untreated Eagle Ford clay and $Sp_{(n\%HL)}$ is the swelling potential at particular hydrate lime percentage ($n\% HL$). SPR value ranges from zero to one. SPR will be zero for untreated Eagle Ford clay because there is no reduction of swelling potential, since there is no lime addition. And SPR will be one when the addition of lime produces 100% of reduction of swelling potential compared with swelling potential in untreated Eagle Ford clay. Therefore, the higher SPR is, the more efficient is the lime addition.

4.2.1. Conventional Free Test Results and Analysis

Three series of conventional free swell tests were conducted. The first set of tests was performed with the purpose to evaluate the effect of lime percentage on swelling reduction. The second one was conducted with specimens cured at different times varying also the lime percentage. And the third group of experiments was carried out to observe the effect of mellowing period on swelling behavior. The experimental plan of conventional free swell tests was presented in Table 3.3.

4.2.1.1. Evaluation of Lime Percentage Effect on Swelling Behavior

The conventional free swell tests conducted for evaluating the hydrated lime percentage effect was carried out using specimens of untreated Eagle Ford clay and lime-treated Eagle Ford clay compacted at the same moisture content (in average 23%), and at the same dry density equivalent to 1.51 g/cm^3 . All these conventional free swell tests were conducted applying setting load of 6 kPa. Table 4.5 summarizes the initial and final characteristics (moisture content, void ratio and saturation) of the specimens used in this set of experiments. Figure 4.14 and Figure 4.15 depict the swelling percent vs. log time curves obtained with variations of lime percentage between 0% and 4%.

Table 4.5. Variations of moisture content, void ratio and saturation during conventional free swell tests for evaluating the hydrated lime effect

Hydrated lime (%)	Moisture content		Void ratio		Saturation	
	Initial	Final	Initial	Final	Initial	Final
0.0	23.2%	43.7%	0.79	1.10	84.9%	100%
0.5	23.0%	40.7%	0.75	0.94	84.0%	100%
1.0	23.4%	36.4%	0.74	0.85	85.7%	100%
1.5	23.4%	33.5%	0.73	0.80	84.5%	100%
2.0	22.9%	47.9%	0.72	0.79	85.0%	100%
2.5	23.0%	32.9%	0.72	0.78	85.3%	100%
3.0	22.9%	32.4%	0.73	0.72	84.7%	100%
3.5	22.9%	32.2%	0.72	0.73	84.7%	100%
4.0	23.0%	27.1%	0.71	0.71	86.5%	100%

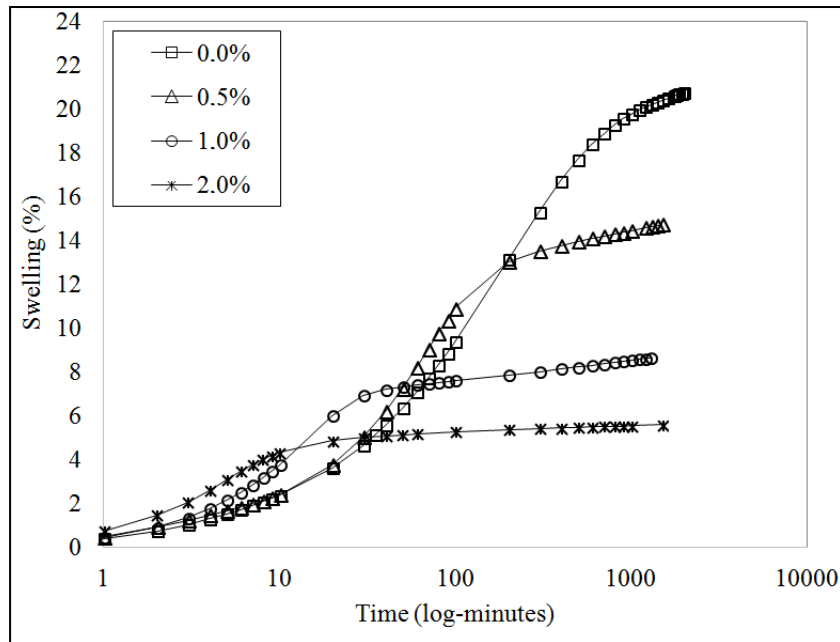


Figure 4.14. Semi-log plot of conventional free swell tests results for lime-treated Eagle Ford clay with lime variation between 0% and 2%.

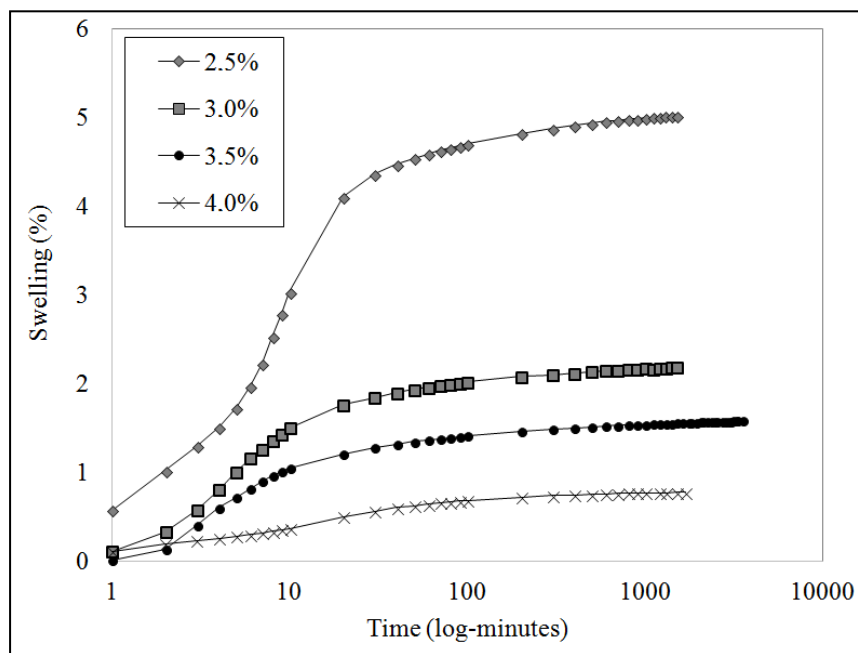


Figure 4.15. Semi-log plot of conventional free swell tests results for lime-treated Eagle Ford clay with lime variation between 2.5% and 4.0%.

By observation Figure 4.14 and Figure 4.15, it can be noticed that the shape of the curves changed after hydrated lime addition. The curve obtained for untreated Eagle Ford clay presented a well defined initial part, but after lime addition, these curves only present two parts corresponding to primary swelling and secondary

swelling. Also, the lime-treated Eagle Ford clay exhibit earlier beginning of the secondary swelling than untreated Eagle Ford clay.

As stated above, the Swelling Potential Reduction Ratio (SPR) allows to estimate the efficiency of lime percentage on the reduction of swelling potential. For this set of experiments, the SPR was calculated and collected in Table 4.6 along with the values of swelling potential and slopes of primary and secondary swelling.

Table 4.6. Swelling potential, SPR, and slopes of primary and secondary swelling of unthread and lime-treated Eagle Ford clay with different hydrated lime percentage.

Hydrated lime (%)	Swelling Potential	SPR	Primary Swelling Slope	Secondary Swelling Slope
0.0	22.1%	0.00	11.54%	2.95%
0.5	12.9%	0.41	9.70%	1.74%
1.0	7.2%	0.67	7.19%	0.99%
1.5	5.0%	0.77	4.41%	0.37%
2.0	4.7%	0.79	4.16%	0.24%
2.5	4.3%	0.81	4.32%	0.24%
3.0	1.7%	0.92	1.62%	0.13%
3.5	1.1%	0.95	1.07%	0.11%
4.0	0.6%	0.97	0.35%	0.08%

The SPR values of Table 4.6 show that 1% of hydrated lime was able to reduce 67% the swelling potential of Eagle Ford clay, whereas 4% of hydrated lime was able to eliminate 97% of swelling potential. Figure 4.16 depicts the Swelling potential (Sp) and swelling potential reduction ratio (SPR) vs. different hydrated lime percentage. It can be seen that swelling potential decreased in exponential way with the hydrated lime increase. Consequently, the increase of SPR fits a natural logarithmic function with excellent correlation ($R^2=0.96$).

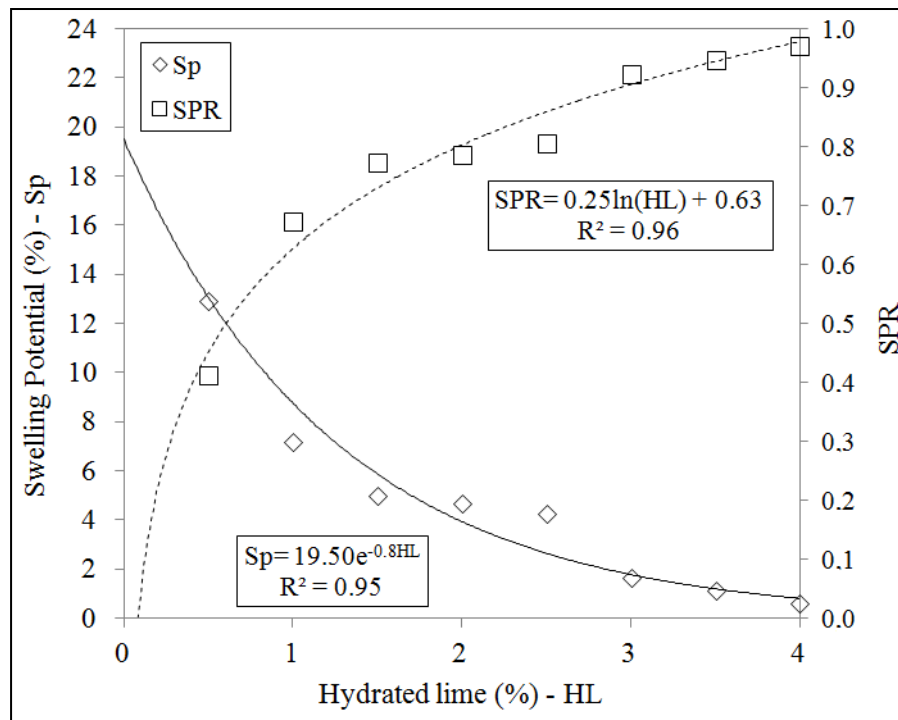


Figure 4.16. Swelling potential (Sp) and swelling potential reduction ratio (SPR) vs. hydrated lime percentage

The primary swelling slope (PSS) and the secondary swelling slope (SSS) variations with hydrated lime percentage were depicted in Figure 4.17 and Figure 4.18, respectively. It can be seen a decrease in PSS and SSS values with an increase in hydrated lime percentage. Specimens treated with hydrated lime higher than 1% presented very small values of SSS, suggesting that the swelling was developed basically during the primary phase due to capillary process.

Sridharan & Gurtug (2004) compared the swelling behavior of kaolinite with montmorillonite clay and stated that the higher plasticity index (PI) of the soil, the larger is the time taken to reach near equilibrium. Based on this, it can be inferred that the slope of primary and secondary swelling decreases due to the lime effect on the plasticity reduction (Figure 4.1). The authors also reported that for kaolinite, the secondary swelling was very small and the swelling percent vs. log-time relationship was almost horizontal in the secondary swelling phase. This also came up in lime-treated Eagle Ford clay analyzed in the present study: the secondary swelling slope became lower than 1% when hydrated lime addition exceeds 1%, indicating that the secondary swelling does not represent a significant amount in the overall swelling.

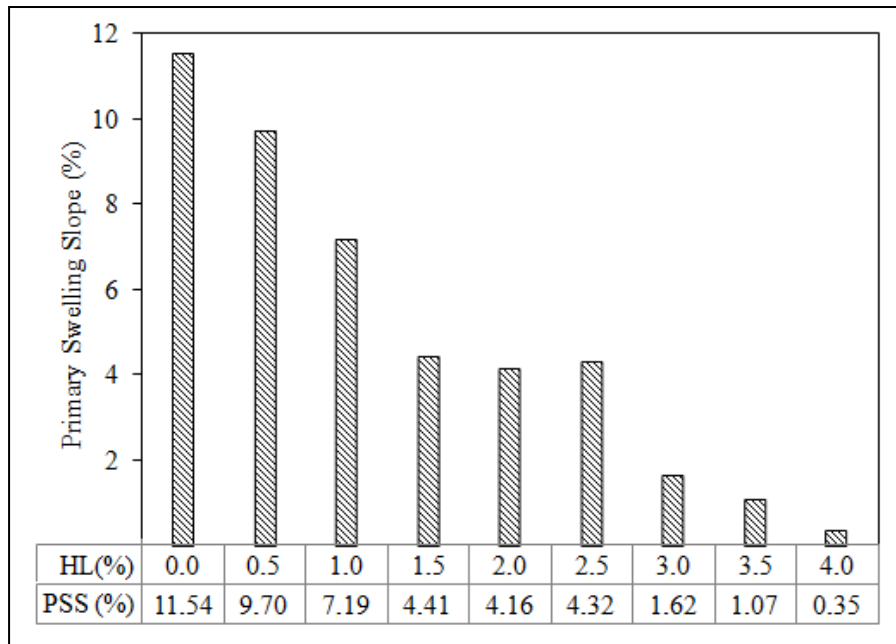


Figure 4.17. Primary swelling slope (PSS) variation with hydrated lime percentage

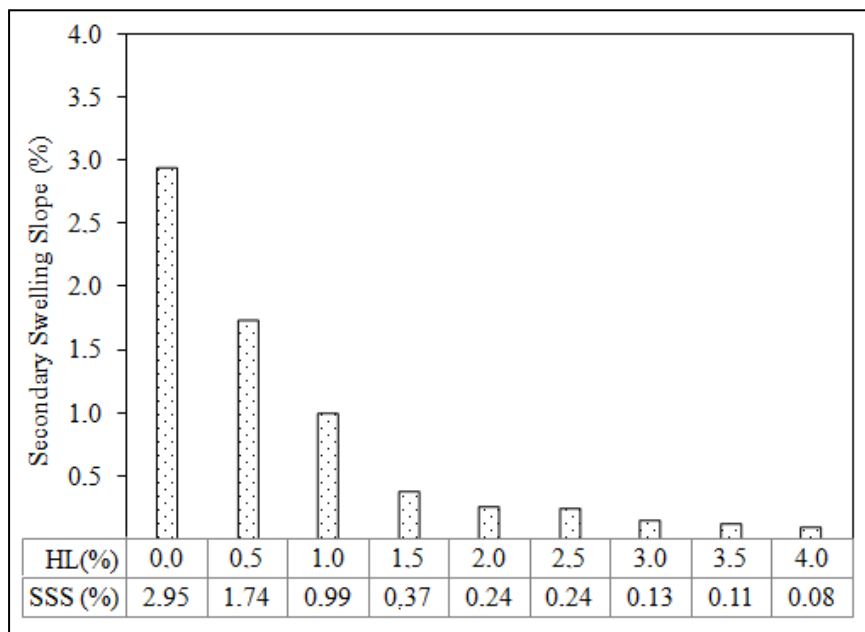


Figure 4.18. Secondary swelling slope (SSS) variation with hydrated lime percentage

In order to determine if a relationship exists between the PSS and SSS in untreated and lime-treated Eagle Ford clay, these two values were plotted against one another in Figure 4.19 for each of the hydrated lime percentage used in this set of experiments. An exponential decreasing relationship between primary and secondary swelling slopes was observed. With low percentages of hydrated lime, there is a clear difference between the secondary and primary swelling slopes.

When a quantity of hydrated lime increases in the lime-soil mixture, the variation between the primary and secondary slopes was small.

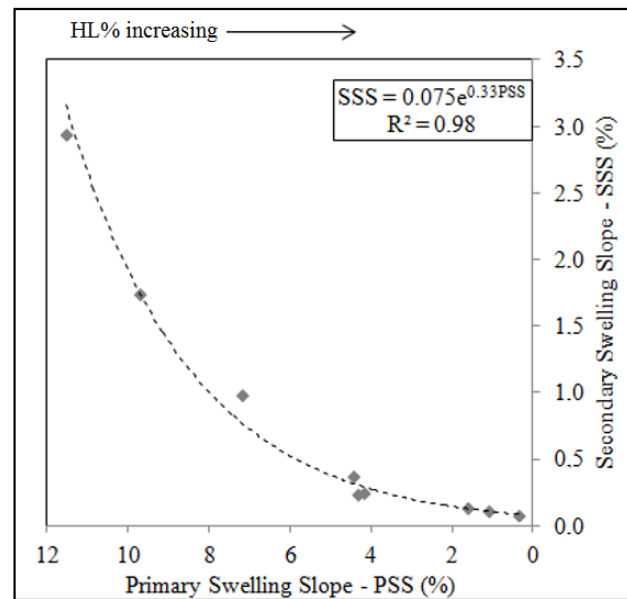


Figure 4.19. Relationship between primary and secondary swelling slope at different lime contents

Considering that the primary swelling is driven by capillarity and secondary swelling might be driven by a long-term process of hydrating clay particles, as proposed by Kuhn (2010), the relationship depicted in Figure 4.19 might indicate that the capillarity and hydration process contributed almost in the same percentage for the total swelling of lime-treated Eagle Ford specimens, since both PSS and SSS had similar values with high hydrated lime percentage, such as 3% or 4%. On the other hand, in untreated Eagle Ford clay, the entrance of water was mainly due to capillarity process, since PSS was high.

Detailed comparison of time-swelling relationship for lime-soil mixtures with hydrated lime percentage variation could not be easily carried out, since the development of swelling varies considerably from one amount of lime to another. Hence, the semi-log plots of this set of conventional free swell tests were re-plotted as time vs. percentage of total swelling for hydrated lime percentage varying from 0% to 4% (Figure 4.20 and Figure 4.21). Here, it was calculated the ratio of the swelling reached at a certain time to the total swelling of the lime-soil mixture. It can be observed that lime-treated Eagle Ford clay developed faster swelling than the natural Eagle Ford clay. In Figure 4.20, it is clear that the mixture with 2% of

hydrated lime reached almost 80% of the total swelling in the first 10 minutes of test, whereas the natural Eagle Ford clay needed almost 1000 minutes to reach the same percentage of the total swelling. The lime-soil mixtures with more than 2% of hydrated lime showed similar velocity to reach the total swelling.

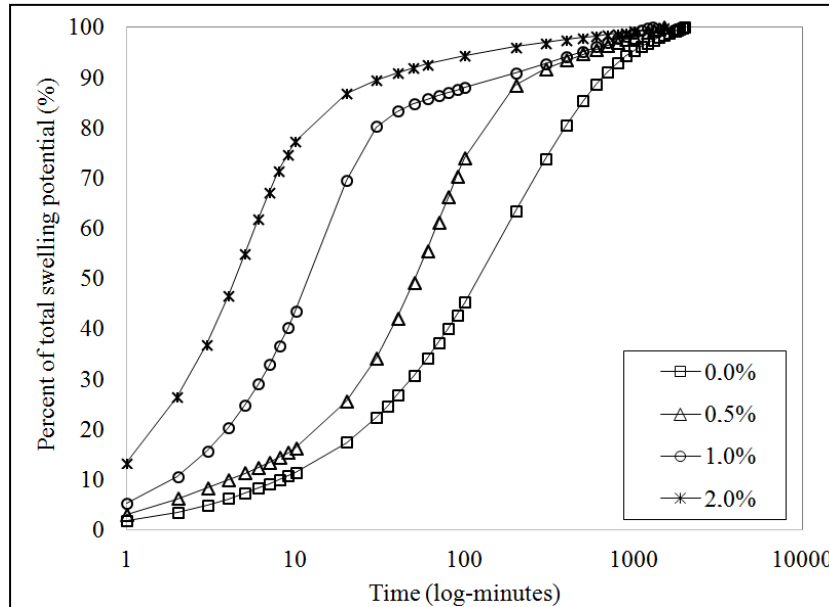


Figure 4.20. Semi-log plot of percentage of total swelling potential vs. time for untreated and lime-treated Eagle Ford clay with lime additions between 0% and 2%.

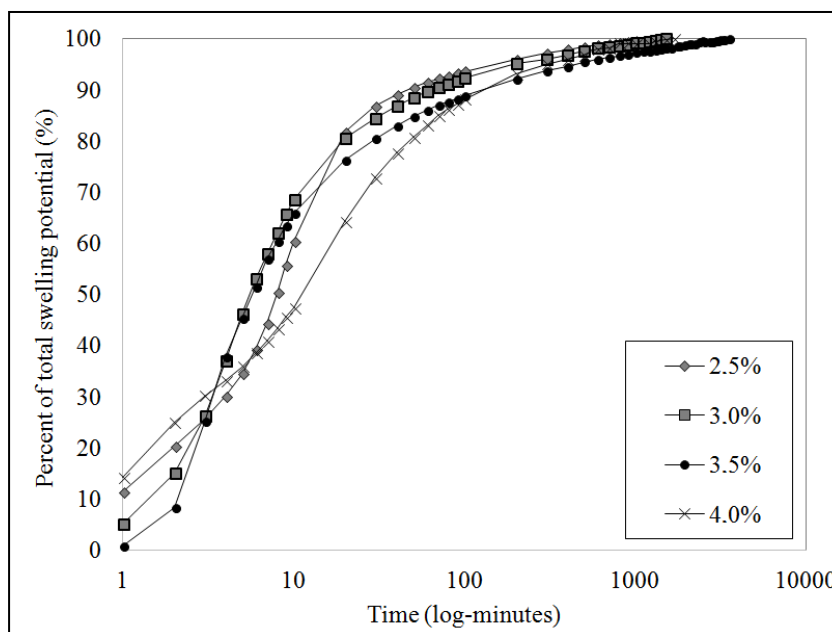


Figure 4.21. Semi-log plot of percentage of total swelling potential vs. time for lime-treated soils with lime additions between 2.5% and 4.0%.

Bin *et al.* (2007), working on clayey soil microstructure with nitrogen adsorption and desorption test, found that the addition of lime leads to an increase

in the amount of pores related to the flocculation process. This may explain why lime-treated Eagle Ford clay reached faster their total swelling than the untreated Eagle Ford clay. The entrance of water into the lime-treated specimen may be facilitated by the presence of big pores of the flocculated structure. On the other hand, the entrance of water into natural Eagle Ford clay may be difficult, because of its small pores, making the development of the total swelling slower.

4.2.1.2.

Evaluation of Curing Time Effect on Swelling Behavior

The second set of conventional free swell tests was conducted varying the curing time in 0, 1, 7 and 28 days in specimens treated with 1%, 2%, 3% and 4% of hydrated lime. The compaction moisture content was kept constant around 23%. All these conventional free swell tests were conducted applying setting load of 6 kPa. Table 4.7 summarizes the initial and final characteristics (moisture content, void ratio and saturation) of the specimens used in this set of experiments.

Table 4.7. Variation of Moisture content, Void ratio and saturation during conventional free swell tests for evaluating the curing time effect

Hydrated lime (%)	Curing time (days)	Moisture content		Void ratio		Saturation	
		Initial	Final	Initial	Final	Initial	Final
1	0	23.2%	43.7%	0.78	1.16	82.5%	100%
	1	24.0%	39.6%	0.90	0.96	72.3%	100%
	7	23.6%	38.6%	0.90	0.96	71.1%	100%
	28	22.2%	38.8%	0.89	0.95	67.5%	100%
2	0	22.9%	47.9%	0.88	0.79	85.0%	100%
	1	22.9%	35.0%	0.87	0.92	70.7%	100%
	7	22.6%	33.1%	0.87	0.89	69.7%	100%
	28	21.0%	34.5%	0.87	0.90	64.7%	100%
3	0	22.9%	38.4%	0.85	0.92	84.7%	100%
	1	23.0%	36.6%	0.86	0.91	70.1%	100%
	7	22.8%	37.0%	0.86	0.93	69.9%	100%
	28	22.9%	37.2%	0.86	0.93	70.0%	100%
4	0	23.0%	37.1%	0.71	0.71	86.5%	100%
	1	22.6%	35.0%	0.86	0.88	69.0%	100%
	7	22.4%	35.1%	0.86	0.87	69.2%	100%
	28	22.6%	34.9%	0.87	0.88	70.0%	100%

The resulting curves of the evaluation of curing time effect on swelling for specimens treated with 1% and 2% of hydrated lime are depicted in Figure 4.22 and Figure 4.23, respectively. Additionally, Figure 4.24 summarizes the swelling potential obtained at different curing times and different hydrated lime percentages. From these results, it is evident that there is a reduction of swelling behavior produced by the combined effect of lime addition and curing time. It can be noticed that there are significant reductions of swelling potential after one day of curing for all hydrated lime percentages. As can be seen in Figure 4.24, the swelling potentials in specimens with 1 day of curing were 36% to 50% smaller than those obtained at 0 days of curing. However, longer curing times, such as 7 and 28 days, produced reductions of swelling potential around 40 to 100% with respect to the value obtained at 0 days of curing.

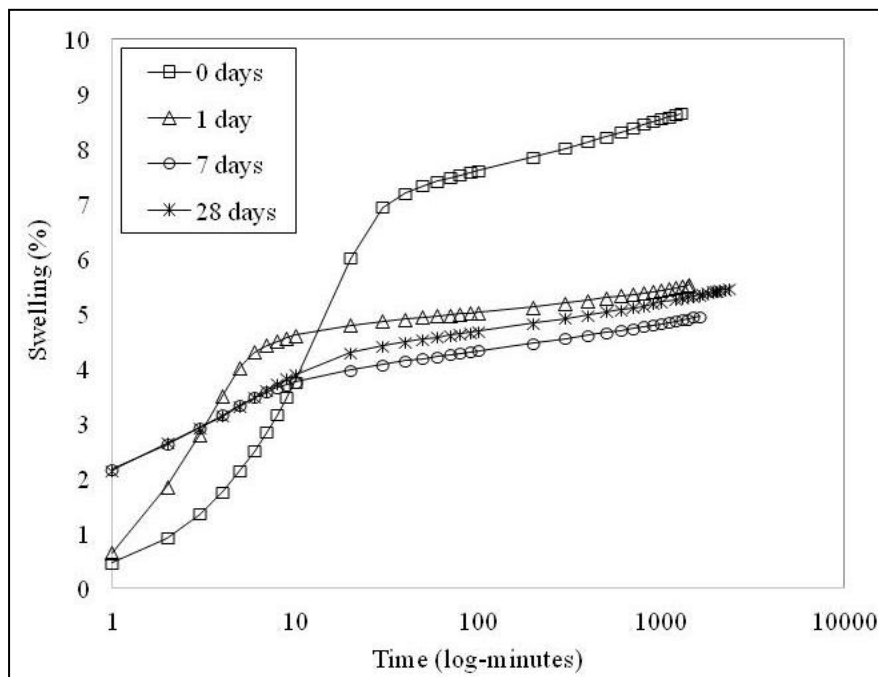


Figure 4.22. Semi-log plot of conventional free swell test results for lime-treated soil with 1% of hydrated lime at different curing times

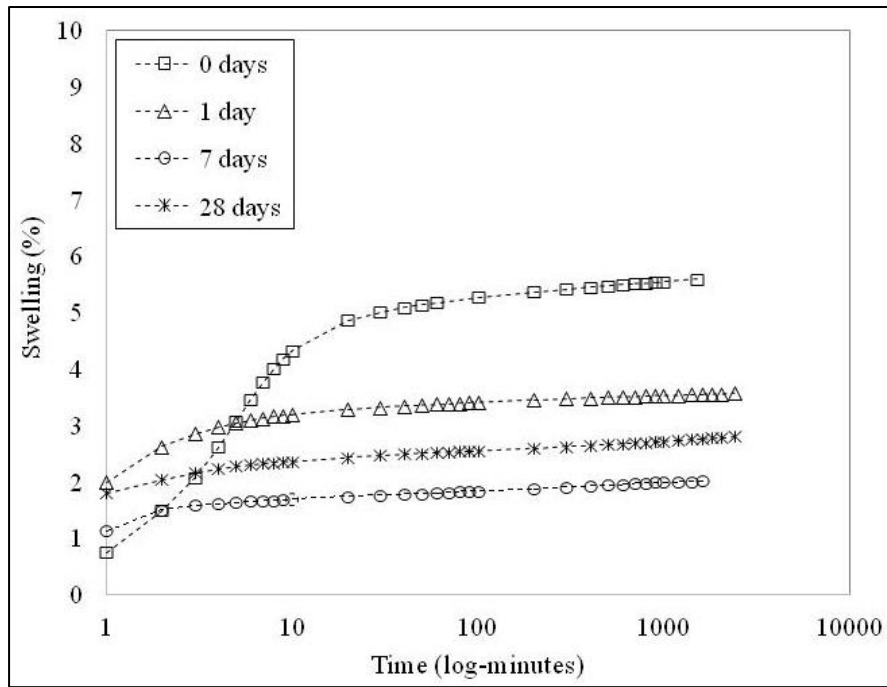


Figure 4.23. Semi-log plot of conventional free swell test results for lime-treated soil with 2% of hydrated lime at different curing times

PUC-Rio - Certificação Digital N° 1212916/CA

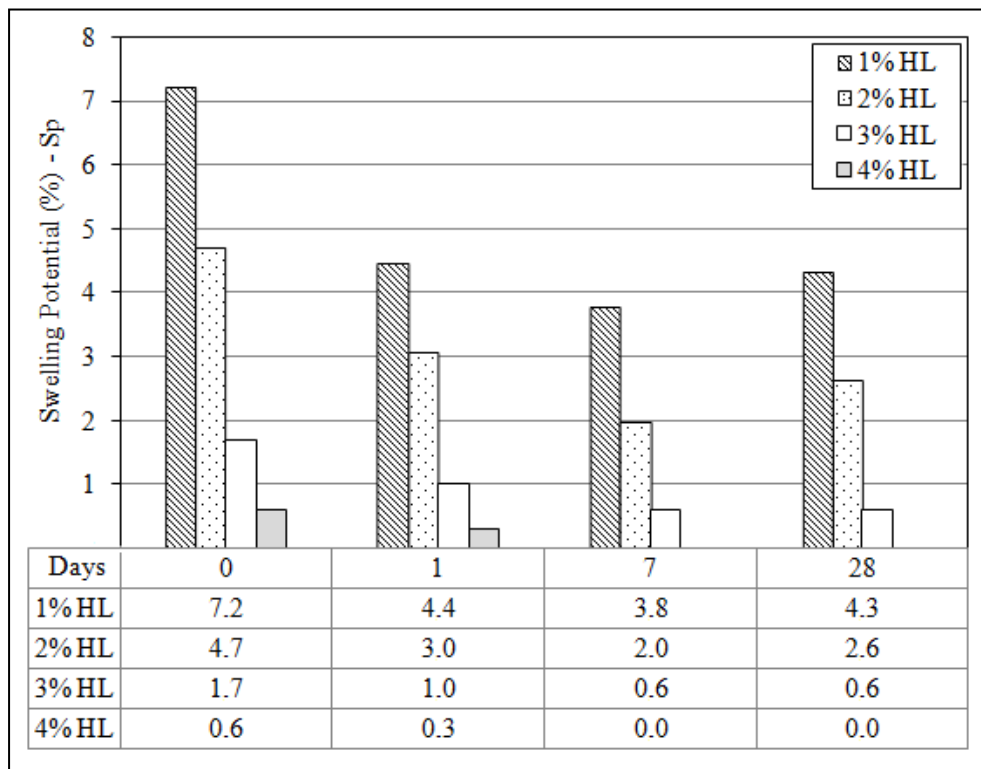


Figure 4.24. Curing time (days) effect on swelling potential

Similar swelling potentials were found in specimens cured for 7 and 28 days. This may be explained considering that short curing times lead to pore-volume

increase, and long curing times allow cemented compounds formation. The presence of these cemented compounds can stop the increase of pore volume making the swelling potential constant in longer curing times.

The SPR (Swelling Potential Reduction Ratio) value was calculated by equation (4.2), taking as reference the value of swelling potential of untreated Eagle Ford clay obtained in the previous set of experiments, i.e., $Sp_{(0\%HL)} = 22.1\%$. The SPR values obtained for different curing times were plotted in Figure 4.25. The results showed that the SPR values obtained at 1, 7 and 28 days of curing were fairly similar. Thus, the effect of curing time, more than 1 day, on swelling potential reduction does not have significant impact. One day of curing was enough to reach remarkable enhancement in swelling potential reduction, since curing times longer than 1 day produce SPR reduction with few variations.

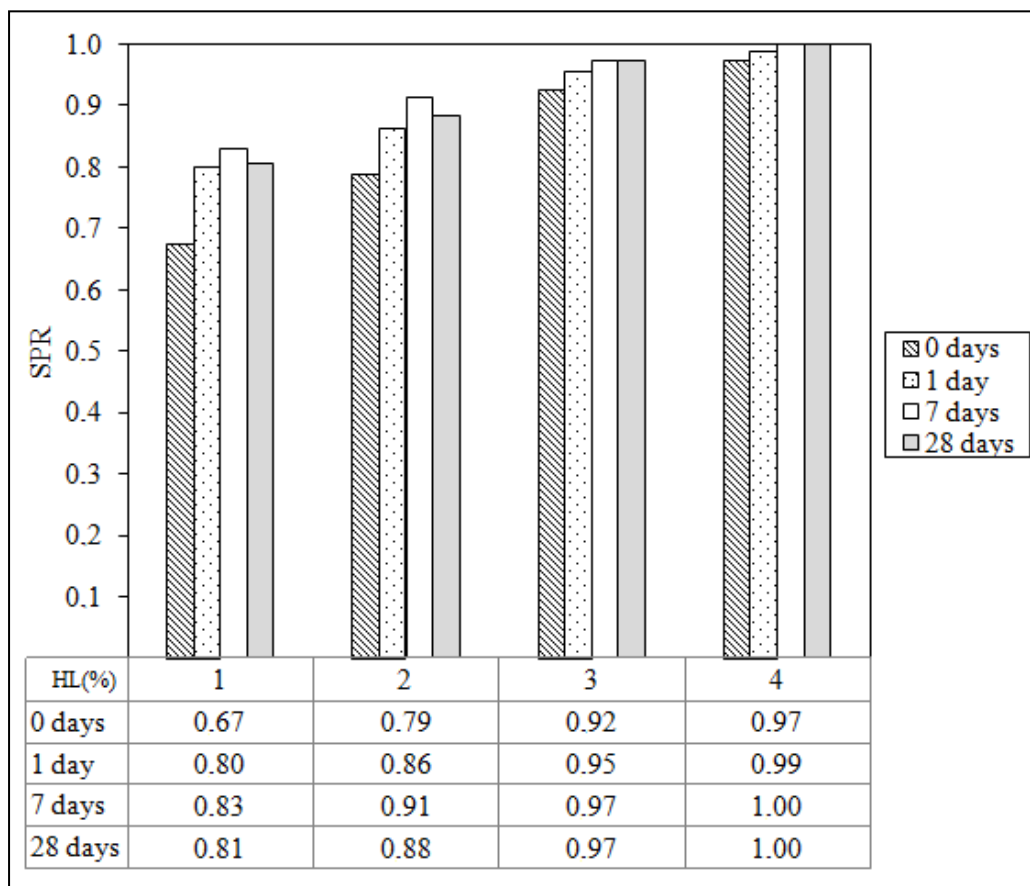


Figure 4.25. Swelling potential reduction ratio (SPR) for different curing times

In order to estimate the effect of curing time on the swelling mechanism, the primary swelling slope and secondary swelling slope variations with curing time

were plotted in Figure 4.26 and Figure 4.27, respectively. The primary swelling slope variations, depicted in Figure 4.26, show a clear trend of reduction of this slope due to curing time. The reduction of primary swelling slopes indicates that the capillary forces diminish with the increase of curing time, thus, the water infiltration becomes more difficult and occurs in a slower manner for specimens cured for long time.

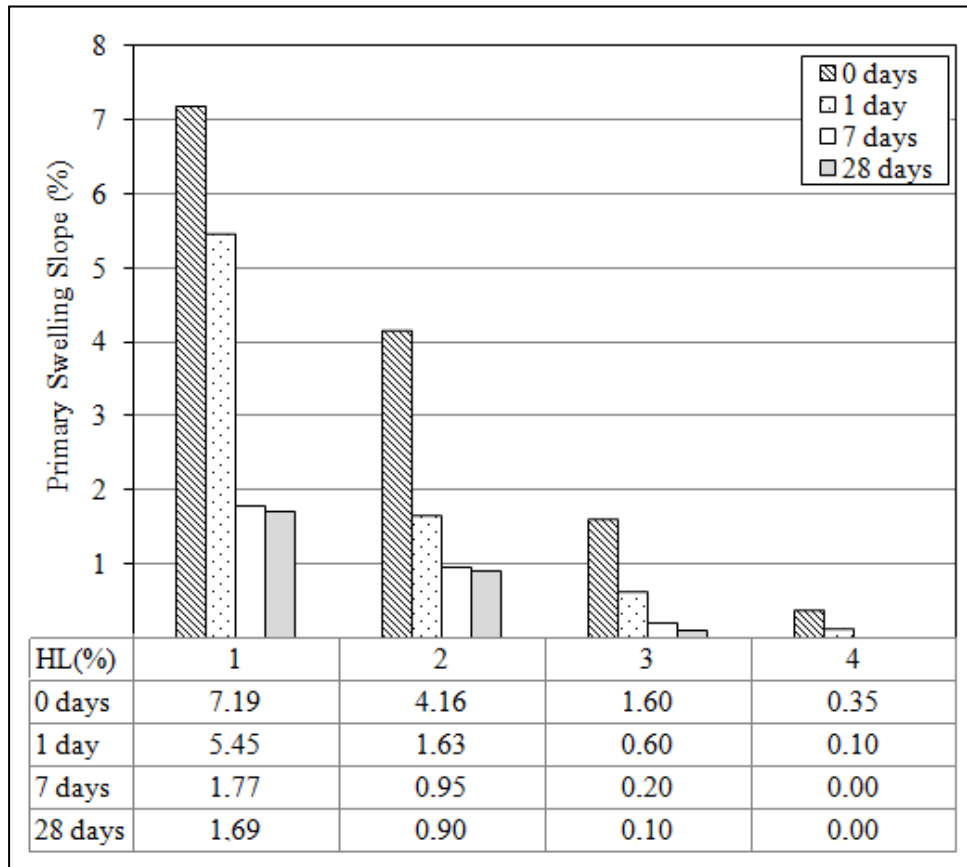


Figure 4.26. Curing time effect on primary swelling slope

The behavior of secondary swelling slope due to curing time effect, depicted in Figure 4.27, shows barely variations between specimens cured at different times. Also, the values of secondary swelling slopes were smaller than 1% making difficult the comparisons related to curing time. Even though, it can be seen a reductions in these slopes when the specimens were cured compared with specimens without curing.

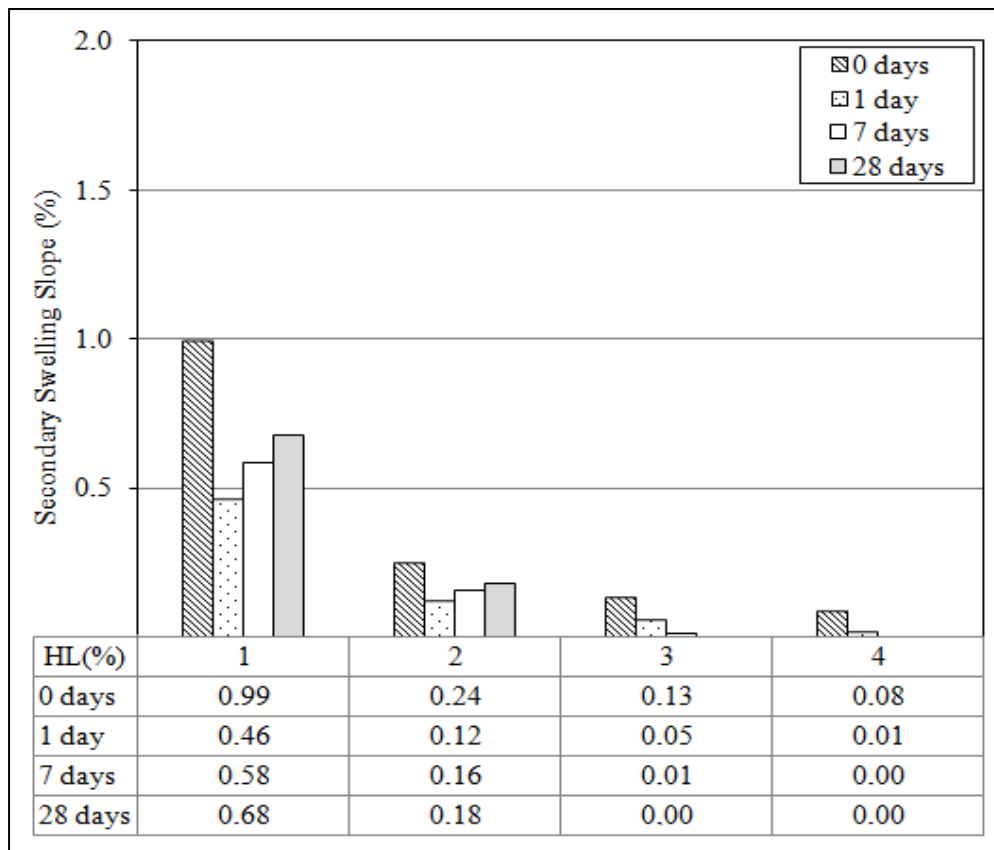


Figure 4.27. Curing time effect on secondary swelling slope

In the same way that it was explained why the curing time reduced the primary swelling slopes, the reduction in the secondary swelling slopes also can be attributed to the fact of the formation of cemented compounds during the curing time. These cemented compounds may difficult the water entrance responsible for hydration process that cause secondary swelling. High lime percentages, such as 3% and 4%, might generate higher amount of cemented compounds during the curing time, and consequently these percentages presented very small, or almost null, secondary swelling slope for 7 or 28 days of curing, as shown in Figure 4.27.

4.2.1.3.

Evaluation of Mellowing Period Effect on Swelling Behavior

The third set of conventional free swell tests was performed to analyze the influence of mellowing period on the swelling behavior of lime-treated Eagle Ford clay. Mellowing is the period time elapsed between the time when the lime-soil mixture was prepared and when final specimen compaction happened. Three types of specimens were prepared in order to analyze the effect of mellowing period. All

of these three types of specimens used the lime-soil mixtures (with 1% and 3% of hydrated lime) prepared at same day. The difference of these types is the day when the compaction was made.

The first type of specimen was prepared with no mellowing period (NM), or zero days mellowing, i.e., the specimens were compacted into the metal ring at the same day that the lime-soil mixtures were prepared. After compaction, these specimens were enveloped in plastic wrap and aluminum foil, and kept into the environmental chamber for curing during 7 days. After this time of curing, the compacted specimens were taken out from the environmental chamber and were subjected to the conventional free swell test. These specimens, with zero days of mellowing, were the same previously used for evaluating the effect of 7 days of curing.

The second type of specimen (designated as M3) was prepared compacting the specimens with 3 days of mellowing. After compaction, these specimens were kept into the environmental chamber, along with the first type of specimens (NM), for more 4 days in order to complete 7 days of curing.

The third type of specimens (designated as M7) was compacted with 7 days of mellowing. Thus, this third type of specimens also completed 7 days of curing, but in loose state. Immediately after finalizing the compaction of specimens type M7, the three types of specimens (NM, M3 and M7) were subjected to the conventional free swell.

Table 4.8 summarizes the initial and final characteristics (moisture content, void ratio and saturation) of the specimens used in this set of experiments and Figure 4.28 depicts the swelling vs. time curves in order to evaluate the effect of mellowing periods. It can be observed in Figure 4.28 an unfavorable effect of mellowing, due to the fact that the swelling occurred in specimens allowed to mellow (M3 and M7) was higher than the swelling reached in specimens with no mellowing period (NM).

Table 4.8. Variations of moisture content, void ratio and saturation during conventional free swell tests for evaluating the mellowing period effect

Hydrated lime (%)	Mellowing period (days)	Specimen label	Moisture content (%)		Void ratio		Saturation	
			Initial	Final	Initial	Final	Initial	Final
1	0	NM	23.6%	38.6%	0.95	1.01	69.2%	100%
	3	M3	23.1%	35.6%	0.95	1.00	72.1%	100%
	7	M7	23.0%	39.0%	0.96	1.07	75.4%	100%
3	0	NM	23.8%	34.0%	0.94	0.95	70.2%	100%
	3	M3	23.0%	35.3%	0.90	0.93	69.3%	100%
	7	M7	22.1%	39.7%	0.99	1.02	74.4%	100%

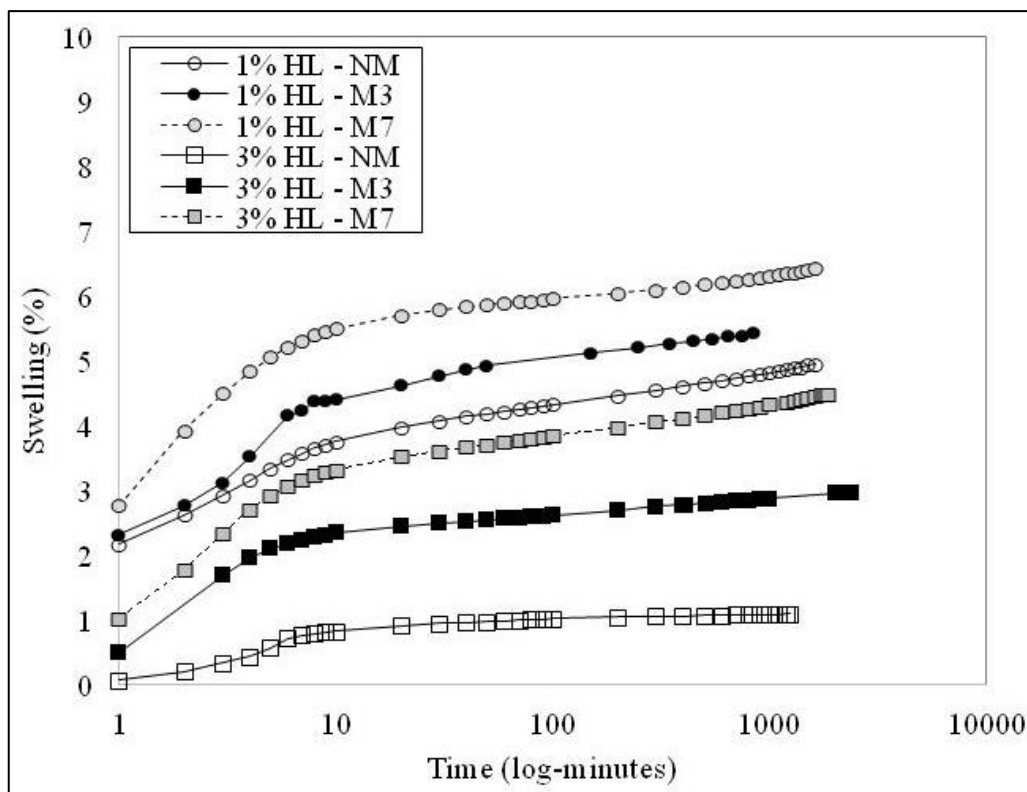


Figure 4.28. Semi-log plot of conventional free swell test results evaluating the effect of mellowing periods

Table 4.9 summarizes the swelling potential and the slopes of primary and secondary swelling obtained for this set of experiments. It seems that the higher lime percentage used, the higher will be the adverse effect of mellowing period on swelling behavior. So that the specimen treated with 1% of hydrated lime registered an increase of 74% of swelling potential, comparing M7 with NM. On the other hand, the specimen treated with 3% of hydrated lime and mellowed for 7 days

increased its swelling potential in more than 200% compared with no mellowed (NM) specimen.

These mellowing results are consistent with those obtained by Holt *et al.* (2000). Their research was about the effect of mellowing on the modification process of four British soils treated with quicklime. They reported that a half day mellowing period produced a decrease in volume change (volume calculated by measuring the height and diameter of specimens subjected to soaking), but mellowing periods above half a day produced gradually an increase in volume change, so that generally after one day mellowing period, the volume change was greater than the volume change without mellowing. This behavior was attributed to the presence of excessive air voids, generated during mellowing, that made the specimen more susceptible to water ingress, resulting in strength loss and volumetric expansion.

Table 4.9. Swelling potential and slopes of primary and secondary swelling of specimens with and without mellowing

Hydrated lime (%)	Mellowing period (days)	Specimen label	Swelling Potential	Primary Swelling Slope	Secondary Swelling Slope
1	0	NM	3.8%	1.77%	0.58%
	3	M3	5.0%	3.65%	0.45%
	7	M7	6.6%	3.75%	0.60%
3	0	NM	0.9%	0.85%	0.06%
	3	M3	2.2%	1.88%	0.25%
	7	M7	3.3%	2.93%	0.59%

The results obtained in the present study can support the generation of excessive air voids during mellowing periods. By observing the results obtained for the primary swelling slopes (PSS), it can be noticed that the increase in mellowing duration led to higher PSS. So that, the entrance of water due to the capillary process took place faster in the specimens with prolonged mellowing (3 or 7 days), indicating that these specimens may have had excessive air voids.

Another possible explanation for the increase of swelling potential due to mellowing period might be the undesirable development of a carbonation process in specimens that were not compacted immediately after lime-soil mixing (in this study, M3 and M7 type specimens). In the carbonation reaction, lime reacts with

atmospheric carbon dioxide to form a relatively insoluble carbonate. Thus, mellowing period might generate mixtures with less active lime.

Table 4.10 contains the values of swelling potential reduction ratio (SPR) for different mellowing periods. It can be noted that the specimen with 3% of hydrated lime and mellowed for 7 days reached almost the same SPR of the specimen with 1% of hydrated lime and no mellowing period. Since it should be expected higher SPR in specimens with higher hydrated lime, the assumption that less active lime might be found in specimen allowed to mellow (M3 and M7) than in the specimens without mellowing period (NM) can be corroborated.

Table 4.10. Swelling potential reduction ratio (SPR) for different mellowing periods

Hydrated lime (%)	Mellowing period (days)	Specimen label	Swelling potential (%)	SPR
1	0	NM	3.8	0.83
	3	M3	5.0	0.77
	7	M7	6.6	0.70
3	0	NM	0.9	0.96
	3	M3	2.2	0.90
	7	M7	3.3	0.85

Accordingly, considering the hypotheses of carbonation development during long mellowing periods, the best practical solution appears to be to compact the lime-treated soils immediately after mixing, in order to minimize the entrance of carbon dioxide and avoid the undesirable carbonation reaction. Otherwise, when longer delays to compaction cannot be avoided, it might be necessary to incorporate a small additional amount of lime into the mixer to compensate the lime lost due to carbonation.

4.2.2. Centrifuge Test Results and Analysis

The centrifuge testing plan was designed to evaluate the combined effect of lime addition with alteration of compaction moisture condition, compaction dry density (relative compaction percentage) and applied stress (by g-level) on swelling behavior of the expansive soil Eagle Ford clay. The experimental plan of centrifuge test was reported in Table 3.4 and the results are presented and analyzed below.

4.2.2.1. Evaluation of Compaction Moisture Condition Effect on Swelling Behavior

Although several researchers have been demonstrated that the swelling potential in expansive soils can be reduced with compaction at high moisture contents (Walker, 2012; Armstrong, 2014; Snyder, 2015), there are no studies about the effect of moisture condition on the swelling potential of lime-treated soils. In order to examine the combined effect of lime addition with compaction moisture condition variations on swelling behavior, the specimens with different percentages of hydrated lime were compacted at three different moisture conditions, designated as dry of optimum (DOP), optimum (OPT) and wet of optimum (WOP).

Based on the optimum moisture content values obtained for untreated Eagle Ford clay (22%) and for lime-treated mixtures with 4% of hydrated lime (26%), as shown in Figure 4.9, the OPT value was fixed as the average of those percentages (24%) in order to establish a baseline for comparison. So, the DOP condition was established equivalent to 21% of moisture content, the OPT condition was equivalent to 24% of moisture content and the WOP condition was equivalent to 27% of moisture content. An acceptable variation of +/-1% in the moisture content was established. The dry density was kept constant at 1.51 g/cm^3 with acceptable variation of +/- 0.1 g/cm^3 . This set of experiments was carried out keeping constant the applied g-level at 5g's. Table 4.11 summarizes the initial and final characteristics (moisture content, void ratio and saturation) of the specimens used in this set of experiments.

Table 4.11. Variation of moisture content, void ratio and saturation during centrifuge tests for evaluating the compaction moisture effect

Hydrated lime (%)	Compacted moisture condition	Moisture content		Void ratio		Saturation	
		Initial	Final	Initial	Final	Initial	Final
0.0	DOP	21.8%	49.6%	0.91	1.25	65.6%	100%
	OPT	22.9%	48.6%	0.93	1.18	67.9%	100%
	WOP	28.1%	43.1%	0.92	1.03	84.1%	100%
0.5	DOP	20.9%	44.0%	0.85	1.01	66.1%	100%
	OPT	24.1%	43.6%	0.87	0.98	75.2%	100%
	WOP	27.0%	42.2%	0.86	0.91	85.0%	100%
1.0	DOP	20.3%	41.3%	0.87	1.00	62.9%	100%
	OPT	23.2%	42.0%	0.85	0.95	74.0%	100%
	WOP	27.7%	42.7%	0.89	0.94	84.2%	100%
2.0	DOP	20.8%	36.5%	0.85	0.93	68.9%	100%
	OPT	22.3%	37.4%	0.85	0.90	70.7%	100%
	WOP	27.3%	37.2%	0.87	0.89	84.0%	100%
3.0	DOP	20.7%	38.0%	0.85	0.90	65.2%	100%
	OPT	23.9%	36.6%	0.86	0.90	76.1%	100%
	WOP	26.9%	34.2%	0.90	0.90	87.4%	100%
4.0	DOP	20.6%	39.6%	0.94	0.95	58.0%	100%
	OPT	24.5%	39.7%	0.93	0.96	66.7%	100%
	WOP	27.3%	39.2%	0.91	0.91	89.9%	100%

The swelling vs. log-time curves obtained by centrifuge test of untreated and lime-treated Eagle Ford clay, with percentages of lime ranging between 0.5% and 4%, and prepared at different compaction moisture condition are depicted in Figure 4.29 to Figure 4.31. Likewise the observations made in the conventional free swell test, it can be noticed that the centrifuge test also exhibited changes in the swelling vs. time curves when hydrated lime was added to the expansive soil Eagle Ford clay. The lime-treated specimens reached the final of primary swelling faster than the untreated Eagle Ford clay (0% HL), regardless the compaction moisture condition (DOP, OPT or WOP). Also, it can be seen that the secondary swelling increased less after lime addition, because after the swelling potential was reached, i.e., when the curve pass the inflexion point, the second part of the curve becomes almost horizontal.

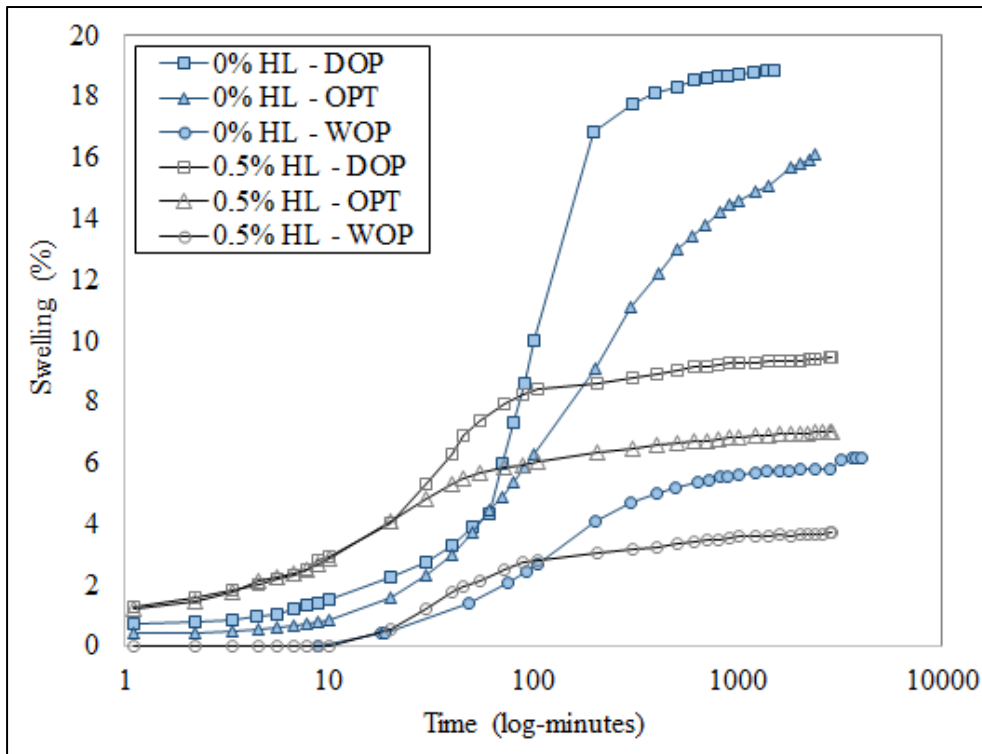


Figure 4.29. Semi-log plot of centrifuge test results from specimens with 0% and 0.5% of hydrated lime compacted at different moisture conditions

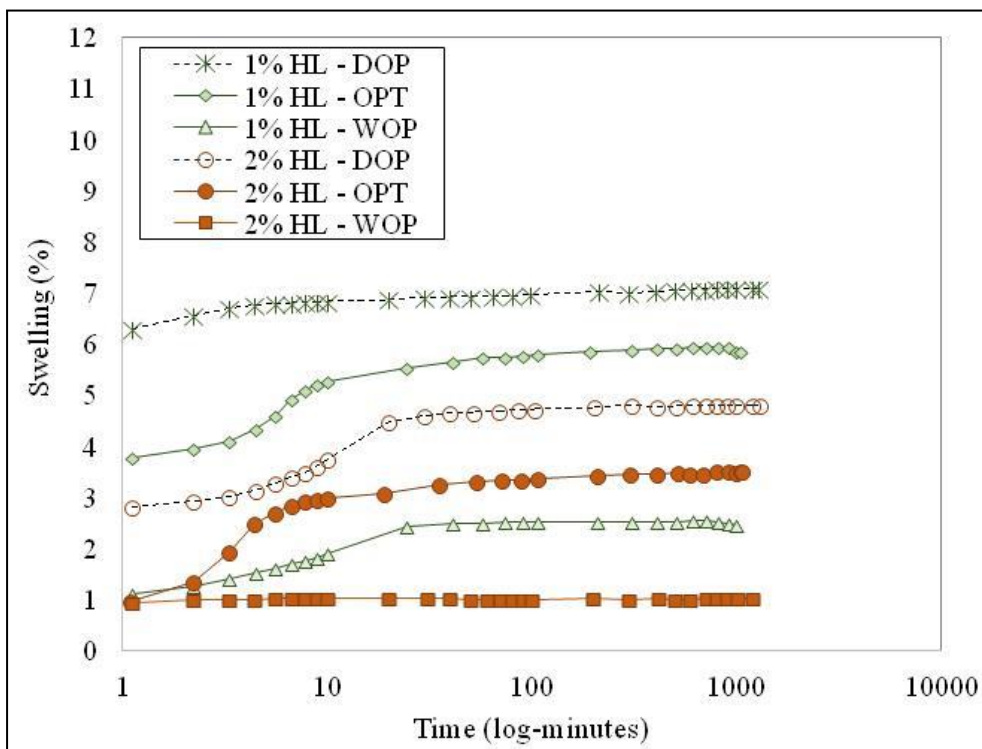


Figure 4.30. Semi-log plot of centrifuge test results from specimens with 1% and 2% of hydrated lime compacted at different moisture conditions

In Figure 4.31, it can be noticed that the swelling potential obtained for specimens treated with 4% of hydrated lime and compacted at moisture conditions OPT and WOP resulted in small negative values. From the physical point of view, these values might be interpreted as small compressions undergone by the specimens, however, since the aim of this research is the expansion evaluation, they will be taken as zero swelling.

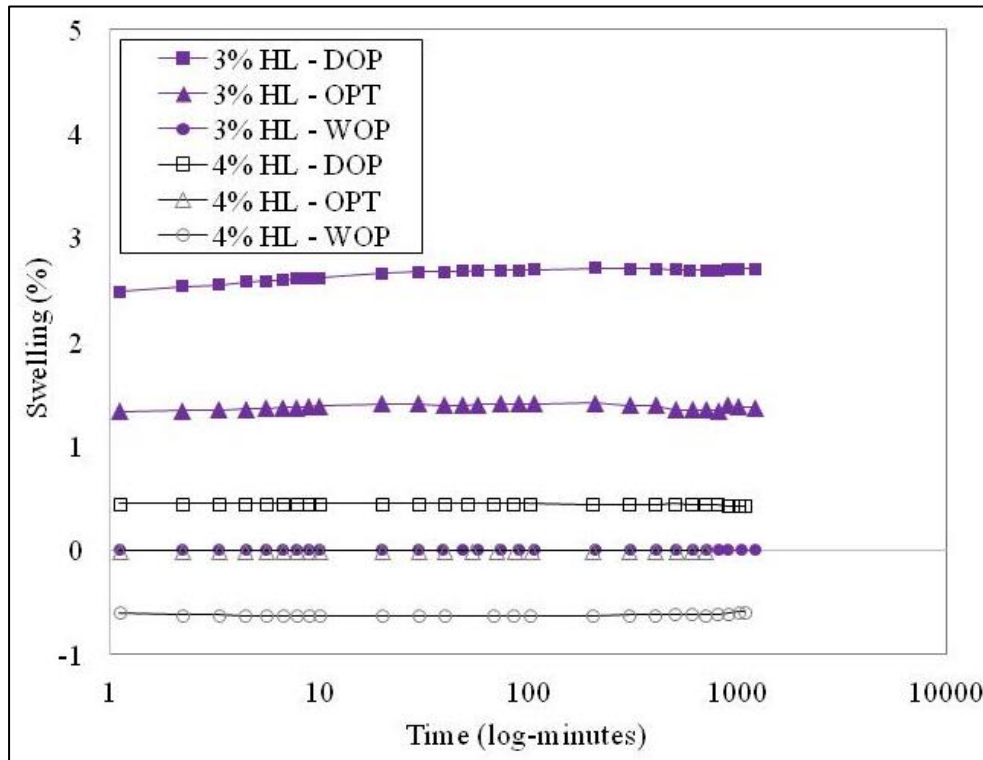


Figure 4.31. Semi-log plot of centrifuge test results from specimens with 3% and 4% of hydrated lime compacted at different moisture conditions

The compaction moisture condition effect on swelling potential for different hydrated lime percentages is depicted in Figure 4.32. It can be observed that when the compaction moisture condition changed from OPT to WOP in the untreated specimens (0% HL), the swelling potential was similar to those reached from specimens with 0.5% and 1.0% of hydrated lime and compacted at OPT moisture condition. This suggests that the increase in moisture content is able to substitute somehow the lime addition in order to reduce the swelling potential. However, in field applications, if the moisture content is too high, the clayey soil might become so sticky and plastic that the equipment cannot handle the soil properly, and besides that, the soil can lose significant bearing capacity. Thus, the use of high moisture

contents to reduce the swelling potential could not be applicable or recommendable in a lot of cases.

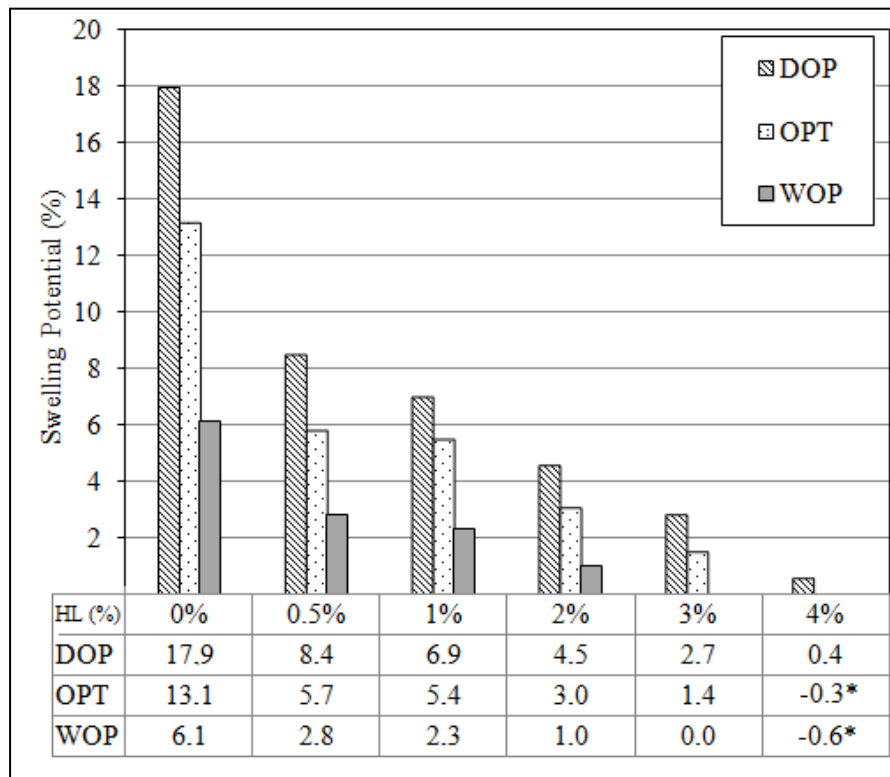


Figure 4.32. Compaction moisture condition effect on swelling potential for different hydrated lime percentages

Comparing the swelling potential obtained at DOP and WOP compaction conditions, it can be observed a reduction of 66% of swelling potential in untreated Eagle Ford clay, from DOP to WOP. Making the same comparison for lime-treated specimens, it can be seen that the increase of compaction moisture content, from DOP to WOP condition, can reduce up to 100% of swelling potential, as shown in Figure 4.32 for specimens with 3% and 4% of hydrated lime.

In order to estimate the swelling potential reduction ratio (SPR), defined by equation (4.2), the baseline swelling potential was established as the swelling potential obtained from untreated Eagle Ford clay at OPT moisture condition, i.e., $Sp_{(0\%HL)} = 13.1\%$, as shown in Figure 4.32, using the centrifuge test. Figure 4.33 illustrate the SPR at different compaction moisture conditions and hydrated lime percentages.

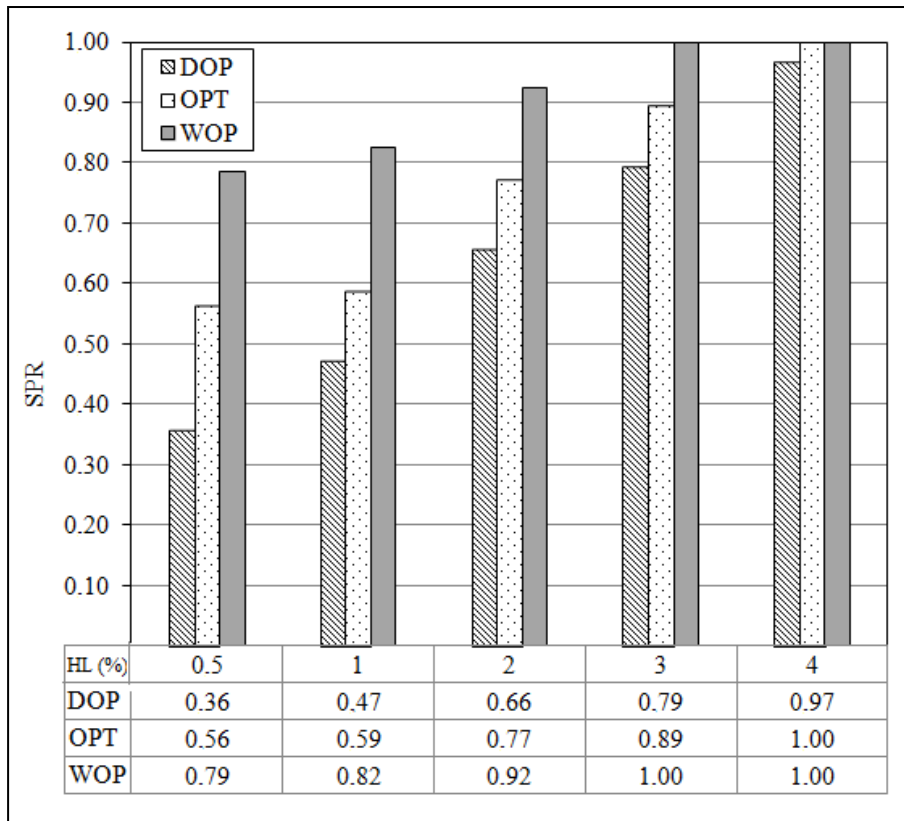


Figure 4.33. Swelling potential reduction ratio (SPR) at different compaction moisture conditions

Based on the patterns exposed in Figure 4.33, the WOP condition produced the highest SPR values for all percentages of hydrated lime applied. Furthermore, it can be noticed that while the hydrated lime percentage is increased, the difference between the SPR at the three compaction moisture conditions DOP, OPT and WOP seems to be reduced.

Also, the increment of compaction moisture content, e.g. from OPT to WOP condition, might reduce the amount of hydrated lime needed to avoid swelling behavior. For instance, in Figure 4.33, it was observed a slightly higher SPR value for the specimen treated with 1% HL and compacted at WOP than the SPR value obtained from the specimen treated with 2% HL and compacted at OPT condition. Therefore, an increase of 3% in compaction moisture content (i.e. from OPT = 24% to WOP = 27%) might result in almost the same swelling reduction produced by an additional of 1% of hydrated lime into the mixture. Since the lime addition also reduces the clay plasticity, problems related with workability are not be expected with increasing compaction moisture content, as could be expected in the case of natural expansive soils compacted at high moisture contents.

Conversely, the DOP condition exhibited an adverse effect on swelling reduction. As can be observed in Figure 4.33, the SPR value obtained in the specimen treated with 3% HL and compacted at DOP condition was similar to the one obtained with 2% HL and compacted at OPT condition. Since the DOP moisture condition may result in higher swelling potential, regardless the hydrated lime percentage, as can be seen in Figure 4.32, the lime-treated soil moisture should be checked before compaction in construction processes in order to ensure that this soil had not lost too much water. In the cases of the lime-treated expansive soils that are found very dry, additional hydration must be necessary in order to reach the intended swelling potential reduction.

In order to examine the combined effect of lime addition with compaction moisture condition variation on the swelling mechanism, the primary swelling slope (PSS) and secondary swelling slope (SSS) were analyzed as follows.

The compaction moisture condition effect on primary swelling slope was depicted in Figure 4.34. The untreated Eagle Ford specimens (0% HL) showed an abrupt decrease in the primary swelling slope when the compaction moisture content was increased. The capillary absorption occurred very fast in the DOP condition, where the primary swelling slope was very high, due to the fact that in the DOP there were many available air voids for being filled by water. When the compaction moisture condition changes from DOP to OPT or DOP to WOP, the void volume filled with water increases while the void volume filled with air decreases, thus it is expected in this case a slower infiltration process during the primary phase of swelling.

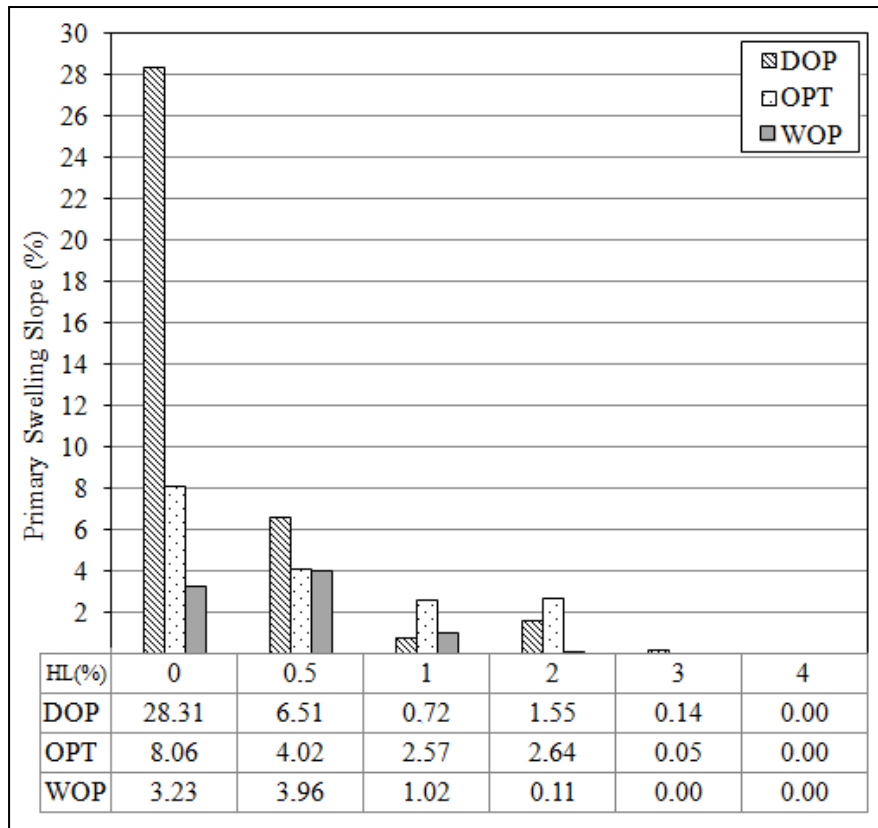


Figure 4.34. Compaction moisture condition effect on primary swelling slope

There is no clear pattern for slopes of primary swelling due to the combined effect of compaction moisture condition with lime addition, as shown in Figure 4.34. However, it can be seen just a few decrease of primary swelling slope when the compaction moisture condition changes from OPT to WOP in lime-treated Eagle Ford specimens. This behavior was also observed for the untreated Eagle Ford clay specimens.

On the other hand, no clear trend can be seen with respect to the DOP moisture condition in lime-treated specimens, because for 0.5% and 3% of hydrated lime, the primary swelling slope of DOP was higher than OPT and WOP, whereas for 1% and 2% of hydrated lime, the primary swelling slope of DOP was lower than OPT condition. The scattered behavior of primary swelling slope in DOP specimens may be attributed to a possible uneven water distribution into these specimens causing an uneven lime reaction through them.

In addition, it can be identified that the primary swelling slope observed in treated Eagle Ford specimens with 3% and 4% of hydrated lime was almost null

for the three compaction moisture condition (DOP, OPT and WOP). This is because of the insignificant swelling potential reached for these hydrated lime percentages.

The compaction moisture condition effect on secondary swelling slope was depicted in Figure 4.35. It can be seen that the untreated Eagle Ford specimens (0% HL) exhibited also a decrease in the secondary swelling slope when the compaction moisture condition was increased from DOP to OPT and DOP to WOP conditions. This is understandable because specimens with higher compaction moisture content contain particles nearer to the total hydration. Thus, the secondary swelling, which is supposed to be driven by hydration process, is expected to decrease with an increase of compaction moisture content.

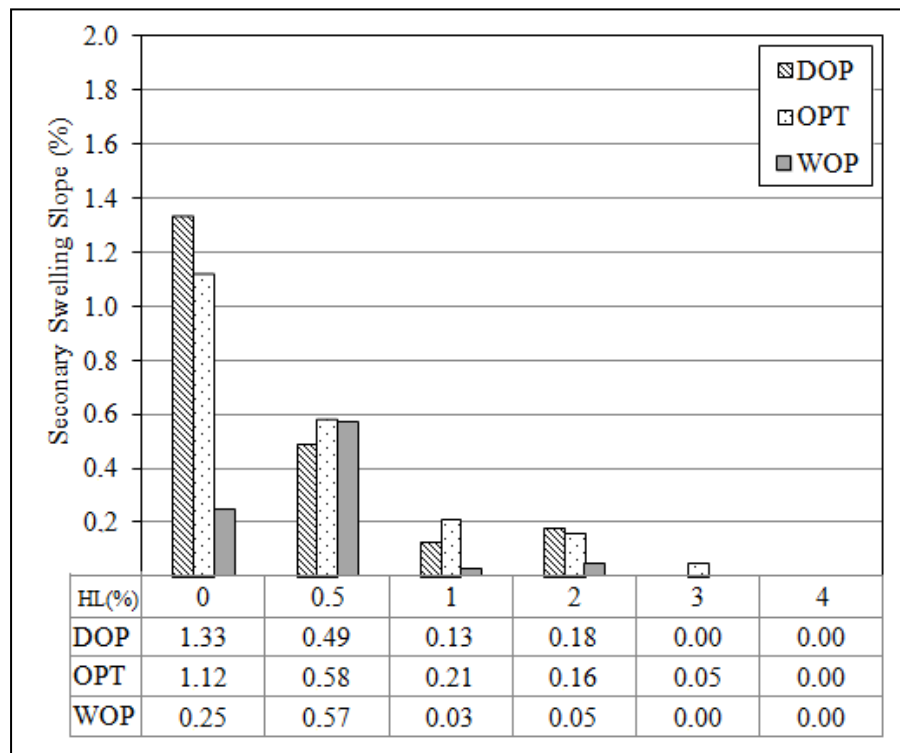


Figure 4.35. Compaction moisture condition effect on secondary swelling slope

When hydrated lime was added, it can be observed a high scatter pattern on the secondary swelling slope along with compaction moisture condition. Despite the scattering behavior on the secondary swelling data, it can be noticed that the lime addition produced very small secondary swelling slopes ($< 0.6\%$), so that, the secondary swelling do not represent a significant portion over the total swelling in lime-treated Eagle Ford clay specimens.

4.2.2.2.

Evaluation of Compaction Dry Density Effect on Swelling Behavior

In order to quantify the combined effect of lime addition with compaction dry density variations on swelling behavior, the specimens were compacted at 94% and 100% of relative compaction (RC). According to the results of standard Proctor compaction test carried out in untreated Eagle Ford clay, presented in section 4.1.5, the maximum dry density was 1.51g/cm^3 . Thus, the specimens with $\text{RC} = 100\%$ were compacted as close as possible to this dry density, whereas specimens with $\text{RC} = 94\%$ were compacted with dry density equivalent to 1.42g/cm^3 . In this set of experiments, the specimens were spun at 5g's into the centrifuge. The moisture content was kept constant and close to the OPT condition of 24%. Table 4.12 summarizes the initial and final characteristics (moisture content, void ratio and saturation) of the specimens used in this set of experiments.

Table 4.12. Variation of moisture content, void ratio and saturation during centrifuge tests for evaluating the compaction dry density effect

Hydrated lime (%)	RC (%)	Moisture content		Void ratio		Saturation	
		Initial	Final	Initial	Final	Initial	Final
0	100	22.9%	48.6%	0.93	1.18	67.9%	100%
	94	22.9%	50.6%	1.03	1.26	60.9%	100%
0.5	100	23.1%	43.6%	0.87	0.98	75.2%	100%
	94	23.1%	46.4%	1.00	1.09	65.4%	100%
1.0	100	23.2%	42.0%	0.85	0.95	74.0%	100%
	94	23.2%	44.3%	0.99	1.08	63.8%	100%
2.0	100	22.9%	37.4%	0.85	0.90	70.7%	100%
	94	22.9%	40.8%	0.90	0.95	68.0%	100%
3.0	100	23.9%	36.6%	0.86	0.90	76.1%	100%
	94	23.9%	40.6%	0.97	0.99	64.8%	100%
4.0	100	24.5%	39.7%	0.93	0.96	66.7%	100%
	94	23.8%	39.6%	0.99	1.00	63.4%	100%

Figure 4.36 and Figure 4.37 depict the swelling vs. log-time curves obtained by centrifuge testing of untreated and lime-treated Eagle Ford clay specimens that were compacted at $\text{RC} = 100\%$ and $\text{RC} = 94\%$. By observing these figures, the general trend noticed is a higher swelling in specimens compacted at $\text{RC} = 100\%$ than specimens compacted at $\text{RC} = 94\%$, except for the specimens with 4% of hydrated lime. Moreover, it was observed that while the percentage of lime

increases, the difference between the swelling developed by specimens at RC = 94% tends to become the same to swelling developed by specimens at RC = 100.

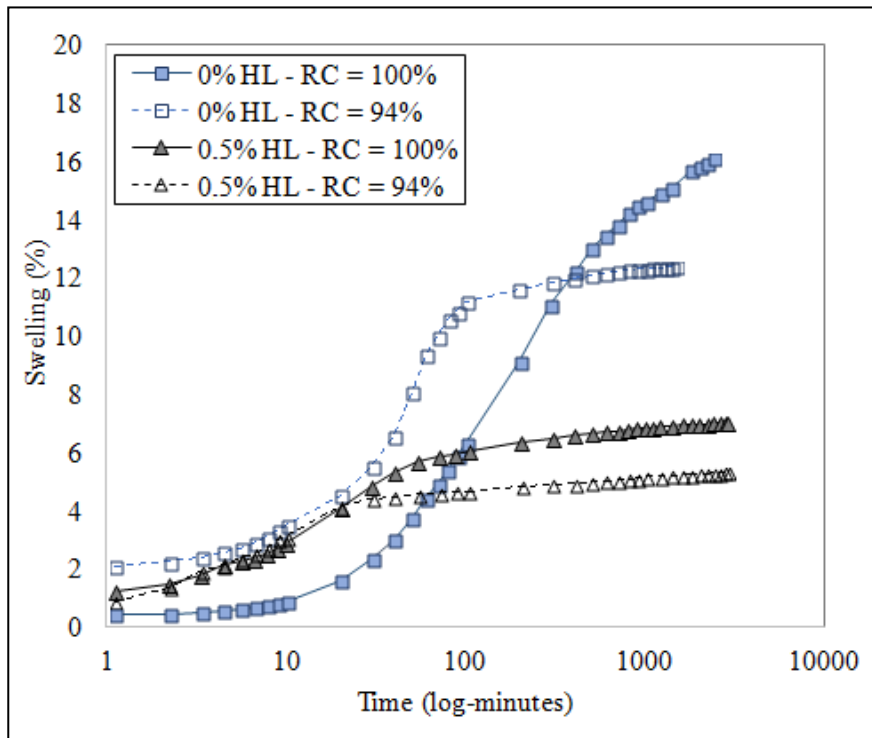


Figure 4.36. Semi-log plot of centrifuge test results of specimens with 0% and 0.5% of hydrated lime and compacted at 94% and 100% relative compaction (RC)

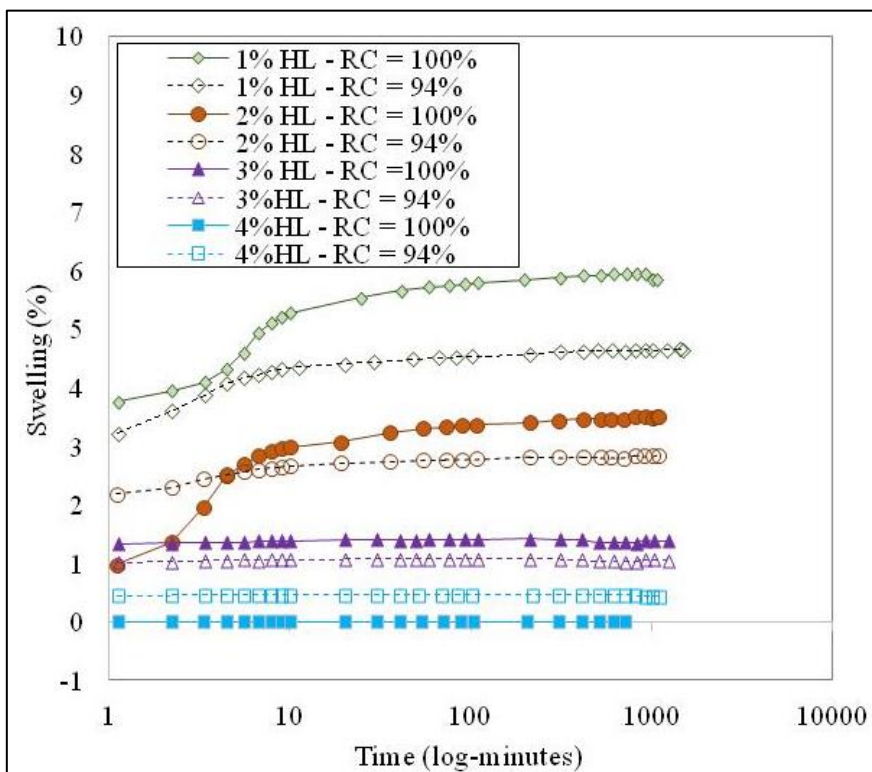


Figure 4.37. Semi-log plot of centrifuge test results of specimens with 1%, 2%, 3% and 4% of hydrated lime and compacted at 94% and 100% relative compaction (RC)

The swelling potential obtained in specimens compacted at RC = 100% and at RC = 94%, with different percentages of lime, are depicted in Figure 4.38. The untreated and lime-treated Eagle Ford specimens with lime addition of 0.5%, 1%, 2% and 3%, reduced their swelling potential ranging from 13% to 25% for the same lime percentage, when RC was decreased from 100% to 94%. Contrariwise, the lime-soil mixture with 4% of hydrated lime showed a slightly increase in swelling potential when RC was decreased from 100% to 94%. As stated above, the negative value of swelling potential should be interpreted as null swelling potential in this study.

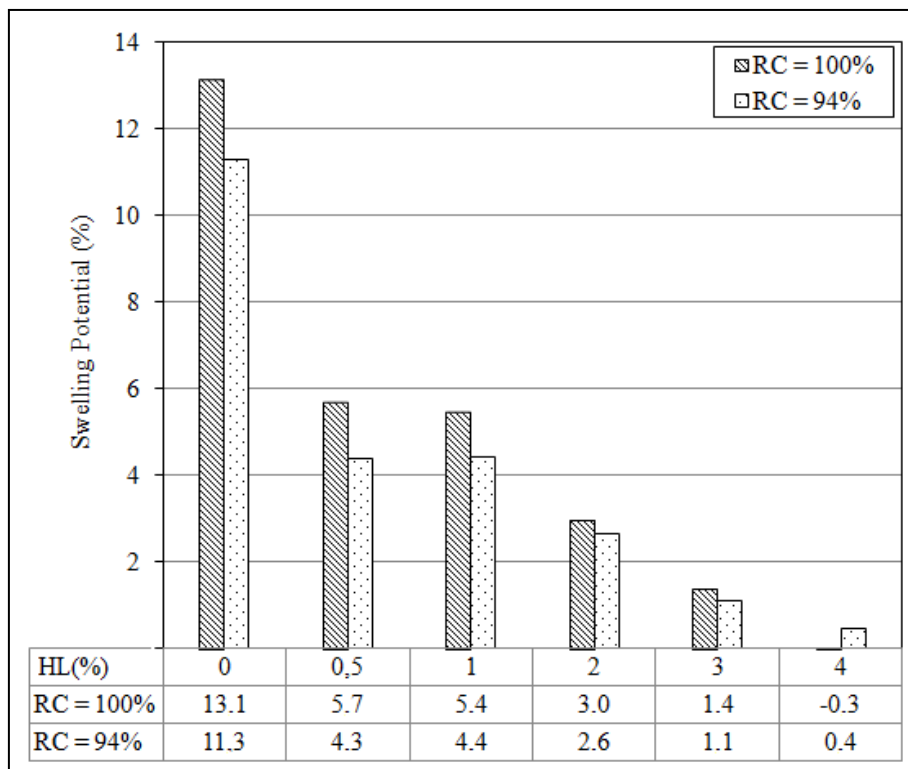


Figure 4.38. Relative compaction effect on swelling potential for different hydrated lime percentages

Likos and Lu (2006) analyzed axial strain of Na and Ca smectite specimens compacted to different initial void ratios and hydrated within the crystalline swelling regimen. The results showed that denser specimens swelled more than initially loose specimens. They indicated that loosely compacted specimens exhibit more inefficient translation from particle-scale swelling to bulk-scale swelling because the interlayer volume changes occurring on the particle scale are internally adsorbed by the larger scale pores. Conversely, densely compacted specimens exhibit more efficient translation from particle-scale swelling to bulk-scale swelling

because the interlayer volume changes are less well accommodated by the internal pores. Therefore, in the present study, it might be observed that the lime addition affects directly the mechanisms of swelling translation from particle-scale swelling to bulk-scale swelling.

The combined effect of relative compaction reduction with lime addition on swelling potential was estimated by the swelling potential reduction ratio (SPR) value, as defined by equation (4.2). The baseline swelling potential was established as the swelling potential obtained from untreated Eagle Ford clay compacted at OPT moisture condition and RC = 100, i.e., $Sp_{(0\%HL)} = 13.1\%$, as shown in Figure 4.38, using the centrifuge test. Therefore, the SPR values were calculated using the swelling potential obtained with different hydrated lime percentages and both relative compaction RC=100% and RC=94. The results are reported in Figure 4.39.

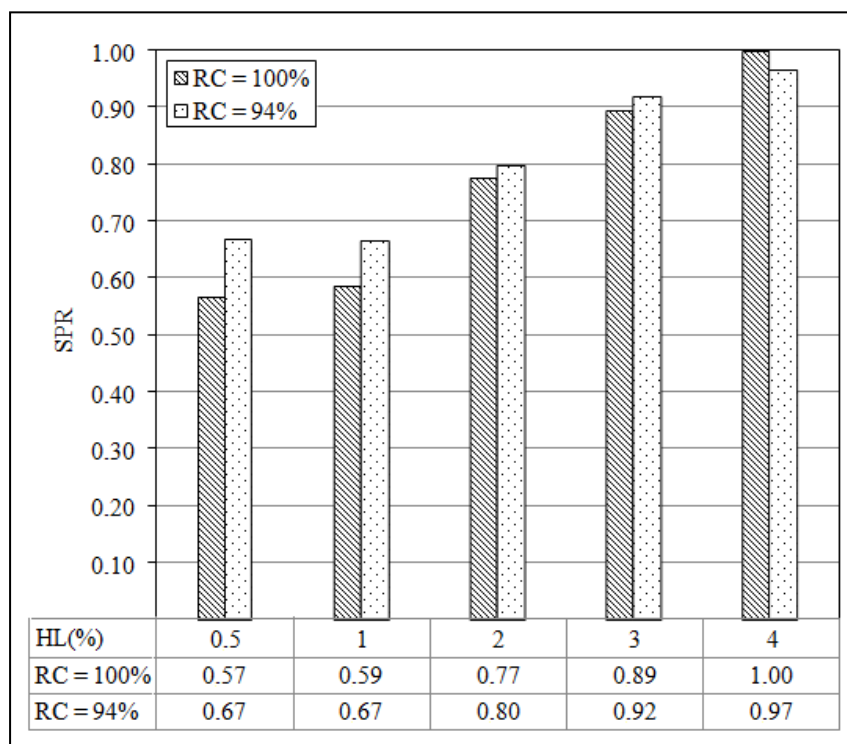


Figure 4.39. Relative compaction effect on swelling potential reduction ratio (SPR) for different hydrated lime percentages

The results suggest that when the hydrated lime percentage was increased, the SPR difference between specimens with RC = 94% and 100% was reduced. Also, it can be observed that SPR for all hydrated lime percentages was greater in specimens compacted at RC = 94% than those compacted at RC = 100%, except

for 4% of hydrated lime. Thus, the reduction in dry density (or RC) leads to increase of lime addition efficiency on swelling reduction. However, unlike to what was observed for variations of compaction moisture content (see explanation for Figure 4.33), the dry density variation could not offset the effect of a greater percentage of lime.

The primary swelling slopes (PSS) and secondary swelling slopes (SSS) obtained in specimens compacted at RC = 100% and at RC = 94%, with different percentages of lime, are depicted in Figure 4.40 and Figure 4.41. In Figure 4.40, it can be observed that primary swelling slope in untreated Eagle Ford specimen compacted at RC = 94% was higher than specimen compacted at RC = 100%. Conversely, the lime-treated Eagle Ford specimen presented smaller PSS compacted at RC = 94% than those compacted at RC = 100%.

Therefore, for untreated Eagle Ford specimens, a faster primary swelling development was observed in loose specimen than in denser one, whereas in lime-treated Eagle Ford clay, the primary swelling occurred faster in specimens compacted at higher dry density. The primary swelling slope changes its behavior from untreated to lime-treated Eagle Ford clay because the generation of cemented compounds, due to lime addition, may modify the process of water absorption by the capillarity process responsible for the primary swelling.

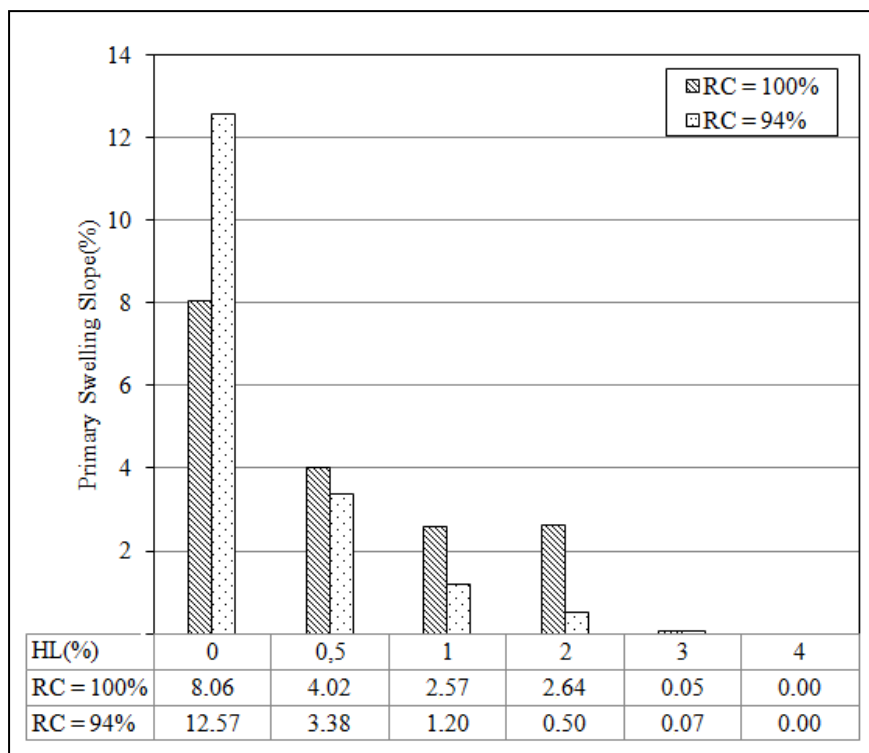


Figure 4.40. Relative compaction effect on primary swelling slope

On the other hand, in Figure 4.41, it can be noticed that both untreated and lime-treated Eagle Ford specimens compacted at RC = 94% presented SSS smaller than those compacted at RC = 100%. Furthermore, it can be seen that lime-treated Eagle Ford clay for hydrated lime of 3% and 4% presented negligible PSS and SSS values due to null (or almost null) swelling.

From these results, it is possible to conclude that the hydration process, responsible for development of secondary swelling, depends on the compaction dry density in both untreated and lime-treated Eagle Ford clay. The behavior of secondary swelling is in accordance with the observations reported by Walker (2012) and Das (2014), for untreated expansive soils.

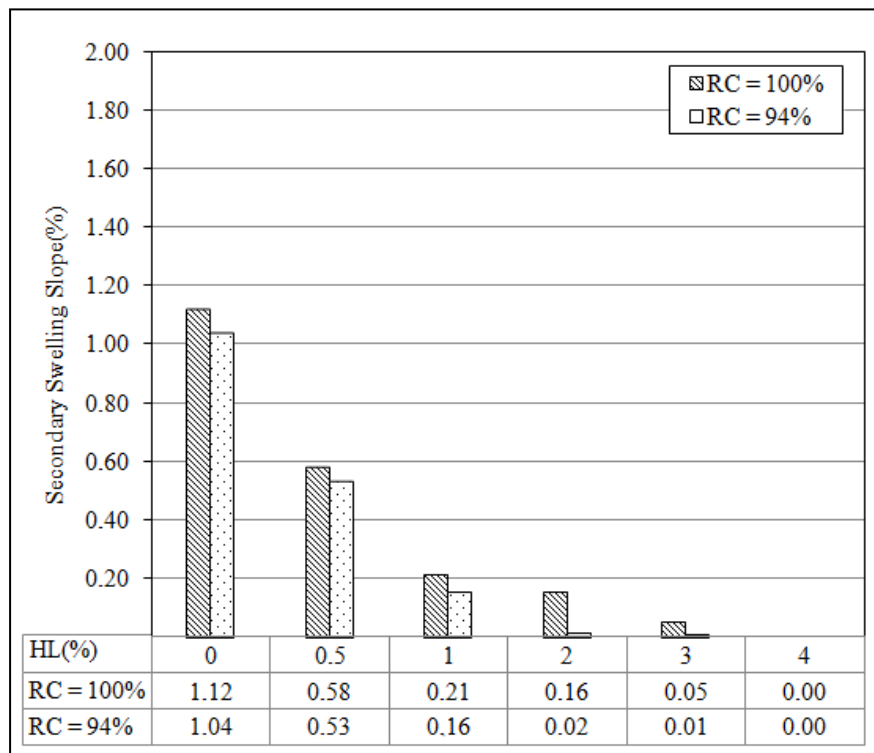


Figure 4.41. Relative compaction effect on secondary swelling slope

4.2.2.3.

Evaluation of G-Level Effect on Swelling Behavior

The g-level within the soil specimens was controlled through regulating the rotational velocity of the centrifuge. In this set of experiments, the untreated and lime-treated Eagle Ford clay with 1% and 2% hydrated lime were subjected to g-levels of 5, 50 and 200 g's. Untreated and lime-treated Eagle Ford specimens, regardless the percentage of hydrated lime, were compacted at the same dry density

of 1.51 g/cm^3 (with acceptable variation of $\pm 0.1 \text{ g/cm}^3$) and at the same initial moisture content of 24% (with acceptable variation of $\pm 1\%$). Since a constant water height of 2 cm (corresponding to 80 grams of water) was added to atop of the soil specimen, the total stress applied over the specimen varied only with the g-level. For these tests, the effective stress varied between approximately 5 and 61 kPa. Table 4.13 summarizes the initial and final characteristics (moisture content, void ratio and saturation) of the specimens used in this set of experiments.

Table 4.13. Variation of moisture content, void ratio and saturation during centrifuge tests for evaluating the g-level effect

Hydrated lime (%)	g -level	Effective stress (kPa)	Moisture content		Void ratio		Saturation	
			Initial	Final	Initial	Final	Initial	Final
0	5	5	22.9%	48.6%	0.93	1.18	67.9%	100%
	50	18	23.6%	43.5%	0.89	1.04	72.9%	100%
	200	61	23.5%	38.1%	0.77	0.87	83.9%	100%
1	5	5	22.8%	42.2%	0.91	1.05	74.2%	100%
	50	18	22.9%	40.8%	0.88	0.97	87.0%	100%
	200	61	23.4%	33.5%	0.79	0.84	81.8%	100%
2	5	5	22.3%	37.4%	0.85	0.90	70.7%	100%
	50	18	22.8%	37.1%	0.86	0.90	70.8%	100%
	200	61	23.0%	36.9%	0.82	0.83	75.5%	100%

Figure 4.42 and Figure 4.43 show the swelling vs. log-time curves obtained by centrifuge testing for untreated and lime-treated Eagle Ford clay specimens subjected at different g-levels. It can be seen in these figures that less swelling was developed when the g-level was increased. This is because the increasing g-level results in an increase of effective stress applied on the specimens.

The swelling potential, SPR values and the primary and secondary swelling slopes were collected in Table 4.14. Based on the swelling potential (S_p) and g-level applied on the specimen, reported in Table 4.14, the graphic of Figure 4.44 was constructed. It can be seen that the relationship between swelling potential and g-level, in centrifuge test, fits trend lines described by natural logarithmic functions for both untreated and lime-treated Eagle Ford clay. If the swelling potential is estimated by using these natural logarithmic functions for a g-level equal to 1, then the S_p results will be 16.33% for 0% HL, 6.87% for 1% HL and 3.99% for 2% HL.

These Sp values are relatively close to those obtained by using the conventional free swell test, as shown in Table 4.6.

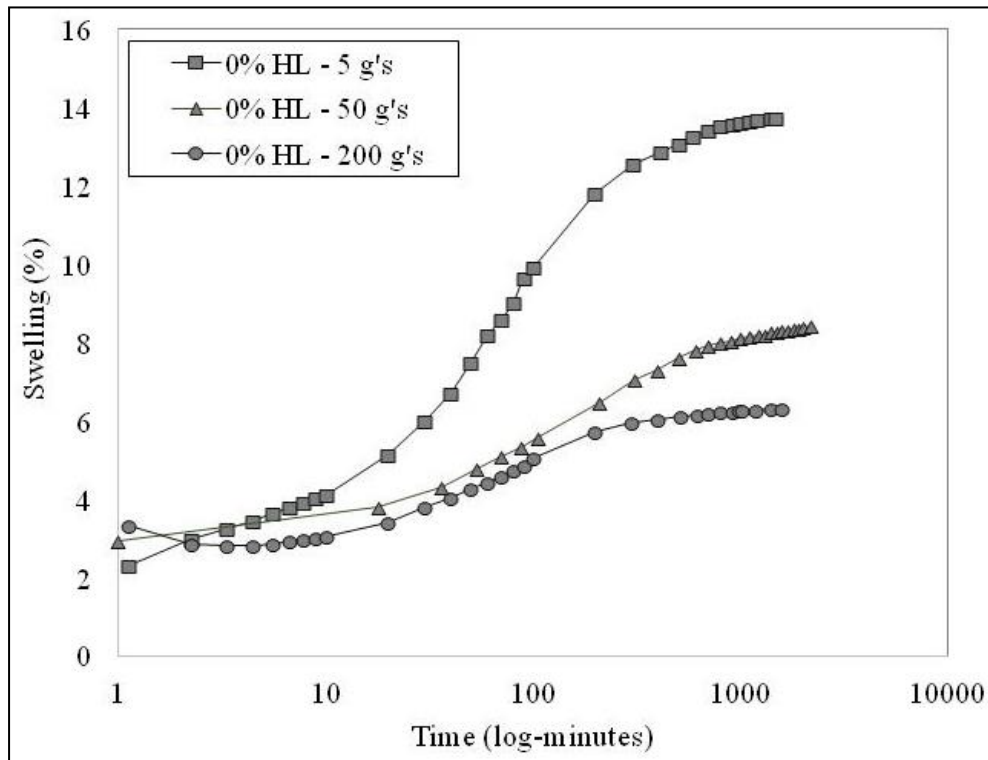


Figure 4.42. Semi-log plot of centrifuge test results of untreated Eagle Ford clay specimens subjected to different g-levels.

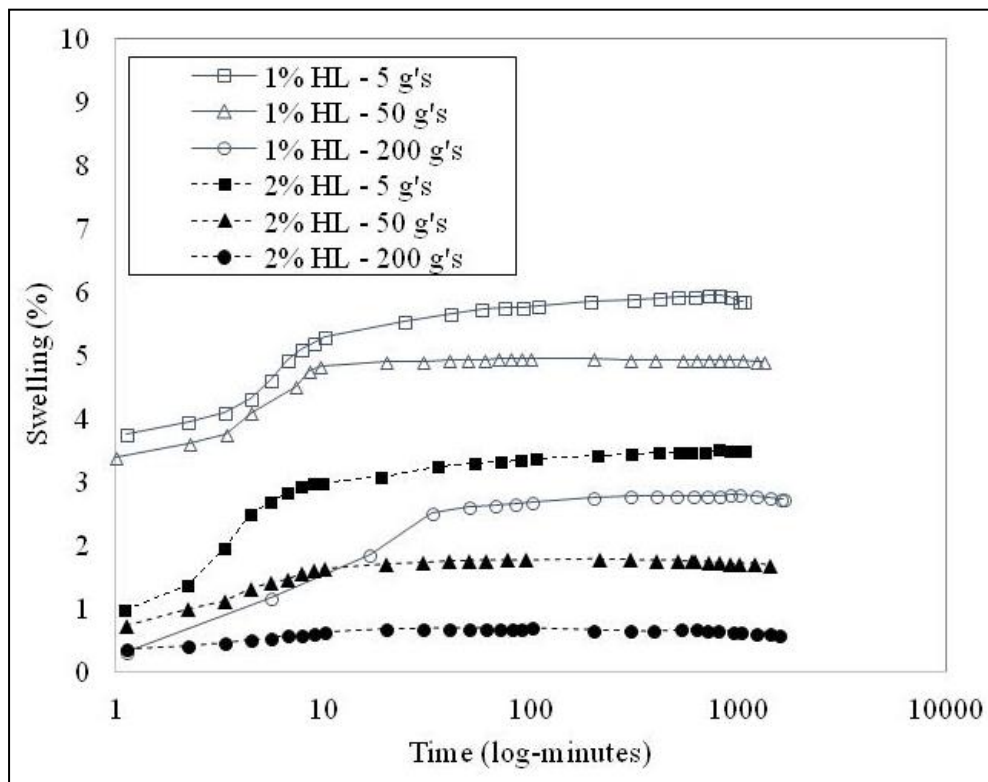


Figure 4.43. Semi-log plot of centrifuge test results at different g-levels for lime-treated soils with 1% and 2% of hydrated lime.

Significant drop in swelling potential occurred when the g-level was increases from 5 to 50 g's. For instance, in untreated and lime-treated Eagle Ford clay specimens with 2% hydrated lime, there was approximately 40% reduction in swelling potential from 5 to 50 g's. However, once the specimen was subjected to stresses related to 50 and 200 g's, the swelling potential showed change less significant.

Table 4.14. Swelling potential, SPR values and primary and secondary swelling slopes for untreated and lime-treated Eagle Ford clay subjected at different g-levels in centrifuge test

Hydrated lime (%)	g-level	Effective stress (kPa)	Swelling potential	SPR	Primary swelling slope	Secondary swelling slope
0	5	5	13.1%	-	8.06%	1.12%
	50	18	8.0%	0.39	3.46%	0.97%
	200	61	5.6%	0.57	2.14%	0.67%
1	5	5	5.4%	0.59	2.57%	0.21%
	50	18	4.8%	0.63	1.04%	0.11%
	200	61	2.6%	0.80	1.38%	0.05%
2	5	5	3.0%	0.77	2.64%	0.16%
	50	18	1.7%	0.87	0.96%	0.03%
	200	61	0.7%	0.95	0.37%	0.09%

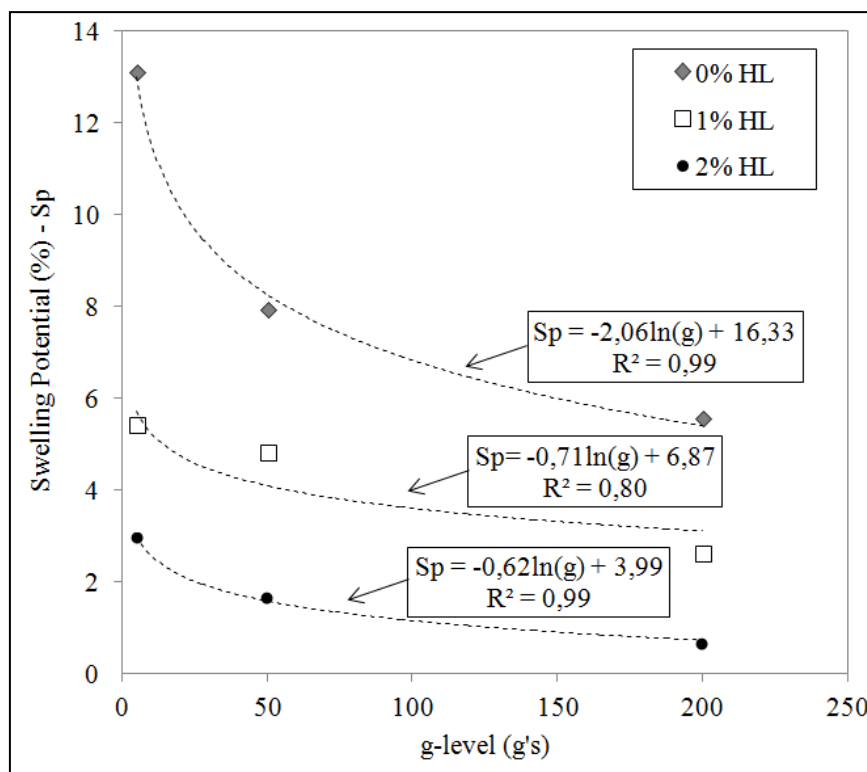


Figure 4.44. Relationship between g-level and swelling potential in centrifuge tests of specimens with different percentage of hydrated lime

The combined effect of effective stress (produced by variations of g-level) with lime addition on swelling potential was estimated by the swelling potential reduction ratio (SPR) value, as defined by equation (4.2). The baseline swelling potential was established as the swelling potential obtained from untreated Eagle Ford clay compacted at OPT moisture condition, RC = 100% and subjected to 5g's, i.e., $Sp_{(0\%HL)} = 13.1\%$, as shown in Table 4.14, using the centrifuge test. Therefore, the SPR values were calculated using the swelling potential obtained with different hydrated lime percentages and g-levels variation. The results are reported also reported in Table 4.14 and plotted in Figure 4.45.

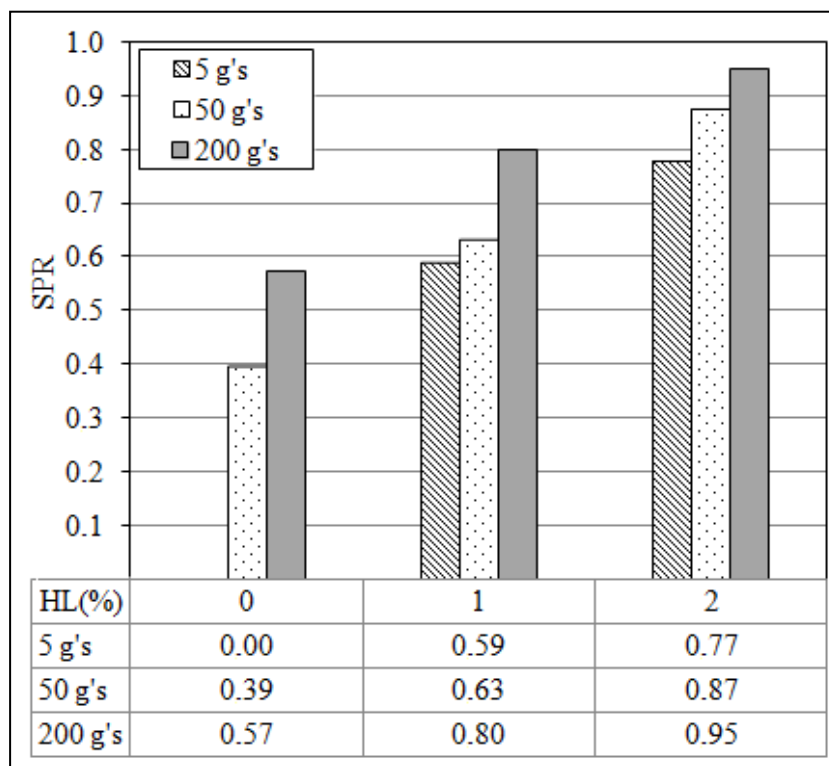


Figure 4.45. g-level effect on swelling potential reduction ratio (SPR) for different hydrated lime percentages

The SPR results suggest that when the g-level (i.e. applied effective stress) increases, the SPR values also increases. Thus, the increase of effective stress leads to increase of lime addition efficiency on swelling reduction. Also, the increment of g-level might reduce the amount of hydrated lime needed to avoid the swelling behavior. So that, the percentage of lime needed to prevent the swelling behavior depends on the applied vertical stress generated by the structure projected on the expansive soil.

For instance, in Figure 4.45, it was observed a similar SPR value (0.57) for the untreated specimen and subjected to 200g's to the SPR value (0.59) obtained from the specimen treated with 1% HL and subjected to 5g's. Likewise, similar SPR value (0.80) for the specimen treated with 1% HL and subjected to 200g's to the SPR value (0.77) obtained from the specimen treated with 2% HL and subjected to 5g's was indentified. Since the artificial g-levels are correlated with effective stress applied on the specimen, the amount of lime needed to prevent the swelling behavior also depends on the vertical stress that will be applied by the weight of the structure projected on the expansive soil.

The effect of g-level on the primary and secondary swelling slopes for 0%, 1% and 2% of hydrated lime is depicted in Figure 4.46 and Figure 4.47. There is an evident decreasing in primary and secondary swelling between results obtained at 5g's and those results at 200g's, independently on the hydrated lime percentage. Das (2014) reported a decrease in the secondary swelling slope upon increasing the g-level for four types of untreated expansive soils (Eagle Ford, Tan Taylor, Houston Black and Black Taylor), which in accordance with the secondary swelling slope results found here.

It was expected that for specimens subjected to 5g's, the water infiltration happen in slower manner than in the specimens subjected to 200g's. So, it was expected that primary and secondary swelling slopes for low g-level should have lower values than specimens subjected to high g-level. However, reverse behavior in primary and secondary swelling was observed here. Probably the applied g-level changed the capillarity and hydration processes into the swelled particles. Even though these processes are still dependent on the effective stress applied on the soil specimen.

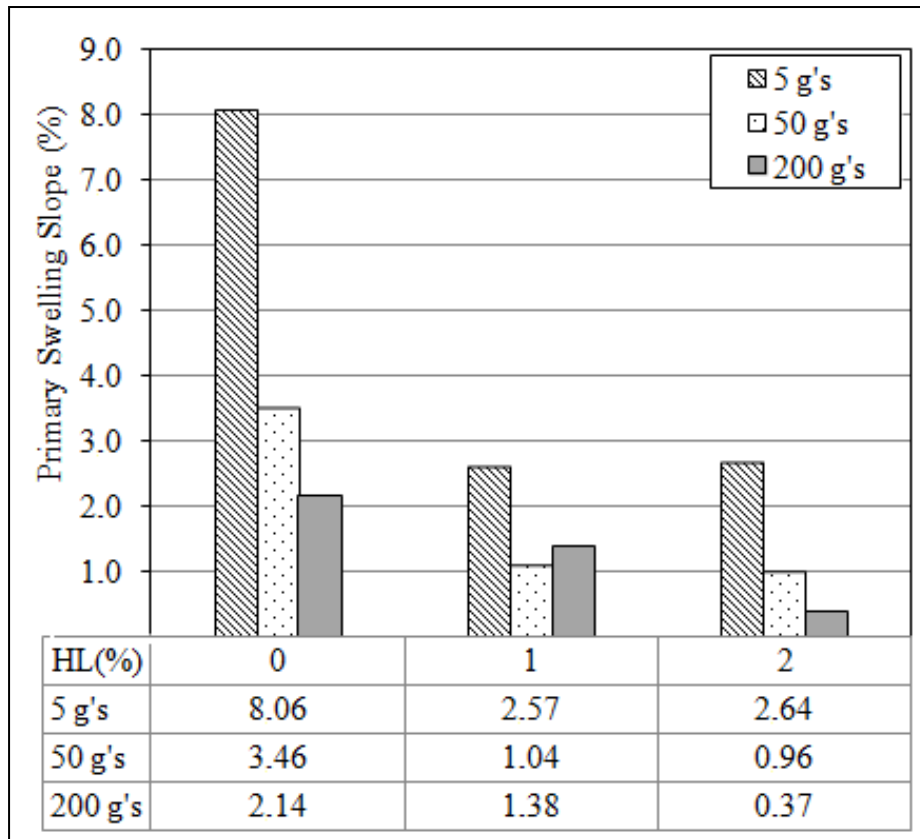


Figure 4.46. g-level effect on primary swelling slope

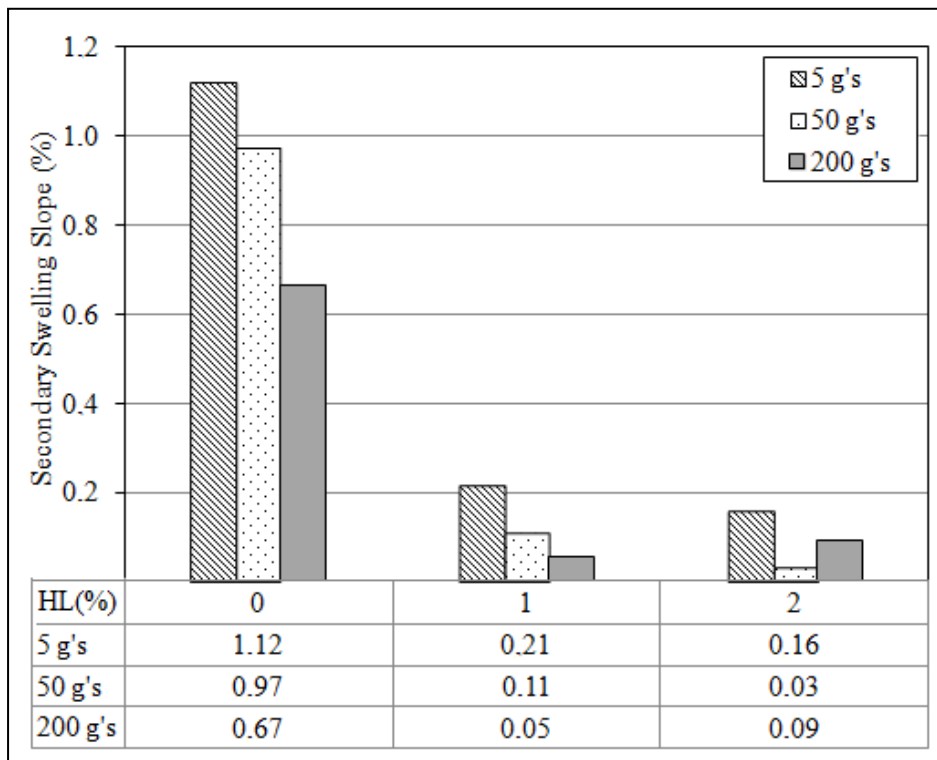


Figure 4.47. g-level effect on secondary swelling slope

4.3. Mineralogical and Micro-structural Observations

The mineralogical test was carried out by using X-Ray Diffraction (XRD) technique, whereas the micro-structural observations were performed by using Environmental Scanning Electron Microscopy (ESEM) and X-Ray Computer Micro-Tomography (Micro-CT) tests. In this section, the results obtained from the experimental plan summarized in Table 3.6 are presented and analyzed.

4.3.1. X-Ray Diffraction (XRD) Analysis

Clay mineralogy is a fundamental factor for controlling expansive soil behavior. The X-Ray Diffraction (XRD) analysis was used to find evidences of mineralogical changes due to lime addition. Figure 4.48 depicts the X-ray diffractogram that shows the intensity as function of incident angle (Two-Theta) for the different minerals in untreated and lime-treated Eagle Ford clay with 3% of hydrated lime. The mineral symbols in this figure are represented as follows: M = montmorillonite, K = kaolinite, I = illite and Q = quartz. It can be noticed that the highest relative intensity represents the quartz peak, indicating the strong X-Ray absorption characteristic of this mineral.

The X-Ray diffractogram of untreated Eagle Ford clay is in agreement with the mineralogical analysis presented by Lin (2012). According to Lin (2012), the untreated Eagle Ford clay has as principal compounds montmorillonite (28%), illite (27%) and kaolinite (11%). These percentages represent the clay minerals proportions in the entire Eagle Ford soil sample, not only in the clay size portion.

The XRD results showed that the lime-treated Eagle Ford clay with 3% HL caused significant increase in minerals' peaks intensities. This could be attributed to reactions between lime and clay minerals that promote the formation of new crystalline phase identified as Calcium Silicate Hydrates (CSH). The X-Ray diffractogram contain additional peaks of CHS in the lime-treated specimen, around the diffraction degree $2\theta = 30^\circ$, 25° and 55° . Additional pozzonalic compounds could not be detected in the X-Ray diffractogram, because they may be present in small quantities or they may not be formed at 3% of hydrated lime.

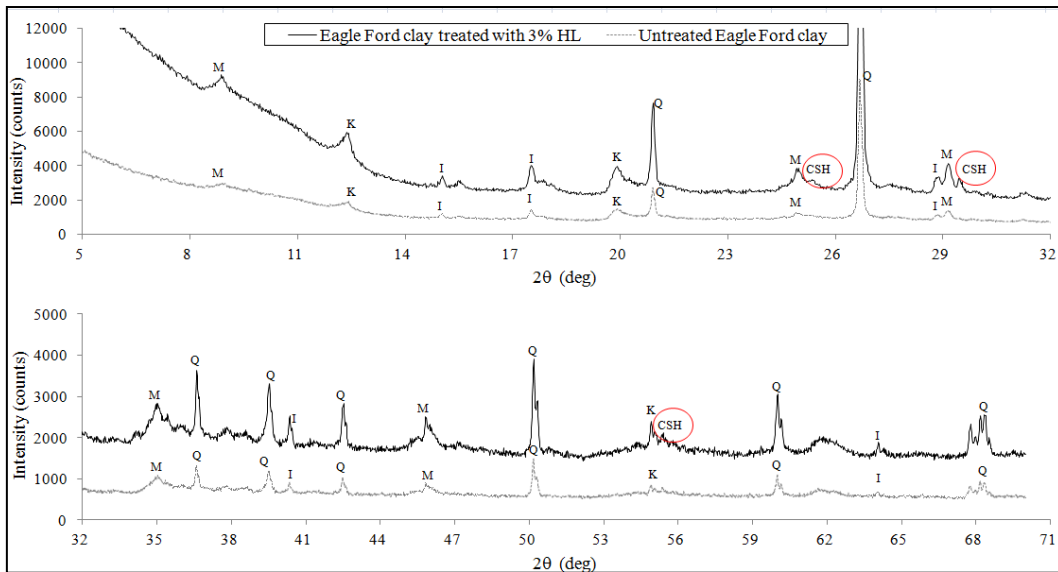


Figure 4.48. X-ray diffractogram of untreated and treated Eagle Ford clay with 3% of hydrated lime

Figure 4.49 depicts the X-ray diffractogram for untreated and lime-treated Eagle Ford clay with 3% of hydrated lime at 0 and 7 days of curing. It can be seen a slight reduction in all clay minerals' peak intensity when curing time was increased (from 0 days to 7 days) in the lime-treated specimen. Also, no new pozzolanic compounds were detected for 7 days of curing.

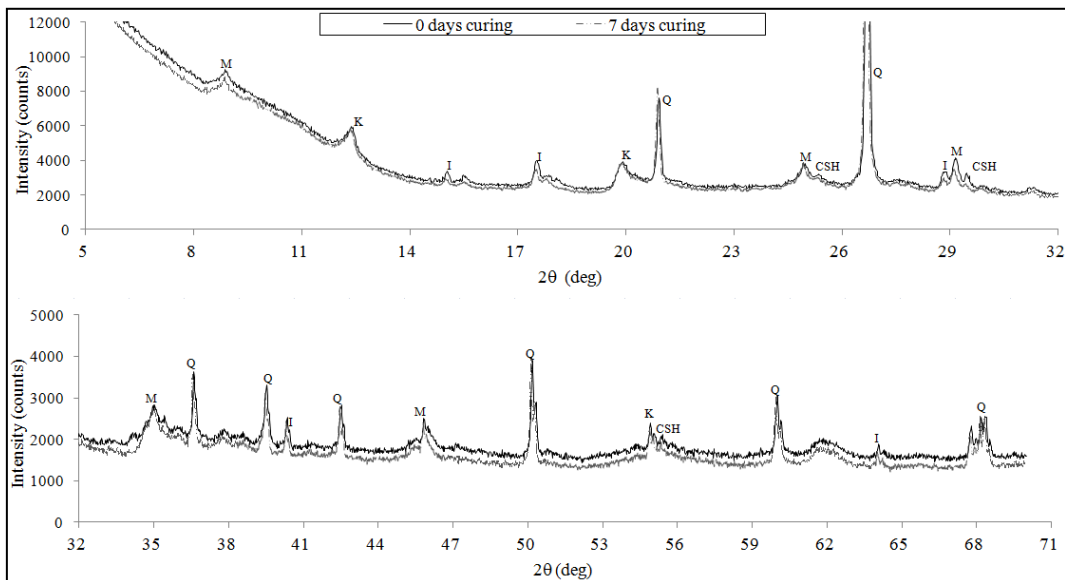


Figure 4.49. X-ray diffractogram of lime-treated Eagle Ford clay with 3% of hydrated lime at 0 and 7 days of curing

Figure 4.50 depicts the X-ray diffractogram for untreated and lime-treated Eagle Ford clay with 3% of hydrated lime with no mellowing and 7 days of mellowing period. It seems that mellowing period does not compromise the development of pozzolanic reactions. The X-Ray diffractogram of the specimen compacted at the same day of mixing, i.e., no mellowing allowed (NM) overlapped the X-Ray diffractogram of the specimen compacted after 7 days of mixing, i.e., 7 days of mellowing period (M7), indicating that there was no change in mineralogical composition due to mellowing application.

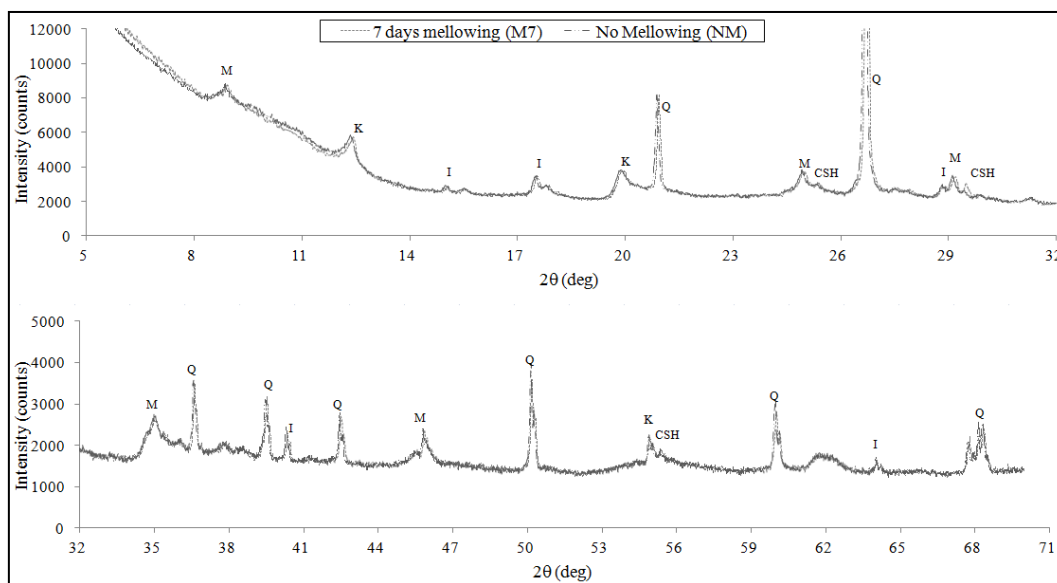


Figure 4.50 X-ray diffractogram of lime-treated Eagle Ford clay with 3% of hydrated lime with no mellowing and 7 days of mellowing period

The adverse effect of mellowing period on lime-treated Eagle Ford clay was previously attributed to the possible undesirable carbonation process. The detection of carbonation products was not possible by the present XRD test, because in low lime percentage (3% HL used here), the amount of carbonation products may be small enough to be detected. Therefore, the carbonation process should not be discarded as the explanation of the adverse effects of mellowing.

4.3.2. Environmental Scanning Electron Microscopy (ESEM) Analysis

The Environmental Scanning Electron Microscopy (ESEM) was used to obtain ESEM micrographs at two different magnifications, low magnification

(200x) and high magnification (1000x), in order to observe the general arrangement of the soil matrix and the microstructure arrangement of untreated and lime-treated Eagle Ford clay. In addition, the ESEM equipment allowed to obtain EDX (energy dispersive x-ray) spectra to do a qualitative elemental analysis on certain selected areas in order to analyze the elemental distribution.

Figure 4.51 and Figure 4.52 illustrate the ESEM micrograph amplification of 200x and 1000x, respectively, of untreated Eagle Ford Clay. The results showed that the untreated Eagle Ford clay exhibits a dense clay matrix (Figure 4.51) with a laminar structure compound of dispersive and thin clay platelets, or aggregates mostly associated in the face to face style (Figure 4.52), as also reported by Lin & Cerato (2014). According to Nelson & Miller (1992), Clay particle contact, alignment and aggregation determine the swelling potential in expansive soils. Untreated Eagle Ford clay structure presents platelets aligned in parallel form. The more dispersive the structure, the more effective surface area is accessible for the contact between particles and water molecules resulting in greater swelling potential. Eagle Ford clay exhibit strong face to face contact that allows great volume increase during swelling process.

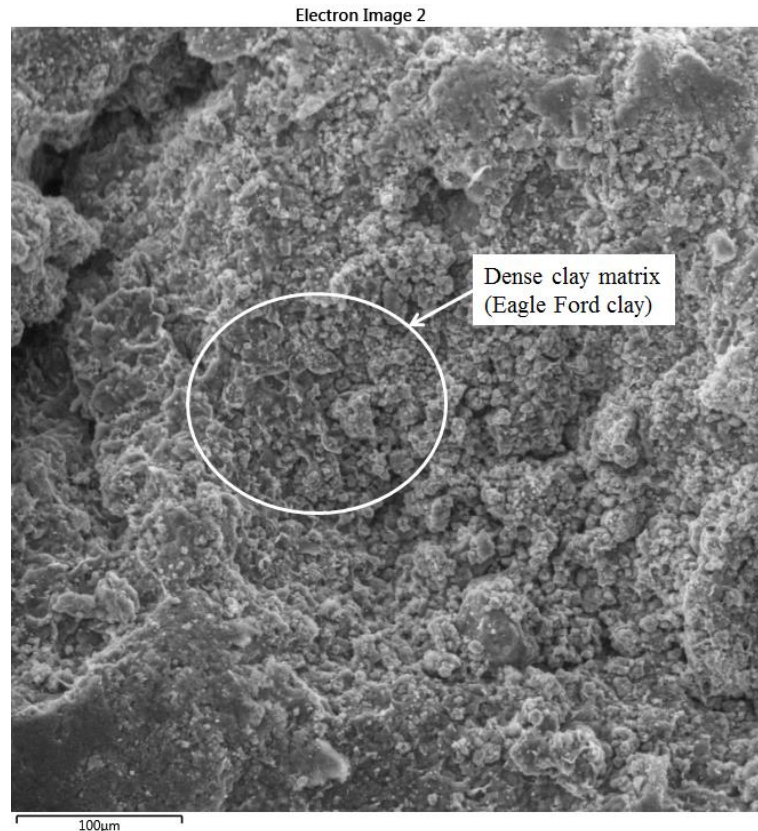


Figure 4.51. ESEM micrograph amplification of 200x of untreated Eagle Ford Clay

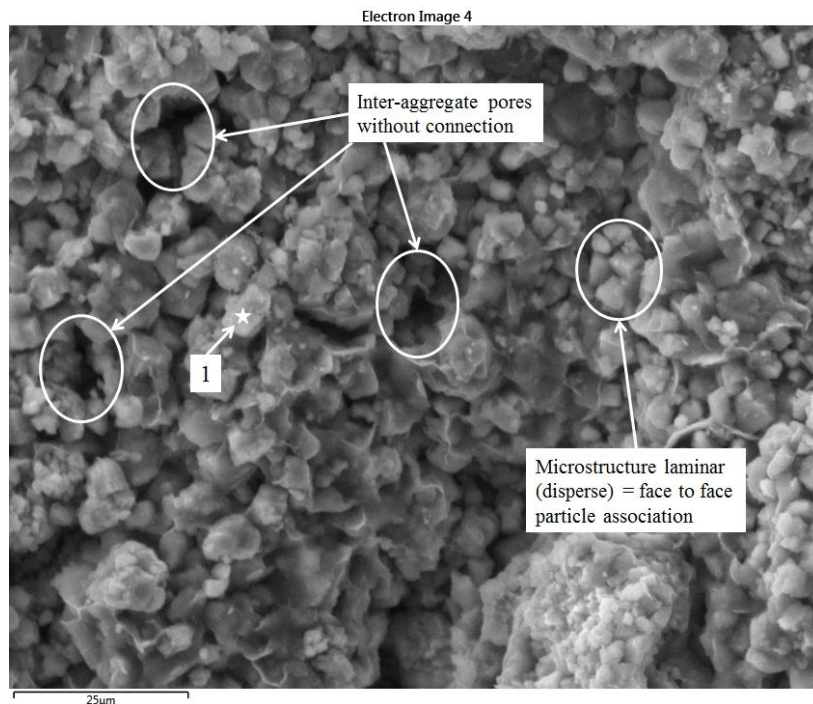


Figure 4.52. ESEM micrograph amplification of 1000x of untreated Eagle Ford Clay

The EDX spectrum of untreated Eagle Ford clay is depicted in Figure 4.53. This spectrum corresponds to point No.1 indicated in the ESEM micrograph of Figure 4.52. Consistently with the XRD results presented in section 4.3.1, the EDX spectrum depicted in Figure 4.53 shows peaks for oxygen (O), aluminum (Al) and silicon (Si), and smaller peaks for sodium (Na), iron (Fe), potassium (K) and magnesium (Mg), and traces of titanium (Ti) and sulfur (S) impurities. The height ratio between the peaks Si and Al is approximately 2:1, that suggests the presence of montmorillonite.

The images shown in Figure 4.54 and Figure 4.55 illustrate the ESEM micrographs amplification of 200x and 1000x, respectively, of Eagle Ford clay treated with 3% of hydrated lime, in order to Figure 4.55 describe the effect of lime addition on the micro-structural features. In the low magnification (200x), it is possible to see that the dense matrix of untreated Eagle Ford clay was converted into a solid matrix with smoother surface. The pozzolanic reactions, responsible for forming Calcium Silicate Hydrate (CSH), generated soil structure flocculation and cementation in clay particles. The flocculation due to chemical bonds forms hydrophobic aggregates that cannot experience intra-aggregate expansion. Consequently, flocculation is a mechanism that increases soil strength and decrease swelling.

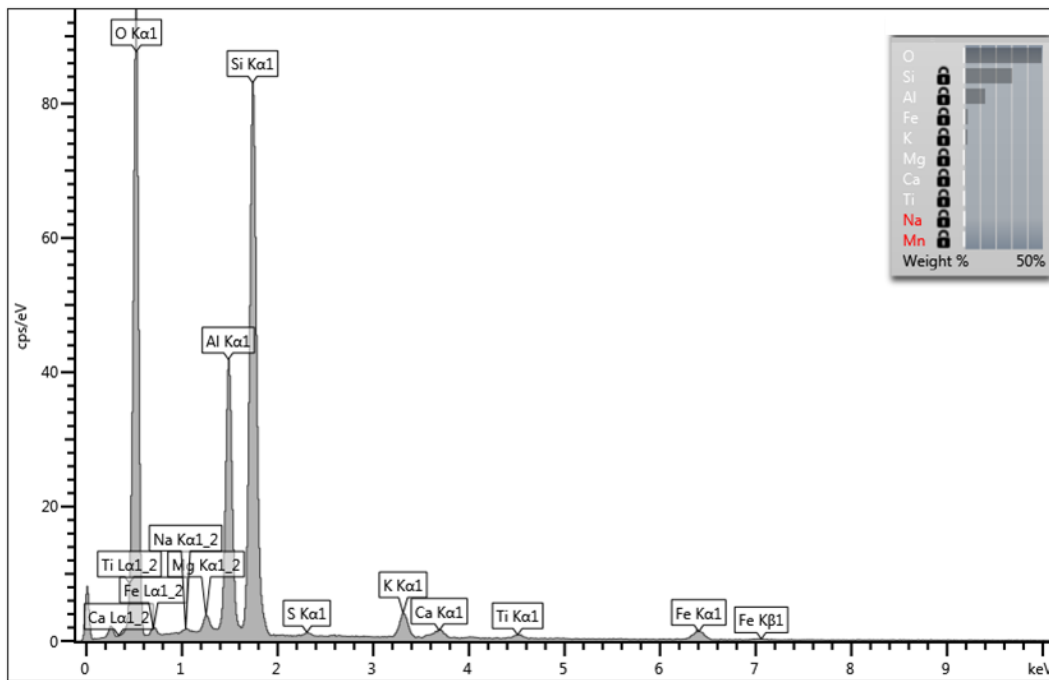


Figure 4.53. EDX spectra of untreated Eagle Ford clay

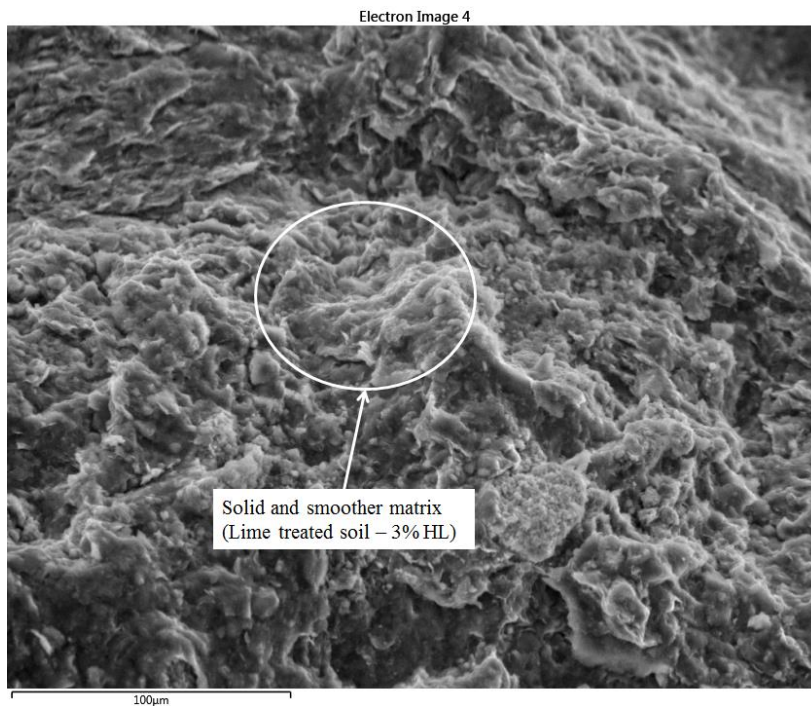


Figure 4.54. ESEM micrograph amplification of 200x of Eagle Ford clay treated with 3% of hydrated lime

The irregular large agglomerations of the clay particles are evident in Figure 4.55. This likely reflects the effect of the strength developed in the clay-lime-water

system. Also, the increase in inter-assemblage pore-size and good pore connection dominate the fabric after lime addition.

According to Stoltz *et al.* (2012), the fabric of the untreated and lime-treated soils may consist of two classes of pores usually called “double structure”. The smallest pores (micro-pores) correspond to the pores inside the aggregates, while the largest pores (macro-pores) are the spaces between these aggregates. The study carried out by them assessed the lime addition effect on the fabric of expansive soils using mercury intrusion porosimetry (MIP) and concluded that the lime addition increases the macro-pore sizes and consequently the void ratio.

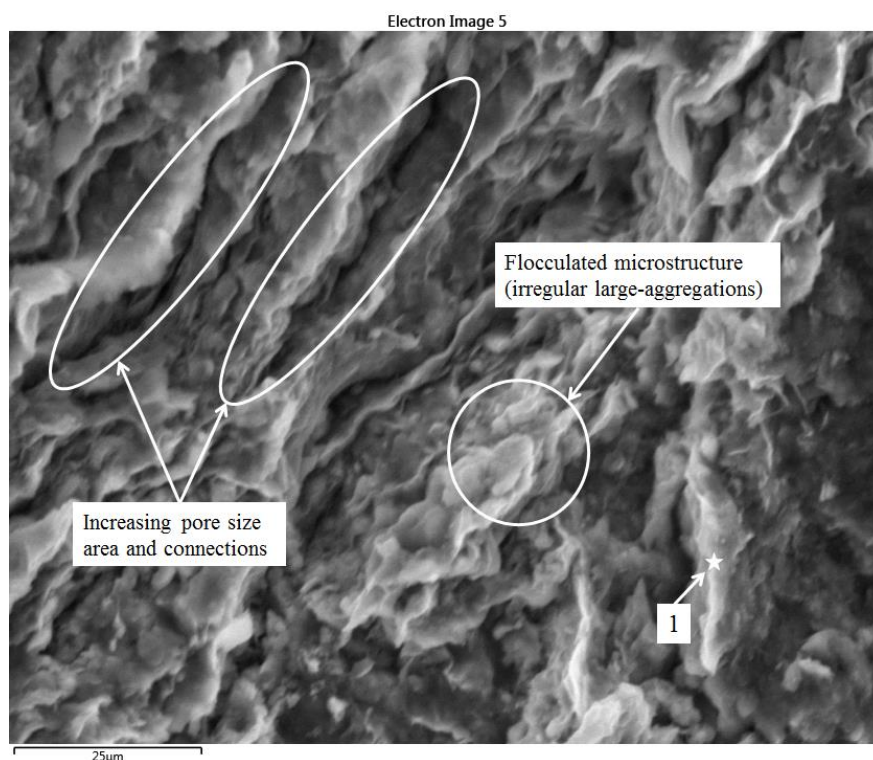


Figure 4.55. ESEM micrograph amplification of 1000x of Eagle Ford clay treated with 3% of hydrated lime

As explained by Yazdandoust & Yasrobi (2010), during the saturation process, molecules of water tend to migrate from the larger pore spaces into the smaller pores by suction in order to establish equilibrium conditions. However, the formation of larger inter-assemblage pore spaces causes reduction in number and volume of intra-assemblage pore spaces, and this fact obstructs some water molecules to reach the overall clay matrix and, consequently swelling potential reduces.

The EDX spectrum of Eagle Ford clay treated with 3% of hydrated lime, corresponding to point No.1 indicated in the ESEM micrograph of Figure 4.55, is shown in Figure 4.56. This spectrum exhibits a strengthened Ca peak in response to lime addition and cemented products formation into the soil.

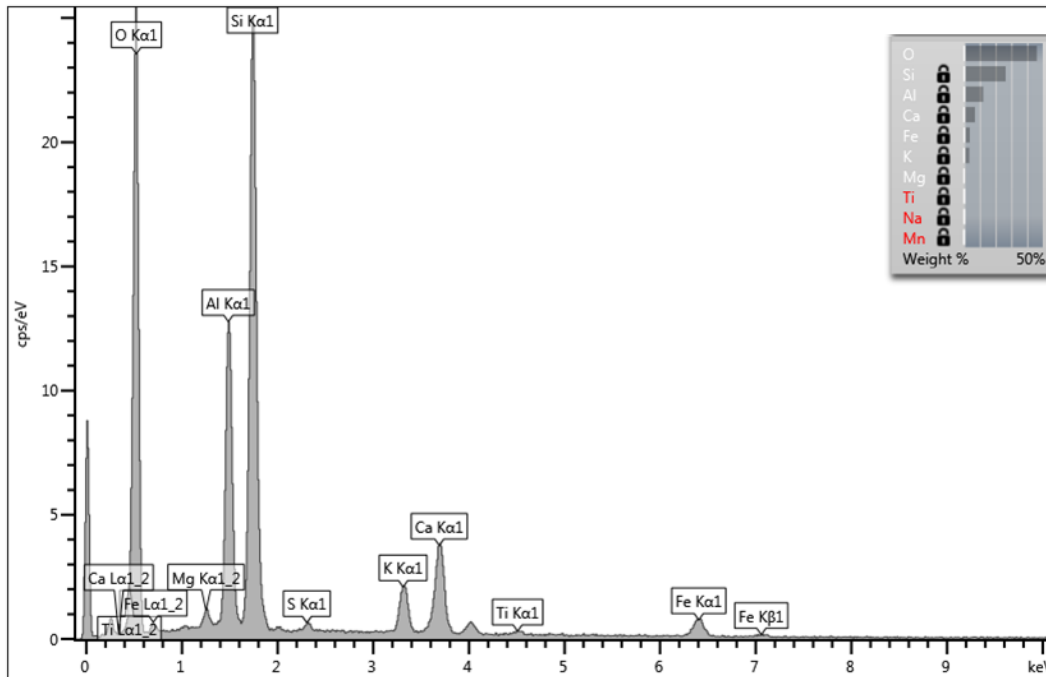


Figure 4.56. EDX spectra of Eagle Ford Clay treated with 3% hydrated lime

4.3.2.1.

Curing and Mellowing Period Effect on Micro-Structural Features

Previous data analysis in this study demonstrated that curing time enhances the strength (section 4.1.6) of lime-treated Eagle Ford clay and reduces its swelling potential (section 4.2.1.2). These effects of curing time on lime addition are strongly related with the micro-structural changes undergone by the specimens along the time.

Figure 4.57 illustrates ESEM micrograph amplification of 1000x of untreated and lime-treated Eagle Ford clay with 3% of hydrated lime and with 1 and 7 days of curing. When the specimen was prepared without lime, the observed microfabric was still open, as shown in Figure 4.57 (a). When hydrated lime was added, the cation exchanges flocculated the soil into larger lumps (Figure 4.57 (b)). With 7 days of curing, the large pores were filled with the cemented products, as shown in

Figure 4.57 (c). Thus, the total pore volume decreases resulting in the development of strength and reduction of swelling potential.

The application of mellowing periods in the lime-treated Eagle Ford clay has shown adverse results in this study. Slight decreasing in compressive strength (section 4.1.6) and increasing in swelling potential (section 4.2.1.3) were observed in specimens that were mixed and left to mellow for 7 days.

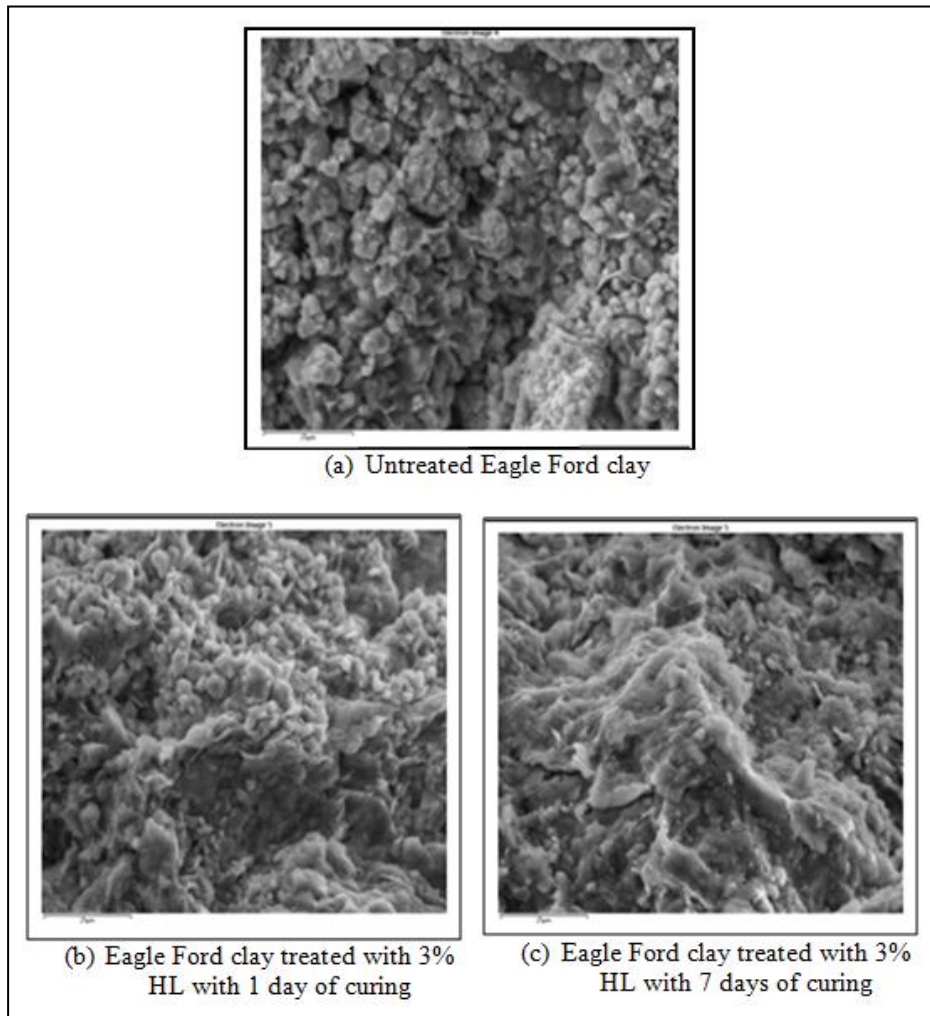


Figure 4.57. ESEM micrograph amplification of 1000x of untreated and lime-treated Eagle Ford clay with 3% of hydrated lime and with 1 and 7 days of curing

Figure 4.58 illustrates the ESEM micrograph amplification of 1000x of lime-treated Eagle Ford clay with 3% of hydrated lime (HL) with no mellowing (NM) and 7 days of mellowing period (7M). It demonstrates that the particle aggregation occurred in both specimens, the one compacted immediately after mixing (NM) and the specimens compacted after 7 days of mixing (M7). The aggregation size in

specimen M7 seems to be bigger than specimen NM, thus the inter-aggregates pores in specimen M7 seem to be bigger, too.

Based on the microstructural difference observed here and in the XRD observations, it is evident that the pozzolanic reactions took place, even if the lime-soil mixture was in uncompact state, and then greater porosity was observed in specimens compacted with mellowing periods. Some studies confirmed the reduction in dry density and increase in the percentages of air voids was due to mellowing periods (Bell, 1996; Holt & Freer-Hewish, 1998; Di Sante *et al.*, 2015). The strength reduction because of mellowing might be due to the formation of big clods that difficult the interaction between lime and the clay material into the clods. Also, the increase of swelling potential due to mellowing can be explained by same reason.

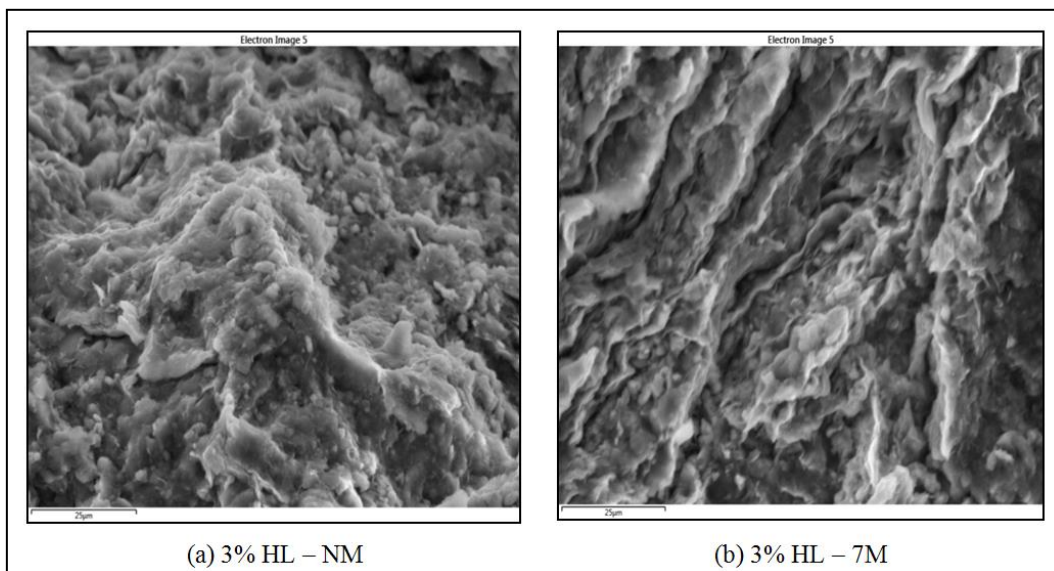


Figure 4.58. ESEM micrograph amplification of 1000x of lime-treated Eagle Ford clay with 3% of hydrated lime (HL) with no mellowing (NM) and 7 days of mellowing period (7M)

4.3.3. Micro-CT Analysis

The Micro-CT data results initially came as a set of 2D images which can be stacked together to form a 3D volume. The provided data contained approximately 200 2D images for each specimen (untreated specimen and lime-treated specimen with 4% of hydrated lime). Entire specimen images, including solid particles and pores, for the untreated and lime-treated Eagle Ford clay are shown in Figure 4.59 and

Figure 4.60, respectively. It can be seen that the specimens contain some cracks due to their small thickness (1cm approximately) and shrinkage produced by the drying process executed after swelling tests. However, this fact did not affect the pore size analysis because the established pore size range disregarded these features.

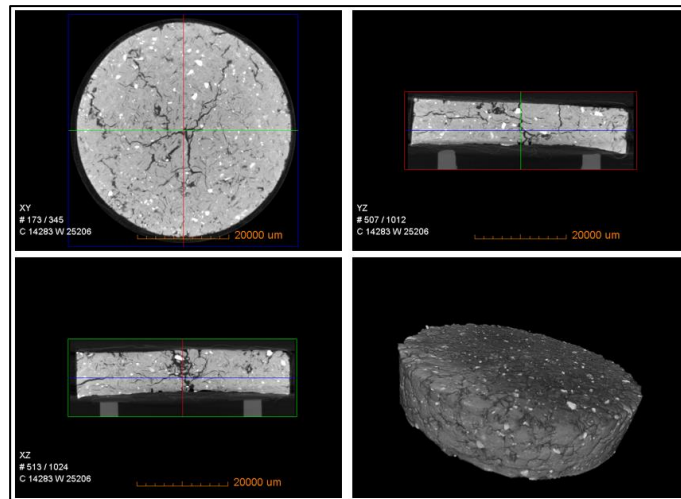


Figure 4.59. Micro-CT images taken from untreated Eagle Ford clay specimen

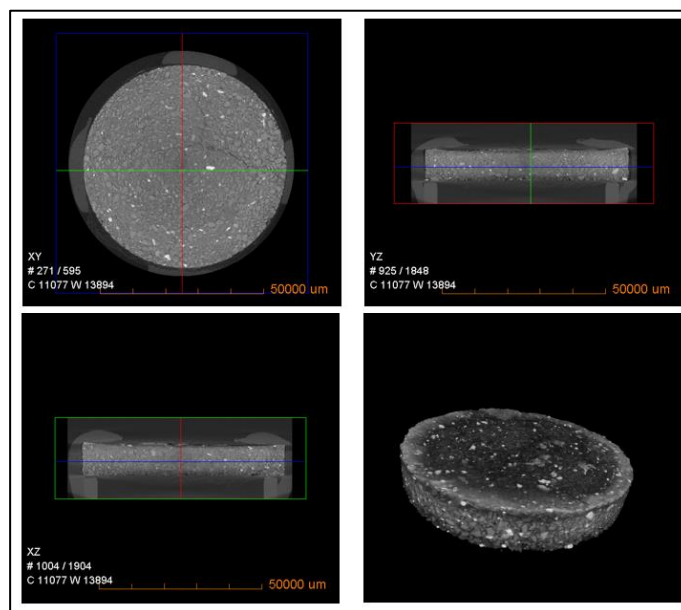


Figure 4.60. Micro-CT images taken from lime-treated specimen with 4% HL

The image processing program used for analyzing the micro-CT images was the ImageJ³, because it is a public domain software. The main steps for analyzing

³ <https://imagej.nih.gov/ij/index.html>

the porosity inside the specimens by using the ImageJ program are described as follows:

The first step was the pre-processing. In this step, 100 images from each specimen were selected, avoiding images taken from the top and bottom specimen extremes, in order to be prepared for the analysis. The pre-processing step included the scale calibration (the specimen diameter was correlated with a number of pixels in the image) and the improvement of image quality by applying “mean” filter and adjusting the brightness and contrast. The mean filter smooths the current image by replacing each pixel with the neighborhood mean. Figure 4.61 shows an example of images before and after pre-processing.

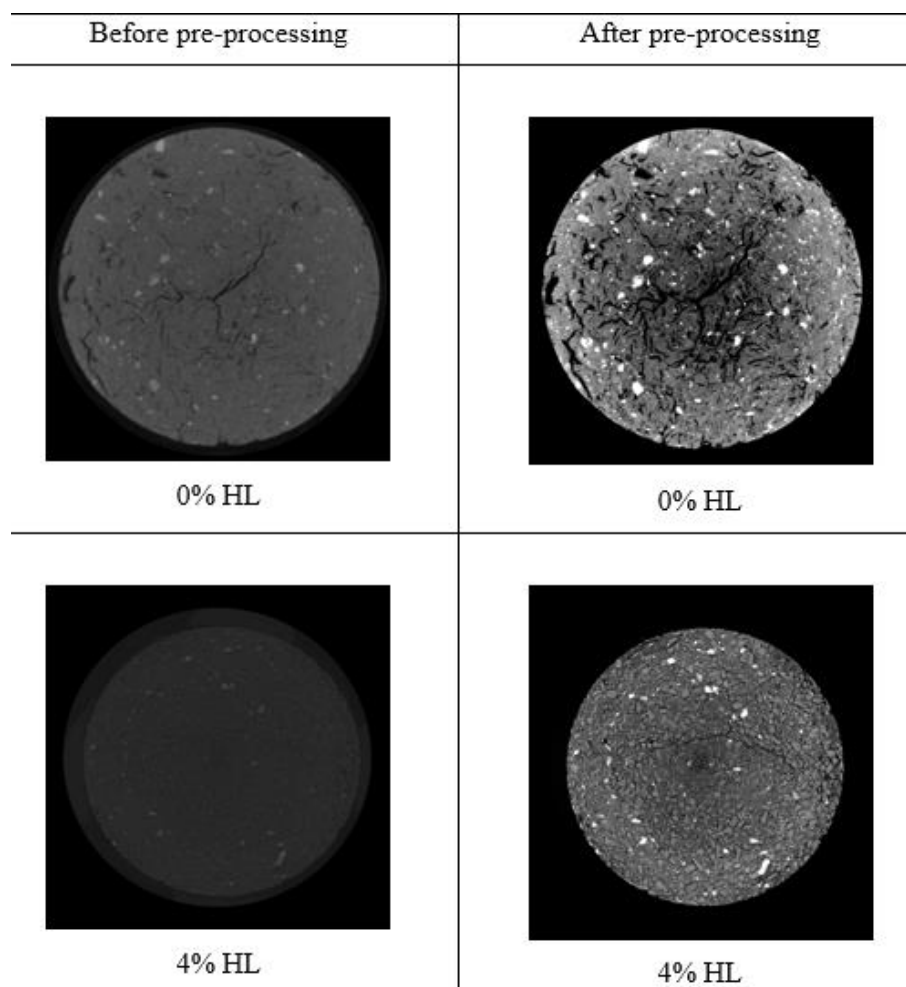


Figure 4.61. Micro-CT images before and after pre-processing

The second step was the segmentation. This step allowed to separate the pores from the specimens by converting the pre-processing image (in gray scale) to a binary image, i.e., a black and white image. So that, it was necessary to set the

thresholds in the gray scale to establish what tones should become black and white. Also, in this step, the specimen holes (pores) were filled with white color in order to facilitate their visualization (Figure 4.62).

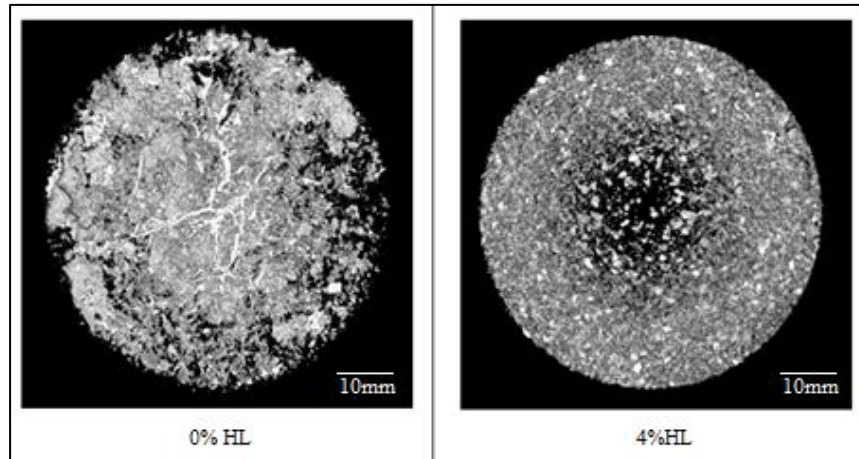


Figure 4.62. Micro-CT images after segmentation depicting pore distribution

The final step was the post-processing and result analysis. After segmentation step, the ImageJ program allowed to obtain the percentage of pores with different area in mm^2 . The pore size distribution carried out here only considered pores with areas between 0.001 to 0.01 mm^2 . The inferior limit was established because of the tomography resolution and the superior limit was fixed in order to omit the cracks in the specimen for the analysis. Based on this, the pore areas were classified in five groups (0.0010, 0.0028, 0.0046, 0.0064 and 0.0082 mm^2) and the pores percentage for each area was calculated, as shown in Figure 4.63.

The results showed that pores with the smallest area (0.001 mm^2) were the most predominant in both untreated and lime-treated specimens, compared with the other established pore areas. However, the percentage of pores with areas smaller than 0.046 mm^2 was 74% for untreated specimen (0% HL) and 52% for the specimen with 4% HL. Additionally, the specimen with 4% HL presented higher percentage of pores with area equal or bigger than 0.046 mm^2 (around 48%) than the untreated specimen where these big pores were around 26%. As explained above in ESEM analysis, the lime addition increases the inter-assembly pore-size. The Micro-CT results also confirmed that the formation of aggregates due to lime addition affected the soil macro-porosity, so that the specimen with 4% HL displayed higher percentage of big pores than the untreated specimen (0% HL).

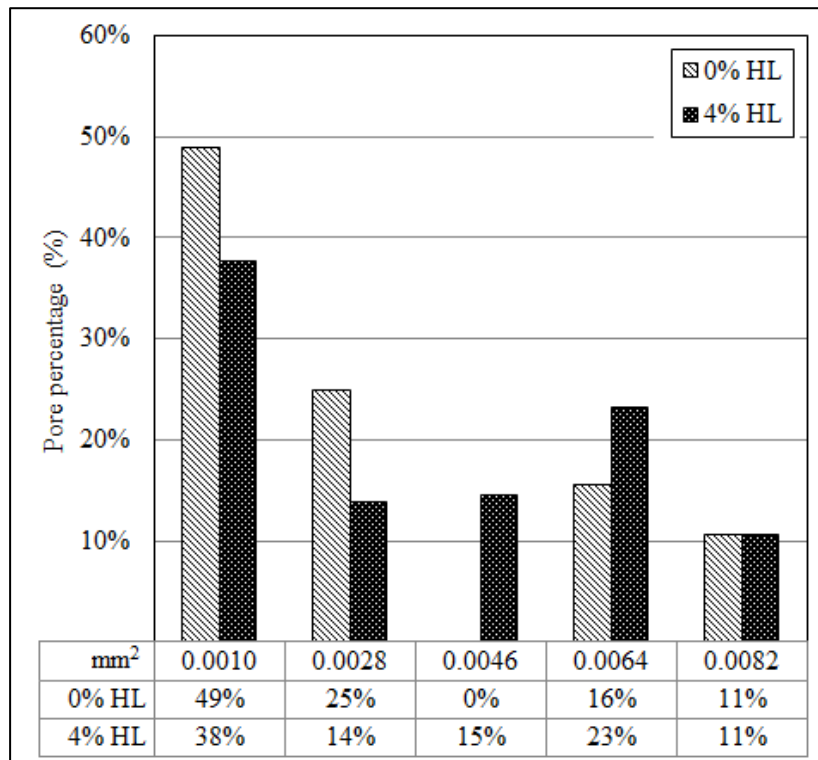


Figure 4.63. Pore area distribution for untreated and lime-treated Eagle Ford clay

5 Conclusions and Recommendations

At the end of this experimental study, important findings about the main parameters that affect the efficiency of lime treatment on the swelling reduction in expansive soils can be drawn. This chapter summarizes these main findings and offers recommendations for further investigations.

5.1. Conclusions

Based on the results presented and analyzed in the previous chapters, and within the established general and specific objectives, it was possible to infer the conclusions presented below:

- In this study, it was successfully verified the capability of the centrifuge technology to analyze the swelling reduction in expansive soils using lime treatment. So far, only expansion measurements of natural soils had been done with this technology. However, the present results demonstrated that this technology also can facilitate the evaluation of treatments to reduce the swelling behavior of expansive soils.
- The index properties of the expansive Eagle Ford clay were modified immediately after lime addition. The lime addition was responsible for creating an alkaline environment into the pore water of the lime-treated soil that promotes pozzolanic reactions and flocculation process. The flocculation process that took place into the lime-soil mixtures was reflected in all the properties analyzed in this study. The flocculation process led to increase the particle size with consequent reduction of cation exchange capacity (CEC) and plastic index (PI) values. Additionally, after lime addition, it was observed a reduction of maximum dry density related to the increase in particle size and air voids;
- Compressive strength and stiffness of the natural Eagle Ford clay were increased with hydrated lime addition. The lime addition produced changes

in the failure response from ductile to brittle behavior. The curing time increased the compressive strength. Furthermore, the strength was also influenced by the elapsed time between mixing and compaction (i.e. mellowing period). The specimens with 7 days of mellowing exhibited lower compressive strength peak than specimens with no mellowing. This reduction in strength was attributed to three factors during mellowing period: loss of water, lime consumption and high air void generation;

- The evaluation of the effect of lime percentage in lime-soil mixtures confirmed that the swelling potential reduction due to lime addition fits a natural logarithmic function between lime percentage and the swelling potential reduction ratio (SPR) with an excellent correlation. It was observed that 1% of hydrated lime was able to reduce 67% of swelling potential of Eagle Ford clay, whereas 4% of hydrated lime was able to eliminate 97% of swelling potential of the natural Eagle Ford clay;
- It was observed clear relationship between the primary swelling slope (PSS) and secondary swelling slope (SSS) in the untreated and lime-treated specimens. Considering that primary swelling is driven by capillarity and secondary swelling by hydration process and analyzing the PSS and SSS, it can be concluded that these processes contributed equally to the total swelling for lime-treated Eagle Ford specimens, since the PSS and SSS values were very close. On the other hand, in untreated Eagle Ford clay, the entrance of water was mainly due to capillarity process, since PSS was high and SSS was low;
- An evident reduction of swelling behavior in expansive Eagle Ford clay was obtained by the combined effect of lime addition with curing time. The swelling potentials in specimens with 1 day of curing were 36% to 50% smaller than those obtained at 0 days of curing (i. e. no curing). Longer curing times, such as 7 and 28 days, produced reductions of swelling potential around 40 to 100% with respect to the value obtained at 0 days of curing. Similar swelling potentials were found in specimens cured during 7 and 28 days. This was explained due to the fact that short curing times lead to the increase of pore-volume, and long curing times allow cemented compounds formation. The presence of these cemented compounds can stop the increase of pore volume making the swelling potential constant in longer curing times;

- Fairly similar reduction of swelling potential was obtained at 1, 7 and 28 days of curing. One day of curing was enough to reach remarkable enhancement in swelling potential reduction compared with specimens without curing (0 days). Longer curing times produced similar potential reduction obtained at 1 day of curing. Since reduction in PSS was detected, the capillary forces into the soil seem to diminish with the increase in curing time. Thus, the water infiltration becomes more difficult and occurs in a slower manner for specimens cured for long time. Furthermore, reduction in SSS was also noticed with the increase in curing time. This reflects that the formation of cemented compounds, during the curing time, makes difficult the entrance of water responsible for the final hydration process;
- The mellowing period was defined as the elapsed time between lime-soil mixture preparation and the final specimen compaction. An adverse effect of prolonged mellowing period on swelling reduction was identified, and it was attributed to two possible causes: (i) the presence of excessive air voids generated during the mellowing period and (ii) the lost of lime due to carbonation process during the mellowing period;
- The swelling behavior of untreated and lime-treated Eagle Ford clay was found to be highly sensitive to variations in compaction moisture condition. When the compaction moisture content was varied from DOP (dry of optimum) to WOP (wet of optimum) condition, it was detected a reduction of 66% of swelling potential in untreated Eagle Ford clay. Likewise, in lime-treated specimens, it was detected reductions up to 100% of swelling potential with the same variation in compaction moisture condition from DOP to WOP. Furthermore, it was found that the increment of compaction moisture content, e.g. from OPT to WOP condition, was able to substitute in some quantity the percentage of hydrated lime needed to reduce the swelling potential of Eagle Ford clay. Since the lime addition also reduces the clay plasticity, problems related with workability are not expected with increasing compaction moisture content, as it could be expected in the case of natural expansive soils compacted at high moisture contents;
- The compaction moisture condition DOP was found to have an adverse effect on lime-treatment efficiency for swelling reduction. This moisture condition

resulted in higher swelling potentials than those found in OPT or WOP conditions. So that, in construction processes, it would be recommended to check the moisture of the lime-soil mixture in order to ensure that it is not in the DOP condition;

- The compaction moisture content affects the mechanism of swelling in untreated and lime-treated Eagle Ford clay. A decrease in the primary swelling slope was detected when the compaction moisture content was increased. So that, the capillary absorption occurred very fast at DOP condition because of the many available air voids for being filled by water. Conversely, slower infiltration process was observed in compaction moisture condition OPT and WOP, where the void volume are filled with more water than in DOP condition;
- The evaluation of compaction dry density on swelling behavior of untreated and lime-treated Eagle Ford clay showed that the swelling potential slightly decreases with a decrease in relative compaction. This behavior was attributed to the fact that loosely compacted specimens exhibit more inefficient translation from particle-scale swelling to bulk-scale swelling because the interlayer volume changes occurring on the particle scale are internally adsorbed by the larger scale pores. Conversely, densely compacted specimens exhibit more efficient translation from particle-scale swelling to bulk-scale swelling because the interlayer volume changes are less well accommodated by the internal pores;
- The lime addition efficiency can be increased with the reduction of compaction dry density. However, unlike to what was observed for variations of compaction moisture content, a reduction in compaction dry density was not able to offset the effect of a greater percentage of hydrated lime for swelling mitigation;
- The combined variation of compaction dry density and lime addition produced changes in the swelling mechanism of untreated and lime-treated Eagle Ford clay. While for untreated Eagle Ford specimens, a faster primary swelling development was observed in loose specimen than in denser one, in lime-treated Eagle Ford clay, the primary swelling occurred faster in specimens compacted at higher dry density. The change in the primary

swelling slope from untreated to lime-treated Eagle Ford clay was attributed to the generation of cemented compounds, due to lime addition, which are able to modify the water absorption by capillarity process generated during the primary swelling. Conversely, the hydration process, responsible for development of secondary swelling, depends only on the compaction dry density because its behavior was the same trend for untreated and lime-treated Eagle Ford clay. The final hydration process occurred in faster manner in specimens with high dry density;

- The combined effect of lime addition with stress variation on the swelling behavior of untreated and lime-treated soils was evaluated by variations in g-level during centrifuge tests. A decreasing natural logarithmic function was found to describe the relationship between swelling potential and g-level. Considering that the artificial g-level is correlated with the effective stress applied on the specimen, it was observed that the percentage of lime needed to prevent the swelling behavior also depends on the applied vertical stress that will be applied by the weight of the structure projected on the expansive soil;
- Even the swelling mechanisms (i.e. absorption by capillarity and hydration process) in both untreated and lime-treated Eagle Ford clay presented dependency on the g-level applied into the centrifuge specimens, the results contradicted the expected behavior. Thus, it was observed that the water infiltration happened in faster manner in specimens subjected to 5g's than those subjected to 200g's, which was reflected in higher values of primary and secondary swelling in the specimens subjected to 5g's;
- The mineralogical analysis allowed to corroborate that lime addition alters the clay composition by formation of new crystalline compounds identified as Calcium Silicate Hydrate (CSH). Also slight reduction in all clay minerals' peak intensity, due to curing time, were detected by XRD results. However, the detection of carbonation products was not possible by the present XRD results, because probably the percentage of hydrated lime used for this test should have been higher than 3% in order to facilitate the detection of carbonation products;

- By ESEM and Micro-CT observations, the disperse particle structure of the natural expansive Eagle Ford clay was found altered by the lime addition. Lime-treated soil exhibited irregular large agglomerations that obstruct the water molecules to reach the overall clay matrix, producing reduction of swelling potential. The Micro-CT analysis displayed reduction in the percentage of small area pores and increase in the percentage of big pores after lime addition. It was further found that the curing time leads to large pores to be filled by cemented products generating additional reduction of swelling potential. Also, ESEM observations allowed to support the hypothesis that prolonged mellowing period results in increasing the pore size in the specimen.

The main contribution of this study was to reveal the combined effect of lime addition with different specimen preparation conditions (such as, curing time, mellowing periods, compaction moisture content, compaction dry density and effective stress) in expansive soils, in order to formulate recommendations to achieve greater efficiency in reduction of swelling behavior. The practical engineering recommendations that can be drawn from this study are:

1. The amount of lime required to prevent swelling will vary from one expansive soil to another, and also will depend on the loading conditions that the expansive soil would be submitted;
2. An efficient lime addition for swelling reduction should avoid prolonged periods between lime-soil mixing and compactions (i.e. mellowing periods). Otherwise, when longer delays to compaction cannot be avoided, a small additional amount of lime should be added to compensate the adverse effect of mellowing;
3. A short period of curing, around 7 days, might be recommended to increase the effect of lime on swelling reduction;
4. If the objective of lime addition is only the swelling decreasing and not the strength gain, the amount of lime can be reduced by increasing the compaction moisture content and/or by decreasing the compaction dry density.

5.2. Future Works

Additional investigations to be undertaken in order to further substantiate the results obtained in the present research work include:

- Further centrifuge testing on different types of expansive soils subjected to different types of treatments for swelling reduction;
- Investigations about the application of lime percentages higher than 4% for Eagle Ford clay, in order to corroborate if the trends observed in this study persists;
- Some of the parameters studied here need to be analyzed in a more detailed manner. For example, the effect of compaction dry density on swelling reduction could be explored with more percentages of relative compaction, not only with 94% and 100%, as was done here. Also, different compaction energies can be applied during specimen preparation in order to analyze the effect of this energy on the swelling behavior.
- The adverse effect of mellowing period on swelling reduction need to be corroborated by analyzing more percentages of hydrated lime and smaller mellowing periods. Also, studies including thixotropic effect on swelling behavior of natural and stabilized expansive soils should be developed.
- Investigations on the empirical and numerical models for predicting the effect of lime addition on the expansive behavior.
- Mercury intrusion porosimetry (MIP) studies to analyze the variations in pore size distribution resultant from alterations of the different parameters studied here (lime percentage, curing time, mellowing period, compaction moisture content, compaction dry density and effective stress).
- X-Ray diffraction tests need to be carried out with percentages higher than 3% of hydrate lime in Eagle Ford clay and longer periods of curing, in order to facilitate the detection of pozzolanic products and undesirable carbonation products.
- Create correlations involving properties such as strength, porosity and swelling in order to predict the effect of lime on hydraulic and mechanical properties of expansive soils.

6

References

AFNOR (NF P 94-068) (1998). **Mesure de la capacité d'adsorption de bleu de méthylène d'un sol ou d'un matériau rocheux**. Association Française de Normalisation, La Defense, Paris.

AL-HOMOUD, A. S., BASMA, A. A., HUSEIN MALKAWI, A. I., & AL BASHABSHEH, M. A. (1995). **Cyclic swelling behavior of clays**. Journal of geotechnical engineering, 121(7), 562-565.

AL-RAWAS, A. A., HAGO, A. W., & AL-SARMI, H. (2005). **Effect of lime, cement and Sarooj (artificial pozzolan) on the swelling potential of an expansive soil from Oman**. Building and Environment, 40(5), 681-687.

AL-RAWAS, A. A. (2002). **Microfabric and mineralogical studies on the stabilization of an expansive soil using cement by-pass dust and some types of slags**. Canadian geotechnical journal, 39(5), 1150-1167.

AL-RAWAS, A. A., TAHA, R., NELSON, J. D., AL-SHAB, T. B., & AL-SIYABI, H. (2002). **A comparative evaluation of various additives used in the stabilization of expansive soils**. ASTM geotechnical testing journal, 25(2), 199-209.

AL-ZOUBI, M. S. (2008). **Swell characteristics of natural and treated compacted clays**. EJGE, Journal of Geotechnical Engineering, 13.

ALONSO, E. E., ROMERO, E., HOFFMANN, C., & GARCÍA-ESCUADERO, E. (2005). **Expansive bentonite–sand mixtures in cyclic controlled-suction drying and wetting**. Engineering geology, 81(3), 213-226.

ARASAN, S., YILMAZ, G., AKBULUT, R. K., & YETIMOGLU, T. (2007). **Engineering properties of compacted clay liners contaminated by salt solution**. In Geotechnical Symposium, Turkish Chamber of Civil Engineers, Adana, Turkey pp (pp. 415-425).

ARMSTRONG, C. P. (2014). **Effect of fabric on the swelling of highly plastic clays**. (Master thesis). The University of Texas at Austin.

ASTM C837-09 (2014). **Standard Test Method for Methylene Blue Index of Clay**. ASTM International, West Conshohocken, PA. www.astm.org.

ASTM D2166/D2166M-13 (2013). **Standard Test Method for Unconfined Compressive Strength of Cohesive Soil**. ASTM International, West Conshohocken, PA. www.astm.org

ASTM D2216-10 (2010). **Standard Test Methods for Laboratory Determination of Water (Moisture) Content of Soil and Rock by Mass**. ASTM International, West Conshohocken, PA. www.astm.org

ASTM D422-63 (2007). **Standard Test Method for Particle-Size Analysis of Soils**. ASTM International, West Conshohocken, PA. www.astm.org

ASTM D4318-10 (2010). **Standard Test Methods for Liquid Limit, Plastic Limit, and Plasticity Index of Soils**. ASTM International, West Conshohocken, PA. www.astm.org

ASTM D4546-08 (2008). **Standard Test Methods for One-Dimensional Swell or Collapse of Cohesive Soils**. ASTM International, West Conshohocken, PA. www.astm.org

ASTM D698-12 (2012). **Standard Test Methods for Laboratory Compaction Characteristics of Soil Using Standard Effort (12 400 ft-lbf/ft³ (600 kN-m/m³))**, ASTM International, West Conshohocken, PA. www.astm.org

ASTM D854-14 (2014). **Standard Test Methods for Specific Gravity of Soil Solids by Water Pycnometer**, ASTM International, West Conshohocken, PA. www.astm.org

ATTOM, M.F., ABU-ZREIG, M.M., AND OBAIDAT, M.T. 2001. **Changes in clay swelling and shear strength properties with different sample preparation techniques**. Geotechnical Testing Journal, 24: 157–163.

AZAM, S., SHAH, I., RAGHUNANDAN, M. E., & ITO, M. (2013). **Study on swelling properties of an expansive soil deposit in Saskatchewan, Canada**. Bulletin of Engineering Geology and the Environment, 72(1), 25-35.

BASER, O. (2009). **Stabilization of expansive soils using waste marble dust**. (Master thesis). Civil Engineering Department, Middle East, Technical University.

BASHABSHEH, M. A. (1996). **Swelling-shrinkage behavior of natural expansive clays**. Applied Clay Science, 11(2), 211-227.

BASMA, A. A., AL-HOMOUD, A. S., MALKAWI, A. I. H., & AL-

- BASMA, A. A., & TUNCER, E. R. (1991). **Effect of lime on volume change and compressibility of expansive clays**. Transportation Research Record, (1295).
- BAVEYE, P., ROGASIK, H., WENDROTH, O., ONASCH, I., & CRAWFORD, J. W. (2002). **Effect of sampling volume on the measurement of soil physical properties: simulation with X-ray tomography data**. Measurement Science and Technology, 13(5), 775.
- BEETHAM, P., DIJKSTRA, T., DIXON, N., FLEMING, P., HUTCHISON, R., & BATEMAN, J. (2014). **Lime stabilisation for earthworks: a UK perspective**. Proceedings of the ICE-Ground Improvement, 168(2), 81-95.
- BELL, F. G. (1996). **Lime stabilization of clay minerals and soils**. Engineering geology, 42(4), 223-237.
- BIN, S., ZHIBIN, L., YI, C., & XIAOPING, Z. (2007). **Micropore structure of aggregates in treated soils**. Journal of materials in civil engineering, 19(1), 99-104.
- CAMBI, C., CARRISI, S., & COMODI, P. (2011). **Use of the Methylene Blue Stain Test to Evaluate the Efficiency of Lime Treatment on Selected Clayey Soils**. Journal of Geotechnical and Geoenvironmental Engineering, 138(9), 1147-1150.
- CHEN, F. H. (1975). **Foundations on expansive soils**. (Vol. 12). Elsevier.
- CHIAPPONE, A., MARELLO, S., SCAVIA, C., & SETTI, M. (2004). **Clay mineral characterization through the methylene blue test: comparison with other experimental techniques and applications of the method**. Canadian geotechnical journal, 41(6), 1168-1178.
- CONSOLI, N. C., DA SILVA LOPES JR, L., & HEINECK, K. S. (2009). **Key parameters for the strength control of lime stabilized soils**. Journal of materials in Civil Engineering, 21(5), 210-216.
- CONSOLI, N. C., LOPES JR, L. D. S., PRIETTO, P. D. M., FESTUGATO, L., & CRUZ, R. C. (2010). **Variables controlling stiffness and strength of lime-stabilized soils**. Journal of Geotechnical and Geoenvironmental Engineering, 137(6), 628-632.
- DAS, B., & SOBHAN, K. (2013). **Principles of geotechnical engineering**. Cengage Learning.

- DAS, J. T. (2014). **Evaluation of the rate of secondary swelling in expansive clays using centrifuge technology.** (Master thesis). The University of Texas at Austin.
- CUISINIER, O., AURIOL, J. C., LE BORGNE, T., & DENELEE, D. (2011). **Microstructure and hydraulic conductivity of a compacted lime-treated soil.** *Engineering geology*, 123(3), 187-193.
- DASH, S. K., & HUSSAIN, M. (2011). **Lime stabilization of soils: reappraisal.** *Journal of materials in civil engineering*, 24(6), 707-714.
- DELL'AVANZI, E., ZORNBERG, J. G., & CABRAL, A. R. (2004). **Suction profiles and scale factors for unsaturated flow under increased gravitational field.** *Soils and foundations*, 44(3), 79-89.
- DELAGE, P., HOWAT, M. D., & CUI, Y. J. (1998). **The relationship between suction and swelling properties in a heavily compacted unsaturated clay.** *Engineering geology*, 50(1), 31-48.
- DI SANTE, M., FRATALOCCHI, E., MAZZIERI, F., & BRIANZONI, V. (2015). **Influence of delayed compaction on the compressibility and hydraulic conductivity of soil–lime mixtures.** *Engineering Geology*, 185, 131-138.
- DI MAIO, C. (1996). **Exposure of bentonite to salt solution: osmotic and mechanical effects.** *Geotechnique*, 46(4), 695-707.
- DU, Y., LI, S., & HAYASHI, S. (1999). **Swelling–shrinkage properties and soil improvement of compacted expansive soil, Ning-Liang Highway, China.** *Engineering Geology*, 53(3), 351-358.
- EADES, J. L., & GRIM, R. E. (1966). **A quick test to determine lime requirements for lime stabilization.** *Highway research record*, (139).
- FERREIRA, S. R. M. (2008). **Solos colapsáveis e expansivos: uma visão panorâmica no Brasil.** VI Simpósio Brasileiro de Solos Não Saturados, 593-619.
- FOROUZAN, A. J. (2016). **Prediction of swelling behavior of expansive soils using modified free swell index, methylene blue and swell oedometer tests** (Doctoral dissertation). Middle East Technical University.
- FRYDMAN, S., & WEISBERG, E. (1991). **Study of centrifuge modeling of swelling clay.** In *Proceedings of the International Conference Centrifuge* (Vol. 113).

- GADRE, A. D., & CHANDRASEKARAN, V. S. (1994). **Swelling of black cotton soil using centrifuge modeling**. *Journal of geotechnical engineering*, 120(5), 914-919.
- GENS, A., & ALONSO, E. E. (1992). **A framework for the behaviour of unsaturated expansive clays**. *Canadian Geotechnical Journal*, 29(6), 1013-1032.
- GUNEY, Y., SARI, D., CETIN, M., & TUNCAN, M. (2007). **Impact of cyclic wetting–drying on swelling behavior of lime-stabilized soil**. *Building and Environment*, 42(2), 681-688.
- HARRIS, J., SEBESTA, S., & SCULLION, T. (2004). **Hydrated lime stabilization of sulfate-bearing vertisols in Texas**. *Transportation Research Record: Journal of the Transportation Research Board*, (1868), 31-39.
- HOLT, C. C., & FREER-HEWISH, R. J. (1998). **The use of lime-treated British clays in pavement construction. Part 1: The effect of mellowing on the modification process**. In *Proceedings of the Institution of Civil Engineers. Transport (Vol. 129, No. 4, pp. 228-239)*. Institution of Civil Engineers.
- HOLT, C. C., FREER-HEWISH, R. J., & GHATAORA, G. S. (2000). **The use of lime-treated British clays in pavement construction. Part 2: The effect of mellowing on the stabilization process**. In *Proceedings of the Institution of Civil Engineers-Transport (Vol. 141, No. 4, pp. 207-216)*. Thomas Telford Ltd.
- HOLTZ, R. D., & KOVACS, W. D. (1981). **An introduction to geotechnical engineering**. Englewood Cliffs, Prentice-Hall.
- HOLTZ, W. G., & GIBBS, H. J. (1956). **Engineering properties of expansive clays**. *Transactions of the American Society of Civil Engineers*, 121(1), 641-663.
- HUNTER, D. (1988). **Lime-induced heave in sulfate-bearing clay soils**. *Journal of geotechnical engineering*, 114(2), 150-167.
- JOHANN, A. D. R. (2013). **Metodologias para a previsão do comportamento mecânico e para a análise da variação da porosidade de um solo siltoso tratado com cal em diferentes tempos de cura**. (Doctoral dissertation). Federal University of Rio Grande do Sul (UFRGS).
- KATTI, D. R., & SHANMUGASUNDARAM, V. (2001). **Influence of swelling on the microstructure of expansive clays**. *Canadian Geotechnical Journal*, 38(1), 175-182.
- KOMINE, H. (2004). **Simplified evaluation for swelling characteristics of bentonites**. *Engineering geology*, 71(3), 265-279.

- KUHN, J. A. (2010). **Characterization of the swelling potential of expansive clays using centrifuge technology**. (Doctoral dissertation). The University of Texas at Austin.
- LAMBE, T. W. (1958). **The engineering behavior of compacted clay**. Journal of the Soil Mechanics and Foundations Division, 84(2), 1-35.
- LE RUNIGO, B., CUISINIER, O., CUI, Y. J., FERBER, V., & DENELEE, D. (2009). **Impact of initial state on the fabric and permeability of a lime-treated silt under long-term leaching**. Canadian Geotechnical Journal, 46(11), 1243-1257.
- LIKOS, W. J., & WAYLLACE, A. (2010). **Porosity evolution of free and confined bentonites during interlayer hydration**. Clays and Clay minerals, 58(3), 399-414.
- LIN, B. (2012). **A comprehensive investigation on microscale properties and macroscopic behavior of natural expansive soils**. (Doctoral dissertation). The University of Oklahoma.
- LIN, B., & CERATO, A. B. (2014). **Applications of SEM and ESEM in Microstructural Investigation of Shale-Weathered Expansive Soils along Swelling-Shrinkage Cycles**. Engineering Geology, 177, 66-74.
- LITTLE, D. N. (1994). **Handbook for Stabilization of Pavement Subgrades and Base Courses with Lime**. National Lime Association, Arlington, Virginia.
- LITTLE, D. N., & NAIR, S. (2009). **Recommended practice for stabilization of subgrade soils and base materials. National Cooperative Highway Research Program**. Transportation Research Board of the National Academies.
- LIU, Z. B., SHI, B., INYANG, H. I., & CAI, Y. (2005). **Magnification effects on the interpretation of SEM images of expansive soils**. Engineering geology, 78(1), 89-94.
- MADSEN, F. T., & MÜLLER-VONMOOS, M. (1989). **The swelling behaviour of clays**. Applied Clay Science, 4(2), 143-156.
- MCCARTNEY, J. S., & ZORNBERG, J. G. (2005). **The centrifuge permeameter for unsaturated soils (CPUS)**. In Proceedings of an International Symposium on Advanced Experimental Unsaturated Soil Mechanics, Trento, Italy (pp. 299-304).
- MISHRA, A. K., OHTSUBO, M., LI, L., & HIGASHI, T. (2011). **Controlling factors of the swelling of various bentonites and their correlations with the**

hydraulic conductivity of soil-bentonite mixtures. Applied Clay Science, 52(1), 78-84.

MITCHELL, J. K., & SOGA, K. (2005). **Fundamentals of soil behavior.** John Wiley & Sons, Inc.

MITCHELL, J. K., & HOOPER, D. R. (1961). **Influence of time between mixing and compaction on properties of a lime-stabilized expansive clay.** Highway Research Board Bulletin, (304).

MONGA, O., NGOM, F. N., & DELERUE, J. F. (2007). **Representing geometric structures in 3D tomography soil images: Application to pore-space modeling.** Computers & geosciences, 33(9), 1140-1161.

MONTES-H, G. (2005). **Swelling–shrinkage measurements of bentonite using coupled environmental scanning electron microscopy and digital image analysis.** Journal of colloid and interface science, 284(1), 271-277.

NALBANTOGLU, Z., & TUNCER, E. R. (2001). **Compressibility and hydraulic conductivity of a chemically treated expansive clay.** Canadian geotechnical journal, 38(1), 154-160.

NAYAK, N. V., & CHRISTENSEN, R. W. (1971). **Swelling characteristics of compacted expansive soils.** Clays and Clay Minerals, 19(4), 251-261.

NELSON, J. D., & MILLER, D. J. (1992). **Expansive soils - problems and practice in foundation and pavement engineering.** John Wiley & Sons, Inc.

OSINUBI, K. J., & NWAIWU, C. M. (2006). **Compaction delay effects on properties of lime-treated soil.** Journal of materials in Civil Engineering, 18(2), 250-258.

OSIPOV, V. I., BIK, N. N., & RUMJANTSEVA, N. A. (1987). **Cyclic swelling of clays.** Applied clay science, 2(4), 363-374.

PANJAITAN, S. R. N. (2014). **The effect of lime content on the bearing capacity and swelling potential of expansive Soil.** Journal of Civil Engineering Research, 4(3A), 89-95.

PLAISTED, M. D. (2009). **Centrifuge testing of expansive clay.** (Master thesis). The University of Texas at Austin.

PETRY, T. M., & LITTLE, D. N. (2002). **Review of stabilization of clays and expansive soils in pavements and lightly loaded structures-history, practice, and future.** Journal of Materials in Civil Engineering, 14(6), 447-460.

- PIRES, L. F., BORGES, J. A., BACCHI, O. O., & REICHARDT, K. (2010). **Twenty-five years of computed tomography in soil physics: A literature review of the Brazilian contribution**. *Soil and Tillage Research*, 110(2), 197-210.
- PITRE, B. (2012). **Application of the Modified Methylene Blue Test to Detect Clay Minerals in Coarse Aggregate Fines**. (Master thesis). Texas A&M University.
- PUPPALA, A. J., INTHARASOMBAT, N., & VEMPATI, R. K. (2005). **Experimental studies on ettringite-induced heaving in soils**. *Journal of Geotechnical and Geoenvironmental Engineering*, 131(3), 325-337.
- PUPPALA, A. J., & CERATO, A. (2009). **Heave distress problems in chemically-treated sulfate-laden materials**. *Geo-Strata—Geo Institute of ASCE*, 10(2), 28-30.
- PUPPALA, A. J., MANOSUTHIKIJ, T., & CHITTOORI, B. C. (2014). **Swell and shrinkage strain prediction models for expansive clays**. *Engineering Geology*, 168, 1-8.
- PUPPALA, A., & MUSENDA, C. (2000). **Effects of fiber reinforcement on strength and volume change in expansive soils**. *Transportation research record: Journal of the transportation research board*, (1736), 134-140.
- RAJASEKARAN, G., & NARASIMHA RAO, S. (2005). **Sulphate attack in lime-treated marine clay**. *Marine Georesources and Geotechnology*, 23(1-2), 93-116.
- REEVES, G. M., SIMS, I., & CRIPPS, J. C. (2006). **Clay materials used in construction**. Geological Society of London.
- ROMERO, E., & SIMMS, P. H. (2008). **Microstructure investigation in unsaturated soils: a review with special attention to contribution of mercury intrusion porosimetry and environmental scanning electron microscopy**. In *Laboratory and Field Testing of Unsaturated Soils* (pp. 93-115). Springer Netherlands.
- SATYANARAYANA, B., & RANGANATHAM, B. V. (1969). **Interaction of primary factors on swell and swell pressure**. *Soil Mechanics & Foundation Engineering*.
- SCHANZ, T., & ELSAWY, M. B. (2015). **Swelling characteristics and shear strength of highly expansive clay–lime mixtures: A comparative study**. *Arabian Journal of Geosciences*, 8(10), 7919-7927.

- SEED, H. B., WOODWARD JR, R. J., & LUNDGREN, R. (1962). **Prediction of swelling potential for compacted clays**. Journal of the soil mechanics and foundations division, 88(3), 53-88.
- SEED, H. B., & CHAN, C. K. (1959). **Structure and strength characteristics of compacted clays**. Journal of the Soil Mechanics and Foundations Division, 85(5), 87-128.
- SHI, B., JIANG, H., LIU, Z., & FANG, H. Y. (2002). **Engineering geological characteristics of expansive soils in China**. Engineering Geology, 67(1), 63-71.
- SIMÕES DE OLIVEIRA, A. G., JESUS, A. C., & MIRANDA, S. B. (2006). **Estudo Geológico–Geotécnico dos Solos Expansivos da Região do Recôncavo Baiano**. II Simpósio Brasileiro de Jovens Geotécnicos-II Geojovem, Nova Friburgo/RJ.
- SIVAPULLAIAH, P. V., SRIDHARAN, A., & STALIN, V. K. (1996). **Swelling behaviour of soil bentonite mixtures**. Canadian Geotechnical Journal, 33(5), 808-814.
- SIVAPULLAIAH, P. V. (2005). **Kaolinite–alkali interaction and effects on basic properties**. Geotechnical & Geological Engineering, 23(5), 601-614.
- SNETHEN, D. R., TOWNSEND, F. C., JOHNSON, L. D., PATRICK, D. M., & VEDROS, P. J. (1975). **A review of engineering experiences with expansive soils in highway subgrades**. Interim Report Army Engineer Waterways Experiment Station, Vicksburg, MS., 1.
- SNYDER, L. M. (2015). **Determination of potential vertical rise in expansive soils using centrifuge technology**. (Master thesis). The University of Texas at Austin.
- SOLANKI, P., & ZAMAN, M. (2012). **Microstructural and mineralogical characterization of clay stabilized using calcium-based stabilizers**. INTECH Open Access Publisher.
- STOLTZ, G., CUISINIER, O., & MASROURI, F. (2012). **Multi-scale analysis of the swelling and shrinkage of a lime-treated expansive clayey soil**. Applied Clay Science, 61, 44-51.
- SRIDHARAN, A., & GURTUG, Y. (2004). **Swelling behaviour of compacted fine-grained soils**. Engineering Geology, 72(1), 9-18.
- TEDESCO, D. (2006). **Hydro-mechanical behaviour of lime-stabilised soils**. (Doctoral dissertation). Università degli Studi di Cassino Facoltà di Ingegneria.

- TALLURI, N. (2013). **Stabilization of High Sulfate Soils**. (Doctoral dissertation). The University of Texas at Arlington.
- TALLURI, N., PUPPALA, A., CHITTOORI, B., GAILY, A., & HARRIS, P. (2013). **Stabilization of high-sulfate soils by extended mellowing**. Transportation Research Record: Journal of the Transportation Research Board, (2363), 96-104.
- TAYLOR JR, W. H., & ARMAN, A. (1960). **Lime stabilization using preconditioned soils**. Highway Research Board Bulletin, (262).
- TEXAS DEPARTMENT OF TRANSPORTATION (TxDOT). (2002). **Designation Tx-121-E: Soil-lime testing**. Texas Department of Transportation, Austin, TX.
- TIPPKÖTTER, R., EICKHORST, T., TAUBNER, H., GREDNER, B., & RADEMAKER, G. (2009). **Detection of soil water in macropores of undisturbed soil using microfocus X-ray tube computerized tomography (μ CT)**. Soil and Tillage Research, 105(1), 12-20.
- TRAN, T. D., CUI, Y. J., TANG, A. M., AUDIGUIER, M., & COJEAN, R. (2014). **Effects of lime treatment on the microstructure and hydraulic conductivity of Héricourt clay**. Journal of Rock Mechanics and Geotechnical Engineering, 6(5), 399-404.
- ULERY, A. L., & DREES, L. R. (2008). **Methods of soil analysis: Mineralogical methods**. Part 5 (Vol. 5). ASA-CSSA-SSSA.
- VIJAYVERGIYA, V. N., & GHAZZALY, O. I. (1973). **Prediction of swelling potential for natural clays**. In Proceedings of the Third International Conference on Expansive Clay Soils (Vol. 1, pp. 227-234).
- VILLAR, M. V., & LLORET, A. (2008). **Influence of dry density and water content on the swelling of a compacted bentonite**. Applied Clay Science, 39(1), 38-49.
- WALKER, T. M. (2012). **Quantification Using Centrifuge of Variables Governing the Swelling of Clays**. (Master thesis). The University of Texas at Austin.
- WAYLLACE, A. (2008). **Volume change and swelling pressure of expansive clay in the crystalline swelling regime**. (Doctoral dissertation). University of Missouri-Columbia.

- WEST, G. (1959). **A Laboratory Investigation into the effect of elapsed time after mixing on the compaction and strength of soil-cement.** *Geotechnique*, 9(1), 22-28.
- WISE, J. R., & HUDSON, W. R. (1971). **An examination of expansive clay problems in Texas.** (Master's thesis). University of Texas at Austin.
- YAZDANDOUST, F., & YASROBI, S. S. (2010). **Effect of cyclic wetting and drying on swelling behavior of polymer-stabilized expansive clays.** *Applied Clay Science*, 50(4), 461-468.
- YILMAZ, I. (2006). **Indirect estimation of the swelling percent and a new classification of soils depending on liquid limit and cation exchange capacity.** *Engineering Geology*, 85(3), 295-301.
- ZORNBERG, J. G., & MCCARTNEY, J. S. (2010). **Centrifuge permeameter for unsaturated soils. I: Theoretical basis and experimental developments.** *Journal of Geotechnical and Geoenvironmental Engineering*, 136(8), 1051-1063.
- ZORNBERG, J. G., KUHN, J. A., & PLAISTED, M. D. (2009). **Characterization of the Swelling Properties of Highly Plastic Clays Using Centrifuge Technology.** Center for Transportation Research (CTR), Report No. FHWA/TX-09/0-6048-1, Austin, Texas.